

**ADJUSTING ASPHALT MIXES FOR
INCREASED DURABILITY AND
IMPLEMENTATION OF A
PERFORMANCE TESTER TO EVALUATE
FATIGUE CRACKING OF ASPHALT
CONCRETE**

Final Report

SPR 785



Oregon Department of Transportation

**ADJUSTING ASPHALT MIXES FOR INCREASED
DURABILITY AND IMPLEMENTATION OF A
PERFORMANCE TESTER TO EVALUATE FATIGUE
CRACKING OF ASPHALT CONCRETE**

Final Report

SPR 785

by

Erdem Coleri, PhD

Shashwath Sreedhar; Sogol Haddadi; Blaine Wruck

School of Civil and Construction Engineering
Oregon State University
101 Kearney Hall
Corvallis, OR 97331
Phone: 541-737-0944

for

Oregon Department of Transportation
Research Section
555 13th Street NE, Suite 1
Salem OR 97301

and

Federal Highway Administration
400 Seventh Street, SW
Washington, DC 20590-0003

January 2018

1. Report No. FHWA-OR-18-06	2. Government Accession No.	3. Recipient's Catalog No.	
4. Title and Subtitle Adjusting Asphalt Mixes for Increased Durability and Implementation of a Performance Tester to Evaluate Fatigue Cracking of Asphalt		5. Report Date January 2018	
		6. Performing Organization Code	
7. Author(s) Erdem Coleri, PhD; Shashwath Sreedhar; Sogol Haddadi; Blaine Wruck		8. Performing Organization Report No. SPR 785	
9. Performing Organization Name and Address School of Civil and Construction Engineering Oregon State University 101 Kearney Hall, Corvallis, OR 97331		10. Work Unit No. (TRAIS)	
		11. Contract or Grant No.	
12. Sponsoring Agency Name and Address Oregon Dept. of Transportation Research Section and Federal Highway Admin. 555 13 th Street NE, Suite 1 400 Seventh Street, SW Salem, OR 97301 Washington, DC 20590-0003		13. Type of Report and Period Covered Draft Report	
		14. Sponsoring Agency Code	
15. Supplementary Notes			
16. Abstract Cracking is a common failure mechanism in asphalt concrete pavement structures. It is one of the main reasons for large road maintenance and rehabilitation expenditures, as well as reduced user comfort and increased fuel consumption due to high road roughness. The resistance of the pavement to this distress mechanism is dependent upon the ductility of the asphalt pavement mixture. The use of recycled asphalt materials in asphalt mixtures are also becoming increasingly common. A drawback of this practice is a reduction in ductility of the asphalt mixture, which causes a significant reduction in the fatigue life of the pavement in many cases. In Oregon, asphalt pavements are commonly failing prematurely due to cracking-related distresses, necessitating costly rehabilitation and maintenance at intervals of less than half of the intended design lives in some cases. For this reason, it is necessary to accurately quantify the impact of increasing the recycled asphalt content in asphalt pavement on the structural cracking resistance of the pavement through use of low-cost and efficient testing procedures that can be implemented easily. This study focuses on characterizing the cracking performance of asphalt pavements in Oregon by considering four tests commonly used to evaluate fatigue cracking resistance and proposing implementation of the most cost-effective and efficient test procedure for agencies and contractors. Also, the impact of asphalt mixture properties, such as binder content, air-void content, aggregate gradation, polymer modification, and aging, on cracking performance of asphalt mixtures was investigated. Mechanistic-empirical (ME) design modeling and life-cycle costs analysis were also conducted to determine cost and performance effectiveness of asphalt mixtures with varying properties. Finally, recommended strategies were proposed for Oregon to address the issue of early pavement fatigue failure based on the test results, statistical analysis, ME models, and life cycle cost analysis (LCCA). The goal of this study is to provide a better decision-making structure during the pavement design stage to address fatigue cracking susceptibility, with the intent of avoiding premature pavement failure and expensive early maintenance and rehabilitation. Additionally, the study aims to reliably facilitate an increase in recycled materials content in asphalt pavement through advanced testing procedures and design recommendations proposed in this study. These recommendations will reduce the life cycle cost of pavements in Oregon, reduce network-level pavement roughness and increase the sustainability of the paving industry.			
17. Key Words Fatigue cracking, top-down cracking, pavement durability, recycled asphalt pavements, mechanistic-empirical design, polymer modified hot mix asphalt, life-cycle cost.		18. Distribution Statement Copies available from NTIS, and online at http://www.oregon.gov/ODOT/Programs/Pages/Research-Publications.aspx	
19. Security Classification (of this report) Unclassified	20. Security Classification (of this page) Unclassified	21. No. of Pages 204	22. Price

SI* (MODERN METRIC) CONVERSION FACTORS

APPROXIMATE CONVERSIONS TO SI UNITS					APPROXIMATE CONVERSIONS FROM SI UNITS				
Symbol	When You Know	Multiply By	To Find	Symbol	Symbol	When You Know	Multiply By	To Find	Symbol
<u>LENGTH</u>					<u>LENGTH</u>				
in	inches	25.4	millimeters	mm	mm	millimeters	0.039	inches	in
ft	feet	0.305	meters	m	m	meters	3.28	feet	ft
yd	yards	0.914	meters	m	m	meters	1.09	yards	yd
mi	miles	1.61	kilometers	km	km	kilometers	0.621	miles	mi
<u>AREA</u>					<u>AREA</u>				
in ²	square inches	645.2	millimeters squared	mm ²	mm ²	millimeters squared	0.0016	square inches	in ²
ft ²	square feet	0.093	meters squared	m ²	m ²	meters squared	10.764	square feet	ft ²
yd ²	square yards	0.836	meters squared	m ²	m ²	meters squared	1.196	square yards	yd ²
ac	acres	0.405	hectares	ha	ha	hectares	2.47	acres	ac
mi ²	square miles	2.59	kilometers squared	km ²	km ²	kilometers squared	0.386	square miles	mi ²
<u>VOLUME</u>					<u>VOLUME</u>				
fl oz	fluid ounces	29.57	milliliters	ml	ml	milliliters	0.034	fluid ounces	fl oz
gal	gallons	3.785	liters	L	L	liters	0.264	gallons	gal
ft ³	cubic feet	0.028	meters cubed	m ³	m ³	meters cubed	35.315	cubic feet	ft ³
yd ³	cubic yards	0.765	meters cubed	m ³	m ³	meters cubed	1.308	cubic yards	yd ³
NOTE: Volumes greater than 1000 L shall be shown in m ³ .									
<u>MASS</u>					<u>MASS</u>				
oz	ounces	28.35	grams	g	g	grams	0.035	ounces	oz
lb	pounds	0.454	kilograms	kg	kg	kilograms	2.205	pounds	lb
T	short tons (2000 lb)	0.907	megagrams	Mg	Mg	megagrams	1.102	short tons (2000 lb)	T
<u>TEMPERATURE (exact)</u>					<u>TEMPERATURE (exact)</u>				
°F	Fahrenheit	(F-32)/1.8	Celsius	°C	°C	Celsius	$\frac{1.8C+32}{2}$	Fahrenheit	°F

*SI is the symbol for the International System of Measurement

ACKNOWLEDGEMENTS

The authors would like to thank the Oregon Department of Transportation (ODOT) for providing funding for this research. The authors thank the members of the ODOT Project Technical Advisory Committee and ODOT research for their advice and assistance in the preparation of this report. In particular, Norris Shippen, Larry Ilg, Justin Moderie, Cole Mullis, Anthony Boesen, John Duval, and Todd Scholz participated on the TAC. The authors would also like to thank Mike Stennett of ODOT who organized material sampling. The authors would also like to thank Tim Flowerday, Nicholas Kolstad, John Paul Morton, Andrew Johnson, Mostafa Estaji, Ihsan Obaid, Natasha Anisimova, Matthew Haynes, and Jawad Qassem for their help with sieving, batching, and measuring theoretical maximum specific gravity of prepared samples, as well as James Batti for his help in the laboratory. The authors also thank Yuqi Zhang for performing the MEPDG analyses for this study. Also, a special thank you to Owens Corning for providing asphalt binders, and to Lakeside Industries for providing aggregates, production mix, and RAP materials used in this study.

DISCLAIMER

This document is disseminated under the sponsorship of the Oregon Department of Transportation and the United States Department of Transportation in the interest of information exchange. The State of Oregon and the United States Government assume no liability of its contents or use thereof.

The contents of this report reflect the view of the authors who are solely responsible for the facts and accuracy of the material presented. The contents do not necessarily reflect the official views of the Oregon Department of Transportation or the United States Department of Transportation.

The State of Oregon and the United States Government do not endorse products of manufacturers. Trademarks or manufacturers' names appear herein only because they are considered essential to the object of this document.

This report does not constitute a standard, specification, or regulation.

TABLE OF CONTENTS

1.0	INTRODUCTION	1
1.1	KEY OBJECTIVES OF THIS STUDY	2
1.2	ORGANIZATION OF THE REPORT	3
2.0	LITERATURE REVIEW	5
2.1	FATIGUE CRACKING MECHANISMS IN ASPHALT PAVEMENTS	5
2.2	FACTORS AFFECTING FATIGUE CRACKING	6
2.2.1	<i>Air-Void and Binder Content.....</i>	6
2.2.2	<i>Binder Modification.....</i>	9
2.2.3	<i>Aging</i>	10
2.2.4	<i>Binder Performance Grade</i>	12
2.2.5	<i>Mixture Segregation</i>	13
2.2.6	<i>Aggregate Gradation and Volumetrics.....</i>	15
2.2.7	<i>Aggregate Type.....</i>	17
2.3	TEST METHODS TO EVALUATE FATIGUE CRACKING PERFORMANCE OF ASPHALT CONCRETE	17
2.3.1	<i>Bending Beam Fatigue (BBF)</i>	18
2.3.2	<i>Indirect Tension (IDT).....</i>	19
2.3.3	<i>Repeated Direct Tension</i>	20
2.3.4	<i>Simplified Viscoelastic Continuum Damage (S-VECD)</i>	21
2.3.5	<i>Semi-Circular Bend (SCB) Test.....</i>	22
2.4	FATIGUE CRACKING MODELS	24
2.4.1	<i>Mechanistic-Empirical Pavement Design Guide (MEPDG) Models.....</i>	24
2.4.1.1	<i>Shell Oil Model</i>	26
2.4.1.2	<i>Asphalt Institute (MS-1) Model.....</i>	27
2.4.2	<i>Continuum Damage Models</i>	28
2.4.2.1	<i>Continuum Damage Mechanics-Based Fatigue Model.....</i>	28
2.4.2.2	<i>Simplified Viscoelastic Continuum Damage (S-VECD) model</i>	30
2.4.3	<i>Parameters to Evaluate Fatigue Cracking Performance</i>	32
2.4.3.1	<i>Paris Law of Crack Propagation</i>	32
2.4.3.2	<i>Dissipated Energy Approach</i>	33
2.4.3.3	<i>Critical Strain Energy Release Rate</i>	34
2.4.3.4	<i>Pseudo Strain Energy Release Rate</i>	34
2.5	PREDICTION OF FIELD FATIGUE CRACKING PERFORMANCE USING LABORATORY TEST RESULTS.....	35
2.5.1	<i>Bending Beam Fatigue Test.....</i>	35
2.5.2	<i>Indirect Tension Test</i>	37
2.5.3	<i>Simplified Viscoelastic Continuum Damage (S-VECD) Test.....</i>	37
2.5.4	<i>Semi-Circular Bend Test</i>	38
2.6	SUMMARY.....	39
3.0	IMPLEMENTATION OF PERFORMANCE TESTER TO EVALUATE FATIGUE CRACKING OF ASPHALT CONCRETE	41
3.1	INTRODUCTION	41
3.2	OBJECTIVES	42
3.3	MATERIALS	42
3.4	EXPERIMENTAL DESIGN	47

3.4.1	<i>Experimental Design for Plant Mixed-Field Compacted Specimens</i>	47
3.4.2	<i>Experimental Design for Plant Mixed - Laboratory Compacted Specimens</i>	48
3.4.2.1	from viscosity versus temperature plots for the binder provided by Owens Corning. A sample Preparation of PMLC Specimens	49
3.4.3	<i>Experimental design for laboratory mixed-laboratory compacted specimens</i>	51
3.5	TEST METHODS	52
3.5.1	<i>Semi-Circular Bend (SCB) Test</i>	52
3.5.1.1	Sample Preparation.....	52
3.5.1.2	Testing.....	53
3.5.1.3	Parameters Obtained from SCB Test Results	54
3.5.1.4	Comparison of Fracture Energy (Gf) to Flexibility Index (FI)	58
3.5.2	<i>Indirect Tension (IDT) Test</i>	59
3.5.3	<i>Bending Beam Fatigue (BBF) Test</i>	60
3.5.4	<i>Direct Tension Cyclic Fatigue (DTCF) Test</i>	61
3.5.5	<i>Resilient Modulus (MR) Test</i>	63
3.5.6	<i>Dynamic Modulus (DM) Test</i>	65
3.5.7	<i>Flow Number (FN) Test</i>	67
3.5.7.1	Francken model	68
3.6	RESULTS AND DISCUSSION	69
3.6.1	<i>Plant Mixed-Field Compacted (PMFC) Specimens</i>	69
3.6.1.1	Semi-Circular Bend (SCB)Test	69
3.6.1.2	Indirect Tension (IDT) Test.....	73
3.6.1.3	Bending Beam Fatigue (BBF) Test	74
3.6.1.4	Resilient Modulus (MR) Test.....	75
3.6.1.5	One-to-One Correlations Between the Output Parameters of Different Tests	76
3.6.2	<i>Plant Mixed-Laboratory Compacted (PMLC) Specimens</i>	77
3.6.2.1	Semi-Circular Bend (SCB) Test	77
3.6.2.2	Indirect Tension (IDT) test	83
3.6.2.3	Bending Beam Fatigue (BBF) Test	85
3.6.2.4	Direct Tension Cyclic Fatigue (DTCF) Test.....	86
3.6.2.5	Dynamic Modulus (DM) Test	87
3.6.2.6	Flow Number (FN) Test	89
3.6.3	<i>Laboratory Mixed-Laboratory Compacted (PMLC) Specimens</i>	90
3.7	SUMMARY AND CONCLUSIONS	92
4.0	CONTRIBUTIONS OF MIXTURE PROPERTIES TO DURABILITY	94
4.1	INTRODUCTION	94
4.2	OBJECTIVES	94
4.3	MATERIALS AND METHODS	95
4.3.1	<i>Experimental Plan to Determine the Impact of Mixture Properties on Durability</i>	95
4.3.2	<i>Materials</i>	96
4.3.2.1	Aggregates.....	96
4.3.2.2	Recycled asphalt pavement (RAP) aggregates	96
4.3.2.3	Binders	96
4.3.3	<i>Sample preparation</i>	96
4.3.3.1	Target gradations	96
4.3.3.2	Batching	99
4.3.3.3	Mixing and compaction	99
4.3.3.4	Air void content.....	99
4.3.4	<i>Testing methods</i>	100
4.4	RESULTS AND DISCUSSION	100
4.4.1.1	Semi-circular bend (SCB) test	100
	ANOVA table.....	102
4.4.1.2	Dynamic modulus (DM) test	103
4.4.1.3	Flow number (FN) test	109
	ANOVA Table	110
4.5	SUMMARY AND CONCLUSIONS	110

5.0	IMPACT OF INCREASED DUST CONTENT ON CRACKING PERFORMANCE	112
5.1	INTRODUCTION	112
5.2	OBJECTIVE	112
5.3	MATERIALS AND METHODS	112
5.3.1	<i>Mix Design Process</i>	114
5.4	RESULTS AND DISCUSSION	115
5.4.1	<i>Semi-Circular Bend (SCB) Test</i>	115
5.4.2	<i>Dynamic Modulus (DM) Test</i>	116
5.4.3	<i>Flow Number (FN) Test</i>	118
5.5	SUMMARY AND CONCLUSIONS	119
6.0	THE EFFECT OF LABORATORY LONG-TERM AGING ON CRACKING PERFORMANCE OF ASPHALT MIXTURES	120
6.1	INTRODUCTION	120
6.2	OBJECTIVES	120
6.3	MATERIALS AND METHODS	121
6.4	RESULTS AND DISCUSSION	121
6.4.1	<i>Semi-Circular Bend (SCB) Test</i>	121
6.4.2	<i>Dynamic Modulus (DM) Test</i>	123
6.4.2.1	Master curves for dynamic modulus	123
6.4.2.2	Master curves for phase angle	124
6.4.3	<i>Flow Number (FN) Test</i>	124
6.5	SUMMARY AND CONCLUSIONS	125
7.0	MECHANISTIC-EMPIRICAL PAVEMENT DESIGN GUIDE (MEPDG) SIMULATIONS AND LIFE CYCLE COST ANALYSIS	126
7.1	INTRODUCTION	126
7.2	MEPDG RUTTING AND FATIGUE CRACKING MODELS	126
7.2.1	<i>Fatigue Cracking Models</i>	126
7.2.2	<i>Rutting Models</i>	128
7.3	LEVEL 1 MEPDG SIMULATIONS USING EXPERIMENTAL RESULTS	130
7.4	COST CALCULATION TOOL	134
7.5	LIFE-CYCLE COST ANALYSIS	137
7.6	RESULTS AND DISCUSSION	139
7.6.1	<i>MEPDG Performance Predictions</i>	139
7.6.2	<i>Life-Cycle Cost Analysis</i>	143
7.7	SUMMARY AND CONCLUSIONS	146
8.0	SUMMARY AND CONCLUSIONS	148
8.1	CONCLUSIONS	148
8.2	RECOMMENDATIONS AND FUTURE WORK	150
8.2.1	<i>Implementation of Performance Tester to Evaluate Fatigue Cracking of Asphalt Concrete</i>	150
8.2.2	<i>Contributions of Mixture Properties to Durability</i>	151
8.2.3	<i>Impact of Increased Dust Content on Cracking Performance</i>	151
8.2.4	<i>The Effect of Laboratory Long-Term Aging on Cracking Performance of Asphalt Mixtures</i>	152
8.2.5	<i>Mechanistic-Empirical Pavement Design Guide (MEPDG) Simulations and Life Cycle Cost Analysis</i>	152
9.0	REFERENCES	154

APPENDIX

LIST OF FIGURES

Figure 2.1: Predicted pavement fatigue life versus air void content and binder content for conventional overlays of thin structure (Harvey and Tsai 1996).	8
Figure 2.2: Predicted pavement fatigue life versus air void content and binder content for conventional and “rich bottom overlays” of thick structure (Harvey and Tsai 1996).	8
Figure 2.3: Segregation and cracking (Harmelink et al. 2008).	9
Figure 2.4: Comparison of G^* (shear modulus) before aging and after long-term aging for the different FAM specimens (Arega et al. 2013).	12
Figure 2.5: Comparison of fatigue life before and after long-term aging for FAM specimens (Arega et al. 2013). ...	12
Figure 2.6: Strain versus number of cycles to failure (50 percent of initial load) (Khedaywi and White 1996).	14
Figure 2.7: Four-point bend testing system (<i>Source: www.pavementinteractive.org</i>).	19
Figure 2.8: (a) Superpave Indirect Tension Test (IDT) with LVDT mounted on the sample (Roque et al. 2002); (b) IDT with LVDT mounted around the sample (Newcomb et al. 2015).	20
Figure 2.9: Configuration of controlled-strain RDT test (Luo et al. 2013).	21
Figure 2.10: (a) S-VECD test setup (<i>source: www.worldhighways.com</i>); (b) gluing jig.	22
Figure 2.11: SCB test apparatus (Wu et al. 2005).	23
Figure 2.12: (a) Constant stress test and (b) constant strain test (Witczak et al. 2004).	26
Figure 2.13: Estimated versus observed fatigue lives (Tayebali et al. 1992).	36
Figure 2.14: Effect of mode of loading and temperature (Tayebali et al. 1992)	37
Figure 2.15: Comparison of FEP++ predicted and measured fatigue life of FHWA ALF mixtures (Underwood et al. 2012).	38
Figure 2.16: Correlation between cracking rates of pavement sections and J_c values from SCB tests (Mohammad et al. 2012).	39
Figure 3.1: Asphalt mix sampling at the production plant.	44
Figure 3.2: Gradation curve for Mix 1 obtained from the plant.	44
Figure 3.3: Gradation curve for Mix 2 and Mix 3 obtained from the plant.	45
Figure 3.4: Field sampling (a) Cores for SCB and IDT tests (b) Slab samples for BBF test (c) Cutting field slabs to produce blocks that can fit the lab saw (d) Cutting field blocks.	48
Figure 3.5: Mechanical Splitting of Asphalt Mixtures	50
Figure 3.6: Mixing and Compaction Curve for PG 70-22ER.	50
Figure 3.7: Laboratory Compaction; (a) Superpave Gyratory Compactor and cylindrical specimens; (b) Roller Compactor and beam specimens	51
Figure 3.8: Cutting and notching procedure for SCB sample preparation.	53
Figure 3.9: SCB loading set up and test	54
Figure 3.10: Load versus displacement (P-u) curve (AASHTO TP 105-13).	55
Figure 3.11: Illustration of load-displacement curve and slope at inflection point (m).	58
Figure 3.12: Illustration of load-displacement curve of ductile and brittle mixtures	59
Figure 3.13: Indirect tension test; (a) Cylindrical specimens from SGC; (b) IDT test apparatus.	60
Figure 3.14: Bending beam fatigue test; (a) Beam specimens prepared with roller compactor; (b) four-point bending test apparatus.	61
Figure 3.15: DTCF test setup	62
Figure 3.16: Gluing setup for DTCF testing.	63
Figure 3.17: Resilient modulus test setup	64
Figure 3.18: Dynamic modulus test setup	65
Figure 3.19: Gauge point gluing setup	66
Figure 3.20: Relationship between permanent strain and load cycles in FN test	67
Figure 3.21: Fracture energy for PMFC samples	70
Figure 3.22: Fracture toughness for PMFC samples	70
Figure 3.23: Secant modulus for PMFC samples	71
Figure 3.24: Flexibility index from SCB test for PMFC samples	71
Figure 3.25: Flexibility index for mixtures with different RAP contents (30% and 40%), binder grades (PG 58-34, PG 64-22, and PG 76-22), and binder contents (6%, 6.4%, and 6.8%) (Coleri et al. 2017)	72
Figure 3.26: Tensile strength for PMFC samples.	73

Figure 3.27: Flexibility index from IDT test for PMFC samples	74
Figure 3.28: Fatigue life from BBF test for PMFC samples	75
Figure 3.29: Resilient modulus for FMFC samples.....	76
Figure 3.30: One-to-one correlation plots (a) flexibility index and fracture energy from SCB (b) flexibility indices from SCB and IDT tests (c) SCB flexibility index and BBF fatigue life (d) Resilient modulus and SCB flexibility index	77
Figure 3.31: Flexibility index from SCB tests for PMLC samples.....	78
Figure 3.32: General procedure followed for extraction	81
Figure 3.33: Comparison of plant and extracted aggregate gradations	82
Figure 3.34: Histogram of binder contents for production mix samples	83
Figure 3.35: Tensile strength from IDT tests for PMLC samples	84
Figure 3.36: Flexibility index from IDT tests for PMLC samples	84
Figure 3.37: Fatigue life from BBF tests for PMLC samples.....	85
Figure 3.38: Fatigue life from DTCF tests for PMLC samples	86
Figure 3.39: Dynamic modulus for PMLC samples.....	88
Figure 3.40: Phase angle for PMLC samples	88
Figure 3.41: Flow number for PMLC samples.....	89
Figure 3.42: The impact of mixing method and compaction type on SCB flexibility index	91
Figure 3.43: SCB results evaluating gyratory and roller compaction.....	91
Figure 4.1: Target, extracted RAP, and stockpiled aggregate gradations for Mix 1.....	97
Figure 4.2: Target, extracted RAP, and stockpiled aggregate gradations for Mix 2 and 3.....	98
Figure 4.3. SCB results comparing plant and laboratory compaction.	101
Figure 4.4. SCB results for the mixtures with different binder contents (5.3% and 6%), and air void contents (5%, and 7%).	102
Figure 4.5. Master curves of dynamic modulus for M1 with different binder contents (5.3% and 6%), air void contents (5%, and 7%).	103
Figure 4.6. Master curves of dynamic modulus for M2 with different binder contents (5.3% and 6%), air void contents (5%, and 7%).	104
Figure 4.7. Master curves of dynamic modulus for M3 with different binder contents (5.3% and 6%), air void contents (5%, and 7%).	104
Figure 4.8. Master curves of dynamic modulus comparing field mixed and laboratory mixed samples.....	106
Figure 4.9. Phase angle master curves for M1 with different binder contents (5.3% and 6%), air void contents (5%, and 7%).	107
Figure 4.10. Phase angle master curves for M2 with different binder contents (5.3% and 6%), air void contents (5%, and 7%).	108
Figure 4.11. Phase angle master curves for M3 with different binder contents (5.3% and 6%), air void contents (5%, and 7%).	108
Figure 4.12. Flow number for mixes with different binder contents (5.3% and 6%), air void contents (5% and 7%).	109
Figure 5.1: Gradations selected to evaluate the effect of increased dust content on durability.	114
Figure 5.2: Mix design curve – Binder content versus air-void content.....	115
Figure 5.3. SCB results for dust content effect.....	116
Figure 5.4. DM master curves comparing finer and coarse gradations.	117
Figure 5.5. DM master curves comparing finer and coarse gradations.	118
Figure 5.6. FN test results for dust content effect.....	119
Figure 6.1. SCB results comparing long-term aged and only short-term aged samples.	122
Figure 6.2. Correlation between FI for long-term aged and only short-term aged samples.	122
Figure 6.3. DM master curves comparing aged and unaged samples.....	123
Figure 6.4. Phase angle master curves comparing aged and unaged samples.	124
Figure 6.5. FN test results comparing aged and unaged samples.	125
Figure 7.1: Cross sections of structures used for MEPDG modeling (a) initial rehabilitation (overlay) b) Structure after the 2 nd rehabilitation.	133
Figure 7.2: Air temperature distribution for Portland.....	133
Figure 7.3: Cost calculation tool input tab (Coleri et al. 2017).	135
Figure 7.4: Cost calculation tool output tab (Coleri et al. 2017).	136
Figure 7.5: Diagram used for LCCA - PG70-22ER binder, fine gradation, 5.3% binder content, and Portland climate.	138
Figure 7.6: Predicted asphalt concrete (AC) rutting for all mixes (a) AADTT=3,000 (b) AADTT=6,000.....	140

Figure 7.7: Predicted bottom-up cracking (alligator) for all mixes (a) AADTT=3,000 (b) AADTT=6,000.....	141
Figure 7.8: Cracking performance curves for the section with for the section with PG70-22ER binder, fine gradation, 5.3% binder content, and Portland climate.....	142
Figure 7.9: Calculated material cost NPVs for all cases for 4% interest rate.....	144
Figure 7.10: Calculated material cost NPVs for all cases for 5% interest rate.....	145
Figure 7.11: Correlation between NPVs calculated by using 4% and 5% interest rates.	145
Figure A.1: PMS for OR-22 Sublimity Section	2
Figure A.2: PMS for OR-99W JUNCTION CITY.....	3
Figure A.3: PMS for OR-99W BRUTSCHER ST	4
Figure A.4: PMS for OR-99EB JCT HWY.....	5
Figure B.1: ODOT mix design summary-Mix 1	2
Figure B.2: ODOT mix design summary-Mix 1 (continued).....	3
Figure B.3: Specific gravity and absorption of coarse and fine aggregates-Mix 1	4
Figure B.4: Field worksheet for HMAC (plant report)-Mix 1.....	5
Figure B.5: ODOT mix design summary – Mix 2 and Mix 3	6
Figure B.6: ODOT mix design summary– Mix 2 and Mix 3 (continued).....	7
Figure B.7: Specific gravity and absorption of coarse and fine aggregates– Mix 2 and Mix 3.....	8
Figure B.8: Field worksheet for HMAC (plant report) – Mix 2 and Mix 3.....	9
Figure C.1: PG 70-22 binder consensus properties	1
Figure C.2: PG 70-22 binder mixing and compaction curve.....	2
Figure C.3: PG 70-22ER binder consensus properties	3
Figure C.4: PG 70-22ER binder mixing and compaction curve.....	4
Figure D.1: Flexural fatigue stiffness versus cycle number for 6.0% BC.....	1
Figure D.2: Flexural fatigue stiffness versus cycle number for 6.4% BC.....	2
Figure D.3: Flexural fatigue stiffness versus cycle number for 6.8% BC.....	2
Figure D.4: Number of BBF cycles required to reach failure of samples with varying RAP and binder contents.	4

LIST OF TABLES

Table 2.1: Asphalt mixture information on I-20 experimental sections (Hu et al. 2011)	7
Table 2.2: Project information and mixtures designation (Wu et al. 2005).....	24
Table 3.1. RAP aggregate gradations-Mix 1	46
Table 3.2. RAP aggregate gradations-Mix 2 and Mix 3	46
Table 3.3: Experimental plan for Plant Mixed Field Compacted (PMFC) samples	47
Table 3.4: Experimental plan for Plant Mixed Laboratory Compacted (PMFC) samples.....	49
Table 3.5: Experimental plan to investigate the effect of compaction and mixing on cracking results.....	52
Table 3.6: Minimum average FN requirement for different traffic levels (AASHTO TP 79-13)	68
Table 3.7: Calculated binder contents of production mix samples	82
Table 3.8: Ranking of the tests	93
Table 4.1: Experimental plan for durability evaluation.....	95
Table 4.2. Target, extracted RAP, and stockpiled aggregate gradations for Mix 1	97
Table 4.3. Target, extracted RAP, and stockpiled aggregate gradations for Mix 2 and Mix 3.....	98
Table 4.4. ANOVA table for the regression model correlating FI test results with mix type, gradation, binder content and air void content	103
Table 4.5. ANOVA table for the regression model correlating FN test results with mix type, binder content and air void content	110
Table 5.1: Experimental plan for dust content effect evaluation.....	113
Table 6.1: Experimental plan for aging evaluation	121
Table 7.1: Cases modeled with MEPDG.....	131
Table 7.2: Summary of calibration factors for Oregon (Williams and Shaidur 2013).	132
Table 7.3: Results of life cycle costs analysis.	143
Table D.1. Number of Cycles Required to Reach a 50% Reduction in Stiffness	3
Table E.1: G_{mm} and air voids for Mix 1	1
Table E.2: G_{mm} and air voids for Mix 2.....	2
Table E.3: G_{mm} and air voids for Mix 3.....	3
Table F.1: Quantity of virgin aggregates and RAP materials for the mixture with 20% RAP, 5.3% binder content, and binder grade of PG 70-22ER.....	1
Table F.2: Quantity of binder, RAP materials, and total aggregates for Mix 1 with 20% RAP, 5.3% binder content, and binder grade of PG 70-22ER.....	2

1.0 INTRODUCTION

Cracking is a common failure mechanism in asphalt concrete pavement structures. It is one of the main reasons for large road maintenance and rehabilitation expenditures, as well as reduced user comfort and increased fuel consumption due to high road roughness. The fatigue mechanism in asphalt pavements is a complex phenomenon that varies across a wide range of temperatures and loading conditions. Asphalt concrete is a heterogeneous matrix of crushed stone and bitumen with nonlinear viscoelastic material properties, which makes analysis of the material very complicated. Furthermore, the increased use of polymer modification and recycled materials in asphalt pavement convolutes the mix design process and adds additional analysis challenges. Although the use of recycled materials is beneficial in most cases, it also makes the mixtures more susceptible to cracking (West et al., 2013). As a consequence of all these factors, cracking characterization of asphalt pavement is challenging and it is imperative to address this issue in order to arrive at a performance-based mix design that yields satisfactory pavement performance.

Asphalt concrete fatigue cracking is recognized as a major distress mode in Oregon. The Oregon Department of Transportation (ODOT) Pavement Management System (PMS) has shown that asphalt mixes placed in the last 20 years have had a tendency to develop premature fatigue cracking after 6 to 8 years of service life, necessitating maintenance or rehabilitation before reaching the intended structural design life of 15 years. The widespread nature of this distress suggests that it is an issue with mix design and production processes and is not a problem specific to certain highway construction projects. Thus, current test methods and design guidelines should be modified and improved to be able to develop more durable asphalt mixtures that last for their intended service lives. In order to determine the most feasible test method and analysis protocol to be used in district and contractor laboratories in Oregon, the accuracy, precision, time, cost, efficiency and practicality of different cracking tests should be evaluated.

In this study, asphalt mixtures used in the state of Oregon are analyzed for their fatigue performance. In order to assess asphalt pavement fracture properties, it is essential to have a laboratory test method that is simple, practical and cost effective to use and implement for agencies and contractors. Therefore, four of the most commonly used cracking experiments were evaluated in order to investigate their effectiveness in determining the fatigue cracking performance of asphalt mixtures. This study was conducted in three phases. In the first phase (Chapter 3.0), the effectiveness of four different cracking experiments used to predict the in-situ cracking performance of existing pavements were evaluated. The four tests were ranked based on their performance, ease of use and the cost involved with implementing them. In the second phase (Chapter 4.0, Chapter 5.0, and Chapter 6.0), using the selected cracking experiment from Phase I, the impact of asphalt mixture properties, such as binder content, air-void content, aggregate gradation, and polymer modification, and aging, on asphalt concrete cracking performance was determined. Finally, mechanistic-empirical pavement design guide (MEPDG) simulations and life cycle cost analyses were conducted to determine the cost and performance effectiveness of asphalt mixtures evaluated in Chapter 4.0.

Once the best tool for quantifying cracking susceptibility was determined, it was important to come up with recommendations that would improve the fatigue performance of asphalt mixtures in Oregon. To be able to provide recommendations for asphalt mixture design properties, the impacts of aggregate gradation, binder content, polymer modification, compactive effort (density) and laboratory long-term aging on cracking test results were studied and quantified. In this study, laboratory test results were used to develop mechanistic-empirical (ME) pavement models for different asphalt mixtures. Varying each of the properties named above allowed for robust Level 1 ME models to be developed. Through development of ME models to predict fatigue cracking based on these parameters, a greater understanding of the cracking performance of asphalt pavements in Oregon was gained. Life-cycle costs analyses were also conducted using the cracking performances predicted by ME design methods to determine cost effectiveness of asphalt mixtures with varying properties.

The intent of this study is to provide the industry and ODOT with better insight on how to combat fatigue-related failure issues by providing quantitative methods to more accurately forecast the fatigue life of asphalt pavements in Oregon. This research study developed testing methods and procedures to ensure that agencies can use high amounts of recycled material in their asphalt mixes reliably, without running the risk of premature failure, costly excess maintenance and reduced user comfort due to high pavement roughness. This will create monetary savings for agencies in the long-run while also encouraging a greater degree of sustainability in the industry.

1.1 KEY OBJECTIVES OF THIS STUDY

The main objectives of this study are to:

- Compare the results of direct tension cyclic fatigue (DTCF), indirect tension (IDT), semi-circular bending (SCB) and bending beam fatigue (BBF) tests using various energy and fatigue life parameters to determine how well they agree;
- Determine the effectiveness of all evaluated testing methods in identifying the in-situ cracking performance of pavements with different mixture properties;
- Select the best cracking experiment by considering testing time, cost, efficiency, complexity and practicality for use in district and contractor laboratories in Oregon;
- Determine the effect of mixing (laboratory and plant mixing) and compaction method (field roller compaction and laboratory gyratory compaction) on the results of the selected cracking experiment;
- Determine the effects of gradation, binder content, air void content (density) and binder type (PG70-22 versus PG70-22ER binder) on the cracking resistance of asphalt mixtures;
- Determine the cracking performance of asphalt mixtures with higher dust contents;

- Determine whether the long-term aging process has any impact on cracking performance ranking of asphalt mixtures; and
- Develop mechanistic-empirical (ME) pavement design models and conduct life-cycle cost analyses to determine cost and performance effectiveness of asphalt mixtures with varying properties.

1.2 ORGANIZATION OF THE REPORT

This report is organized as follows:

- This introductory chapter is followed by the literature review.
- Implementation of performance tester to evaluate cracking resistance of asphalt mixtures are discussed in Chapter 3.0.
- Chapter 4.0 presents the impacts of various mixture properties on cracking and rutting resistance of asphalt mixtures.
- The impact of dust content and dust-to-binder ratio on cracking and rutting performance of asphalt mixtures is discussed in Chapter 5.0.
- Chapter 6.0 discusses the impact of asphalt aging on mixture cracking performance prediction.
- Chapter 7.0 presents the results of the mechanistic-empirical pavement design guide (MEPDG) simulations and life cycle cost analysis conducted to determine the cost and performance effectiveness of asphalt mixtures tested in Chapter 4.0.
- Finally, Chapter 8.0 presents the conclusions, summary of the work and recommendations.

2.0 LITERATURE REVIEW

2.1 FATIGUE CRACKING MECHANISMS IN ASPHALT PAVEMENTS

It has been established that cracking is the major cause of premature failure in hot-mix asphalt concrete (HMAC), and fatigue cracking is one of the main modes of failure associated with HMAC cracking (Birgisson et al. 2002). Asphalt concrete fatigue cracking has also been accepted to be a major distress mode in Oregon (ODOT 2013). Oregon Department of Transportation (ODOT)'s Pavement Management system has shown that mixes placed in the last 20 years have had a tendency to develop premature cracking after 6 to 8 years of service life before reaching the structural design life of 15 years.

Historically, fatigue cracking was assumed to initiate only at the bottom of asphalt layer and propagate to the surface (bottom-up cracking). The initiation of bottom-up fatigue cracking is due to the bending action of the pavement layer that leads to tensile stress development at the bottom of the asphalt layer. Thus, generally, bottom-up cracking is a result of structural design problems. Recently, it has been determined that fatigue cracking may also initiate from the surface of the asphalt layer and propagate to the bottom (top-down cracking) (Witczak et al. 2004). The widespread nature of top-down cracking in Oregon suggests that it is a general mix design issue and not a specific project related problem. The increased use of recycled asphalt pavement (RAP) and recycled asphalt shingle (RAS) in surface mixes in Oregon might have increased the occurrence of top-down cracking. Taking cores and trenched sections are the only ways to identify the initiation point of cracking in order to see whether the cracking is bottom-up or top-down (Williams and Shaidur 2015).

High surface tensile stresses for thin asphalt concrete layers and high near tire shear induced tension for thick structures are accepted to be the major causes of top-down cracking (Roque et al. 2010). Large truck loads, aging, low upper layer stiffness, surface mixes with high RAP/RAS contents, and high surface air-void content have been identified as possible causes. Moreover, thermal stresses and moisture are influential in propagating cracks. This distress type cannot be explained by traditional fatigue cracking models since crack initiation and propagation mechanisms for top-down cracking are different from traditional bending related bottom-up cracking. Wambura et al. (1999) investigated the primary reason for initiation of top-down fatigue cracking and concluded that oxidation and age hardening of the top few millimeters of the asphalt concrete surface course is the major reason for top-down fatigue crack initiation. The high surface tensile strain due to heavy wheel loads accompanied with thermally induced strain can be large enough to crack the brittle surface of an age-hardened HMAC surface. For this reason, top-down cracking can occur in structurally well-designed thick asphalt concrete pavements within 3 to 8 years of paving (Uhlmeier et al. 2000).

2.2 FACTORS AFFECTING FATIGUE CRACKING

2.2.1 Air-Void and Binder Content

Air-void and binder content are the two major factors affecting fatigue cracking performance of asphalt mixtures. For equal compaction effort, higher binder content tends to reduce air-void content of the mix resulting in an increase in mix density. Although increasing mix binder content can be accepted to be a viable strategy for increasing asphalt mix fatigue life, increased binder content tends to create a softer mix with lower rutting resistance. In addition, increasing binder content increases the unit cost of the mix.

Hu et al. (2011) investigated several variables that influence the cracking performance of asphalt concrete (Hu et al. 2011). The main objective of this study was to estimate the optimum binder contents for different types of mixtures. Texas A&M Transportation Institute (TTI) Overlay Tester (OT) was used to determine the cracking resistance of HMAC mixtures. Corresponding predictive models were developed (Equations 2.1 and 2.2) and were used to determine the minimum binder content.

$$N_{OT} = a_1 \exp(a_2 \times FT) SA^{a_3} \quad (2.1)$$

Where,

- N_{OT} = Fatigue life (number of repetitions)
 FT = film thickness (μm),
 SA = surface area of the aggregate particles (m^2/kg), and
 a_{1-3} = regression coefficients.

$$FT = \frac{\frac{P_{be}}{G_b}}{SA \times P_s} \times 1000 \quad (2.2)$$

Where,

- P_b = binder content (%), by total mass of mixture,
 P_{be} = effective binder content (%), by total mass of mixture,
 P_{be}/G_b = effective volume of asphalt binder, and
 P_s = aggregate content ($100 - P_b$) (%), by total mass of mixture.

Nine test sections, which comprised of three HMAC mixtures and three types of aggregates, on Interstate 20 near Atlanta, Texas were evaluated in this study. It was observed that in all the test sections, cracking developed within 1 year of service. These test sections were used to evaluate the developed models (Equations 2.1 and 2.2) and it was concluded that binder contents of the cracked sections determined by conventional mix design methods were much lower than the binder contents recommended for meeting the cracking resistance requirement (Table 2.1).

Table 2.1: Asphalt Mixture Information on I-20 Experimental Sections (Hu et al. 2011)

Section No.	Mixture Type	Aggregate Type	In-Place		Asphalt Absorption (%)	Minimum Recommended Asphalt Content (%)
			SA (m ³ /kg)	AC (%)		
1	Superpave C	Gravel	5.25	4.55	0.35	5.67
2		Sandstone	7.24	4.90	1.37	7.00
3		Quartzite	6.88	5.10	0.63	6.30
4	CMHB C	Gravel	6.48	4.70	0.35	6.00
5		Sandstone	7.04	4.57	1.37	7.00
6		Quartzite	5.45	4.77	0.63	5.99
7	Type C	Gravel	6.84	4.08	0.35	6.07
8		Sandstone	8.17	4.76	1.37	7.12
9		Quartzite	7.04	4.70	0.63	6.35

NOTE: CMHB = coarse matrix high binder.

Williams and Shaidur (2015) investigated the causes of early-age cracking on Oregon highways. The aim of this study was to come up with modifications to the current mix design guidelines practiced in Oregon State. This study recommended increasing the percent G_{mm} to 92% to reduce in-situ air voids below 6% in order to increase the density of the mix and increase resistance to cracking. It was further suggested that reducing design air-void content from 4% to 3.5% would increase the design binder content of mixes by about 0.25%, which in turn is assumed to increase the cracking resistance of the mixture.

Using controlled-strain bending beam fatigue (BBF) test with two strain levels (150 and 300 microstrains), Harvey and Tsai (1996) showed that there is considerable correlation between the fatigue life of the asphalt concrete mix and strain level, air void content, and binder content. One aggregate type, five different binder contents (4% to 6%), and three different air void contents (1 to 3%, 4 to 6%, and 7 to 9%) were selected for preparing asphalt mixtures. Results of this study showed that fatigue life increases with decreasing air void content and increasing binder content. Reduction in air void content from 8 to 5 percent leads to a 100 to 200 percent increase in fatigue life. Likewise, 0.5% increase in binder content resulted in a 10 to 20 percent increase in overlay fatigue life (See Figure 2.1 and Figure 2.2).

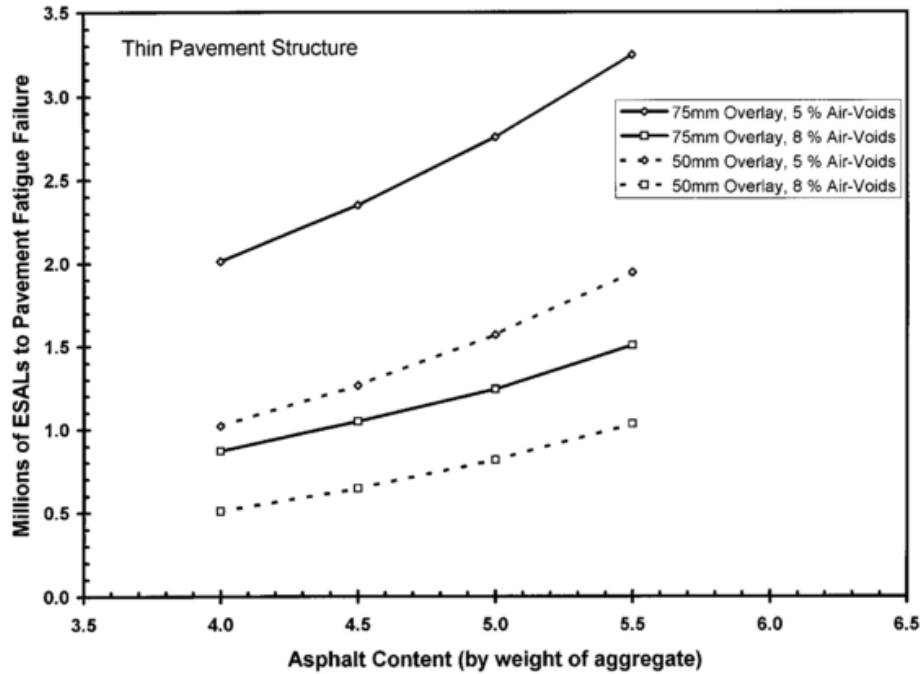


Figure 2.1: Predicted pavement fatigue life versus air void content and binder content for conventional overlays of thin structure (Harvey and Tsai 1996).

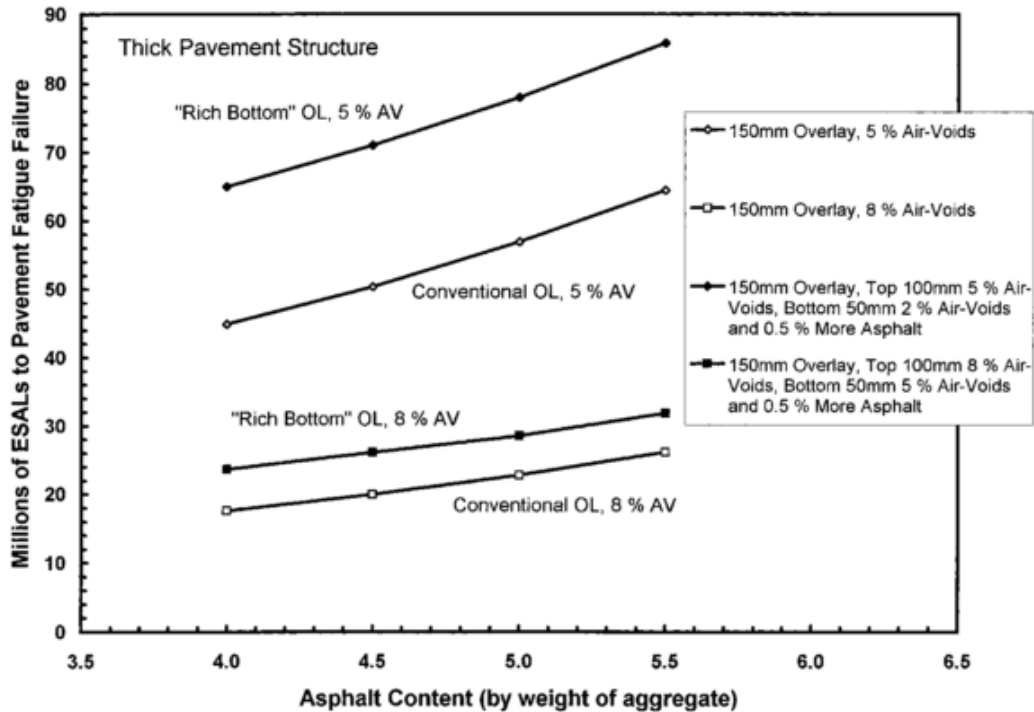


Figure 2.2: Predicted pavement fatigue life versus air void content and binder content for conventional and "rich bottom overlays" of thick structure (Harvey and Tsai 1996).

After a rehabilitation project in a section of I-25 north of Denver with milling and refilling existing surface with new hot mix asphalt, cracking started to appear in the driving lanes after 1 year. In order to investigate the reason for early-age cracking, 28 sites were evaluated from a wide geographic area of Colorado. Results of the study suggested that majority of top-down cracking is a result of the segregation in the upper pavement lift (Figure 2.3). Harmelink et al. (2008) showed that increasing the binder content could create a reduction in segregation and consequently reduce top-down cracking occurrence. This study suggested increasing the binder content in the mix design process by decreasing the number of design gyrations as a function of traffic volume.

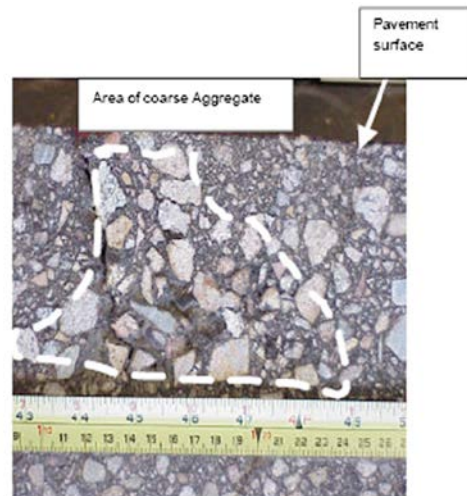


Figure 2.3: Segregation and cracking (Harmelink et al. 2008).

2.2.2 Binder Modification

Over the past couple decades, agencies started to use modified asphalt binders more frequently to reduce amount and severity of rutting and cracking on highways. Although binder modification increases the initial cost of the constructed sections, increased service life can significantly reduce life cycle costs.

Polymers are the most commonly used modifiers. The two major polymer types are elastomers and plastomers. Styrene-Butadiene-Styrene (SBS) is the most frequently used elastomer while crumb rubber is also another elastomer made from discarded tires (Walker 2014). Crumb rubber can be considered as a sustainable engineering material because it reduces tire stockpiles that otherwise mostly go into landfill (Gauff 2010). Rubber modified asphalt is often used as a superior mix for resisting reflective cracking in California when used as the uppermost structural layer. However, Caltrans does not permit rubber modified asphalt to be placed thicker than 60 mm (2.4 inches) based on perceived risk of rutting of the asphalt mix (Coleri et al. 2012).

Bahia et al. (2001) conducted a research on evaluating the efficiency of the Superpave intermediate temperature requirement ($G^*\sin \delta \leq 5000$ kPa) using flexural beam fatigue tests on a combination of two aggregate types (gravel and limestone) and two gradations (coarse and fine) with nine modified asphalt binders. The test temperature was selected for each mixture was

based on the intermediate temperature requirement where the $G^* \sin \delta$ is equal to 5000 kPa under a 10 Hz sinusoidal load with a peak-to-peak strain of 800 $\mu\epsilon$. This study showed that modified asphalt mixtures with PG 82-22 asphalt binder and SBS modifier had fatigue life as two to five times greater than unmodified mixtures with PG 82-22 asphalt binders. Mixtures with elastomeric modified asphalt binders with the same aggregate type showed higher fatigue life compared to other types of binders used in this study.

Raad et al. (2001) have investigated the role of aging on rubberized gap-graded and conventional dense-graded asphalt mixes using beam specimens extracted from a 10-year-old highway section in southern California. For this study, controlled-strain fatigue beam tests were conducted to evaluate the stiffness and fatigue performance of the specimens at two different temperatures (22°C and -2°C). Results indicated longer fatigue lives for rubberized gap-graded asphalt mixes than conventional dense-graded asphalt mixes for both aged and unaged specimens.

Bonnetti et al. (2002) evaluated the effect of binder modifiers on the fatigue cracking performance using cumulative dissipated energy ratio concept (Ghuzlan and Carpenter 2000). Time sweep binder fatigue tests were conducted with five modified asphalts and two base binders. N_{p20} value, *number of cycles at which the dissipated energy ratio shows 20% deviation from the no-damage ratio*, was used to illustrate the failure condition. In general, modified asphalt binders showed longer fatigue lives than unmodified binders. Elastomeric modifiers such as styrene-butadiene-styrene (SBS) of PG 82-22 and styrene-butadiene (SB) cross-linked of PG 58-40 represented better fatigue performance than the aged PG 76-22 mix and PG 76-22 rubber modified asphalt. Moreover, asphalt binder type was influential in fatigue behavior due to the different chemical compositions of the binders.

Based on the previous studies, it can be concluded that laboratory fatigue performances of polymer modified asphalt mixtures were higher than the laboratory fatigue performances of mixtures with unmodified asphalt binders. In general, polymer modified asphalt mixtures have fatigue lives greater than unmodified asphalt mixtures (some reported cases even showed an order of magnitude higher fatigue lives). The fatigue performances of modified mixes are highly influenced by the base asphalt binder used in the mixture (Prowell et al. 2010).

2.2.3 Aging

Asphalt aging occurs during production, construction, and service life of the mixtures. It is a critical factor in evaluating the cracking performance of pavement systems. The aging of asphalt mixtures is mostly affected by the aging of asphalt binder (Bell and Sosnovske 1994). Aging of asphalt binder associated with the oxidation of the binder is a major factor affecting the fatigue performance of asphalt mixtures. As the aromatic compounds in asphalt binders are oxidized, more polar carbonyl compounds are created which results in increased elastic modulus and viscosity, in other words, stiffening of the binder (Glover et al. 2005).

Baek et al. (2012) have investigated the effects of aging on linear viscoelastic response (LVE) and damage characteristics. Four different aging levels were selected (short term aging, and long term aging level 1 to level 3). It was indicated that aging was a significant factor in the damage

growth. They also stated that aging influences the distribution of stress and the way damage is accumulated throughout the pavement structure.

Study conducted by Isola et al. (2014) evaluated laboratory aging methods to simulate the change in asphalt mixture properties in the field. Two aging procedures were used in this study: 1) heat oxidation conditioning (HOC), and 2) cyclic pore pressure conditioning (CPPC) for inducement of moisture related damage. For short-term and long-term aging simulation, standard short-term oven aging (STOA) and long-term oven aging (LTOA) procedures were used (Bell et al. 1994). Three asphalt mixtures (lime-treated granite mixture, granite mixture, and limestone mixture) were produced for Superpave IDT testing (indirect tensile test) for four conditioning levels (STOA, STOA plus CPPC, LTOA, LTOA plus CPPC). It was concluded that oxidative aging causes the reduction of fracture energy¹ (total energy necessary for fracture inducement) and consequently, stiffening and embrittling mixtures. CPPC created effectively generated additional damage and more reduction in fracture energy (FE) and made the aging process more compatible with the damage observed in the field.

Arega et al. (2013) conducted research on evaluating the fatigue cracking resistance of short-term and long-term aged asphalt mortars with fine aggregate matrix (FAM) and warm mix additives. Two different binders (PG76-28 and PG64-22) with four additives and one aggregate type were tested using dynamic mechanical analyzer (DMA) for this study. Fatigue cracking resistance of specimens were measured before and after long term aging. For short term aging, mortars were aged as a loose mix for four hours at 60°C. Then, one batch was compacted with the Superpave Gyratory Compactor (SGC), and other batch was further aged for 30 days in the same environment to simulate long term aging. Stiffness and fatigue life of FAM are illustrated in Figure 2.4 and Figure 2.5, respectively. It can be observed that short-term aged mixtures have lower stiffness (G^*) with longer fatigue life compared to long-term aged mixtures. However, fatigue resistance rankings of mixtures with and without long-term aging were determined to be the same.

¹ FE is the total energy necessary for fracture inducement, and it shows the fracture tolerance of the mixture, therefore, represents the cracking performance of the mixture (Roque et al. 2011).

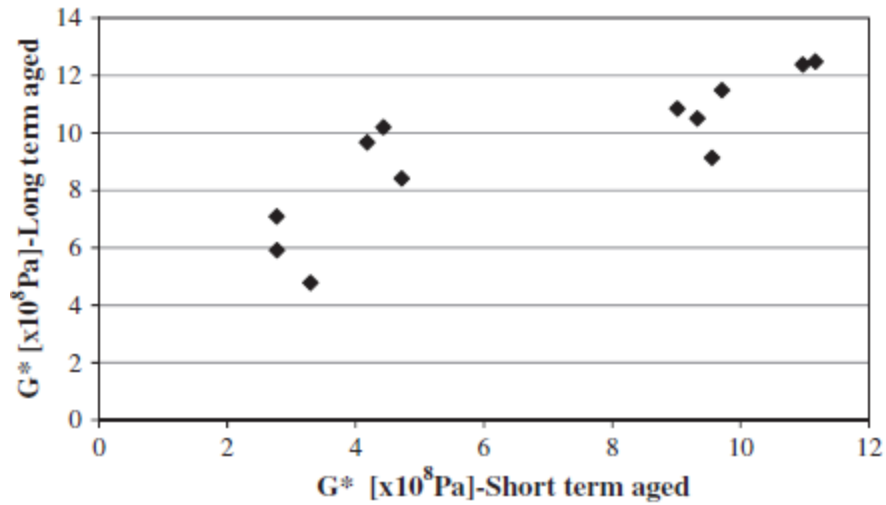


Figure 2.4: Comparison of G^* (shear modulus) before aging and after long-term aging for the different FAM specimens (Arega et al. 2013).

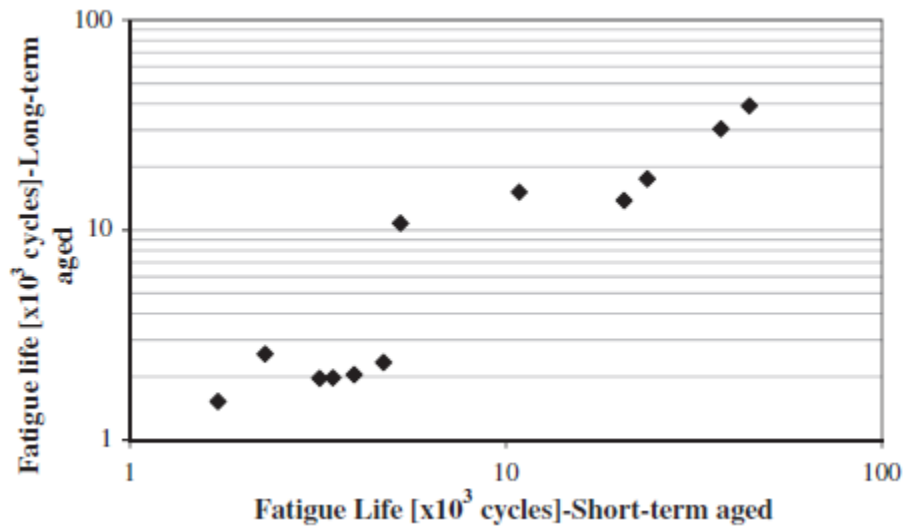


Figure 2.5: Comparison of fatigue life before and after long-term aging for FAM specimens (Arega et al. 2013).

2.2.4 Binder Performance Grade

Performance grading is based on the idea that properties of asphalt binder for a specific road construction should be selected by considering physical and environmental conditions (Kim 2009). Superpave performance grading system follows the same logic as the older penetration and viscosity based grading systems while the relationship between binder properties and

conditions of use are more accurately specified. Several studies in the literature focused on investigating the impact of performance grade and binder stiffness on cracking performance.

Study carried out by Li et al. (2008) investigated the effect of binder grade and reclaimed asphalt pavement (RAP) on the characteristics of asphalt mixtures. In this study, ten different mixtures with two RAP sources, three RAP percentages (0%, 20%, and 40%), two binder grades (PG 58-28 and PG 58-34) were tested by dynamic modulus and semi-circular bend fracture testing (SCB) at different temperatures. Dynamic modulus and fracture energy, representing the fatigue performance and cracking resistance of mixtures (Kandhal et al. 1995, Roque et al. 2011), were measured for all the asphalt mixtures. Specimens with PG 58-28 asphalt binders had higher dynamic modulus (for mixes with and without RAP) values than the PG 58-34 mixes. Additionally, specimens with PG 58-34 asphalt binders showed higher fracture resistance at low temperatures.

Williams and Shaidur (2015) conducted a study on ten highway sections (six with top-down cracking and four without top-down cracking) in Oregon to investigate the possible reasons for early-age cracking. Ten cores from cracked sections and five cores from non-cracked section were taken for laboratory testing. Falling weight deflectometer (FWD) and dynamic cone penetrometer (DCP) tests were conducted to evaluate the pavement structure soundness. Dynamic modulus and indirect tensile strength (IDT) tests were conducted with the specimens extracted from the field. Moreover, binders were extracted and recovered from the cores and tested with dynamic shear rheometer and bending beam rheometer to determine their actual performance grades. Results showed that sections with top-down cracking did not have any structural problems and density variations in the base layer. However, cracked sections had higher dynamic modulus, stiffer binder (with higher complex shear modulus), and lower indirect tensile strength than the sections without cracking. The change in binder performance grades over time due to binder aging resulted in a more brittle mix at the surface of the pavement that is more prone to top-down cracking.

In order to investigate the sensitivity of mixture properties to binders from different suppliers with same PG grades, Kaloush et al. (2012) conducted dynamic modulus and flow number tests with four asphalt mixes prepared by using binders from four different suppliers in Arizona with the same PG grades (PG 76-16) and aggregate gradations. Results of the analyses showed that the differences in measured mixture properties for the four mixes were statistically significant. This result suggests that between-supplier variability can be an important factor affecting the quality of the asphalt mixes.

2.2.5 Mixture Segregation

Asphalt mixture segregation occurs when coarse and fine aggregates are not uniformly distributed in different parts of the mixture. This phenomenon increases the moisture and air permeability of the mixture and creates local weak spots within the asphalt concrete microstructure, and consequently causes distresses including raveling, cracking, or moisture damage. There are various factors inducing segregation such as mixture design (mostly binder content and gradation), stockpiling and handling, and surge and storage silos (Kennedy et al. 1987). Asphalt mix production and construction related segregation results in non-uniform

asphalt mixes with gradations and binder contents different from the original design mixtures (Brock 1986).

Using laboratory bending beam fatigue (BBF) testing, Khedaywi and White (1996) have conducted a laboratory study to evaluate the effect of segregation on fatigue performance of asphalt concrete mixtures. Five different mixtures with various segregation levels (ranging from fine side of the mix design to the coarse side) were prepared for this study: 1) very fine, 2) fine, 3) control mix, 4) coarse, and 5) very coarse. Control mix with median gradation and 4.5 percent binder content was prepared. Control mix was sieved over the 3/8 inch sieve to prepare a highly segregated asphalt mix. Materials remaining on the sieve were considered as very coarse mixtures. Likewise, materials passing through the sieve were used to prepare very fine asphalt mixes. Then, coarse and fine mixtures were prepared by blending specific percentages of very coarse and fine materials. BBF tests were conducted with prepared beam samples (representing intermediate level of segregation). Since standard beam dimensions are used to prepare samples for all 5 gradations, mixes with coarser gradations appear to have more segregation than the mixes with finer gradations. The number of repetitions required to reach 50 percent reduction in initial stiffness was used as the fatigue life. Coarsely segregated asphalt mixes with lower asphalt binder showed shorter fatigue lives. On the other hand, the more finely segregated asphalt mixture with higher binder content had longer fatigue life. On the other hand, mixtures with lower percentage of coarse aggregates and high binder content showed more susceptibility to rutting. Figure 2.6 illustrates the relationship between fatigue life of asphalt concrete mixes and segregation. It can be observed that fatigue lives increased from mix 5 to 1 (very finely segregated mix having the longest fatigue life) for a specific strain level.

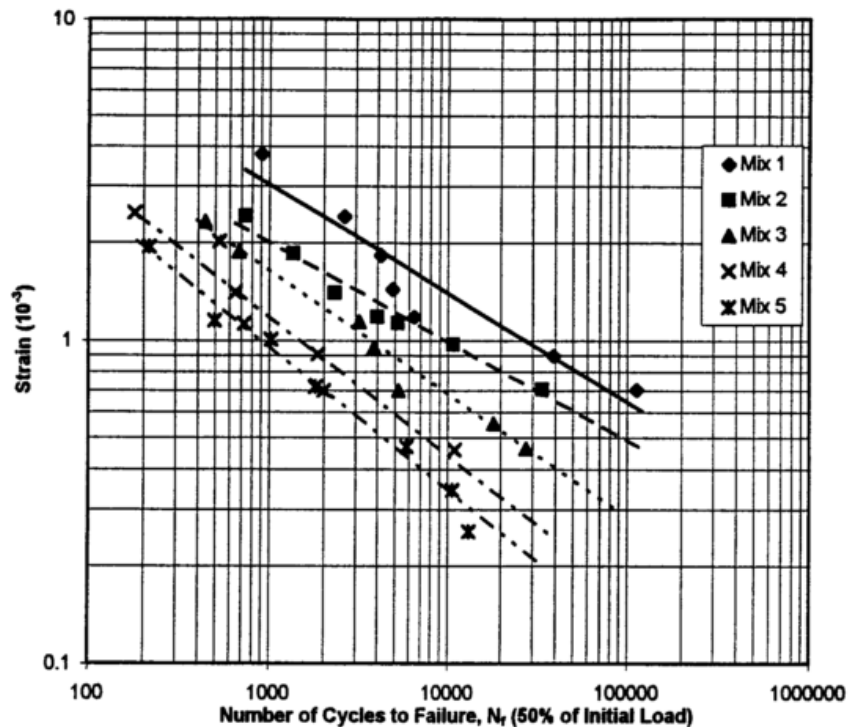


Figure 2.6: Strain versus number of cycles to failure (50 percent of initial load) (Khedaywi and White 1996).

De Freitas et al. (2005) simulated in-situ segregation by accumulating coarse aggregates at the top of the asphalt layer and fine aggregates at the lower part of the wearing course. Using accelerated wheel-tracking device at 3 different temperatures (30°C, 40°C, and 50°C), they observed that cracks were limited to the parts with coarse aggregates at the top and did not propagate to the fine-graded layers.

Schorsch et al. (2003) evaluated the effects of segregation on crack initiation and propagation using laboratory and field investigations. It was concluded that top-down cracks initiated from highly segregated spots and propagated through other areas with various degrees of segregation. Service life of the pavement decreased about 50% due to segregation-related longitudinal cracks (Chang et al. 2001). Using nuclear density measurements, it was determined that non-segregated areas had higher densities than segregated areas. They collected cores from field sections to measure specific gravity, air void content, density, and gradation in order to evaluate the degrees of segregation determined by nuclear density measurements. Degrees of segregation were categorized into heavy, medium, and light segregated areas. Conducting indirect tensile strength tests, they concluded that average tensile strengths of non-segregated specimens were two times higher than the average tensile strengths for the segregated specimens, which resulted in longer fatigue lives for non-segregated mixtures. Moreover, it was also observed that segregated cores had higher air void contents (average of 3.8% for non-segregation cores and 6.1% for segregated cores) and lower specific gravities than non-segregated specimens.

2.2.6 Aggregate Gradation and Volumetrics

Gradation, shape, texture, and angularity are the major aggregate properties affecting cracking performance of asphalt mixtures. Nominal maximum aggregate size (NMAS), *the largest sieve that retains some of the aggregates (generally not more than 10 percent by weight)*, is generally used as a parameter to specify the size distribution of aggregates in an asphalt mix. Gradation curves are also used to more accurately quantify the differences between different aggregate size distributions. The impact of aggregate gradations on mixture volumetrics and cracking performance should be investigated to determine optimum gradations that can be used to develop more durable asphalt mixes. Most of the studies in the literature suggested that adequate balance between volumetric characteristics of mixtures and the amount of raw materials (binder, aggregate, filler, and additives) is crucial for a proper mix design.

Using accelerated wheel-tracking device and 3-D nonlinear viscoelastic finite element modeling, De Freitas et al. (2005) prepared and examined 17 asphalt bituminous slabs with granite aggregates and limestone fillers. Three different gradations were selected for asphalt mixture preparation namely fine graded, coarse graded, and an average grading mixture. Mixture with coarse gradations showed earlier crack initiation than the fine-graded mixtures, especially at higher test temperatures.

Using Bailey method of gradation analysis, Khosla and Sadasivam (2005) determined the optimum gradation resistant to permeability, rutting, and fatigue cracking. 12 mixtures (6 with 12.5 mm and 6 with 9.5 mm nominal maximum size) were tested by FSCH (frequency sweep at constant height) test to evaluate fatigue performance at 20°C. Fatigue lives of the mixtures were assumed to correspond to 50 percent reduction in mixture stiffness. Results showed that both

12.5 mm and 9.5 mm NMA, mixtures with low permeability tended to have longer fatigue lives than the mixtures with high permeability. It was concluded that higher fraction of #4 (4.75 mm) aggregate size increases permeability. Therefore, an upper limit of 25% for #4 size aggregates was specified. Moreover, the inclusion of higher fraction of 3/8" and 1/2" aggregates with #8 (2.36 mm) and #16 (1.18 mm) size aggregates reduced the permeability of mixtures and resulted in mixtures with greater fatigue performance.

Sousa et al. (1998) investigated the effect of aggregate gradation on fatigue performance of asphalt concrete mixes using four-bending fatigue tests. Nine different aggregate gradations with nominal maximum aggregate sizes of 19 mm, 25 mm, and 12.5 mm with 100 percent crushed aggregates were selected for this study. Asphalt mixes were prepared by using two binder grades (PG 58-16 and PG 64-16). This study compared the gradation requirements proposed by Superpave volumetric mix design method with other gradations passing through and above the restricted zone, which met the California Department of Transportation, Arizona Department of Transportation, French, and Portuguese Standard grading specifications. All the fatigue tests were conducted at 20 °C using a sinusoidal wave with a frequency of 10 Hz. Results demonstrated that increasing binder content reduced fatigue lives. Since all the mixtures had 7 percent air voids, this trend was attributed to the lower compaction effort required for mixtures with high binder content. In general, fine gradations (passing through and above the restricted zone) tended to have better fatigue performance than gradations below the restricted zone. Brittle nature of mixtures with higher amount of large aggregates passing below the restricted zone led to lower fatigue performance.

Results of WesTrack experiments showed that bottom-up crack propagation was faster in coarse-graded aggregate mixes than fine and fine-plus mixes but crack initiation took longer time to occur in coarse mixes than mixes with fine and fine-plus gradations (Tsai et al. 2002). Fine-plus mixtures also showed greater fatigue cracking resistance than fine-graded mixes with equal air-void contents.

Using the data from the WesTrack project, Pellinen et al. (2004) compared existing fatigue models and pointed out the strong correlation between fatigue performance of asphalt mixtures and volumetric properties. VFA^2 (voids filled with asphalt) was the main volumetric characteristic correlated with measured cracking in the WesTrack study. Pellinen et al. (2004) suggested that mixtures with 53% VFA, V_{beff} (effective binder content) > 9%, air void content < 6%, and VMA^3 (void in the mineral aggregate) < 14% were mostly resistant to cracking.

Daniel and Lachance (2005) prepared mixtures with 0%, 15%, 25%, and 40% RAP contents to evaluate the effects of RAP content on volumetric and mechanistic properties of asphalt mixtures. Dynamic modulus, creep compliance, and creep flow tests were conducted with specimens with different RAP contents. Results showed that VMA and VFA increased with increasing RAP content (25% and 40%). Increased VFA and VMA, higher binder content, and finer gradation for mixtures with 25% and 40% RAP led to unexpected trends in the test results. Specimen with 15% RAP had higher dynamic modulus and lower compliance compared to

²VFA: The portion of the voids in the mineral aggregate that contain asphalt binder.

³VMA: The volume of intergranular void space between the aggregate particles of a compacted paving mixture that includes the air voids and the effective binder content, expressed as a percent of the total volume of the specimen.

specimens without RAP (more resistance to rutting with lower fatigue life). On the other hand, mixtures with 25% and 40% RAP had dynamic modulus and lower compliance close to the mixture with no RAP. It was concluded that this unexpected trend was a result of the higher binder content, finer gradation, and higher VFA and VMA of mixtures containing 25% and 40% RAP compared with the control mix and 15% RAP mixture.

Using unconfined dynamic modulus and triaxial shear strength tests, Pellinen (2003) determined that decreasing VMA from 23% to 11% by keeping the effective binder content (V_{beff}) constant at 7.5% could increase the stiffness to the same extent as increasing the binder grade from PG 58 to PG 76. Moreover, they concluded that mechanical performance of the mixture was highly correlated with VMA and VFA.

2.2.7 Aggregate Type

Several studies in the literature focused on investigating the impact of aggregate type on cracking performance. Hu et. al (2011) prepared asphalt mixes with hard limestone, medium limestone, soft limestone, quartzite, sandstone, gravel, and granite to evaluate the impact of aggregate type on cracking resistance. TTI Overlay tester is used to evaluate the cracking performance of prepared asphalt mixes. Results of the analyses showed that asphalt binder grade, asphalt absorption, and asphalt film thickness are the major factors affecting cracking performance while aggregate type had a minor effect.

Using the results of several studies in the literature, Tangella et al. (1990) prepared a summary of factors influencing the fatigue life including binder stiffness, air void content, binder content, aggregate gradation, and aggregate type. It was concluded that the effects of binder stiffness and air void content on cracking performance are more significant than all other factors. In addition, it was concluded that aggregate type had less impact on fatigue response of asphalt mixes than all other contributing factors.

Using flexural beam fatigue test, Bahia et al. (2001) investigated the accuracy of intermediate temperature requirement ($G^* \sin \delta \leq 5000$ kPa). This study included combination of two aggregate types (gravel and limestone), two gradations (coarse and fine), and nine asphalt modifiers. Results showed that mixtures with fine-graded limestone aggregates have shorter fatigue lives than coarse-graded mixes. However, mixtures with gravel aggregates represented the opposite trend, greater fatigue life for fine gradations than coarse gradations. The results of this study showed that the effects of binder grade, binder content, and modification on fatigue performance are significantly higher than the influence of aggregate type.

2.3 TEST METHODS TO EVALUATE FATIGUE CRACKING PERFORMANCE OF ASPHALT CONCRETE

High surface tensile stresses for asphalt concrete layers (top-down), high near tire shear induced tension for thick structures (top-down), and high bending stresses at the bottom of the asphalt concrete layers (bottom-up) are the major causes of cracking (Roque et al. 2010). Several researchers have come up with test procedures to evaluate fatigue cracking performance of

asphalt concrete (Tayebali et al. 1992, Lee et al. 2000, Roque et al. 2002, Wu et al. 2005, Kim et al. 2008, Lou et al. 2013). However, it is difficult to come up with a single test method for all conditions since variable material properties, design, traffic, and climate create several different cracking failure mechanisms. In this study, bending beam fatigue (BBF), indirect tension (IDT), repeated direct tension (RDT), simplified viscoelastic continuum damage (S-VECD), and semi-circular bend (SCB) tests are the experiments investigated in order to understand the applicability of these test procedures to be used for mix and structural design in Oregon. The test procedures based on previous studies and standards are presented in the following sections.

2.3.1 Bending Beam Fatigue (BBF)

In a simple flexure test, a uniaxial tensile bending, which simulates the fatigue damage that originates at the bottom of an asphalt layer, is created within the specimen. Hence, these tests are most commonly used to obtain bottom-up fatigue cracking data (Monismith 1981). With the invent of servo hydraulic and computer controlled pneumatic loading systems, the three-point and the four-point bend tests have become very popular. Four-point bend tests are preferred as they simulate crack initiation in an area of stress between two loads (Hartman et al. 2004). This test follows AASHTO T321-07 (2007) standard. In this test, the failure point (fatigue life) is defined as the load cycle at which the specimen undergoes a 50 percent reduction in its original (initial) stiffness.

In this test, 380 mm long by 50 mm thick by 63 mm wide HMA beam specimens obtained from laboratory or field compacted HMA are subjected to flexural bending until failure. A metal block is epoxied to the neutral axis of beam specimen. The specimen is then placed in an environmental chamber maintained at $20.0 \pm 0.5^{\circ}\text{C}$ for 2 hours to ensure the specimen is at the pre-selected temperature prior to testing. The linear variable differential transducer (LVDT) is attached to the specimen by screwing it onto the metal block epoxied on the specimen (Figure 2.7) and the target initial strain (250 – 750 $\mu\epsilon$) and loading frequency are selected. The loading frequency is set within a range of 5 to 10 Hz. Then, 50 load cycles are applied at a constant strain of 250 to 750 $\mu\epsilon$. The specimen stiffness at the 50th load cycle will be the initial stiffness, which will be used as a reference for determining specimen failure. The selected strain level should be low enough so that at least 10,000 load cycles can be applied to the specimen before its stiffness is reduced to 50 percent of its original value. Test results are continuously monitored and recorded and the test is terminated when the specimen has experienced more than 50 percent reduction in stiffness.

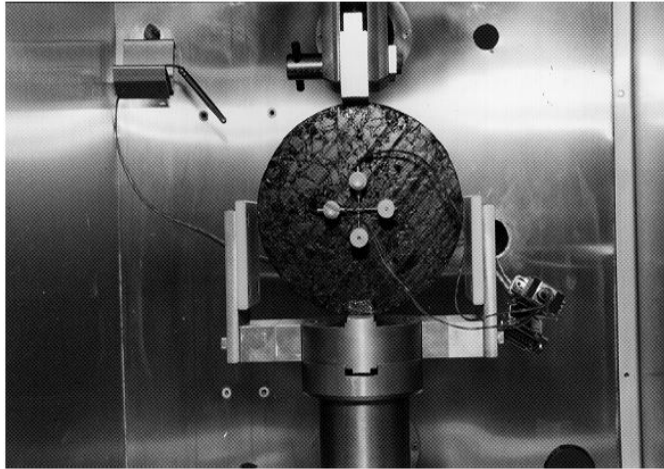


Figure 2.7: Four-point bend testing system (Source: www.pavementinteractive.org).

2.3.2 Indirect Tension (IDT)

Superpave Indirect Tension (IDT) test was developed as a part of Strategic Highway Research Program (SHRP) to evaluate thermal cracking. University of Florida further evaluated and improved IDT for use in evaluation of fatigue cracking (Roque et al. 2002). The main aim of the study was to use the IDT to understand the crack initiation and propagation in asphalt mixtures and to identify the key mixture properties that control cracking performance of different mix types. In this study, field cores from eight sections, two Superpave coarse mixtures and two Superpave fine mixtures were used. Tested specimens had a diameter of 150 mm and a thickness of 25 mm. The test was performed at 10°C with a constant haversine load of 0.1 second and a rest period of 0.9 second. Two horizontal and two vertical displacement measurements, load and the corresponding time were recorded until failure. The test setup is shown in the Figure 2.8a. It was observed that there were some inconsistencies between the laboratory-measured and field crack growth rates indicating that the mechanisms used to induce cracks in the laboratory are different from the field. Based on these observations, the following conclusions were made:

- Total fracture energy (FE_f) and the dissipated creep strain energy to failure ($DCSE_f$) are the two material properties that are easily obtained from the Superpave IDT.
- These properties can be used to evaluate and control fracture for any loading conditions such as stress-controlled, strain-controlled, and repeated loading.



(a)



(b)

Figure 2.8: (a) Superpave Indirect Tension Test (IDT) with LVDT mounted on the sample (Roque et al. 2002); (b) IDT with LVDT mounted around the sample (Newcomb et al. 2015).

This test can also be conducted by using two LVDTs around the sample as shown in the Figure 2.8b. A round robin study was carried out between Texas A&M Transportation Institute (TTI), National Center for Asphalt Technology (NCAT), and University of California Pavement Research Center (UCPRC) to check the variability and bias of the measured resilient modulus between different laboratories (Newcomb et al. 2015). NCAT and TTI used the LVDTs around the specimen (Figure 2.8b) while UCPRC used LVDTs on the sample (Figure 2.8a) (ASTM D7369). It was observed that the differences in measured resilient modulus from these three laboratories were not statistically significant.

2.3.3 Repeated Direct Tension

The repeated direct tension (RDT) test has been used to evaluate tensile properties of asphalt mixtures and to assess the development of fatigue cracking under repeated loading (Bolzan and Huber 1993). Luo et al. (2013) carried out a study to characterize asphalt mixtures using controlled-strain repeated direct tension test. The main aim of the study was to develop an energy-based mechanistic approach to characterize the fatigue damage in asphalt mixtures. The asphalt mixtures used in this study were laboratory-mixed and compacted with an unmodified asphalt binder and a common Texas limestone with a Type C dense aggregate gradation (TxDOT 2004). Superpave gyratory compacted specimens were cored to produce specimens with a diameter of 102 mm and a height of 102 mm. The total air void was controlled at $3.5 \pm 0.5\%$. The controlled strain RDT test was conducted using a servo-hydraulic system at 20°C. The specimens were glued to a pair of end caps and were kept in the system for conditioning. Three axial linear variable differential transducers (LVDTs) were mounted on the specimen to capture the axial deformation of the specimen. The test setup is shown in Figure 2.9. Two RDT tests were performed on the same specimen which included: a non-destructive test with 200 load cycles and a maximum axial strain of 40 $\mu\epsilon$; and a destructive RDT test with 1000 load cycles

and a maximum axial strain of $200\ \mu\epsilon$. The loading frequency was 1 Hz in both cases. The major conclusions of the study were:

- In both RDT tests, stress was composed of a tensile and a compressive component in the same load cycle and it was observed that the measured material properties in the tensile stress portion were different from the material properties in the compressive stress portion.
- Asphalt mixture had a larger complex modulus and phase angle in tensile stress portion than in compressive stress portion.



Figure 2.9: Configuration of controlled-strain RDT test (Luo et al. 2013).

In this test, dissipated strain energy (DSE) and recoverable strain energy (RSE) were measured. Further research is currently being conducted to develop methods to use these parameters in modeling fatigue crack growth rate. Simplified Viscoelastic Continuum Damage (S-VECD) test is also a direct tension test which uses continuum damage approach to characterize fatigue failure and is explained in the next section.

2.3.4 Simplified Viscoelastic Continuum Damage (S-VECD)

The simplified Viscoelastic Continuum Damage (S-VECD) test follows AASHTO TP 107 (2014) protocol. This test is used to determine the damage characteristic curve via direct tension cyclic loading. In this test, a controlled and repeated cyclic load is applied to the specimen until failure. The applied stress and the axial strain response are measured and used to determine damage (S) and the pseudo secant modulus (C) which are expressed as the damage characteristic

curve. The fundamental relationship between damage and material integrity of asphalt mixtures can be determined using the damage characteristic curve. This property, which is independent of temperature, frequency and mode of loading, is combined with viscoelastic properties of asphalt concrete and is used to analyze the fatigue characteristics of asphalt concrete mixtures.

Direct tension testing is performed on the samples cored and obtained from Superpave gyratory compacted specimens. The average diameter is 100 to 104 mm and the average height of the specimen is 127.5 to 132.5 mm. Mounting studs for the axial sensors are attached to the sides of the specimen using epoxy. End plates are then glued to the bottom and top of the specimen using the gluing jig (Figure 2.10b). The specimen is then placed in the testing machine and fastened tightly to the bottom support with screws. Then, the specimen is raised and secured to the top loading platen. The axial sensors are attached to the mounting studs of the specimen. Specimen is kept for conditioning at the pre-selected test temperature for about four hours before starting the test (Figure 2.10a). In general, a total of three specimens at different strain levels are tested. The resulting data is analyzed using the ALPHA-fatigue software to develop the damage characteristic curve.

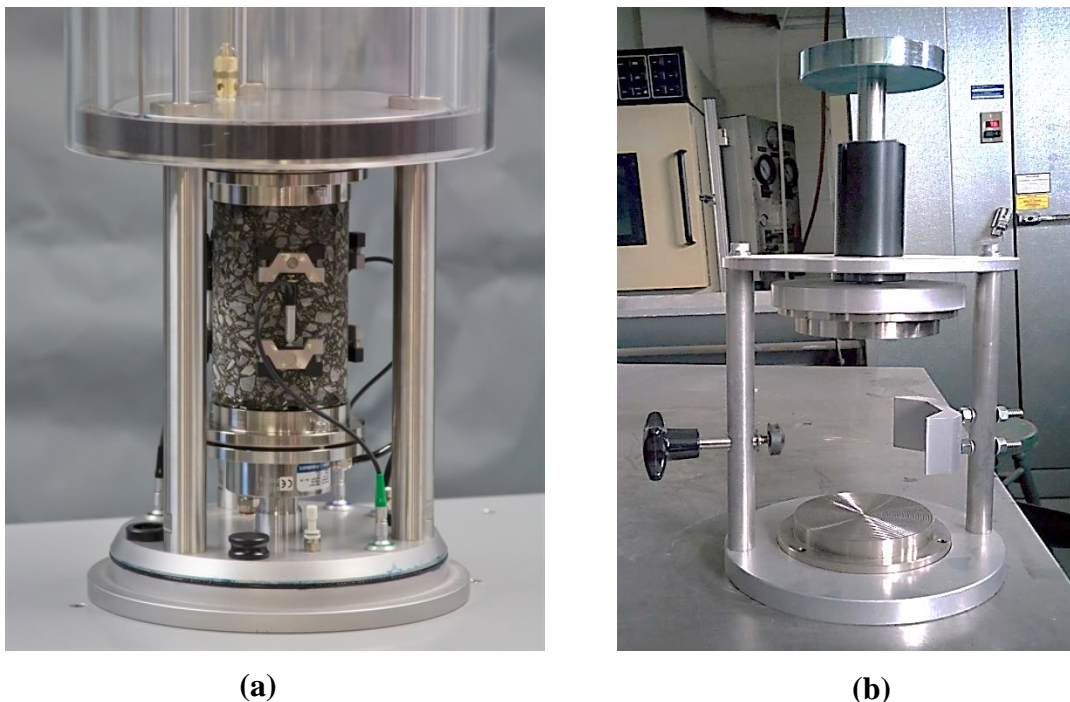


Figure 2.10: (a) S-VECD test setup (*source: www.worldhighways.com*); (b) gluing jig.

2.3.5 Semi-Circular Bend (SCB) Test

Wu et al. (2005) developed the semi-circular bend (SCB) test (Figure 2.11) to determine the fracture resistance characteristics of asphalt concrete. This test works on the principle of elasto-plastic fracture mechanics and uses notched semi-circular specimens to determine the critical energy strain rate of mixtures. Various advantages of this test are: (1) different notch depths can easily be introduced into the samples which makes the evaluation of true fracture properties of

asphalt mixtures with regards to the crack propagation much easier; (2) the test setup and procedure is relatively simple; (3) the SCB specimens can be prepared by taking cores from Superpave gyratory compacted specimens; and (4) multiple specimens can be obtained from the same Superpave gyratory compacted specimen thus reducing the error caused by heterogeneities of different samples. In this test, the semi-circular specimen was loaded monotonically until failure under a constant cross-head deformation rate of 0.5 mm/min at a test temperature of $25 \pm 1^\circ\text{C}$. The load and vertical deformation were measured continuously and load-displacement curve was plotted.

A total of 117 SCB tests were conducted at 25°C , resulted from 13 Superpave mixtures \times 3 notch depths \times 3 replicates for each mixtures. The notch depths that were used in this study were 25.4, 31.8, and 38.0 mm. It is required to have at least two notch depths in the experimental design to be able to calculate the strain energy release rate (J_c) The project information and mixture designations are shown in Table 2.2. The major conclusions of this study were:

- For a single notch depth, the fracture resistance based on average strain energy was found to be consistent with that from average vertical displacement, but different from that based on the peak load.
- Mixtures with higher tensile strengths could be more brittle and less fracture resistant than those with lower tensile strengths.
- The results obtained from the SCB tests with a single notch depth were not found to be able to rank the fracture resistance of Superpave mixtures in a consistent order.
- Superpave mixtures with larger NMAAS were found to have better fracture resistance.
- Superpave mixtures with softer asphalt binders were found to have more fracture resistance.

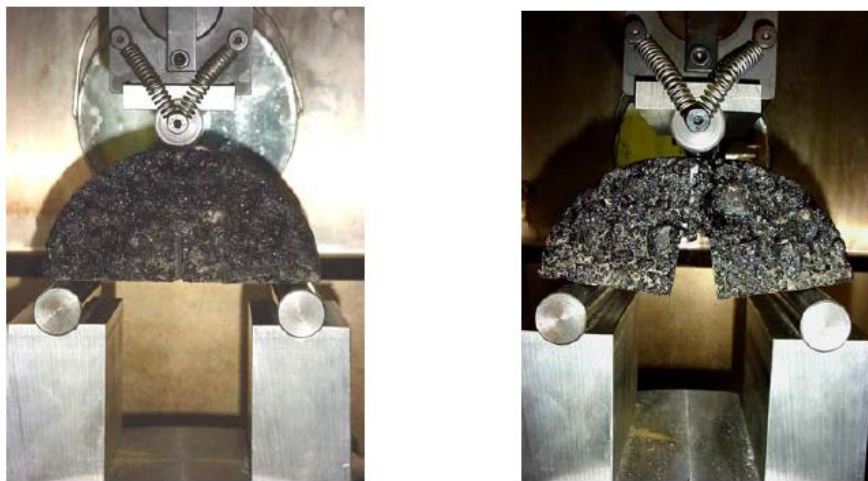


Figure 2.11: SCB test apparatus (Wu et al. 2005).

Table 2.2: Project information and mixtures designation (Wu et al. 2005)

Project Route	Mixture Type	Binder Type	Aggregate			N _{design}	Mix Designation
			NMAS (mm)	Type	Gradation		
LA 361	WC	PG70-22M*	19	Granite	Fine	75	361W
LA 191	WC	PG70-22M	19	Rhyolite	Fine	75	191W
LA 874	WC	PG70-22M	19	Limestone	Coarse	75	874W
LA 121	BC	AC-30	19	Limestone	Coarse	97	121B
LA 22	BC	AC-30	19	Limestone	Coarse	97	22B
LA 4	BC	AC-30	25	Limestone	Coarse	97	4B
US 61	WC	PAC-40	19	Limestone	Coarse	109	61W
US 61	BC	PAC-40	25	Limestone	Coarse	109	61B
US 90	BC	PAC-40	25	Limestone	Coarse	109	90B
Westbank Express	WC	PAC-40	19	Limestone	Coarse	125	WEW
I-10	WC	PG76-22M	19	Limestone	Coarse	125	10W
I-49	WC	PG76-22M	19	Limestone	Coarse	125	49W
I-12	WC	PG76-22M	19	Limestone	Coarse	125	12W

*M = polymer-modified binder; WC = wearing course; BC = binder course.

2.4 FATIGUE CRACKING MODELS

The prediction of fatigue cracking is based on the cumulative damage calculated as the ratio of predicted number of traffic repetitions to the allowable number of load repetitions (fatigue life). The fatigue life of an asphalt mixture is influenced by factors such as binder type, binder content, aging, air void content, climate, and traffic. This section summarizes various models developed to predict the fatigue performance of asphalt mixtures.

2.4.1 Mechanistic-Empirical Pavement Design Guide (MEPDG) Models

Miner's law is one of the most basic recursive-incremental damage accumulation method used in fatigue cracking prediction (Miner, 1945). It is based on the cumulative damage theory and defined as the ratio of number of cycles applied at each stress level to the number of cycles to failure, as shown in Equation 2.3. For fatigue cracking, number of cycles to failure in Miner's law is defined as the number of repetitions to fatigue cracking or allowable number of repetitions. In mechanistic-empirical (ME) pavement design, number of repetitions to fatigue cracking are calculated for all trucks on a highway section with different loads, speeds, and temperatures via transfer functions developed by using laboratory fatigue cracking test results. Then, damage created by a specific axle for a specific time interval (using load, speed, and temperature for the corresponding time interval) is calculated by dividing 1 by the calculated number of repetitions to fatigue cracking. By summing up calculated damage created by all truck axles for a specific design period by considering variable traffic, climate, and changing material properties, total accumulated damage for the design period can be calculated. Fatigue cracking is assumed to occur when the accumulated damage value reaches a value of '1'.

$$\sum_i \frac{\Delta n_i}{n_f(\sigma_i)} = 1 \quad (2.3)$$

Where,

Δn_i = number of cycles applied at each stress level σ_i .

n_f = number of cycles to failure at stress level σ_i .

The most common type of model used to predict the number of load repetitions required for initiation of fatigue cracking is a function of the tensile strain and stiffness of the mix. General form of the number of load repetitions equation (transfer function) used in MEPDG is shown in Equation (2.4) (Witczak et al. 2004).

$$N_f = C k_1 \left(\frac{1}{\varepsilon_t} \right)^{k_2} \left(\frac{1}{E} \right)^{k_3} \quad (2.4)$$

Where:

N_f = Number of repetitions to fatigue cracking.

ε_t = Tensile strain at the critical location.

E = Stiffness of the material.

k_1, k_2, k_3 = Laboratory regression coefficients.

C = Laboratory to field adjustment factor.

Constant stress and constant strain are two test loading types that are used for fatigue characterization. In constant stress tests, applied load remains constant and with increase in number of load repetitions, tensile strain increases. In constant strain tests, strain remains constant and with increase in load repetitions, stiffness of the material reduces and so is the stress to maintain the same strain. These phenomena are shown in Figure 2.12.

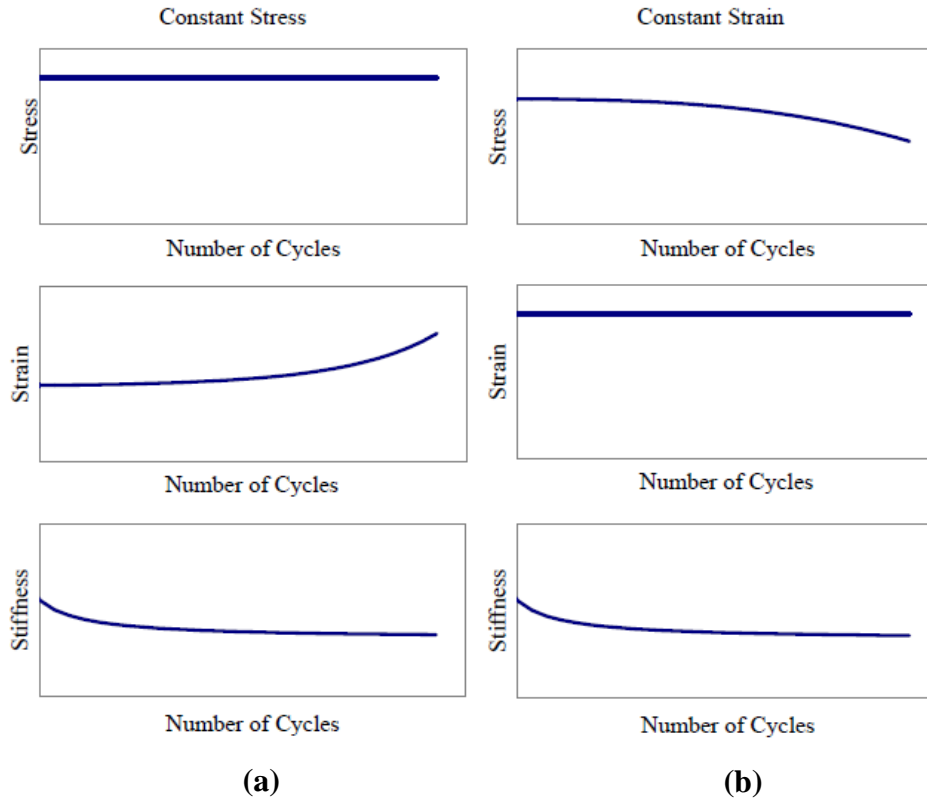


Figure 2.12: (a) Constant Stress Test and (b) Constant Strain Test (Witczak et al. 2004).

The Shell Oil (Bonnaure et al. 1980) and the Asphalt Institute (MS-1 1982) models are the most commonly used fatigue cracking models. Although, general form of each model is similar to the mathematical model shown in Equation (2.4, the difference is in the laboratory regression coefficients and the laboratory to field adjustment factor.

2.4.1.1 Shell Oil Model

The Shell Oil Co. has developed fatigue damage prediction equations by laboratory fatigue testing with constant strain and constant stress methods. The Equations (2.5 and (2.6 are summarized as follows (Bonnaure et al. 1980) :

Constant Strain:

$$N_f = A_f [0.17PI - 0.0085PI(V_b) + 0.0454V_b - 0.112]^5 \epsilon_t^{-5} E^{-1.4} \quad (2.5)$$

Constant Stress:

$$N_f = A_f [0.0252PI - 0.00126PI(V_b) + 0.00673V_b - 0.0167]^5 \epsilon_t^{-5} E^{-1.4} \quad (2.6)$$

Where:

PI	=	Penetration index	=	$\frac{20-500A}{1+50A}$
A	=	temperature susceptibility	=	$\frac{\log(\text{pen at } T_1) - \log(\text{pen at } T_2)}{T_1 - T_2}$
A_f	=	laboratory to field adjustment factor		
T_1 & T_2	=	temperatures in °C at which penetrations are measured		
V_b	=	effective binder content (%)		
ϵ_t	=	Tensile strain at the critical location		
E	=	Stiffness of the material		

Generally, the constant stress method is used for asphalt pavements with layer thicknesses more than 8 inches while constant strain method is considered applicable to thin asphalt pavement layers with thicknesses less than 2 inches. But there was no relationship for intermediate thicknesses, which are more common in flexible pavement constructions. Hence, a numerical transition approach was developed by Witczak et al. (2000) to overcome this problem. The generalized Shell Oil fatigue equation (Equation (2.7) improved by Witczak et al. (2000) is given as:

$$N_f = A_f \left(1 + \frac{13,909E^{-0.4} - 1}{1 + \exp^{1.345h_{ac}-5.408}} \right) (0.0252PI - 0.00126PI(V_b) + 0.00673V_b - 0.0167)^5 \left(\frac{1}{\epsilon_t} \right)^5 \left(\frac{1}{E} \right)^{-1.4} \quad (2.7)$$

Where:

A_f	=	laboratory to field adjustment factor
h_{ac}	=	thickness of asphalt concrete layer in inches

2.4.1.2 Asphalt Institute (MS-1) Model

The Asphalt Institute's fatigue model is based upon the modifications to constant stress laboratory fatigue criteria. The model developed by Witczak et al. (MS-1 1982) utilized

the basic fatigue relationship developed by Hudson et al. (1968). Developed MS-1 model is given below in Equation (2.8):

$$N_f = 0.00432C \left(\frac{1}{\varepsilon_t} \right)^{3.291} \left(\frac{1}{E} \right)^{0.854}$$

$$C = 10^M \quad (2.8)$$

$$M = 4.84 \left(\frac{V_b}{V_a + V_b} - 0.69 \right)$$

Where:

V_b = effective binder content (%).

V_a = air voids (%).

Both Shell Oil model and MS-1 model are of the same form, but the coefficients for the MS-1 model are smaller when compared to the Shell Oil model. The reason behind this was that the Shell Oil model was based upon only laboratory testing whereas the MS-1 model was based upon actual field calibration studies.

2.4.2 Continuum Damage Models

Phenomenological and mechanistic approaches are two major practices for fatigue characterization of asphalt mixtures. The phenomenological approach uses the initial response of the mixture to predict fatigue life and does not account for the evolution of damage throughout the design life. The introduction of fracture mechanics into the mechanistic approach allowed the consideration of fatigue damage growth in asphalt pavement performance prediction. Although this approach is quite complex when compared to the phenomenological approach, it includes a wide range of more realistic loading and environmental conditions and hence can be considered to be a better tool in assessing the fatigue life of pavement structures. The following sections present important continuum damage models that are developed to predict the fatigue life of asphalt mixtures.

2.4.2.1 Continuum Damage Mechanics-Based Fatigue Model

Schapery (1990) developed a model to evaluate the mechanical behavior of elastic media with growing damage and other changes in structure. Asphalt mixture being a viscoelastic material, Lee et al. (2000) replaced the linear strain with a parameter called pseudostrain, *a quantity calculated from actual time dependent strains*, to eliminate the hysteretic behavior due to linear viscoelasticity (Equation (2.9)). The pseudostrain accounts for the time-temperature dependent properties of viscoelastic materials through the convolution integral so that damage is evaluated independent of viscoelastic effects.

$$\varepsilon^R = \frac{1}{E_R} \int_0^t E(1 - \tau) \frac{d\varepsilon}{d\tau} d\tau \quad (2.9)$$

Where,

E_R = reference modulus (typically 1),

$E(t, \tau)$ = relaxation modulus

The simulated stress-pseudostrain behavior revealed the following three important characteristics of damage growth:

- Nonlinearity of loading and unloading paths in every cycle
- Change in slope of each stress-pseudostrain cycle as cyclic loading continues
- Accumulation of permanent pseudostrain in the controlled-stress method

A single parameter called the secant pseudostiffness S^R was used to represent the change in slope of stress-pseudostrain loops and is defined as:

$$S^R = \frac{\sigma_m}{\varepsilon_m^R} \quad (2.10)$$

Where:

ε_m^R = peak pseudo strain

σ_m = stress corresponding to ε_m^R

The generalized form of the constitutive model is presented below:

$$\sigma = I(\varepsilon_e^R)[F + G + H] \quad (2.11)$$

Where:

I = initial pseudostiffness

ε_e^R = effective pseudostrain

F & H = functions to characterize the change in pseudostiffness due to damage growth and micro damage healing respectively

G = function to account for the difference in stress values for loading and unloading paths

The development of continuum damage mechanics-based fatigue model is based on the constant strain testing because fatigue performance prediction is dependent upon accurate modeling of the change in pseudostiffness as a function of loading cycles, and only F and H are required to predict the number of cycles to failure (N_f). The number of cycles to failure of an asphalt mixture subjected to a cyclic loading with M number of rest periods is expressed as:

$$N_{f,Total} = N_{f,w/oRP} + \sum_{i=1}^M \Delta N_{f,i} \quad (2.12)$$

Where:

$N_{f,w/oRP}$ = N_f from a fatigue test without rest.

$\Delta N_{f,i}$ = increase in N_f due to the i th rest period.

2.4.2.2 Simplified Viscoelastic Continuum Damage (S-VECD) model

Continuum damage theories characterize a material using the net effect of microstructural changes on observable properties. It employs the instantaneous pseudo secant modulus to assess the material's integrity. Kim and Little (1990) applied Schapery's (1987) nonlinear viscoelastic constitutive theory to describe the behavior of sand asphalt under controlled strain cyclic loading. Later, Lee and Kim (1998) demonstrated that this theory can also describe the behavior of asphalt concrete under both controlled stress and controlled strain cyclic loading. The concepts which define the VECD model are (Underwood et al. 2010):

- the elastic-viscoelastic correspondence principle based on pseudo strain (ϵ^R),
- work potential theory for modelling the effects of micro cracks, and
- the time-temperature superposition principle to include the joint effect of time and temperature.

The functional forms to characterize the S-VECD model are as shown in Equations (2.13 to (2.15 (Underwood et al. 2012).

$$\varepsilon^R = \begin{cases} \varepsilon^R = \frac{1}{E_R} \int_0^\xi E(\xi - \tau) \frac{d\varepsilon}{d\tau} d\tau & \xi \leq \xi_p \\ \varepsilon_{0,ta}^R = \frac{1}{E_R} \times \frac{\beta + 1}{2} ((\varepsilon_{0,pp})_i \times |E|_{LVE}^*) & \xi > \xi_p \end{cases} \quad (2.13)$$

$$C = \begin{cases} C = \frac{\sigma}{\varepsilon^R \times DMR} & \xi \leq \xi_p \\ C^* = \frac{(\beta+1)\sigma_{0,pp}}{2\varepsilon_{0,ta}^R \times DMR} & \xi > \xi_p \end{cases} \quad (2.14)$$

$$dS = \begin{cases} (dS_{transient})_{timestep j} = \left(-\frac{DMR}{2} (\varepsilon^R)_j^2 \right)^{\frac{\alpha}{1+\alpha}} (\Delta\xi)_j^{\frac{1}{1+\alpha}} & \xi \leq \xi_p \\ (dS_{cyclic})_{cycle i} = \left(-\frac{DMR}{2} (\varepsilon_{0,ta}^R)^2 \right)^{\frac{\alpha}{1+\alpha}} \times [\Delta N_i \times \xi_p \times K_1]^{\frac{1}{1+\alpha}} & \xi > \xi_p \end{cases} \quad (2.15)$$

Where,

ε^R = pseudostrain,

ε = strain,

$E(\xi)$ = linear viscoelastic relaxation modulus,

τ = integration term,

ξ = reduced time,

ξ_p = reduced pulse time,

$\varepsilon_{0,pp}$ = peak-to-peak strain magnitude,

$\varepsilon_{0,ta}^R$ = pseudostrain tension amplitude,

$\sigma_{0,pp}$ = peak-to-peak stress magnitude,

β = load form factor,

dS = increment of damage growth,

ΔC_j = finite difference between C-values at consecutive time steps j and j-1,

ΔC_i = finite difference between C-values at cycle i and i- ΔN ,

$\Delta \xi$ and $j-1$,	=	finite difference between reduced time at consecutive time steps j
ΔN_i	=	number of cycles between calculation steps for cyclic portion,
K_1	=	loading shape factor,
DMR	=	dynamic modulus ratio, and
α	=	damage evolution rate.

This S-VECD model is rearranged in the traditional fatigue relationship in order to predict the number of cycles to failure (N_f) and the final form is shown in Equation (2.16).

$$N_f = \frac{(f_{red})(2^\alpha)(S_{failure})^{\alpha-\alpha C_{12}+1}}{(\alpha-\alpha C_{12}+1)(C_{11}C_{12})^\alpha[(\beta+1)(\epsilon_{0,pp})(|E|_{LVE}^*)]^{2\alpha}(K_1)} \quad (2.16)$$

Where:

f_{red}	=	$f \times \alpha_t$,
f	=	loading frequency (Hz),
$ E _{LVE}^*$	=	linear viscoelastic relaxation modulus,
$S_{failure}$	=	failure damage.

2.4.3 Parameters to Evaluate Fatigue Cracking Performance

2.4.3.1 Paris Law of Crack Propagation

Paris and Erdogan (1963) characterized sub-critical crack growth under fatigue loading using the stress intensity factor. Paris' law is written as:

$$\frac{da}{dN} = C \Delta K^m \quad (2.17)$$

Where:

da/dN	=	crack growth rate
ΔK	=	stress intensity factor
C and m	=	material parameters

Paris' law is only valid for uniaxial loading and linear elastic fracture mechanics (LEFM) conditions. Zhang et al. (2001) determined that Paris law does not incorporate all aspects associated with the mechanism of cracking of asphalt mixtures and hence a concept involving threshold as a failure criterion is required to understand the initiation and propagation of cracks.

2.4.3.2 Dissipated Energy Approach

The four point bend test uses dissipated energy approach to characterize fatigue damage. Under simple loading, crack initiation in an asphalt mixture is a function of stress or strain and can be expressed as (Monismith et al. 1994):

$$N_f = a \left(\frac{1}{\sigma} \right)^b \text{ or } N_f = c \left(\frac{1}{\epsilon} \right)^d \quad (2.18)$$

Where:

- N_f = number of load applications to crack initiation
 σ, ϵ = tensile stress and strain, respectively, and
 a, b, c, d = experimentally determined coefficients

The stress and strain in the above equation were replaced with the energy dissipated during an initial loading cycle, w_o .

$$N_f = e \left(\frac{1}{w_o} \right)^f \quad (2.19)$$

Where:

- e, f = experimentally determined coefficients

Further study established a relationship between number of cycles to failure and cumulative dissipated energy and is given as:

$$W_N = A(N_f)^z \quad (2.20)$$

Where:

- W_N = cumulative dissipated energy to failure, and
 A, z = experimentally determined coefficients

Although the above relationship is a good predictor of cycles to failure, it does not cater for different types and conditions of testing. It was identified that these relationships are different for different mixes and are a function of test temperature and mode of testing.

2.4.3.3 Critical Strain Energy Release Rate

The semi-circular bend (SCB) test uses the concept of critical strain energy release rate to characterize fatigue damage. The linear-elastic fracture mechanics (LEFM) defines the strain energy release rate (G) of a cracked member under Mode I displacement mode as:

$$G = -\left(\frac{1}{b}\right) \frac{dU}{da} = \frac{K^2}{E'} \quad (2.21)$$

Where:

b	=	thickness of the specimen
a	=	the notch depth
U	=	the strain energy to failure
K	=	stress intensity factor
E'	=	Young's modulus

The concept of LEFM was extended to accommodate elasto-plastic behavior of materials, such as asphalt mixtures, using the J-integral. J-integral is the line integral around the crack and is equal to strain energy release rate for a crack in a body subjected to loading. The critical value of J-integral or the fracture resistance, J_C , is determined with the following equation (Rice, 1968):

$$J_C = -\left(\frac{1}{b}\right) \frac{dU}{da} \quad (2.22)$$

2.4.3.4 Pseudo Strain Energy Release Rate

The S-VECD test uses the pseudo strain energy release rate to characterize fatigue damage. In a viscoelastic continuum damage model, the basic equations required for the damage theory are (Underwood et al. 2010):

- the pseudo strain energy density function,

$$W^R = f(\epsilon^R, S) \quad (2.23)$$

- the stress-pseudo strain relationship,

$$\sigma = \frac{\delta W^R}{\delta \epsilon^R} \quad (2.24)$$

- the damage evolution law,

$$\frac{dS}{dt} = \left(-\frac{\delta W^R}{\delta S} \right)^\alpha \quad (2.25)$$

Where:

σ	=	stress,
ϵ^R	=	pseudo strain,
S	=	internal state variable representing damage,
α	=	damage evolution rate.

2.5 PREDICTION OF FIELD FATIGUE CRACKING PERFORMANCE USING LABORATORY TEST RESULTS

2.5.1 Bending Beam Fatigue Test

Tayebali et al. (1992) established a practical and relatively simple approach for predicting fatigue behavior of asphalt mixtures by laboratory testing. Four point bending tests were conducted with laboratory-mixed laboratory-compacted beam specimens with a loading time of 0.1 second. For the controlled-stress tests, a step loading pattern was applied while a haversine loading pattern was used for the controlled-strain tests. For the controlled-stress tests, the number of load repetitions until failure were recorded while in controlled-strain tests, the number of load repetitions at which the specimen experienced a stiffness reduction of 50% were recorded. Figure 2.13 shows the estimated versus observed fatigue lives for specimens tested under controlled-stress and controlled-strain conditions.

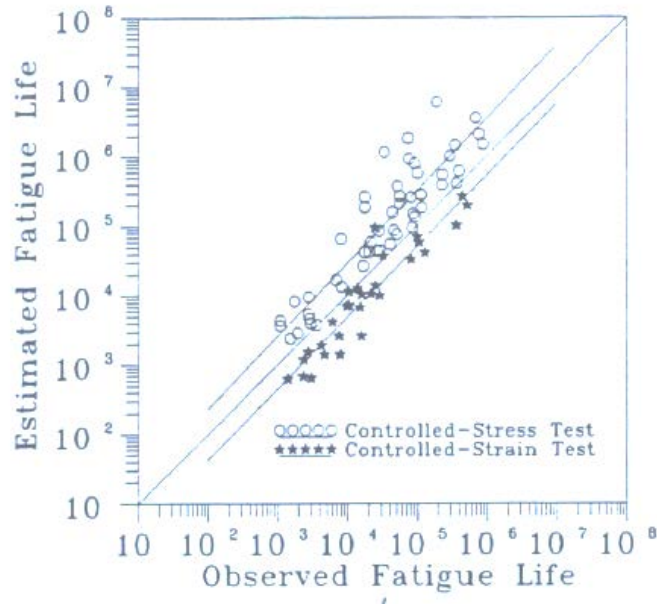


Figure 2.13: Estimated versus observed fatigue lives (Tayebali et al. 1992).

The following conclusions were made in this study:

- For a controlled-stress test, the estimated fatigue lives were greater than the observed fatigue lives. The R^2 for the correlation between estimated and observed fatigue lives was calculated to be 0.8.
- For a controlled-strain test, the estimated fatigue lives were smaller than the observed fatigue lives. The R^2 for the correlation between estimated and observed fatigue lives was calculated to be 0.88.
- It was observed that the number of cycles to failure versus the cumulative dissipated energy relationship is dependent upon the mode of loading and temperature as shown in the Figure 2.14.

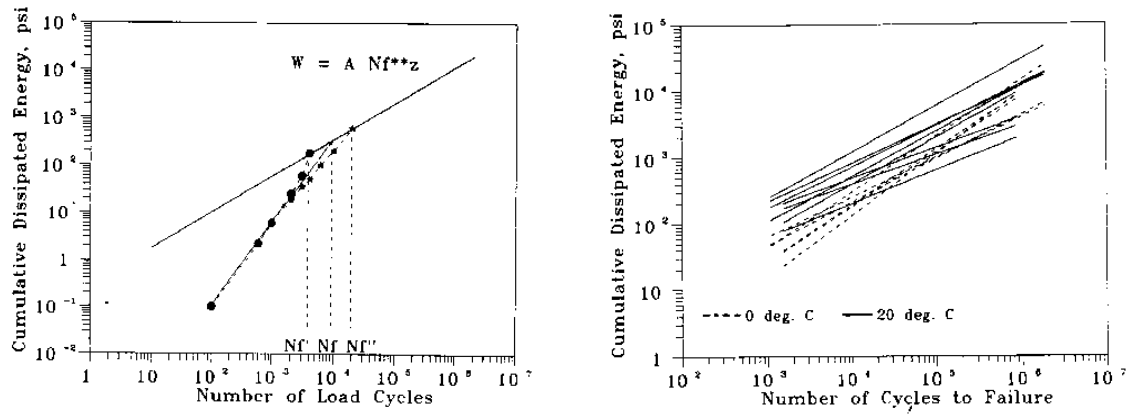


Figure 2.14: Effect of mode of loading and temperature (Tayebali et al. 1992)

2.5.2 Indirect Tension Test

Zhang et al. (2001) carried out a study with an objective to determine the correlation between laboratory-measured crack growth rates and the field performance. In this study, eight field sections comprising of two Superpave coarse mixtures, and two Superpave fine mixtures were used. A total of 225 field cores were collected from these sections to obtain mixture properties. In addition, specimens were compacted using Superpave gyratory compactor and all aggregate and volumetric requirements of Superpave were met. These samples were tested for resilient modulus, creep compliance, and strength tests at -10°C, 0°C, and +10°C using Superpave indirect tension test (IDT). Crack growth rate (da/dN) parameters developed by Roque et al. (1999) were used in the analysis.

From this study, the following conclusions were made:

- The laboratory-measured crack growth rates did not correlate well with field performance. Also, it was observed that laboratory age hardening appeared to reduce the crack growth rate of the Superpave mixtures, which is not quite realistic.
- It was observed that fracture energy density and resilient modulus had no effect on crack growth rate observed in the laboratory, contrary to the fact that fracture energy density is an effective indicator of field cracking performance of asphalt pavements.
- It was concluded that Paris law, one of the first and most widely used fatigue crack propagation criteria, does not incorporate all aspects involved in the mechanism of cracking of asphalt mixtures subjected to generalized loading conditions.

2.5.3 Simplified Viscoelastic Continuum Damage (S-VECD) Test

Underwood et al. (2012) used the S-VECD-FEP++ model to predict the fatigue behavior of the FHWA Accelerated Load Facility (FHWA ALF) pavements. The ALF experiment had 12 lanes of different asphalt concrete mixtures. The pavement structure consisted of 100 mm hot mix asphalt overlaid on 560 mm crushed aggregate base on top of a compacted A-4 subgrade soil.

The lanes that had the control mixture, the styrene butadiene styrene-(SBS) modified mixture, crumb rubber terminal blend mixture (CRTB), and ethylene terpolymer mixture were tested in this study. Figure 2.15 shows the comparisons of fatigue performances between S-VECD-FEP++ simulations and ALF measurements. In the ALF experiments, the failure was defined as the cycle at which 20 % of the lane had cracked while in the simulations, failure was defined as the cycle at which element reaches a pseudostiffness value of 0.25. Two comparisons were made in this study: one with terpolymer and the other without terpolymer. The correlation observed between the measured and predicted failures was quite good in the case where terpolymer lane was not considered. However, it should be noted that R^2 value for the correlation between field and laboratory measurements might be high (0.954) as a result of the limited number of data points available for comparison.

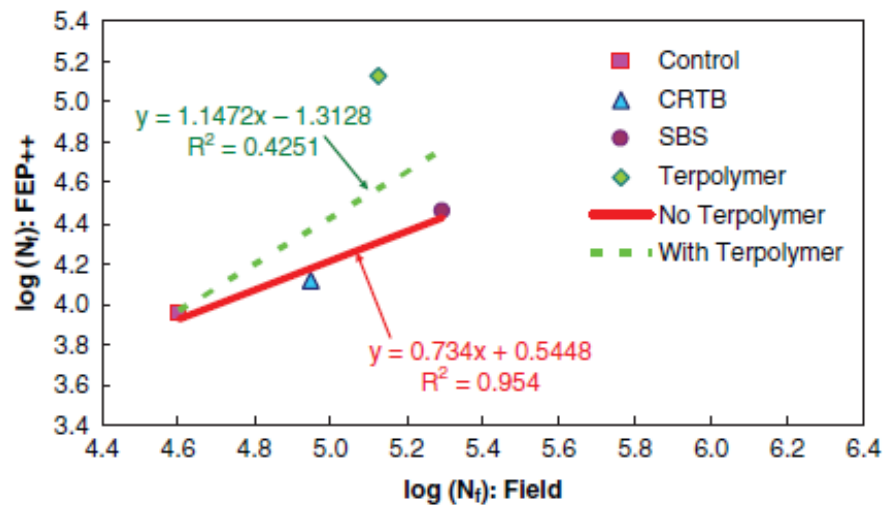


Figure 2.15: Comparison of FEP++ predicted and measured fatigue life of FHWA ALF mixtures (Underwood et al. 2012).

2.5.4 Semi-Circular Bend Test

Mohammad et al. (2012) carried out a study to evaluate the effectiveness of semi-circular bend (SCB) test for predicting fatigue cracking performance of asphalt pavements by analyzing the relationship between the results obtained from the laboratory prepared asphalt mixtures and the field performance of asphalt pavements. In this study, nine field projects were considered. At the time of construction, the critical strain energy release rate (J_c) of plant mixed-laboratory compacted asphalt mixtures were measured by SCB testing at an intermediate temperature of 25°C. Also, the corresponding cracking data were collected from Louisiana pavement management system database. Finally, a regression analysis was performed to determine the relationship between SCB and field cracking performance. Figure 2.16 portrays the correlation between J_c values and cracking rates. It was observed that cracking rates decreased as J_c value increases. Therefore, from this study it was concluded that SCB measured J_c values demonstrated a good correlation with the field cracking performance data at intermediate service temperatures.

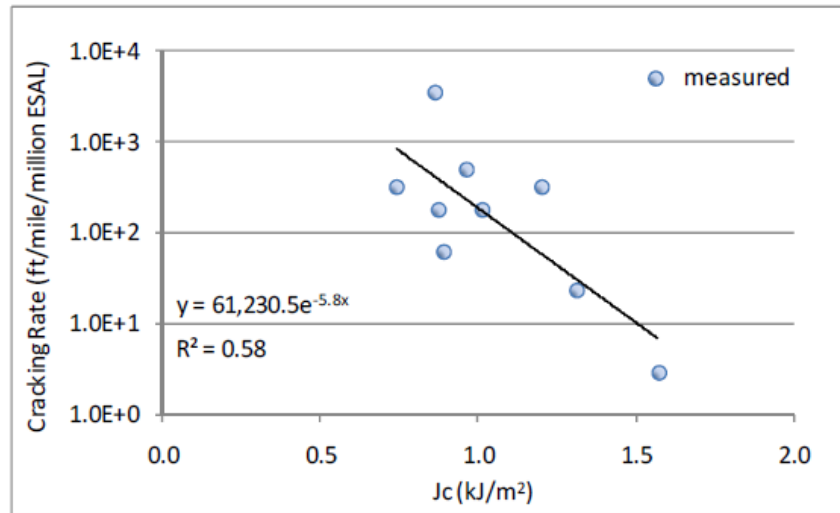


Figure 2.16: Correlation between cracking rates of pavement sections and J_c values from SCB tests (Mohammad et al. 2012).

2.6 SUMMARY

A review of the literature indicated that cracking (especially top-down) is the major distress mode in Oregon and the U.S. According to the literature, binder content, air-void content (density), surface aging, and binder grade are the most important factors affecting asphalt pavement cracking performance. Aggregate gradation and mixture segregation are the other two factors that influence crack resistance.

Harvey and Tsai (1996) suggested that 0.5% increase in binder content can result in a 10 to 20 percent increase in overlay fatigue life while Williams and Shaidur (2015) suggested to increase design binder content of asphalt mixes in Oregon by about 0.25% to increase the cracking resistance of the mixture and reduce top-down cracking. Harmelink et al. (2008) showed that increasing the binder content could create a reduction in segregation and consequently reduce top-down cracking occurrence. Although increasing mix binder content can be accepted to be a viable strategy for increasing asphalt mix fatigue life, increased binder content tends to create a softer mix with lower rutting resistance. In addition, increasing binder content increases the unit cost of asphalt mixes. Thus, the impact of increased binder content on crack resistance, rutting performance, and segregation should be investigated. By using mechanistic-empirical design methods and life-cycle cost analysis, cost benefits of increasing asphalt binder content should be quantified and evaluated.

In general, results of previous studies suggested higher crack resistance for asphalt mixes with finer gradations. In all the reviewed literature, using fine gradation with increased binder content increased crack resistance by increasing ductility, reducing air-void content, and reducing segregation. It was also suggested that adequate balance between volumetric characteristics of mixtures and the amount of raw materials (binder, aggregate, filler, and additives) is crucial for a proper mix design. Literature review also showed that the effect of binder grade, binder content, and modification on fatigue performance is significantly higher than the influence of aggregate

type. Thus, effect of aggregate type on cracking performance will not be investigated in this study.

Based on the previous studies, it can be concluded that laboratory fatigue performances of modified asphalt mixtures were higher than the laboratory fatigue performances of mixtures with unmodified asphalt binders. In general, polymer modified asphalt mixtures have fatigue lives about an order of magnitude higher than unmodified asphalt mixtures. It was also determined that polymer and rubber modification can create significant improvements in performance. However, high cost of modified binders prevented the widespread use of this technology in development of high performance asphalt mixes. The cost advantage of binder modification should be quantified and evaluated by using mechanistic-empirical modeling and life-cycle cost analysis.

In this study, bending beam fatigue (BBF), indirect tension (IDT), direct tension cyclic fatigue (RDT), direct tension cyclic fatigue (DTCF), and semi-circular bend (SCB) tests are the experiments investigated to understand the applicability of these test procedures to be used for mix and structural design in Oregon. Although the correlation between field and lab-measured cracking performance for the DTCTF test (Underwood et al. 2012) was determined to be high with an R^2 value of 0.954, limited number of field sections used in the study suggests a more comprehensive evaluation with additional field sections. Comparison of results from BBF and SCB experiments with measured field cracking performance showed that these tests can provide parameters that are highly correlated with field performance (Tayebali et al. 1992, Mohammad et al. 2012). However, effectiveness of these tests in characterizing Oregon mixes for different climate regions and traffic levels needs to be investigated. In order to determine the most feasible test method and analysis protocol to be used in district and contractor laboratories in Oregon, accuracy, precision, time, cost, efficiency, and practicality of different cracking tests should be evaluated.

3.0 IMPLEMENTATION OF PERFORMANCE TESTER TO EVALUATE FATIGUE CRACKING OF ASPHALT CONCRETE

3.1 INTRODUCTION

Fatigue cracking is one of the most predominant modes of pavement distress. It occurs due to repeated traffic loading, particularly by heavy axle loads of trucks. It has been observed that the pavements constructed in Oregon over the last two decades are failing prematurely by fatigue cracking. The use of recycled materials, polymers and modified binders in the asphalt mix have altered the performance of the mixtures. Hence, volumetric properties considered in the mix design stage are not sufficient on their own to evaluate the fatigue performance of asphalt mixtures. Therefore, a more comprehensive laboratory evaluation tool is necessary to understand the behavior of paving mixtures.

Several tests are being used around the world to characterize the cracking resistance of asphalt mixtures. Based on a comprehensive literature review (Chapter 2.0), four cracking tests were chosen in this research study as candidate experiments. The Semi-Circular Bend (SCB) test, Indirect Tension (IDT) test, Bending Beam Fatigue (BBF) test and Direct Tension Cyclic Fatigue (DTCF) test are the most commonly used test methods used to evaluate the fatigue performance of asphalt mixtures. The four chosen tests were evaluated for:

- Simplicity: Factors such as sample preparation, testing difficulty and required testing time;
- Sensitivity to mix design parameters: Ability of the tests to identify the impact of fundamental mixture properties, such as binder content, binder type, air void content, polymer modification and recycled materials, on measured performance;
- Correlations to field performance: Ability of the tests to identify field sections with high and low cracking performance;
- Test variability; and
- Cost involved in implementation.

In this part of the study, the effectiveness of each laboratory experiment was first evaluated by comparing test results from PMFC-Old (plant mixed and field compacted - cores from field sections) specimens to the measured in-situ cracking performance of roadway sections. Second, the agreement between the results of different experiments was determined. The major purpose was to determine the effectiveness of different testing methods in identifying the cracking performance of pavements with different mixture properties. Another purpose of this part of the study was to determine the cracking and rutting resistance of Mix 1 (PG70-22ER-Fine gradation), Mix 2 (PG70-22ER-Coarse gradation) and Mix 3 (PG70-22-Coarse gradation), which are asphalt mixtures that are now commonly used in Oregon for pavement construction. Finally, the impact of compaction [(field compaction and Superpave Gyratory Compactor (SGC)] and mixing (laboratory and plant mixing) on cracking test results were determined.

3.2 OBJECTIVES

The major objectives of this part of the study are as follows:

- Determine the agreement between the results of different experiments;
- Determine the effectiveness of different testing methods in identifying the in-situ cracking performance of pavements with different mixture properties;
- Determine the cracking and rutting resistance of Mix 1 (PG70-22ER-Fine gradation), Mix 2 (PG70-22ER-Coarse gradation) and Mix 3 (PG70-22-Coarse gradation) asphalt mixtures that are now commonly used in Oregon for pavement construction;
- Determine the correlations between SCB, IDT, BBF and DTCF test results and measured field performance data;
- Select the best cracking experiment by considering testing time, cost, efficiency, complexity and practicality for use in district and contractor laboratories in Oregon; and
- Determine the effect of mixing (laboratory and plant mixing) and compaction method (field roller compaction and laboratory gyratory compaction) on the results of the selected cracking experiment.

3.3 MATERIALS

This section provides information about virgin binders, virgin aggregates and RAP aggregates used in this study. All the materials were obtained from local sources. In this study, three types of asphalt samples were used for testing and evaluation:

- *Plant Mixed-Field Compacted (PMFC) samples:* These are samples taken from various highway sections and used for laboratory specimen production. Parameters obtained from PMFC samples were expected to reflect actual field performance. However, since control on production variability and compaction is limited for PMFC mixtures, binder content, gradation, RAP content and air-void content can vary from target values.
- *Laboratory Mixed-Laboratory Compacted (LMLC) samples:* The aggregates, virgin binders and RAP material used to produce asphalt mixtures for field construction were sampled from the Lakeside Industries plant in Portland, Oregon (Figure 3.1). These materials were used to produce LMLC samples at the Asphalt Materials Performance Laboratory at Oregon State University. Although laboratory compaction and mixing methods are different from plant mixing and field compaction methods, the binder content, gradation, RAP content and air-void content can be accurately controlled to achieve target values for LMLC samples. In addition, specimens with air-void contents, binder contents and gradations that are different from the plant

production were prepared in this study to determine the impact of these factors on cracking and rutting resistance of asphalt mixtures.

- *Plant Mixed-Laboratory Compacted (PMLC) samples:* Before construction, loose asphalt mixtures were collected from the Lakeside Industries plant to produce PMLC samples in the laboratory. Although PMFC samples are expected to provide more realistic test results reflecting actual in-situ performance, compaction variability and limited layer thickness for laboratory test specimen production required plant sampling of production mixtures and compaction in the laboratory for specimen production.

In this study, production mixtures were collected from the plant before construction to produce PMLC specimens. Aggregates, binders and RAP materials used to produce the plant mixtures were also sampled from the plant before construction to use for LMLC specimen production in the laboratory. PMFC samples were collected (cored) from the roadway sections constructed with these production mixtures. PMFC-Old samples were collected from four different highway sections (two sections with no cracking and two sections with cracking) to conduct different cracking experiments in order to determine the effectiveness of each experiment in identifying the cracking resistance.

Three different asphalt mixtures were used in this study. Mix 1 (M1) was comprised of 3/8" nominal maximum aggregate size (NMAS) aggregates (fine gradation), 20% RAP and PG 70-22ER (polymer modified binder) grade virgin asphalt binder. The binder content of M1 was 6% by total weight. Mix 2 (M2) was comprised of 1/2" NMAS aggregates (coarse gradation), 20% RAP and PG 70-22ER (polymer modified binder) grade virgin asphalt binder. The binder content of M2 was 5.3% by total mixture weight. Mix 3 (M3) was comprised of 1/2" NMAS aggregates (coarse gradation), 20% RAP and PG 70-22 (no polymer modification) grade virgin asphalt binder. The binder content of M3 was 5.3% by total mixture weight. The gradation curves for M1, M2 and M3 are presented in Figure 3.2 and Figure 3.3. The asphalt mix designs for the three mixtures are provided in Appendix B. It should be noted that mixture properties for M2 and M3 are identical other than the binder type. M2 has a polymer modified binder (PG70-22ER) while the binder for M3 (PG70-22) has no modification.



Figure 3.1: Asphalt mix sampling at the production plant.

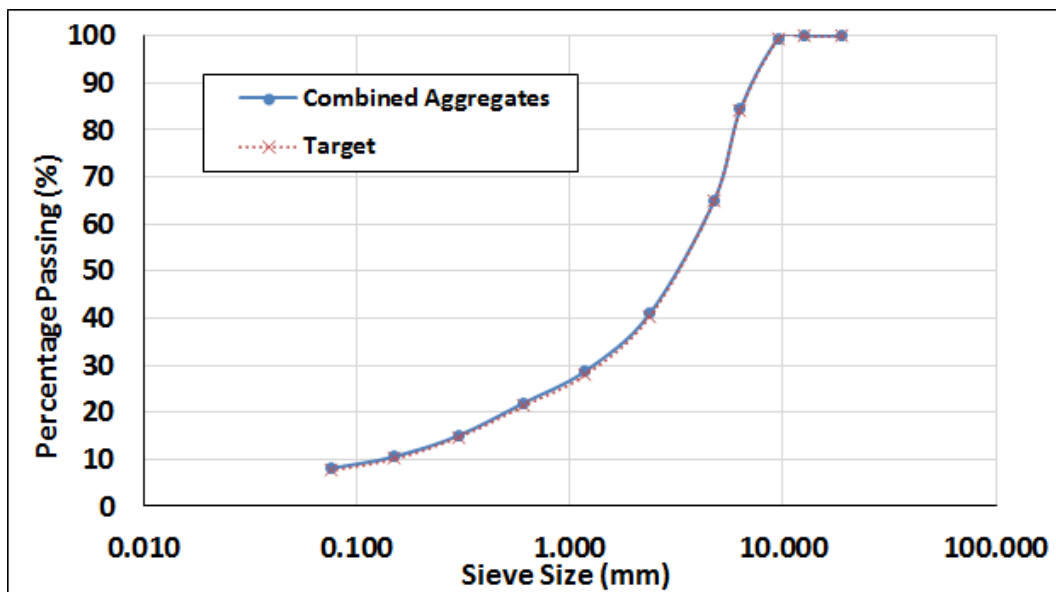


Figure 3.2: Gradation curve for Mix 1 obtained from the plant.

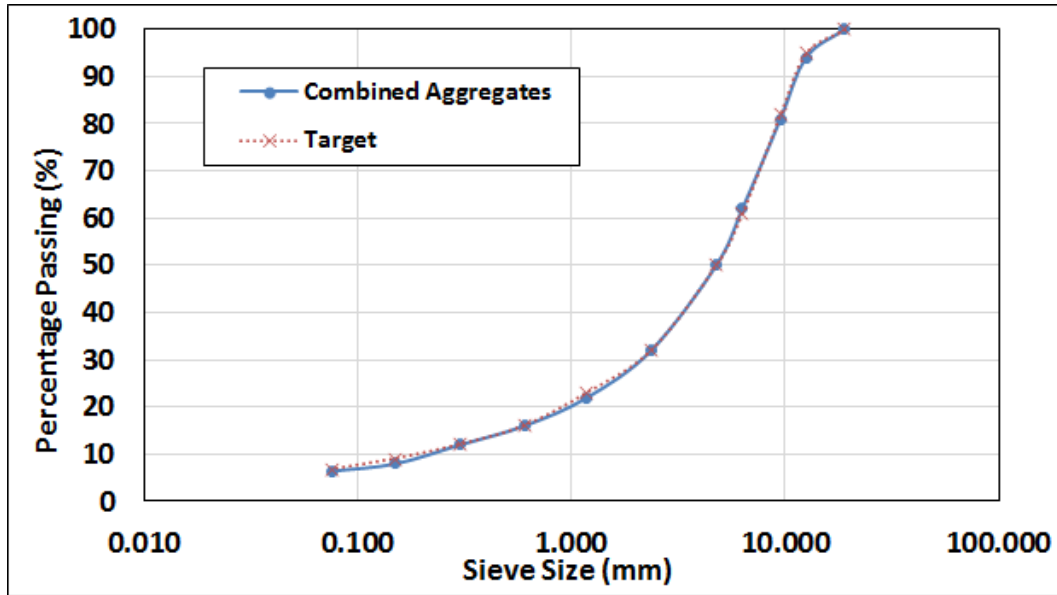


Figure 3.3: Gradation curve for Mix 2 and Mix 3 obtained from the plant.

Gradation, binder content and theoretical maximum specific gravity (G_{mm}) of RAP materials were provided by Lakeside Industries (Appendix B). AASHTO T 308-10 was followed for binder extraction and RAP content measurements. The quantity of binder in RAP materials for Mix 1 was determined as 5.26% while binder content of the RAP used for Mix 2 and Mix 3 production was 5.1%. AASHTO T 30-10 was followed to determine the gradation of extracted RAP aggregates. For five samples of RAP materials for Mix 1, Mix 2, and Mix 3, RAP aggregates were extracted and their gradations were determined, as shown in Table 3.1 and Table 3.2, respectively. Then, to obtain the final RAP aggregate gradation, the percent passing the #200 sieve was reduced by 1 percent. This correction was applied due to the aggregate breakdown in the ignition oven test (AASHTO T 30-10). Detailed information about the RAP gradations, binder contents and theoretical specific gravities are given in Appendix B.

Table 3.1. RAP Aggregate Gradations-Mix 1

Stockpile	Sample 1	Sample 2	Sample 3	Sample 4	Sample 5	Average	Final Gradation
Sieve Size	Percentage Passing						
3/4"	100.0	100.0	100.0	100.0	100.0	100.0	100.0
1/2"	100.0	100.0	100.0	100.0	100.0	100.0	100.0
3/8"	96.1	97.2	97.3	96.3	96.9	96.8	96.8
1/4"	79.7	79.6	77.8	77.0	78.0	78.4	78.4
#4	68.8	67.7	64.9	64.1	66.6	66.4	66.4
#8	46.9	45.6	43.3	43.1	46.5	45.1	45.1
#16	32.8	31.7	30.8	30.8	31.2	31.5	31.5
#30	24.3	23.9	23.3	23.7	23.8	23.8	23.8
#50	17.5	17.5	17.1	17.7	17.4	17.4	17.4
#100	13.1	12.8	12.4	13.1	13.2	12.9	12.9
#200	9.7	9.4	9.1	9.4	9.6	9.4	8.4

Table 3.2. RAP aggregate gradations-Mix 2 and Mix 3

Stockpile	Sample 1	Sample 2	Sample 3	Sample 4	Sample 5	Average	Final Gradation
Sieve Size	Percentage Passing						
3/4"	100.0	100.0	100.0	100.0	100.0	100.0	100.0
1/2"	97.0	97.5	96.8	97.9	98.7	97.6	97.6
3/8"	88.0	86.1	87.7	89.7	89.9	88.3	88.3
1/4"	69.6	68.8	69.9	70.5	70.5	69.9	69.9
#4	59.9	59.3	59.4	59.0	60.4	59.6	59.6
#8	42.1	41.5	42.6	41.8	41.8	42.0	42.0
#16	31.1	30.6	31.6	31.2	30.6	31.0	31.0
#30	24.1	23.6	24.6	24.1	23.7	24.0	24.0
#50	17.6	17.1	18.0	17.4	17.6	17.5	17.5
#100	12.8	12.4	13.2	12.7	12.9	12.8	12.8
#200	9.5	9.3	10.1	9.6	9.7	9.6	8.6

3.4 EXPERIMENTAL DESIGN

3.4.1 Experimental Design for Plant Mixed-Field Compacted Specimens

In this part of the study, the effectiveness of each laboratory experiment was evaluated by comparing test results from PMFC-Old specimens to the measured in-situ cracking performance of roadway sections. For this purpose, test samples for laboratory testing were collected from two field sections with high cracking resistance (sections with no cracking) and two with low cracking resistance (sections with severe cracking). The general experimental design is given in Table 3.3. Field specimens were collected from the following sections: Sections US20-U and OR99-U with no cracking and sections OR99W-C and OR99EB with severe cracking. The Pavement Management System (PMS) Data Sheets for these four sections are presented in Appendix A. DTCF tests were not carried out with field specimens since it was not possible to obtain 6-inch-tall specimens from field sections due to limited layer thicknesses. All the field cores and samples were taken along the wheel path as shown in Figure 3.4.

Table 3.3: Experimental Plan for Plant Mixed Field Compacted (PMFC) samples

Test type	Mix Type	Temp.	Strain levels	Replicates	Total Tests	Total specimens
Beam fatigue (BBF)	4 sections ¹	20°C	400 μ strain	3	12	12
SCB	4 sections	25°C	N/A	9	36	20
IDT	4 sections	25°C	N/A	6	24	24
Resilient modulus	4 sections	1 run	N/A	5	20	0 ²

Note:

¹ Four sections from ODOT SPR734 (Williams and Shaidur 2015):

1. Section with no cracking: US20-U - OR22:Sublimity Intchg Sect (RW2-WB): High traffic
2. Section with no cracking: OR99-U - OR99: Junction City 1: High traffic
3. Section with cracking (9,300ft/mile): OR99W-C - OR 99W:Brutscher St-Jct Hwy 151: High traffic
4. Section with cracking (15,420ft/mile): OR 99EB: Jct Hwy 001-Comm. St.: High traffic

² Resilient modulus tests were conducted with IDT specimens. Thus, no extra specimens were cut for resilient modulus testing.



Figure 3.4: Field sampling (a) Cores for SCB and IDT tests (b) Slab samples for BBF test (c) Cutting field slabs to produce blocks that can fit the lab saw (d) Cutting field blocks.

3.4.2 Experimental Design for Plant Mixed - Laboratory Compacted Specimens

In this part of the study, the agreement between the results of different experiments was determined. The major purpose was to determine the effectiveness of different testing methods in identifying the cracking performance of pavements with different mixture properties. Another purpose of this part of the study was to determine the cracking and rutting resistance of Mix 1 (PG70-22ER-Fine gradation), Mix 2 (PG70-22ER-Coarse gradation) and Mix 3 (PG70-22-Coarse gradation) asphalt mixtures that are now commonly used in Oregon for pavement construction. Table 3.4 shows the experimental plan followed in this part of the study. In order to evaluate the effectiveness of each experiment, three mixes with different cracking performance (Mix 1, Mix 2 and Mix 3) were used. Loose asphalt mixtures were sampled from the plant and stored in air-tight buckets. Since mixes were sampled during construction, the possibility of using cracking test results from production mixtures to predict long-term cracking performance can be determined in a future study. Cracking performance of these sections can be monitored

over the next 4-5 year period to evaluate the correlations between predicted performance (laboratory testing) and long-term in-situ performance.

Table 3.4: Experimental Plan for Plant Mixed Laboratory Compacted (PMFC) samples

Test type	Mix Type	Temp.	Strain levels	Replicates	Total Tests
Beam fatigue	M1 ¹ M2 M3	20°C	400 μstrain	3	9
DTCF	M1 M2 M3	20°C	200 μstrain	2	6
SCB	M1 M2 M3	25°C	N/A	9	27
IDT	M1 M2 M3	25°C	N/A	6	18
Dynamic modulus	M1 M2 M3	1 run ²	100 μstrain	2	6
Flow number	M1 M2 M3	54.7°C	N/A	2	6

Note: ¹ M1: Mix 1-PG70-22ER-Fine gradation
M2: Mix 2-PG70-22ER-Coarse gradation
M3: Mix 3-PG70-22-Coarse gradation

² Samples were tested at temperatures of 4 °C, 20 °C, and 40 °C and the loading frequencies of 0.1, 0.5, 1, 5, and 10 Hz. A loading frequency of 0.01 Hz was also used for 40 °C tests.

3.4.2.1 from viscosity versus temperature plots for the binder provided by Owens Corning. A sample Preparation of PMLC Specimens

Loose production mixes sampled from the plant were stored in airtight buckets. In the laboratory, these buckets were then placed in the oven at 110 °C for 2 hours. With the help of a mechanical splitter, uniform sampling of the mix was carried out as shown in Figure 3.5. Theoretical maximum specific gravity (G_{mm}) of each mix type was measured to be able to determine the required amount of asphalt mixture to achieve 7% air-void content. The required amount for different samples were weighed out and again kept in the oven at the compaction temperature for 2 more hours. The mixing and compaction temperatures were obtained from viscosity versus temperature plots for the binder provided by Owens Corning. A sample mixing and compaction curve for PG 70-22ER is presented in Figure 3.6. The binder properties are all presented in Appendix C. Cylindrical samples were compacted using a Superpave Gyratory Compactor (SGC) in accordance with the AASHTO T312-12 specification. The slab samples for BBF tests were compacted using a hydraulic roller compactor (Figure 3.7).



Figure 3.5: Mechanical Splitting of Asphalt Mixtures

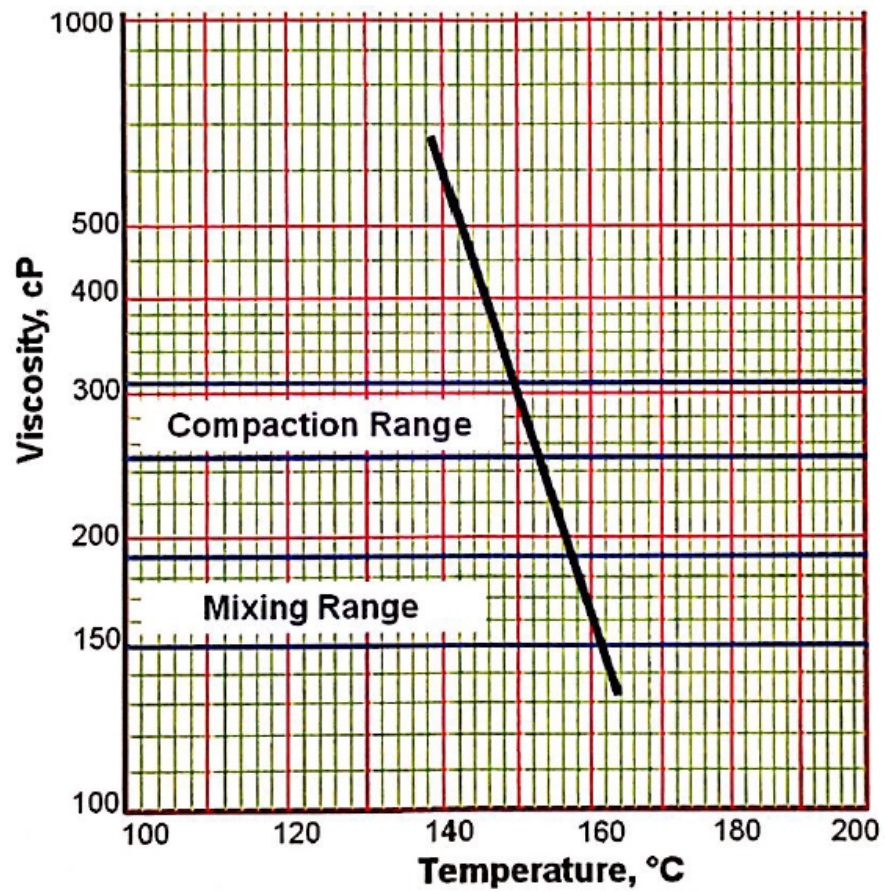


Figure 3.6: Mixing and Compaction Curve for PG 70-22ER

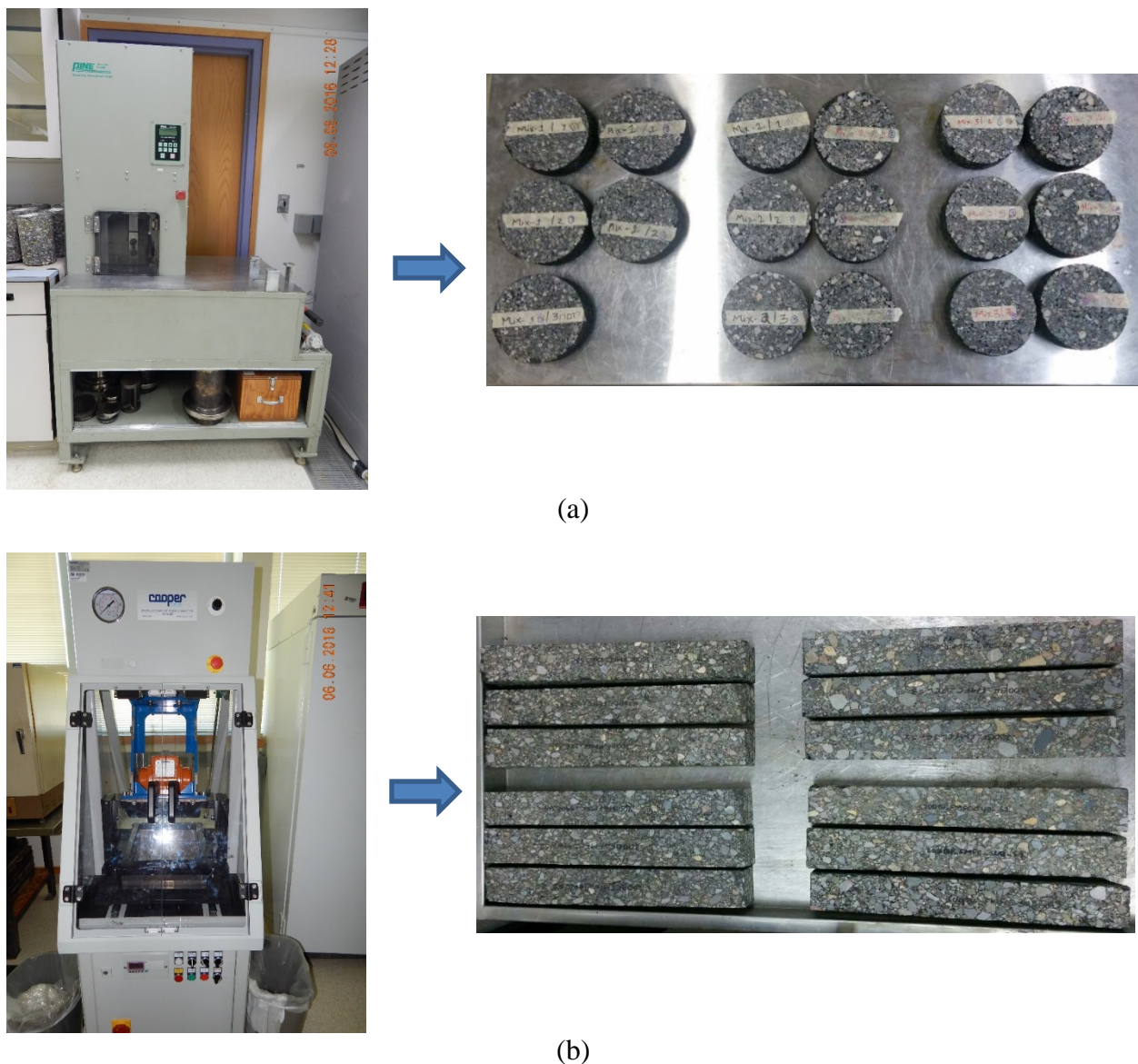


Figure 3.7: Laboratory Compaction; (a) Superpave Gyratory Compactor and cylindrical specimens; (b) Roller Compactor and beam specimens

3.4.3 Experimental design for laboratory mixed-laboratory compacted specimens

In this part of the study, the impact of compaction (field compaction and SGC) and mixing (laboratory and plant mixing) on cracking test results (only SCB) were determined. PMFC samples were collected (cored) from the roadway sections constructed with the production mixtures described in Section 3.4.2. Table 3.5 shows the experimental plan followed in this part of the study. By comparing test results from PMFC and PMLC specimens, the impact of compaction on test results was quantified. By comparing PMLC test results to LMLC test results, the impacts of mixing and batching (laboratory and plant) were determined.

Table 3.5: Experimental Plan to Investigate the Effect of Compaction and Mixing on Cracking Results

Test type	Mix Type	Comp.	Temp .	Repl.	Total Tests
SCB	M2 ¹	PMFC ²	25°C	6	6
SCB	M2	PMLC ³	25°C	4	4
SCB	M2	LMLC ⁴	25°C	4	4

Note: ¹ M2: Mix 2-PG70-22ER-Coarse gradation

² PMFC: Plant Mixed-Field Compacted;

³ PMLC: Plant Mixed-Laboratory Compacted;

⁴ LMLC: Laboratory Mixed-Laboratory Compacted.

3.5 TEST METHODS

Test methods followed in this study (SCB, IDT, BBF, DTCF, resilient modulus, DM and FN tests) to evaluate cracking and rutting performance of asphalt mixtures are presented in this Section.

3.5.1 Semi-Circular Bend (SCB) Test

SCB tests were conducted in this study to determine the cracking performance of asphalt mixtures. The test method for evaluating cracking performance of asphalt concrete at intermediate temperatures developed by Wu et al. (2005) was followed.

3.5.1.1 Sample Preparation

130 mm tall samples were compacted in the laboratory according to AASHTO T 312-12. Two samples with the thicknesses of 57 ± 2 mm were cut from each gyratory compacted sample using a high-accuracy saw (Figure 3.8a). Then the circular samples (cores) were cut into two identical halves (Figure 3.8b) using a special jig designed and developed at Oregon State University (OSU).

Wu et al. (2005) suggested performing tests on samples with different notch depths (25.4 mm, 31.8 mm and 38.0 mm). However, Ozer et al. (2016) and Nsengiyumva (2015) showed that reducing the notch depth reduces the variability. A similar conclusion was also derived based on the results of this study. For this reason, in this study, a 15 mm notch depth was selected for sample preparation. A notch along the axis of symmetry of each half was created with the table saw using another special cutting jig developed at OSU (Figure 3.8c). Notches were 15 ± 0.5 mm in length and 3 mm wide.

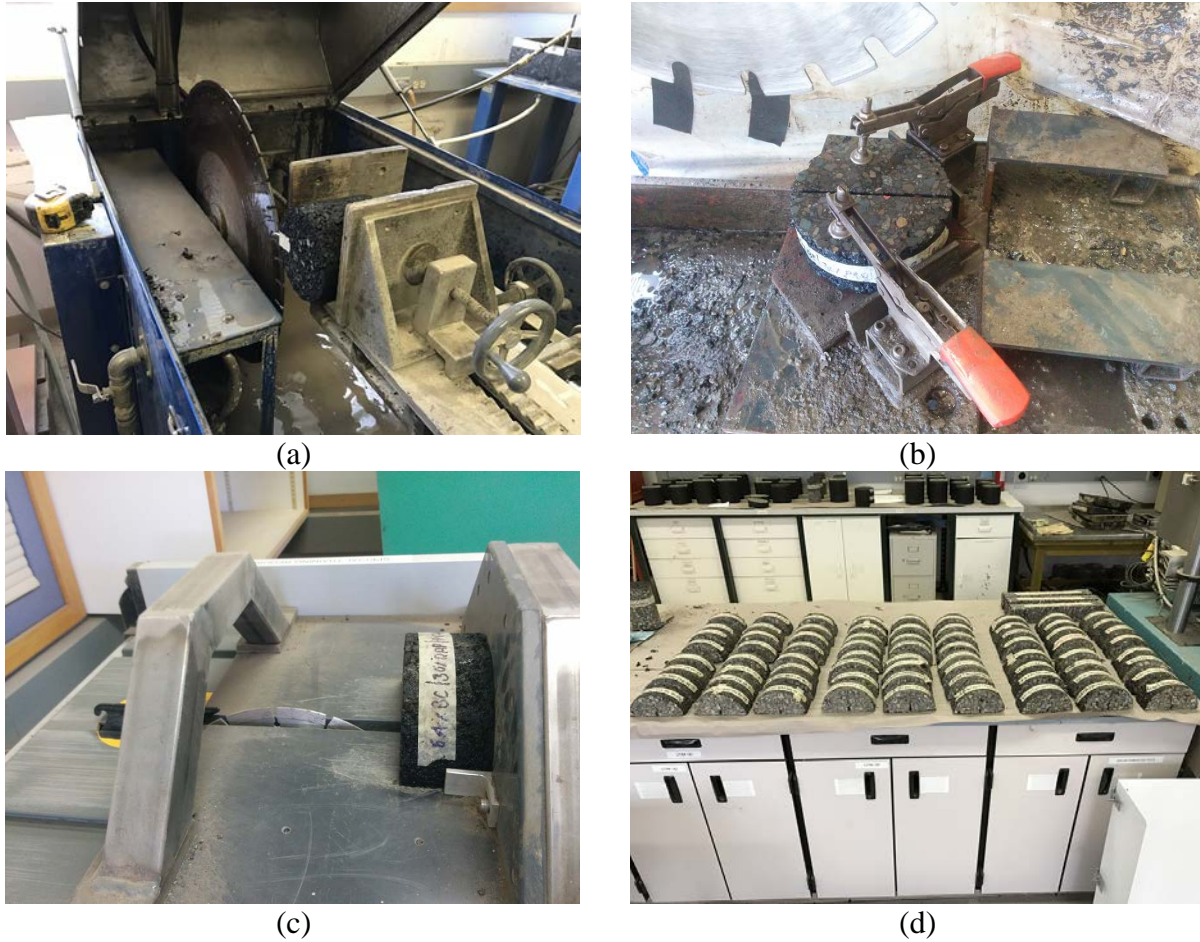


Figure 3.8: Cutting and Notching Procedure for SCB Sample Preparation

3.5.1.2 Testing

Tests were conducted at 25 °C with a displacement rate of 0.5 mm/min (AASHTO TP 105-13). Samples were kept in the chamber at the testing temperature for conditioning the day before being tested. The flat side of semi-circular samples was placed on two rollers (Figure 3.9). As a vertical load with constant displacement rate is applied on the samples, the applied load is measured (AASHTO TP 105-13). The test stops when the load drops below 0.5 kN. Fracture energy (G_f), fracture toughness (K_{IC}), secant stiffness (S) and flexibility index (FI) are the testing parameters obtained from this test. Procedures followed to calculate these test parameters are given in the next section.



Figure 3.9: SCB Loading Set-Up and Test

3.5.1.3 Parameters Obtained from SCB Test Results

This section describes the parameters obtained from SCB test results (displacement vs. load curves) including fracture energy (G_f), fracture toughness (K_{IC}), secant stiffness (S) and flexibility index (FI).

- **Fracture Energy (G_f)**

Fracture energy (G_f) is obtained by dividing the work of fracture (W_f) by the ligament area (A_{lig}) as shown in Equations 3.1 to 3.3. As the G_f increases, the work required for crack initiation and propagation increases. Therefore, asphalt mixtures with higher G_f values are expected to show higher resistance to cracking (Ozer et al. 2016). Work of fracture is the area under load versus displacement (P-u) curve (Figure 3.10). The test stops when the load drops below 0.5 kN. The remainder of the curve is extrapolated to estimate the area under the tail of the P-u curve. W_f is the sum of the area under the curve obtained from the test (W) and the extrapolated tail area (W_{tail}) as it is shown Figure 3.10.

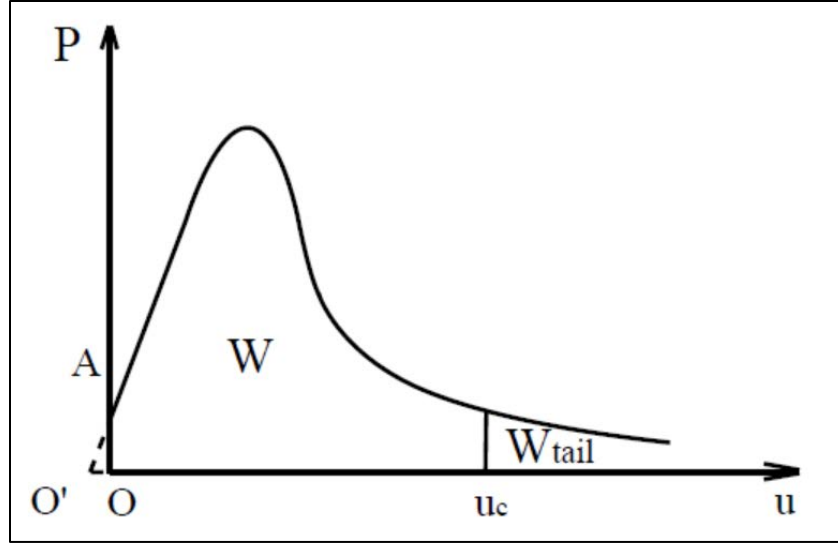


Figure 3.10: Load versus displacement (P-u) curve (AASHTO TP 105-13)

W_f is calculated as follows (AASHTO TP 105-13):

$$G_f = \frac{W_f}{A_{lig}} \quad 3.1$$

$$W_f = \int P \, du \quad 3.2$$

$$A_{lig} = (r-a) \cdot t \quad 3.3$$

Where:

G_f = fracture energy (kJ/m²),

W_f = work of fracture (kJ),

P = applied load (kN),

u = load line displacement (m),

A_{lig} = ligament area (m²),

r = sample radius (m),

a = notch length (m), and

t = sample thickness (m).

The quadrangle rule is used to calculate the area under the curve obtained from the test (W) using Equation 3.4 (AASHTO TP 105-13):

$$W = \sum_{i=1}^n (u_{i+1} - u_i) * (P_i) + \frac{1}{2} * (u_{i+1} - u_i) * (P_{i+1} - P_i) \quad 3.4$$

Where:

P_i = applied load (kN) at the i load step application,

P_{i+1} = applied load (kN) at the i+1 load step application,

u_i = load line displacement (m) at the i step, and

u_{i+1} = load line displacement (m) at the i+1 step.

A power function with a coefficient of -2 is used to fit the post-peak part of the P-u curve starting from the point at which the P value is lower than the 60% of the peak load. After fitting the curve, the coefficient c is obtained using Equation 3.5 (AASHTO TP 105-13). Then the area under the extrapolated tail portion (W_{tail}) is estimated using Equation 3.6 (AASHTO TP 105-13).

$$P = \frac{c}{u^2} \quad 3.5$$

$$W_{tail} = \int_{u_c}^{\infty} P \, du = \int_{u_c}^{\infty} \frac{c}{u^2} \, du = \frac{c}{u_c} \quad 3.6$$

Where:

u = integration variable equal to load line displacement (m), and

u_c = load line displacement value at which the test is stopped (m).

Consequently, total area under the curve (W_f) is obtained as follows (AASHTO TP 105-13):

$$W_f = W + W_{tail} \quad 3.7$$

- **Fracture Toughness (K_{IC})**

Fracture toughness (K_{IC}) is the stress intensity factor at peak load. It shows how much energy is required for crack formation. A higher K_{IC} value indicates higher brittleness of mixtures. The following equations are used to compute K_{IC} (AASHTO TP 105-13):

$$\frac{K_{IC}}{\sigma_0 \sqrt{\pi a}} = Y_{I(0.8)} \quad 3.8$$

$$\sigma_0 = \frac{P_{peak}}{2rt} \quad 3.9$$

$$Y_{I(0.8)} = 4.782 + 1.219 \left(\frac{a}{r} \right) + 0.063 \exp(7.045 \left(\frac{a}{r} \right)) \quad 3.10$$

Where:

P_{peak} = peak load (MN),

r = sample radius (m),

t = sample thickness (m),

a = notch length (m), and

$Y_{I(0.8)}$ = the normalized stress intensity factor (dimensionless).

- **Secant Stiffness (S)**

Secant stiffness (S) is the ratio of the peak load to the vertical deformation required to reach the peak deformation. Higher values for S indicate higher resistance to crack initiation and higher brittleness (Harvey et al. 2015).

$$S \text{ (KN/mm)} = \frac{\Delta y}{\Delta x} = \frac{\text{peak load}}{\text{vertical deformation at peak load}} \quad 3.11$$

- **Flexibility Index (FI)**

Flexibility index (FI) is the ratio of the fracture energy (G_f) to the slope of the line at the post-peak inflection point of the load-displacement curve (Figure 3.11). FI correlates with brittleness, and it was developed for asphalt materials by Ozer et al. (2016). Lower FI values show that the asphalt mixtures are more brittle and have a higher crack growth rate (Ozer et al. 2016). Flexibility index is calculated as follows:

$$FI = A * \frac{G_f}{\text{abs}(m)} \quad 3.12$$

Where:

G_f = fracture energy (KJ/m²),

abs(m) = absolute value of the slope at inflection point of post-peak load-displacement curve,

A = unit conversion factor and scaling coefficient.

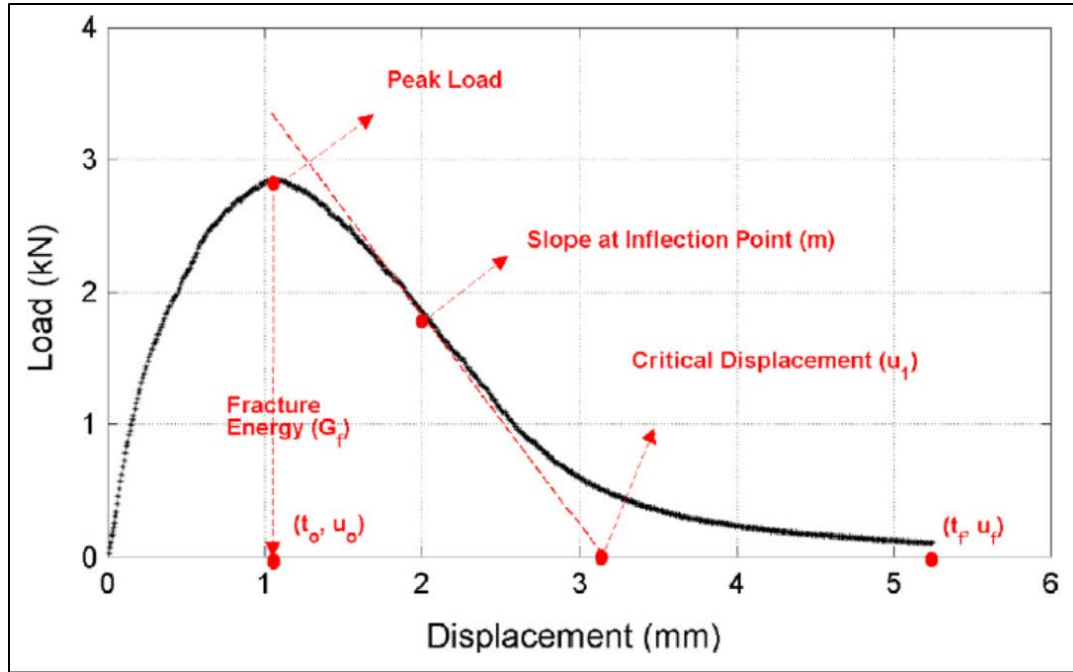


Figure 3.11: Illustration of load-displacement curve and slope at inflection point (m)

(Ozer et al. 2016)

3.5.1.4 Comparison of Fracture Energy (G_f) to Flexibility Index (FI)

Brittle mixtures require higher energy for crack initiation, but once the crack starts, it propagates rapidly. Conversely, ductile mixtures need less energy for crack initiation, but cracks propagate more slowly. Load-displacement curves of ductile and brittle mixtures are shown in Figure 3.12. The area under the load-displacement curve is higher for the brittle mixture compared to the ductile mixture. Thus, the brittle mixture seems to have higher G_f value. On the contrary, since the slope at the inflection point is also higher for the brittle mixture, the FI value decreases. The ductile mixture has a smaller area under the curve and smaller slope at the inflection point and it has higher FI than the brittle mixture. It can be concluded that FI is a better performance indicator than G_f since it properly describes crack initiation and propagation stages of the load-displacement curve (Ozer et al. 2016). Results of this study also show that FI is able to identify the effects of several different mixture properties on cracking resistance.

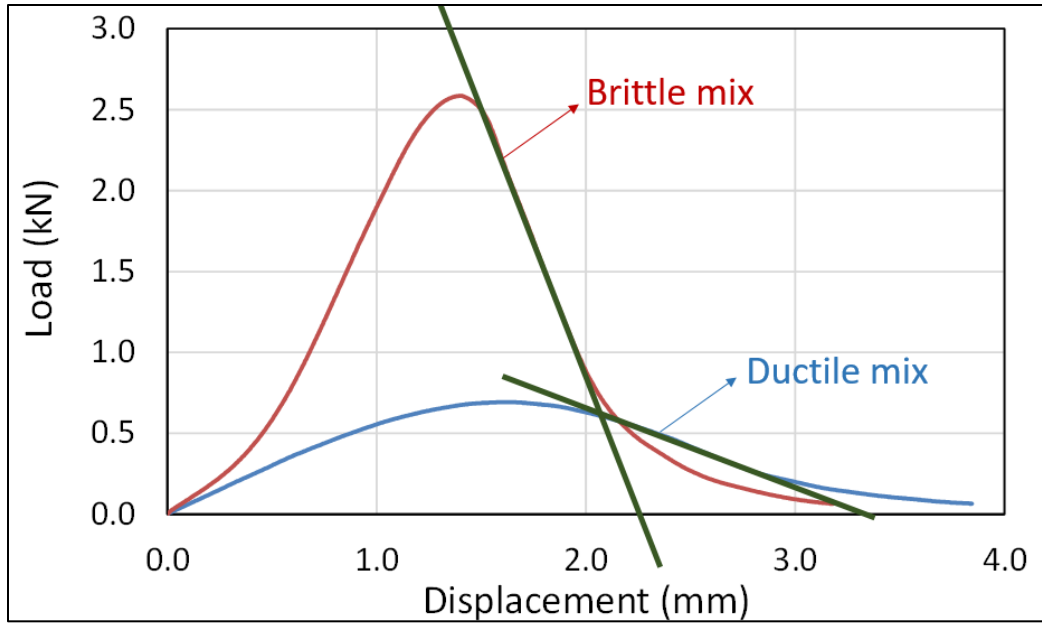


Figure 3.12: Illustration of load-displacement curve of ductile and brittle mixtures

3.5.2 Indirect Tension (IDT) Test

The IDT experiments are carried out by loading cylindrical specimens along their vertical diametric planes. The peak load at failure is used to calculate the IDT strength of the specimen. The ASTM D6931-12 specification is followed to conduct this experiment. The test setup is shown in Figure 3.13.

Sample preparation and testing procedure:

- Cylindrical specimens of 150 mm diameter are produced using SGC per the AASHTO T312 specification.
- The SGC specimen is cut into slices 50 mm in height using a high precision saw. A minimum of three replicate specimens are prepared.
- Samples are placed in the environmental chamber set at $25 \pm 1^\circ\text{C}$ for 2 hours to ensure the specimen is at test temperature prior to beginning the test.
- In this study, deformation rate is set at 50 mm/min and a compressive load is applied until the specimen fails. The load versus displacement curve is plotted and the peak load is recorded.



(a)



(b)

Figure 3.13: Indirect tension test; (a) Cylindrical specimens from SGC; (b) IDT test apparatus

Using the measured peak load, tensile strength for each specimen ($S_{t,n}$) is calculated as:

$$S_{t,n} = \frac{2 \times P_{f,n}}{\pi \times b_n \times D_n} \quad 3.13$$

Where,

$P_{f,n}$ = maximum load observed for specimen, n;

b_n = thickness of the specimen, n;

D_n = diameter of the specimen, n.

3.5.3 Bending Beam Fatigue (BBF) Test

The BBF test, or four-point bend test, is used to estimate fatigue life of pavement layers under repeated traffic loading. In this test, failure is defined as the load cycle at which the specimen undergoes a 50 percent reduction in stiffness relative to the initial stiffness. This test follows the AASHTO T321 specification. The test setup is shown in Figure 3.14.

Sample preparation and testing procedure:

- Sample slabs are prepared using a laboratory roller compactor. The dimensions of the prepared slab specimens were 400 mm (length) by 260 mm (width) by 60 mm (thickness).

- With the help of a saw, these slabs were cut into beam specimens of 380 ± 6 mm in length, 50 ± 6 mm in height and 63 ± 6 mm in width. Three replicate test specimens can be obtained from one slab.
- Samples are then placed in the environmental chamber set at $20 \pm 0.5^\circ\text{C}$ for 2 hours to ensure the specimen is at the test temperature prior to beginning the test.
- Clamps of the four-point bending device are raised and the sample is slid into position. Once the specimen is placed, clamps are lowered and the LVDT is adjusted to read between ± 2 mm.
- The desired strain and loading frequency are entered into the test software. In this study, 400 microstrain and 10 Hz loading frequency were selected.
- The test is terminated when the stiffness of the sample reduces to 50 percent of its initial value. The percent reduction in stiffness versus number of cycles is plotted and the number of cycles required for 50 percent reduction in stiffness is noted.



Figure 3.14: Bending beam fatigue test; (a) Beam specimens prepared with roller compactor; (b) four-point bending test apparatus

3.5.4 Direct Tension Cyclic Fatigue (DTCF) Test

The DTCF test is used to determine the damage characteristic curve of asphalt mixtures subjected to direct tension cyclic fatigue loading. The fatigue test consists of two parts: first, a dynamic modulus fingerprint test to estimate the stiffness of the specimen and then a cyclic fatigue test. In this test, repeated cyclic tensile loads are applied to cylindrical asphalt specimens (150 mm height and 100 mm diameter) until failure. The applied stress and axial strain responses are measured and used to calculate the parameters characterizing cracking resistance. The test process is controlled by the S-VECD fatigue program in the equipment software. This study

followed the AASHTO TP 107 specification to conduct DTCF experiments. The test setup is shown in Figure 3.15.



Figure 3.15: DTCF test setup

Sample preparation and testing procedure:

- Cylindrical specimens of 150 mm diameter and 170 mm height are produced from SGC specimens (AASHTO T312). Then, 100 mm diameter samples were cored and their edges were cut off to obtain 150 mm tall samples.
- The end plates and the ends of the specimen surface are wiped clean using a small amount of acetone.
- About 100 g of adhesive (DEVCON 10110) is weighed out and is distributed uniformly on the end plates and ends of the sample. Then the sample and end plates are placed in the gluing jig and suitable load is applied onto the specimen. The excess glue is scraped off before the glue sets.
- After the curing time has passed, the sample is taken out of the gluing jig and mounting studs for the axial sensors are attached to the sides of the sample using epoxy cement. The gluing process is illustrated in Figure 3.16.

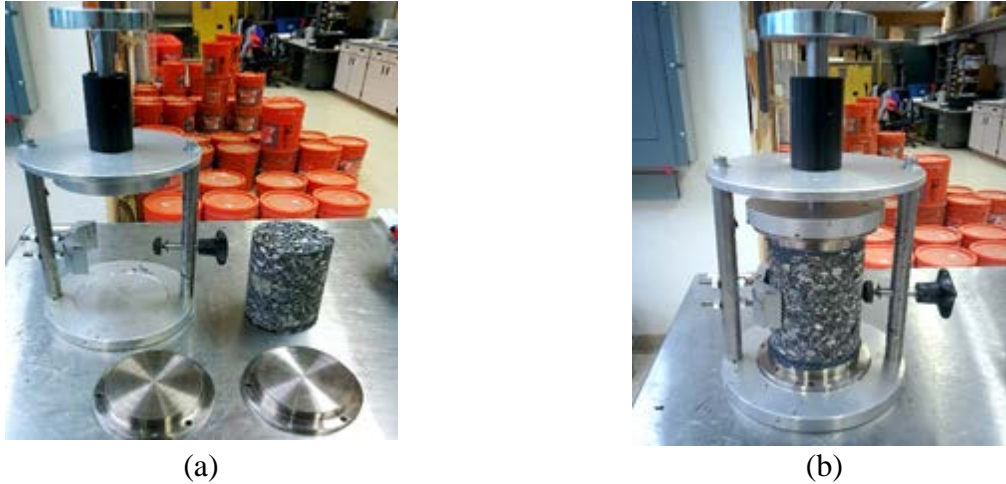


Figure 3.16: Gluing setup for DTCF testing

- The sample is placed in the environmental chamber set at $20 \pm 0.5^\circ\text{C}$ for 2 hours to ensure the sample reaches the test temperature before beginning the test.
- Once the sample attains temperature equilibrium, the sample is bolted to the bottom support of the test equipment. The actuator is brought into position and the upper loading platen is bolted to the specimen.
- LVDTs are attached to the specimen and the sample is left in the chamber for another hour to reach the test temperature.
- A fingerprint dynamic modulus test is run at 10 Hz frequency at target temperature with a target strain range of 50 to 75 microstrain. After the fingerprint test, the sample is allowed to rest for a period of 20 minutes.
- After the rest period, the cyclic fatigue test is initiated with the peak-to-peak on-specimen strain amplitude of 200 microstrain.
- The test is terminated after 100,000 cycles or when the specimen fails from fatigue cracking.

3.5.5 Resilient Modulus (MR) Test

The resilient modulus is defined as the ratio of stress to strain for an instantaneous load. It gives a measure of stiffness for the asphalt mixtures. In this study, the ASTM D7369-11 specification is followed to conduct resilient modulus experiments. The test setup is shown in Figure 3.17.

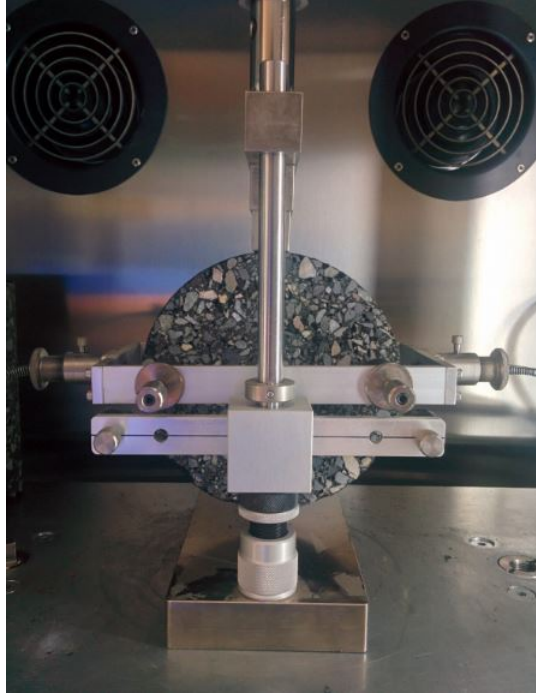


Figure 3.17: Resilient modulus test setup

Sample preparation and testing procedure:

- Cylindrical specimens of 150 mm diameter are produced using SGC (AASHTO T312).
- The SGC core is cut into slices of 50 mm height using a high precision saw. A minimum of three replicate samples are prepared.
- Samples are placed in the environmental chamber set at $25 \pm 1^\circ\text{C}$ for 2 hours to ensure the specimen is at test temperature prior to beginning the test.
- At the end of the conditioning period, an initial vertical contact load is applied to the specimen. The contact load is 4% of the maximum load ($0.04P_{\text{max}}$) and is not less than 22.2 N but not more than 89.0 N.
- After applying the contact load, a cyclic load is applied to the specimen. The cyclic load is calculated as:

$$P_{\text{cyclic}} = P_{\text{max}} - P_{\text{contact}} \quad \mathbf{3.14}$$

- Resilient modulus is calculated automatically by the test software. It is essentially the ratio of peak stress to peak strain for every load cycle.

3.5.6 Dynamic Modulus (DM) Test

Asphalt concrete mixtures are viscoelastic materials that show both viscous and elastic behavior. At lower temperatures and higher loading frequencies, elastic behavior becomes more dominant while viscous components are more apparent at higher temperatures and lower loading frequencies. DM tests are conducted to characterize the elastic modulus of asphalt concrete mixtures at different loading frequencies and temperatures. DM tests are performed at low strain levels (about $100\mu\epsilon$) to determine the elastic modulus in the linear viscoelastic range. The effects of loading time and temperature on elastic modulus is modeled and presented in the form of master curves (Norouzi et al. 2016).

The DM test is a strong indicator of asphalt mixture performance. Dynamic modulus and phase angle are two performance variables obtained from DM tests. Dynamic modulus shows how stiff an asphalt mixture is. A higher dynamic modulus value represents a higher stiffness. The time delay between the time point at which peak stress is applied and the time point at which peak strain is observed is used to calculate phase angle. The phase angle represents viscoelastic characteristics of asphalt mixtures. A higher phase angle indicates that the samples are more viscous, more susceptible to rutting and more resistant to cracking (Darnell and Bell 2015). In this study, the AASHTO TP 79 specification was followed to conduct the dynamic modulus test. The unconfined test was carried out. The test setup is shown in Figure 3.18.



Figure 3.18: Dynamic modulus test setup

Sample preparation and testing procedure:

- In this study, 170 mm tall samples were prepared by using gyratory compaction according to AASHTO PP 60-14. Then, 100 mm diameter samples were cored and their edges were cut off to obtain 150 mm tall samples.
- The gauge points were attached to the specimen at a gauge length of 70 ± 1 mm, measured center-to-center of the gauge points. The process is illustrated in Figure 3.19.



Figure 3.19: Gauge point gluing setup

- Specimens were then placed in the environmental chamber at the testing temperatures for conditioning. Samples were kept in the chamber at the testing temperatures the day before being tested. Each specimen was tested at 4°C, 20°C and 40°C temperatures and 0.1 Hz, 0.5 Hz, 1 Hz, 5 Hz and 10 Hz frequencies. The frequency of 0.01 Hz was also used only for tests conducted at 40°C. These loading frequencies simulate different traffic speeds. Higher frequencies represent higher vehicle speeds.
- The specimen to be tested was placed between the bottom and top loading platens. Then the specimen-mounted deformation-measuring system was installed on the gauge points.
- The chamber is closed and once the specimen reaches the test temperature, cyclic loads that can create a strain level of $100\mu\epsilon$ are applied.
- The calculation of dynamic modulus and phase angle is performed automatically by the test software.

- After conducting the tests, master curves were developed for dynamic modulus and phase angle following the AASHTO PP 61-13 procedure. Master curves display phase angle and dynamic modulus with respect to loading frequencies.

3.5.7 Flow Number (FN) Test

The flow number (FN) test is a performance test for evaluating rutting resistance of asphalt concrete mixtures (Bonaquist et al. 2003). In this test, while constant deviator stress is applied at each load cycle on the test sample, permanent strain at each cycle is measured (Figure 3.20). Permanent deformation of asphalt pavements has three stages: 1) primary or initial consolidation, 2) secondary, and 3) tertiary or shear deformation (Biligiri et al. 2007). Figure 3.20 shows three stages of permanent deformation. FN is the loading cycle at which the tertiary stage starts after the secondary stage.

In this study, testing conditions and criteria for FN testing described in AASHTO TP 79-13 for unconfined tests were followed. The recommended test temperature, determined by LTPPBind Version 3.1 software, is the average design high pavement temperature at 50% reliability for cities in Oregon with high populations and at a depth of 20 mm (0.79 in) for surface courses (Rodezno et al. 2015). Tests were conducted at a temperature of 54.7°C with average deviator stress of 600 kPa and minimum (contact) axial stress of 30 kPa. For conditioning, samples were kept in a conditioning chamber at the testing temperature a day prior to being tested. To calculate FN in this study, the Francken model was used (discussed below).

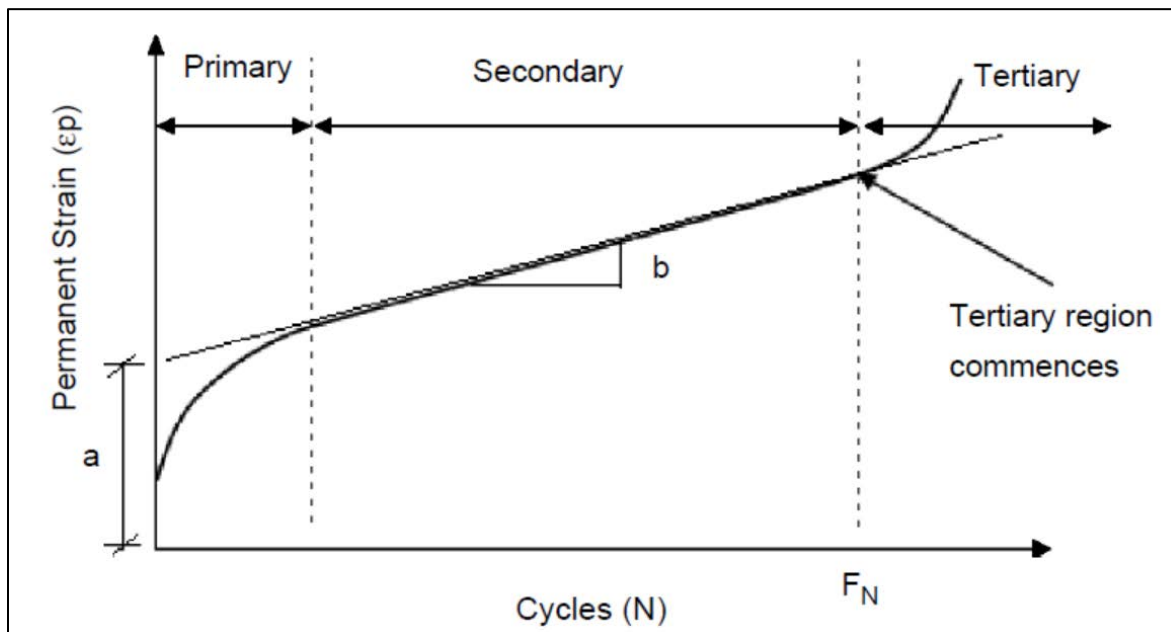


Figure 3.20. Relationship between permanent strain and load cycles in FN test

(Biligiri et al. 2007)

Minimum FN values (calculated by using the Francken model) for different traffic levels recommended by AASHTO TP 79-13 are given in Table 3.6 (Rodezno et al. 2015).

Table 3.6: Minimum Average FN Requirement for Different Traffic Levels (AASHTO TP 79-13)

Traffic (million ESALs)	Minimum Average FN Requirement
<3	NA
3 to <10	50
10 to <30	190
≥30	740

Note: NA= not applicable.

3.5.7.1 Francken model

The Francken Model was developed for triaxial and uniaxial repeated-load tests for different temperatures and stress levels (Francken 1977). A study carried out by Biligiri et al. (2007) showed that this model calculates FN more accurately compared to other mathematical models. This model can also represent all three stages of deformation (1.primary or the initial consolidation of the mix, 2. secondary, and 3. tertiary or shear deformation) more properly. Moreover, Dongre et al. (2009) confirmed the robustness of Francken model by fitting FN data obtained from field projects. The model is given as follows:

$$\epsilon_p(N) = AN^B + C(e^{DN} - 1) \quad 3.15$$

Where:

$\epsilon_p(N)$ = permanent deformation or permanent strain from F_n test,

N = number of loading cycles, and

A, B, C, D = regression constants.

The rate of change of the slope of the permanent strain is obtained by taking the second derivative of the Francken model (Equation 3.16). The inflection point, at which the sign of the rate of change of slope changes is considered as the FN and indicates when the tertiary stage begins. FN is the number of cycles at which the second derivative of the Francken model is zero. The second derivative of the model is as follows (Dongre et al. 2009):

$$\frac{\partial^2 \epsilon_p}{\partial N^2} = A * B * (B-1) * N^{B-2} + (C * D * e^{D * N}) \quad 3.16$$

The model shown in Equation 3.15 is fitted to the permanent strain versus the number of cycles for each sample. After estimating the regression constants (A, B, C, and D), to find the number of load cycles at the inflection point, FN is computed at the point which Equation 3.16 (second derivative of Francken model) is equal to zero. In this study, a code developed by Coleri et al. (2017) is used to analyze the data and calculate regression constants (A, B, C, and D) of the Francken model to find the FN for each test.

3.6 RESULTS AND DISCUSSION

3.6.1 Plant Mixed-Field Compacted (PMFC) Specimens

The purpose of testing PMFC samples was to evaluate the effectiveness of each test in determining the cracking performance of in-situ asphalt pavements. The subsequent sections present the results of SCB, IDT and BBF tests used in this study. DTCF tests were not carried out with field specimens since it was not possible to obtain 6-inch-tall specimens from field sections due to limited layer thicknesses.

3.6.1.1 Semi-Circular Bend (SCB) Test

SCB tests were conducted on the field specimens obtained from four different pavement sections as discussed in Section 3.4.1. Cores of 150 mm diameter were obtained from these sections. Two samples with the thicknesses of 57 mm were cut and semi-circular samples were prepared to conduct SCB experiments by following the process outlined in Section 3.5.1. For each field section, three notch depths were used (1.0 in., 1.25 in. and 1.5 in.) and for each notch depth, three replicate specimens were tested in this study. A total of 36 tests were conducted and four parameters (fracture energy, fracture toughness, secant modulus and flexibility index) were calculated for each test.

The results of the SCB tests are presented in Figure 3.21 to Figure 3.24. Figure 3.21 shows calculated average fracture energy for each section while Figure 3.22 to Figure 3.24 depicts the fracture toughness, secant modulus and flexibility index of the four field sections, respectively. It was observed that the fracture energy parameter was not able to differentiate the fatigue performance of the field sections and cannot identify the sections with poor cracking performance, while the flexibility index was successful in predicting the in-situ cracking performance. The flexibility indices of tested samples from 99E and 99W (the sections with severe cracking – See Appendix A and Section 3.4.1) were much lower than the samples from Junction City (OR99-U) and Sublimity (US20-U) (sections with high cracking performance – See Appendix A and Section 3.4.1). Field performance data from ODOT's PMS for these four sections (See Appendix A) shows that sections 99E and 99W had severe cracking while Junction City and Sublimity sections were in good condition. Therefore, it can be concluded that the flexibility index parameter is an effective parameter in predicting cracking performance of asphalt concrete pavement structures. From Figure 3.22 and Figure 3.23, it was also observed that fracture toughness (K_{IC}) and secant modulus (S) also correlate well with cracking resistance. Lower values

of K_{IC} and S indicate more ductile materials that have higher crack propagation resistance.

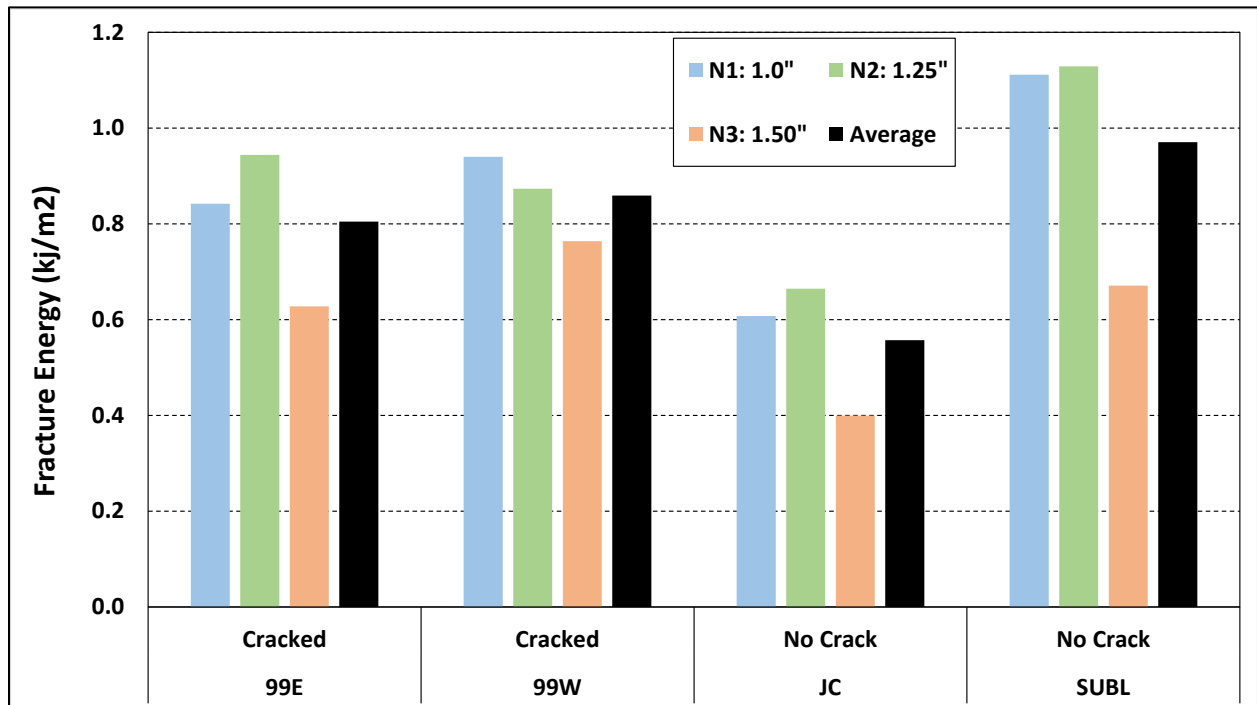


Figure 3.21: Fracture energy for PMFC samples

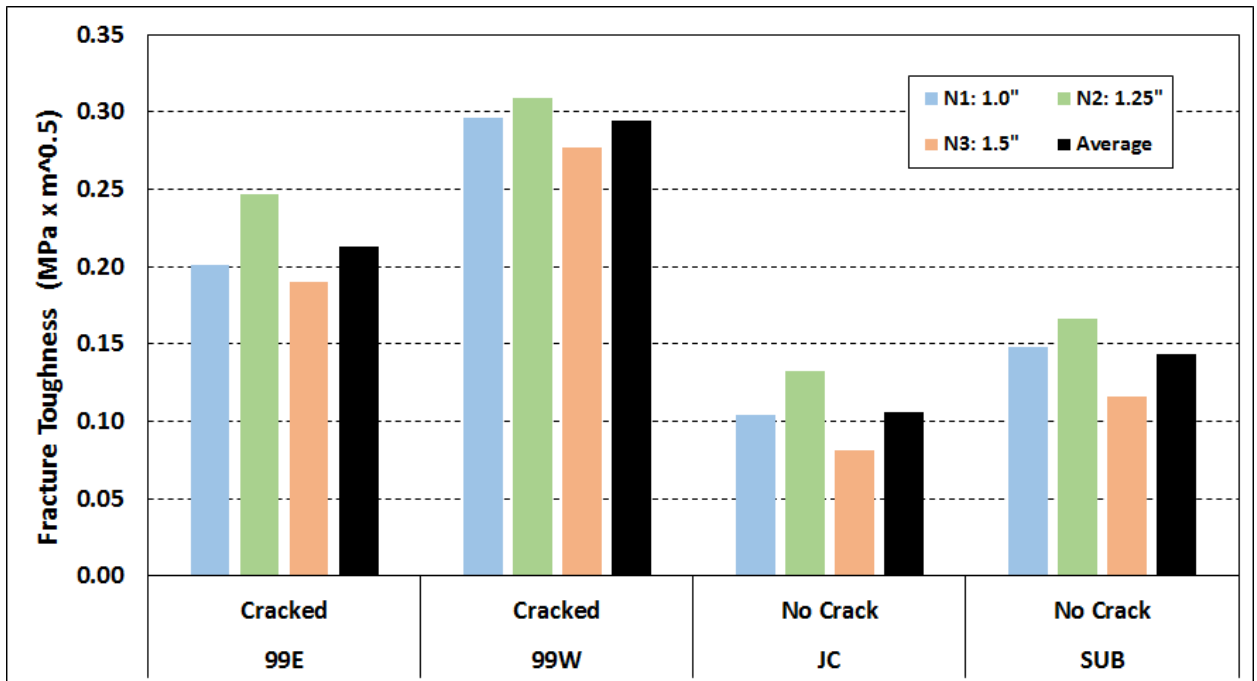


Figure 3.22: Fracture toughness for PMFC samples

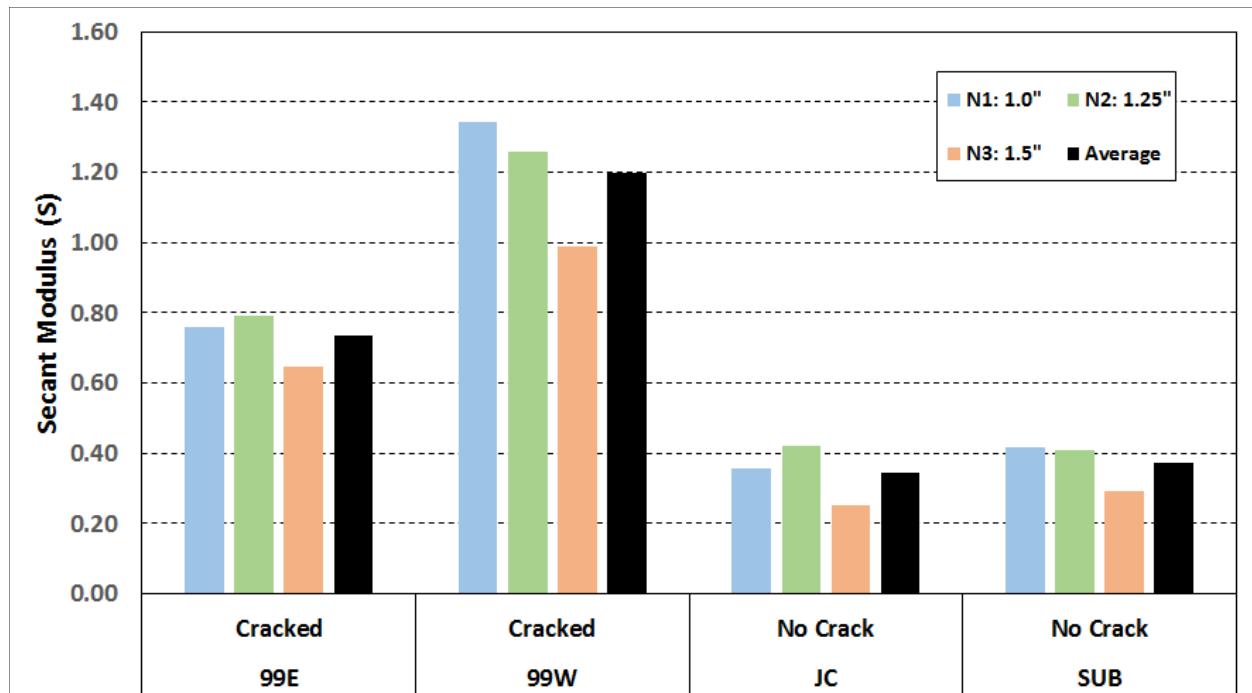


Figure 3.23: Secant modulus for PMFC samples

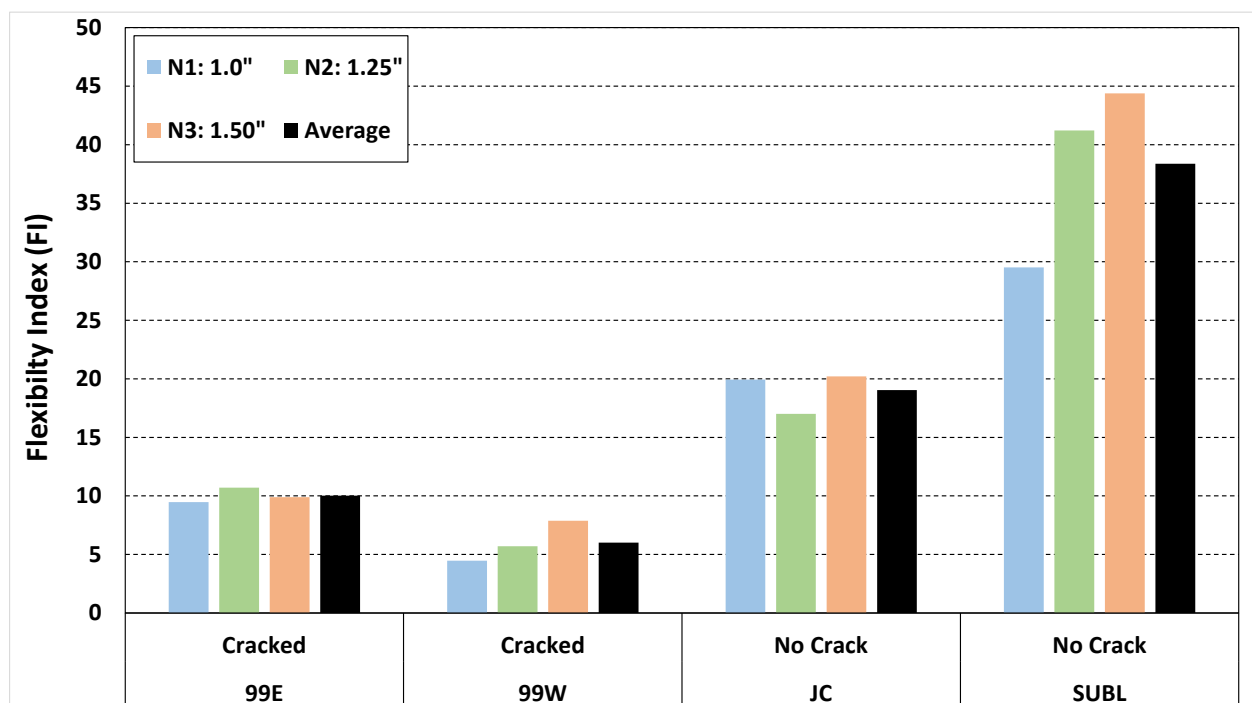


Figure 3.24: Flexibility index from SCB test for PMFC samples

Figure 3.25 illustrates the flexibility index values of laboratory mixed-laboratory compacted specimens from another research study performed at Oregon State University (Coleri et al. 2017). In this study, SCB tests were carried out with samples with two RAP contents (30% and 40%), three different binder contents (6%, 6.4% and 6.8%), and three binder grades (PG 58-34, PG 64-22 and PG 76-22). Four replicate samples were tested for each combination and a total of 72 tests were conducted.

As is shown in Figure 3.25, FI increases as the binder content increases for mixtures with the same RAP contents. Asphalt mixtures with lower binder contents are more brittle and more susceptible to cracking. Results also show that asphalt mixtures with 30% RAP have higher FI than the asphalt mixtures with 40% RAP. Higher RAP contents result in more brittle mixes and less cracking resistance. Moreover, using softer binders increases FI. As was expected, the mixture with the softest binder grade (PG 58-34), the highest binder content (6.8%) and the lowest RAP content has the greatest FI. Conversely, the mixture with PG 76-22 binder grade, 6% binder content and 40% RAP content shows the lowest FI value. All these logical results further suggest that slight changes in mixture properties can effectively be captured by the SCB test and flexibility index parameter.

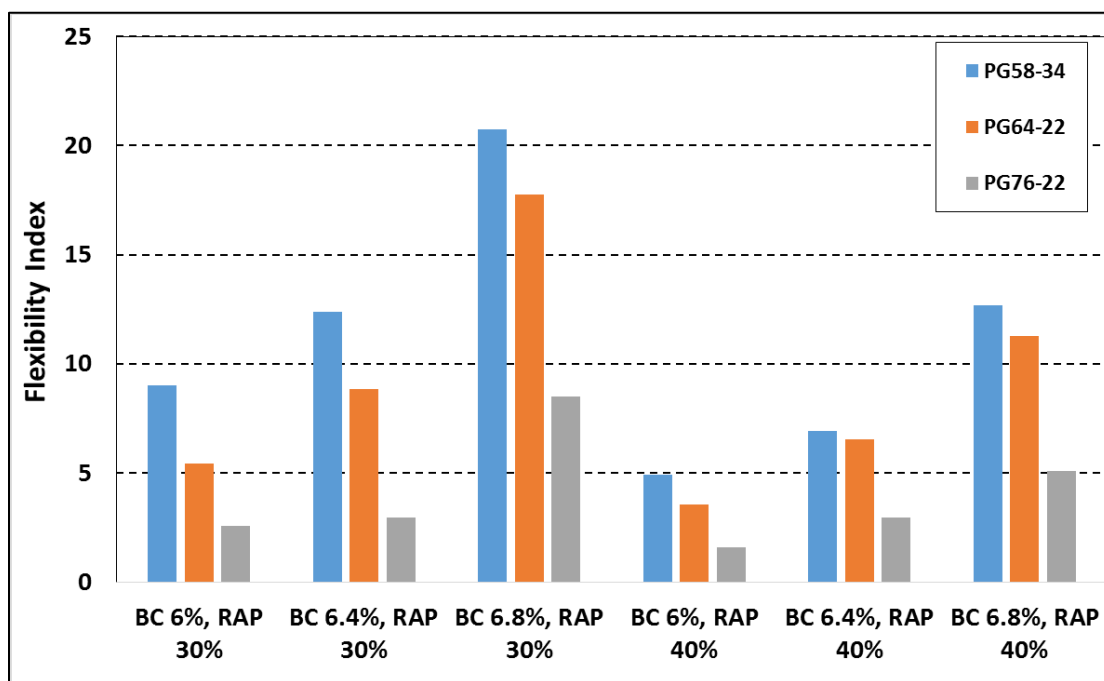


Figure 3.25: Flexibility index for mixtures with different RAP contents (30% and 40%), binder grades (PG 58-34, PG 64-22, and PG 76-22), and binder contents (6%, 6.4%, and 6.8%) (Coleri et al. 2017)

3.6.1.2 Indirect Tension (IDT) Test

IDT tests were conducted with the field cores from the same four field sections discussed in the previous section and Section 3.4.1. Similar to the SCB test, 150 mm diameter cores were obtained from these sections. 50 mm thick slices were then cut from these cores. Six replicate specimens were tested for each section and a total of 24 tests were conducted. Tensile strength from each test was determined by following the procedure outlined in Section 3.5.2. Test results for all field sections are presented in Figure 3.26. The colored bars represent the average strength from six replicate experiments while the length of the error bar on each bar represents the variability of the measured strength for each section (error bar length = two standard deviations). It can be observed that the tensile strength of 99E and 99W (severely cracked sections) are higher than that of Junction City and Sublimity (no cracking sections). Higher tensile strength suggests lower ductility for specimens from 99E and 99W sections and therefore cracking resistances of these two sections are expected to be lower than the sections in Junction City and Sublimity. These results agree with the data from ODOT PMS. Hence, it was concluded that the tensile strength parameter obtained from IDT was successful in evaluating the fatigue performance of in-situ pavements. Also, using the same test results, flexibility indices were determined and shown in Figure 3.27. It can be observed that the flexibility indices from IDT were in agreement with the flexibility indices for SCB test results given in Section 3.6.1.1.

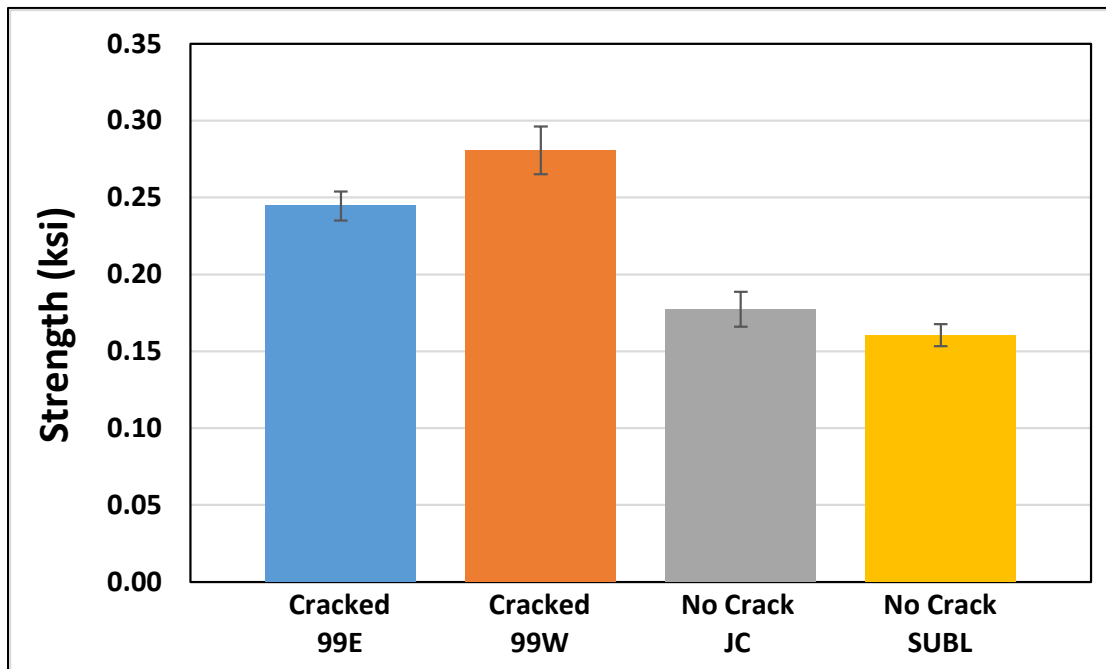


Figure 3.26: Tensile strength for PMFC samples

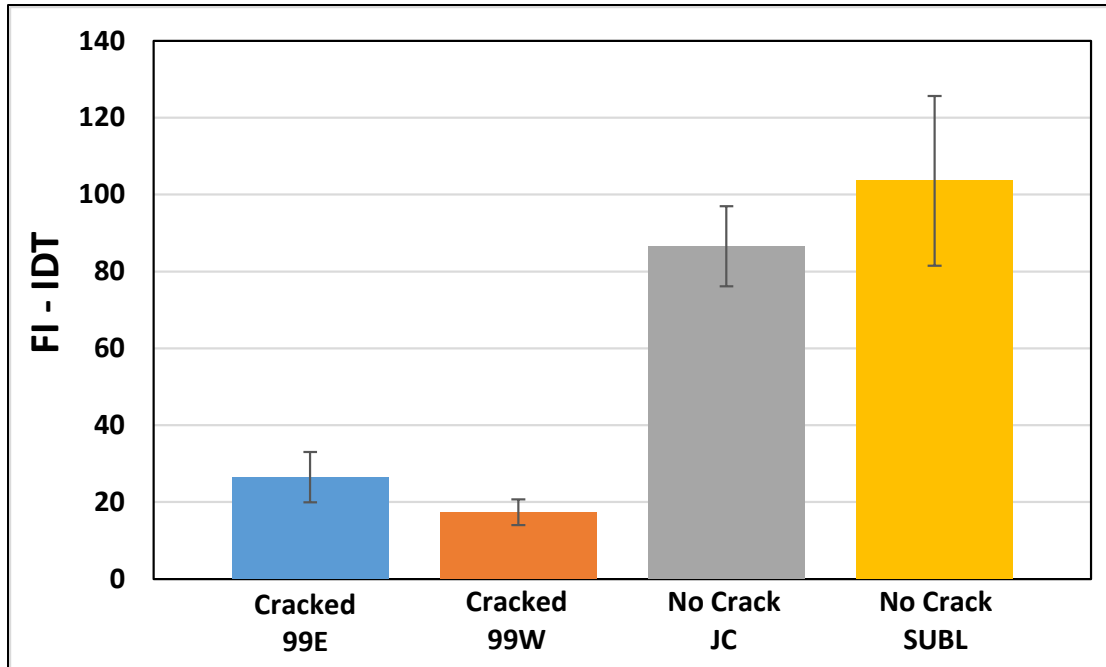


Figure 3.27: Flexibility index from IDT test for PMFC samples

3.6.1.3 Bending Beam Fatigue (BBF) Test

Asphalt concrete slabs obtained from the four pavement sections (Figure 3.4b) were cut in the laboratory to obtain beam samples with 50 mm height, 63 mm width and 380 mm length. Three replicate specimens for each section and a total of nine specimens were prepared and tested at a 400 $\mu\epsilon$ strain level and 10 Hz loading frequency.

The results from the BBF test are presented in Figure 3.28. In this test, fatigue life is defined as the number of load cycles that need to be applied to reach 50% reduction in stiffness. It can be observed from Figure 3.28 that measured fatigue lives for the sections 99E and 99W are higher than the fatigue lives for the samples from sections Junction City and Sublimity. These results contradict the performance data from ODOT's PMS (Appendix A). Hence, it can be concluded that the BBF test is not effective in predicting in-situ pavement fatigue performance. Since BBF is accepted to be an effective test to characterize bottom-up fatigue cracking resistance, it may not be capturing the cracking resistance of the asphalt mixtures that are likely to fail from top-down cracking, which is the most common distress type in Oregon (Williams and Shaidur 2015). Also, the coefficient of variation between the replicates was high as compared to SCB and IDT tests. Further investigations are necessary to study the effectiveness of the BBF test in evaluating the pavement performance.

It should also be noted that field sampling for BBF testing is extremely time consuming and labor intensive. For sections with thick asphalt layers, the heavy weight of the cut asphalt block requires a small-scale crane or a forklift to remove the cut block from the pavement. In addition, cutting BBF test samples from the heavy asphalt blocks requires the use of a concrete chainsaw or a handheld chop saw to reduce the size of the field

block since it is not possible to fit the field block into the stationary laboratory saw (Figure 3.4c). All these factors increase the cost of BBF testing with field cores and reduce practicality.

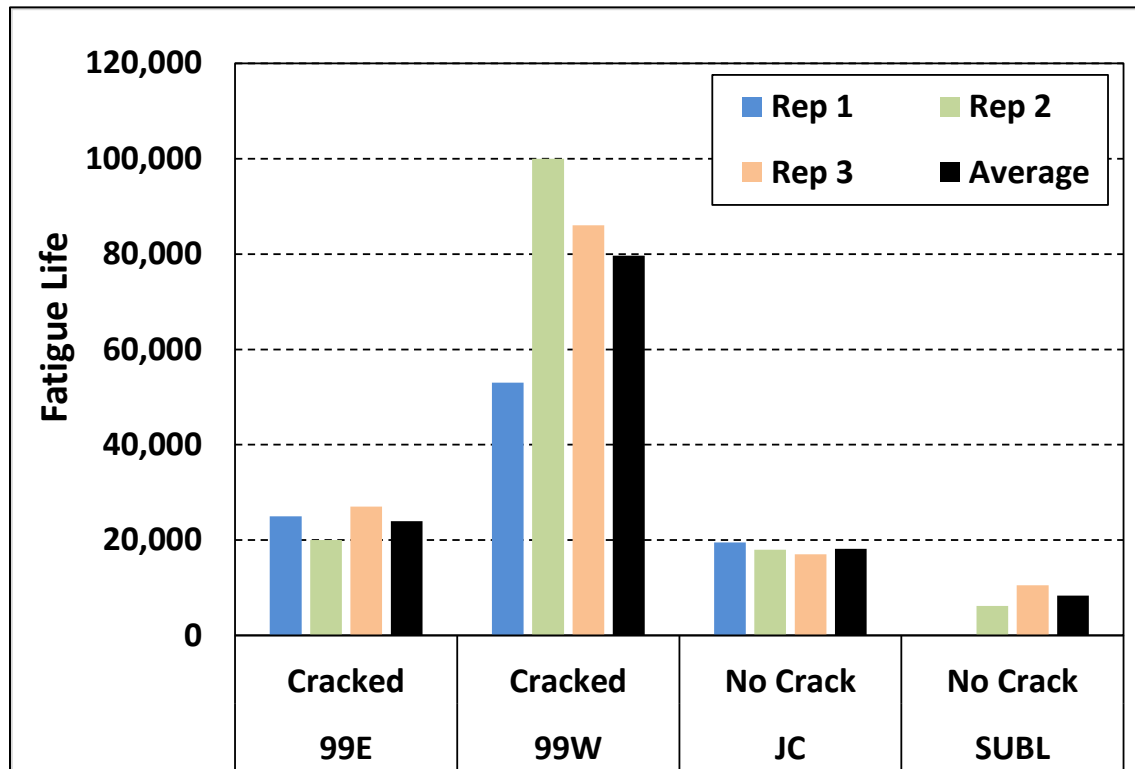


Figure 3.28: Fatigue life from BBF test for PMFC samples

3.6.1.4 Resilient Modulus (M_R) Test

The resilient modulus is a measure of stiffness (elastic properties) of the asphalt material. Similar to SCB and IDT test, 150 mm diameter cores were obtained from the four field sections. Slices of 50 mm were cut from these cores. Five replicate tests were conducted for each section and a total of 20 tests were carried out. Results are presented in Figure 3.29. Higher resilient modulus values suggest lower ductility for specimens from 99E and 99W sections and therefore cracking resistances of these two sections are expected to be lower than the sections in Junction City and Sublimity. These results agree with the performance data from the ODOT PMS. These results are also in agreement with the SCB and IDT results. Hence, it was concluded that the resilient modulus test can be an effective experiment to evaluate the fatigue performance of in-situ pavements.

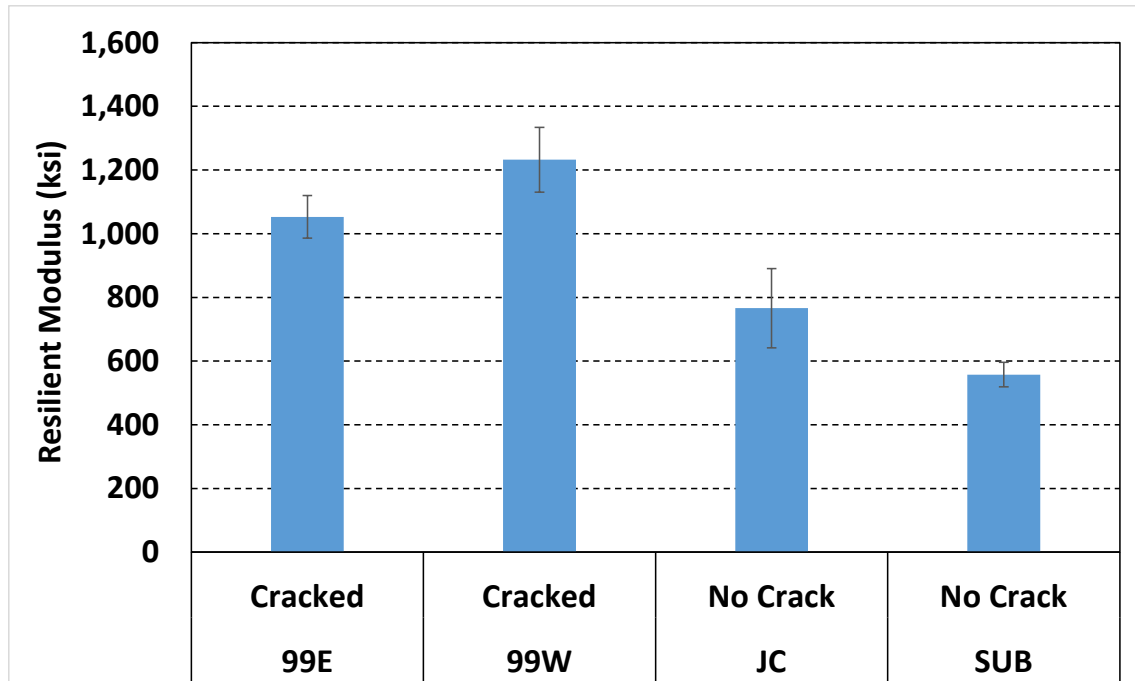


Figure 3.29: Resilient modulus for FMFC samples

3.6.1.5 One-to-One Correlations Between the Output Parameters of Different Tests

Figure 3.30 illustrates the correlations between the output parameters of different tests. Figure 3.30a shows that fracture energy and flexibility index parameters calculated using SCB test results are not correlated. Since flexibility index was determined to be highly correlated with measured field cracking performance, low correlation between flexibility index and fracture energy is a result of the inability of fracture energy parameter in explaining in-situ cracking performance.

Figure 3.30b depicts the correlation between flexibility indices obtained from SCB and IDT tests. The strong correlation between the flexibility indices obtained from SCB and IDT tests indicated that both tests can be used to characterize cracking resistance of asphalt mixtures.

Figure 3.30c shows that the correlation between SCB flexibility index and BBF fatigue life is low. Since flexibility index was determined to be highly correlated with measured field cracking performance, low correlation between flexibility index and BBF fatigue life is a result of the inability of fatigue life parameter to explain in-situ cracking performance.

The strong correlation between resilient modulus and SCB flexibility index given in Figure 3.30d proves that resilient modulus test can be an effective alternative to SCB testing. However, it should be noted that resilient modulus test requires a high-cost hydraulic or pneumatic test system to be able to apply cyclic loads.

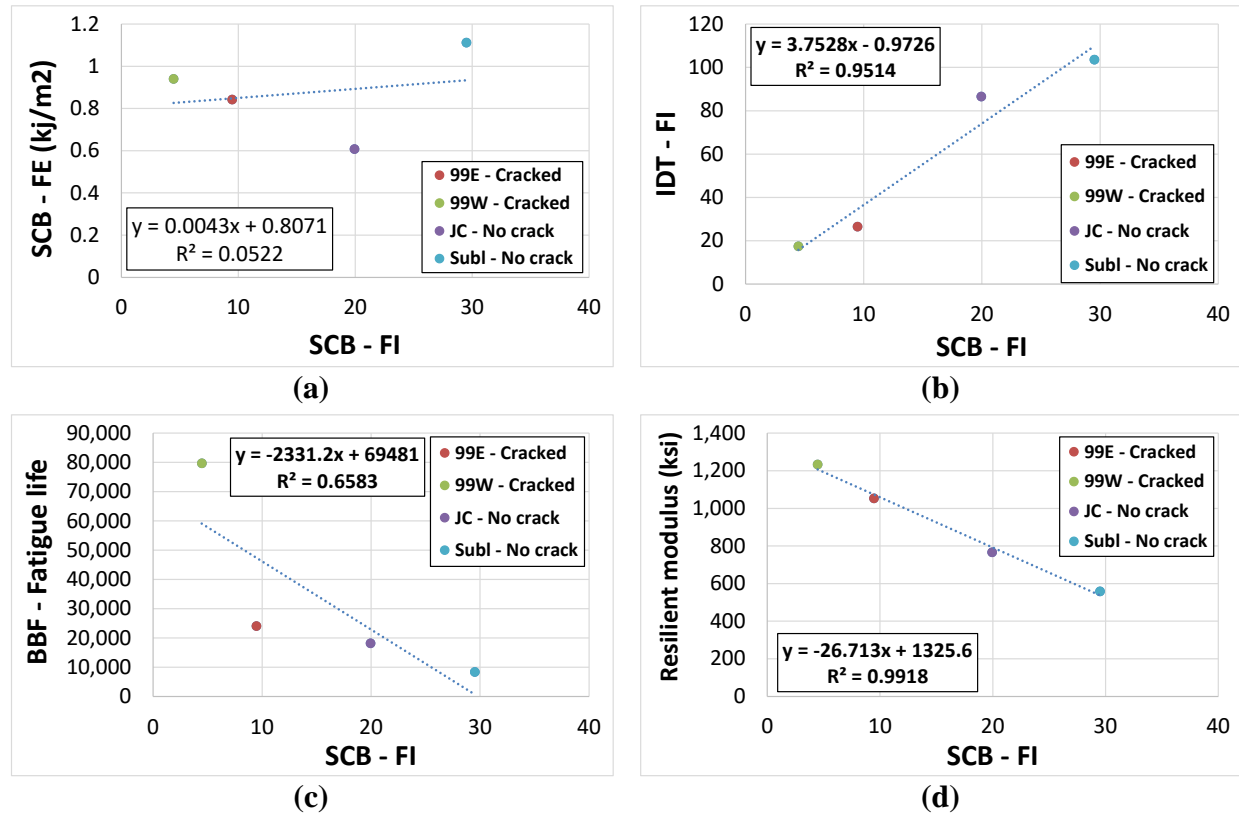


Figure 3.30: One-to-one correlation plots (a) flexibility index and fracture energy from SCB (b) flexibility indices from SCB and IDT tests (c) SCB flexibility index and BBF fatigue life (d) Resilient modulus and SCB flexibility index

3.6.2 Plant Mixed-Laboratory Compacted (PMLC) Specimens

The major purpose of testing PMLC samples was to determine the effectiveness of different testing methods in identifying the cracking performance of pavements with different mixture properties. Another purpose of this part of the study was to determine the cracking and rutting resistance of Mix 1, Mix 2 and Mix 3 asphalt mixtures that are now commonly used in Oregon for pavement construction. Table 3.4 shows the experimental plan followed in this part of the study. In order to evaluate the effectiveness of each experiment, three mixes with different expected cracking performance (Mix 1, Mix 2 and Mix 3) were used. Loose asphalt mixtures were sampled from the plant and used for specimen preparation (See Section 3.4.2). The results of SCB, IDT, BBF, DTCF, DM and FN tests are presented in the following sections.

3.6.2.1 Semi-Circular Bend (SCB) Test

SCB test samples were prepared in the laboratory using the production mix obtained from the asphalt plant. The samples compacted were of 150 mm diameter and 130 mm height. Two samples with the thicknesses of 57 mm were obtained from each compacted specimen. These slices were cut into symmetrical semi-circular halves. For each mix

type, three samples with three notch depths were prepared (0.6 in., 1.0 in. and 1.25 in.). For each notch depth, three replicate samples were prepared. A total of 27 tests were conducted, and flexibility index was calculated for every test.

Test results are presented in Figure 3.31. Mix 1 (modified mix with fine gradation) had the highest flexibility index followed by Mix 3 (unmodified mix with coarse gradation) and Mix 2 (modified mix with coarse gradation). Since Mix 2 and Mix 3 had identical mix designs except the ER binder used in Mix 2, the average flexibility index for Mix 2 was expected to be higher than Mix 3. However, it can be observed that Mix 3 has a higher flexibility index than Mix 2, which is incongruent with what was expected. This unexpected result raised suspicion about the true binder contents of these two mix types. Since binder content is expected to be the most significant factor controlling cracking resistance of asphalt mixtures (Coleri et al. 2017), higher binder content for Mix 3 might have increased the cracking resistance.

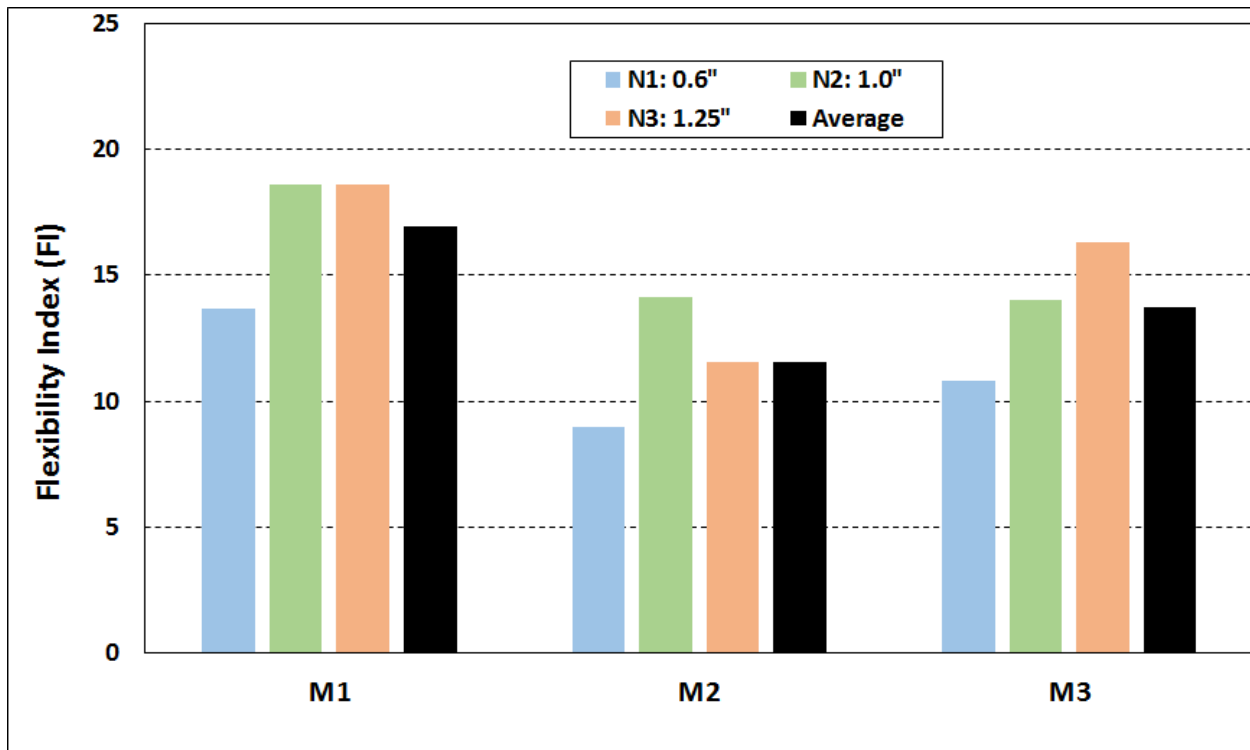


Figure 3.31: Flexibility index from SCB tests for PMLC samples

Note: M1: Mix 1-PG70-22ER-Fine gradation
M2: Mix 2-PG70-22ER-Coarse gradation
M3: Mix 3-PG70-22-Coarse gradation
N: Notch depth

In order to evaluate this disparity in the experimental results of the SCB experiments for Mix 2 and Mix 3, binder extraction was performed on each of the production mixes in order to determine their binder contents. The binder contents for both mix designs for Mix 2 and Mix 3 were supposed to be the same (5.3% from mix design), so the extraction served as a check on the scheduled mix design properties. Mix 1 was also tested for completeness and also to evaluate the accuracy of the extraction process. Extraction was performed with three replicate samples of each mix type in order to determine the average binder content for each mix type.

The procedure followed for the extraction of binder and determination of binder content for each production mix type was adopted from ASTM D2172. The procedure is outlined below and is shown in Figure 3.32.

1. Each production mix type was placed in the oven at 110°C for 2 hours to make the mix workable (Figure 3.32a). Samples of approximately 4kg of each mix type were collected and split using a mechanical splitter according to AASHTO R 47.
2. Once split, samples of approximately 0.5kg each were weighed and individually added to the extraction bowl (Figure 3.32b). The initial mass of the sample and the paper centrifuge filter disk were each recorded.
3. The bowl, mix and filter were assembled and inserted into the centrifuge extractor (Figure 3.32c). The lid was secured and 450 mL of Powersolv solvent was added to the top of the extractor. The sample was allowed to condition for 30 minutes prior to beginning the centrifuge extraction. After the conditioning time, the centrifuge extractor was allowed to run at a speed of 350 RPM and a mixture of solvent and binder was extracted.
4. Three additional washes with 250 mL aliquots and finally one wash with 200 mL were conducted, increasing the speed of the centrifuge extractor by 150 RPM for each wash.
5. The extracted production mix aggregates were collected in a pan and allowed to air dry for 30 minutes. The aggregates were then left in a drying oven at about 120 °C for 1-2 hours to evaporate the remaining solvent from the aggregates (Figure 3.32d). The final mass of the sample and filter disk were obtained.
6. The binder content of each mix sample was calculated according to Equation 3.17 in ASTM D2172 (shown as Equation 3.17 below). The terms W_2 (mass of water in the test portion) and W_4 (mass of the mineral matter in the extract) in the equation were neglected for simplicity and due to their minimal effect on the binder content calculation. The trend in binder contents were of particular interest and not necessarily the specific binder content percentages.

$$\text{Asphalt binder content, \%} = \left[\frac{(W_1 - W_2) - (W_3 + W_4)}{W_1 - W_2} \right] * 100\% \quad 3.17$$

Where:

W_1 = mass of test portion;

W_2 = mass of water in test portion;

W_3 = mass of extracted mineral aggregate; and

W_4 = mass of mineral in the extract

7. Sieve analyses were performed on extracted Mix 2 and Mix 3 to evaluate the performance of the extractions and the gradation of the production mix samples (Figure 3.33). It can be observed that extracted aggregate and plant target gradations are close for Mix 2 and Mix 3.
8. The binder contents and aggregate gradations for each mix sample were recorded in a spreadsheet.
9. The extracted binder solution for each mix type were stored in sealed glass containers for future use, if necessary.



(a)



(b)

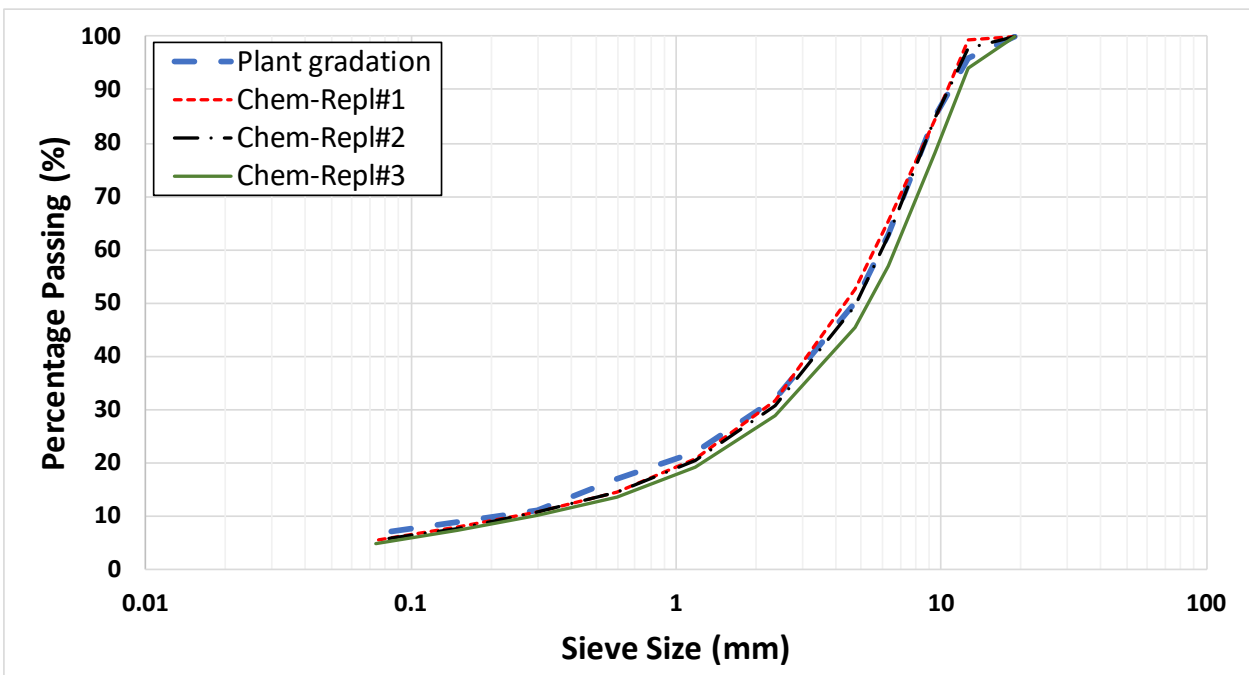


(c)



(d)

Figure 3.32: General procedure followed for extraction



(a)

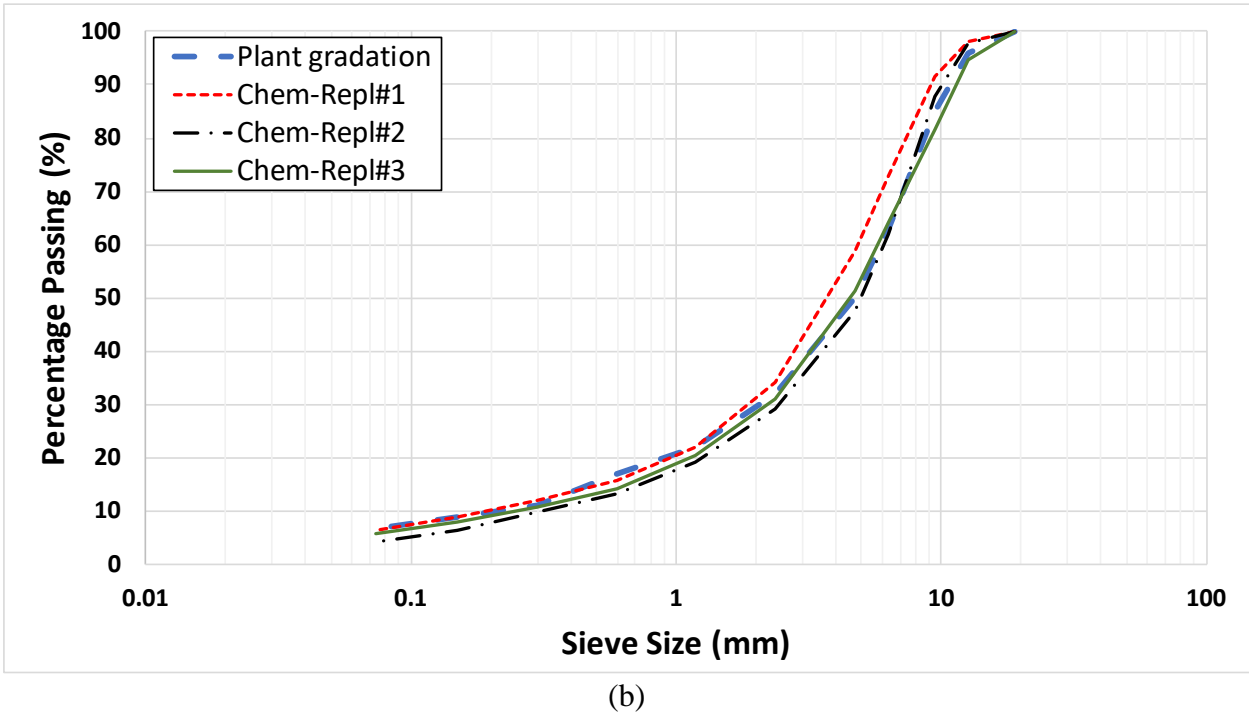


Figure 3.33: Comparison of plant and extracted aggregate gradations

Table 3.7 shows the calculated binder contents of each production mix type obtained from the extraction process.

Table 3.7: Calculated Binder Contents of Production Mix Samples

Sample	Binder Contents		
	Mix 1	Mix 2	Mix 3
1	6.2%	6.2%	6.3%
2	6.4%	5.9%	6.7%
3	6.7%	5.8%	6.4%
Average	6.4%	6.0%	6.5%
Std Dev	0.23%	0.16%	0.22%

Figure 3.34 shows a histogram of the binder contents for each production mix type with error bars indicating one standard deviation above and below the calculated binder content (length of the error bar is equal to two standard deviations).

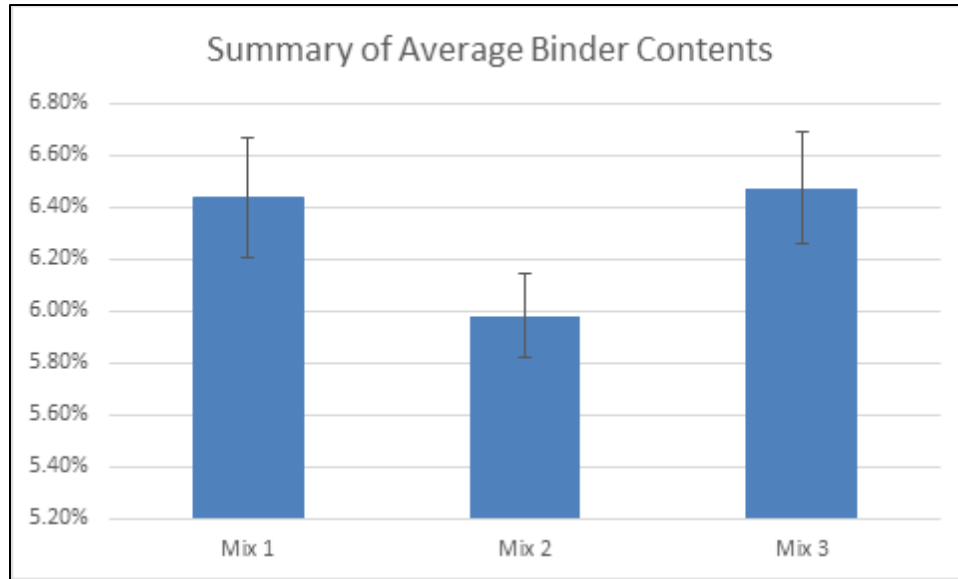


Figure 3.34: Histogram of binder contents for production mix samples

From measured binder contents (Table 3.7 and Figure 3.34), it was observed that Mix 3 had a binder content approximately 0.5% higher, on average, than Mix 2. This result validated the concerns over the experimental results of the SCB experiments. The binder contents for Mix 2 and Mix 3 should have been equal according to the mix designs (5.3%). This elevated binder content in Mix 3 can help to explain the higher FI of Mix 3 in the SCB test results.

3.6.2.2 Indirect Tension (IDT) test

IDT test samples were prepared in the laboratory using the production mix obtained from the asphalt plant. The samples compacted were of 150 mm diameter and 130 mm height. Two slices of 50 mm were obtained from each compacted specimen. For each mix type, six replicate experiments were conducted in this study. A total of 18 tests were conducted. In addition to the tensile strength parameter, flexibility index was determined for each replicate experiment and used for mixture cracking performance comparison.

Tensile strength and flexibility index parameters calculated by using IDT test results are presented in Figure 3.35 and Figure 3.36, respectively. It can be observed that the flexibility index was highest for Mix 1, followed by Mix 3 and Mix 2. Although the flexibility index values obtained from IDT tests were much higher than the flexibility indices obtained from SCB tests, flexibility indices for both experiments followed similar trends. Average tensile strength values for all three mixtures were determined to be close to each other. Tensile strength parameter suggested that Mix 3 has the highest cracking resistance followed by Mix 1 and Mix 2.

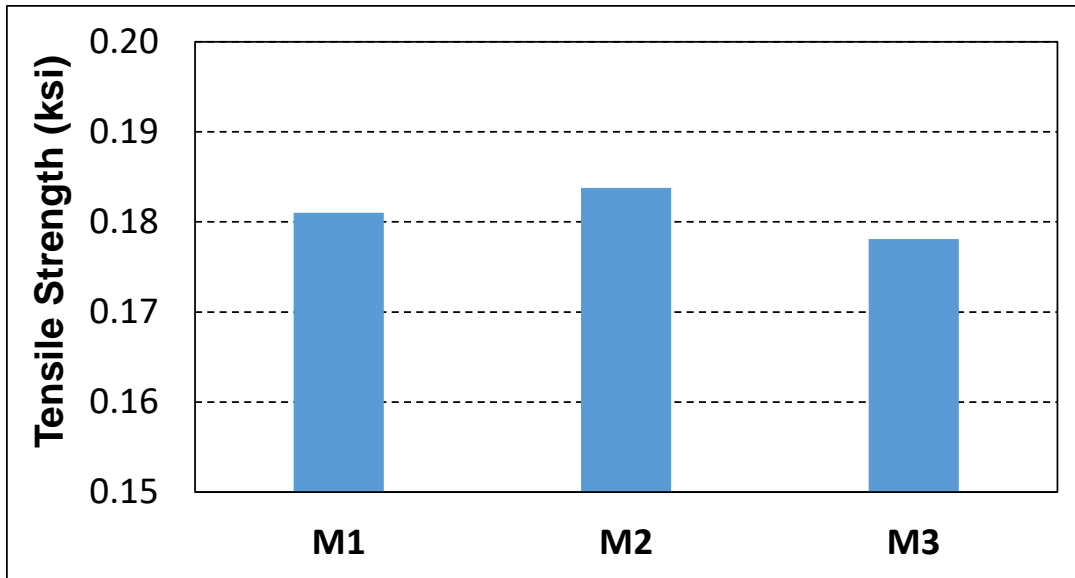


Figure 3.35: Tensile strength from IDT tests for PMLC samples

Note: M1: Mix 1-PG70-22ER-Fine gradation
M2: Mix 2-PG70-22ER-Coarse gradation
M3: Mix 3-PG70-22-Coarse gradation

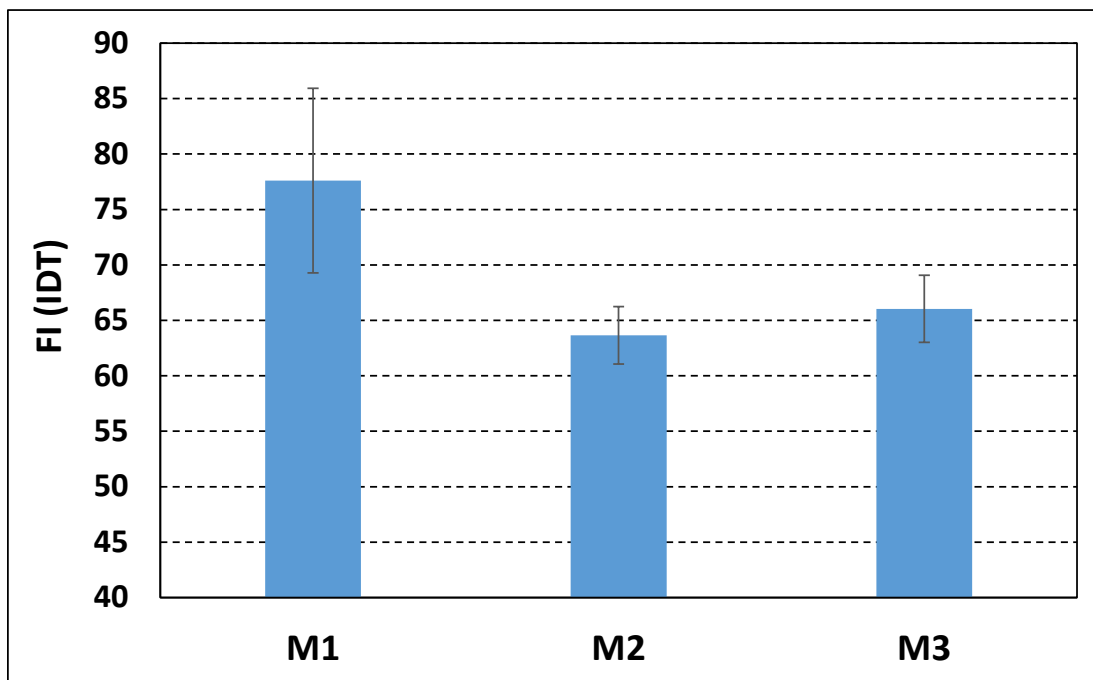


Figure 3.36: Flexibility index from IDT tests for PMLC samples

Note: M1: Mix 1-PG70-22ER-Fine gradation
M2: Mix 2-PG70-22ER-Coarse gradation

3.6.2.3 Bending Beam Fatigue (BBF) Test

Beam samples were prepared by following the procedure described in Section 3.5.3. For each mixture type, three replicate experiments were conducted. A total of 9 samples were tested at $400\mu\epsilon$ strain level and 10 Hz loading frequency. Results are presented in Figure 3.37. Fatigue life of Mix 1 was the highest followed by Mix 3 and Mix 2. These results are in agreement with the results from SCB and IDT tests. However, it can be observed that the coefficient of variation between the replicates of the same mix is high. For example, in Mix 1, replicate 2 had a fatigue life of about 500,000 cycles whereas replicate 3 had a fatigue life of over 5,000,000 cycles. This high variability can introduce bias into the test results leading to inaccurate evaluation of fatigue performance of asphalt mixtures. For this reason, in order to reduce the effects of high variability on average fatigue life, more replicate experiments should be conducted. However, it should be noted that compacting and cutting beam specimens is much harder than preparing core samples for IDT and SCB experiments. In addition, conducting one BBF experiment takes about 1 to 5 days depending on the flexural strength of the mixture. Due to these reasons, BBF test may not be as practical as SCB and IDT experiments. On the other hand, since BBF is a repeated load test, results can be used for mechanistic-empirical design while fracture tests (SCB and IDT) just provide a parameter that can be used to rank the cracking resistance of different mixture types.

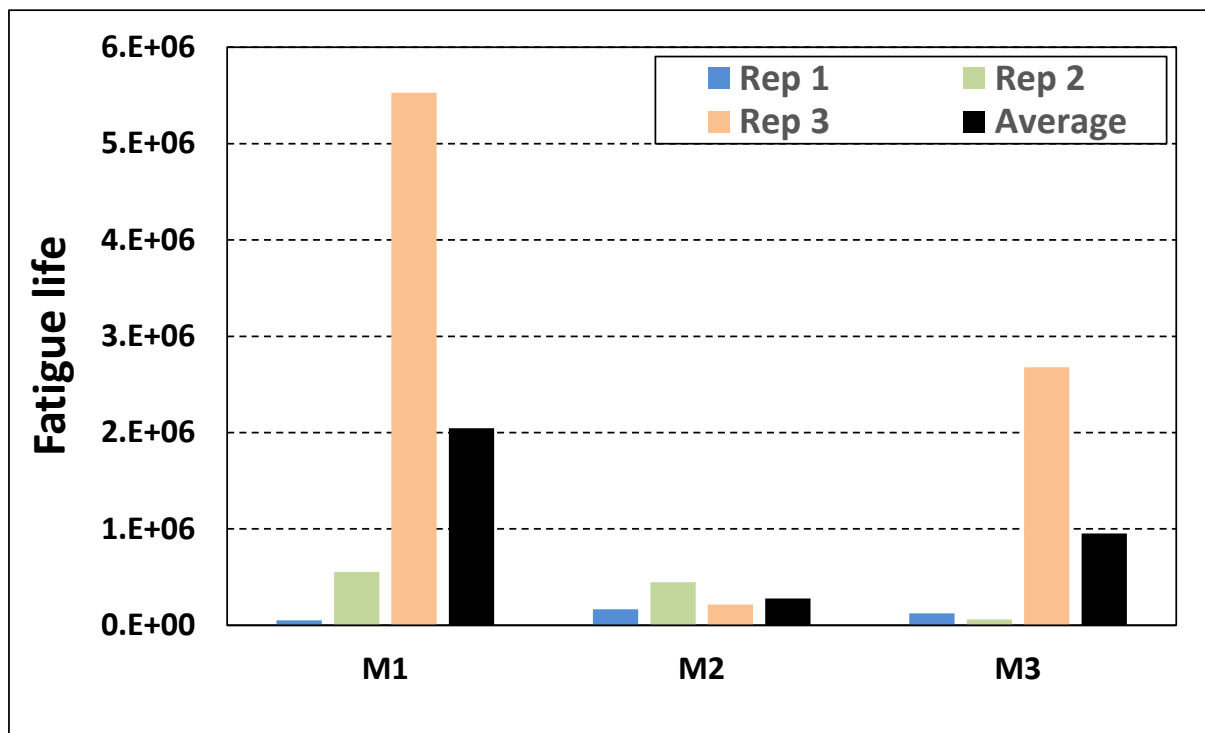


Figure 3.37: Fatigue life from BBF tests for PMLC samples

Note: M1: Mix 1-PG70-22ER-Fine gradation

M2: Mix 2-PG70-22ER-Coarse gradation
M3: Mix 3-PG70-22-Coarse gradation

Appendix D presents the results of BBF tests conducted as a part of another ODOT research project conducted by Oregon State University (Coleri et al. 2017). Results from this study further confirmed that the BBF test results variability is significantly higher than all other tests.

3.6.2.4 Direct Tension Cyclic Fatigue (DTCF) Test

DTCF tests were conducted by following the procedure described in Section 3.5.4. Two replicate samples were produced for each mix type and a total of 6 samples were tested. In this study, fatigue life from the DTCF test was defined as the number of cycles required to reach 50 percent reduction in original stiffness. Figure 3.38 illustrates the DTCF test results. It can be observed that fatigue lives calculated for all three mixes are close. The results for DTCF tests are in agreement with the results from SCB, IDT and BBF tests. However, it can be observed that the coefficient of variation between the replicates of the same mix is high. For example, in Mix 1, replicate 1 had a fatigue life of about 29,000 cycles whereas replicate 3 had a fatigue life of about 130,000 cycles. This high variability can introduce bias into the test results leading to inaccurate evaluation of fatigue performance of asphalt mixtures. For this reason, in order to reduce the effects of high variability on average fatigue life, more replicate experiments should be conducted. However, it was experienced that the sample preparation and testing process for DTCF was tedious, time consuming and requires a significant level of training.

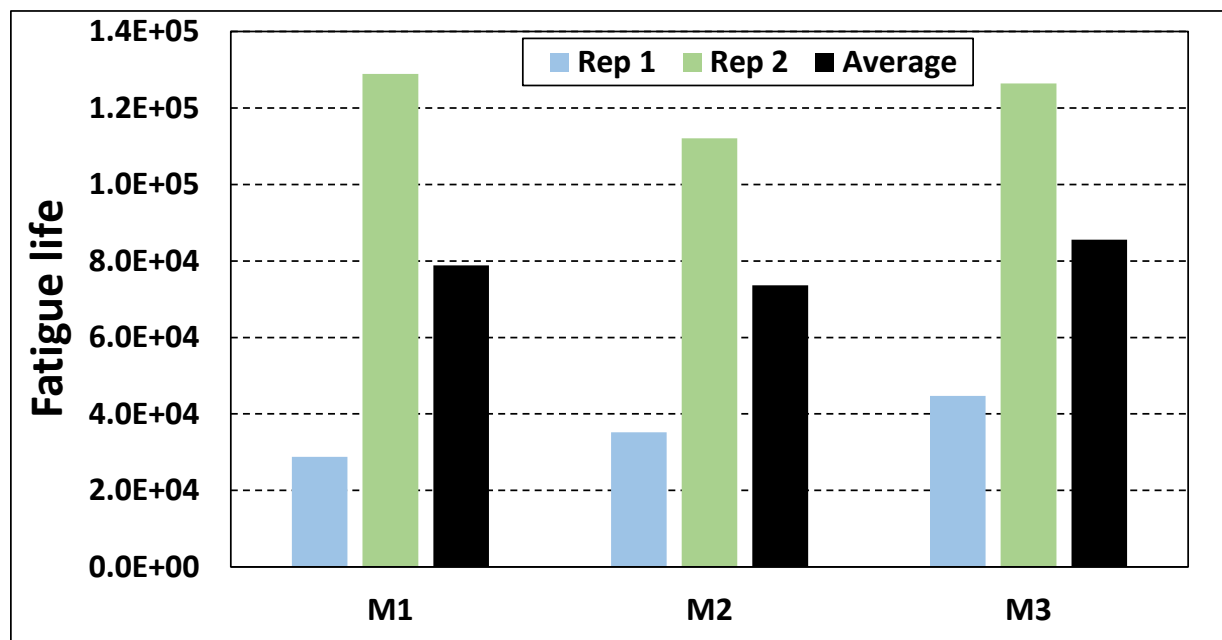


Figure 3.38: Fatigue life from DTCF tests for PMLC samples

Note: M1: Mix 1-PG70-22ER-Fine gradation

M2: Mix 2-PG70-22ER-Coarse gradation

M3: Mix 3-PG70-22-Coarse gradation

3.6.2.5 Dynamic Modulus (DM) Test

Samples for DM tests were prepared and tested by following the process described in Section 3.5.6. Two replicate samples were produced for each mix and a total of six samples were tested. Each specimen was tested at 4°C, 20°C and 40°C temperatures and 0.1 Hz, 0.5 Hz, 1 Hz, 5 Hz and 10 Hz frequencies. The frequency of 0.01 Hz was also used only for tests conducted at 40°C. In this study, Mastersolver V2.2, a spreadsheet developed by Dr. Ramon Bonaquist of Advanced Asphalt Technologies, is used to develop master curves and develop the parameters required to perform Level 1 MEPDG analysis (Chapter 7.0). Figure 3.39 illustrates the dynamic modulus master curves for the three mixes tested in this study. As expected, the non-polymer mix (Mix 3) had higher stiffness than the polymer modified mixes (Mix 2 and Mix 1) as depicted in the figure. The higher the dynamic modulus value, the higher the stiffness will be and therefore the susceptibility to rutting will be lower.

The time delay between the time point at which peak stress is applied and the time point at which peak strain is observed is used to calculate phase angle. Phase angle shows energy absorption capacity of an asphalt mixture and represents viscoelastic characteristics of asphalt mixtures. A higher phase angle indicates that the asphalt mixture is more viscous, more susceptible to rutting and more resistant to cracking (Darnell Jr. and Bell 2015). Dynamic modulus and phase angle are inversely related to each other. A mixture with a comparatively high dynamic modulus (high stiffness) at a given frequency level has a low phase angle at the same frequency (Darnell Jr. and Bell 2015).

Figure 3.40 illustrates the phase angle master curves for the three mixes. The same shift factor values, which were calculated and used for developing the master curves for DM tests, are used to develop the master curves for phase angles. Therefore, these master curves are not as smooth as the master curves of the dynamic modulus. The reference temperature for all master curves is 20°C. The higher the phase angle, the more viscous the mix is. Hence, it will have a higher resistance to cracking. However, mixes with very high phase angles will lead to rutting issues. It can be observed from the figure that Mix 1 has higher phase angle compared to Mix 2 and Mix 3 when the loading frequencies for highway speeds are considered (0.1 Hz to 10 Hz). Dynamic modulus and phase angle are inversely proportional to each other. Therefore, from the dynamic modulus and phase angle values, it can be concluded that Mix 1 has the highest resistance to cracking followed by Mix 2 and Mix 3, respectively.

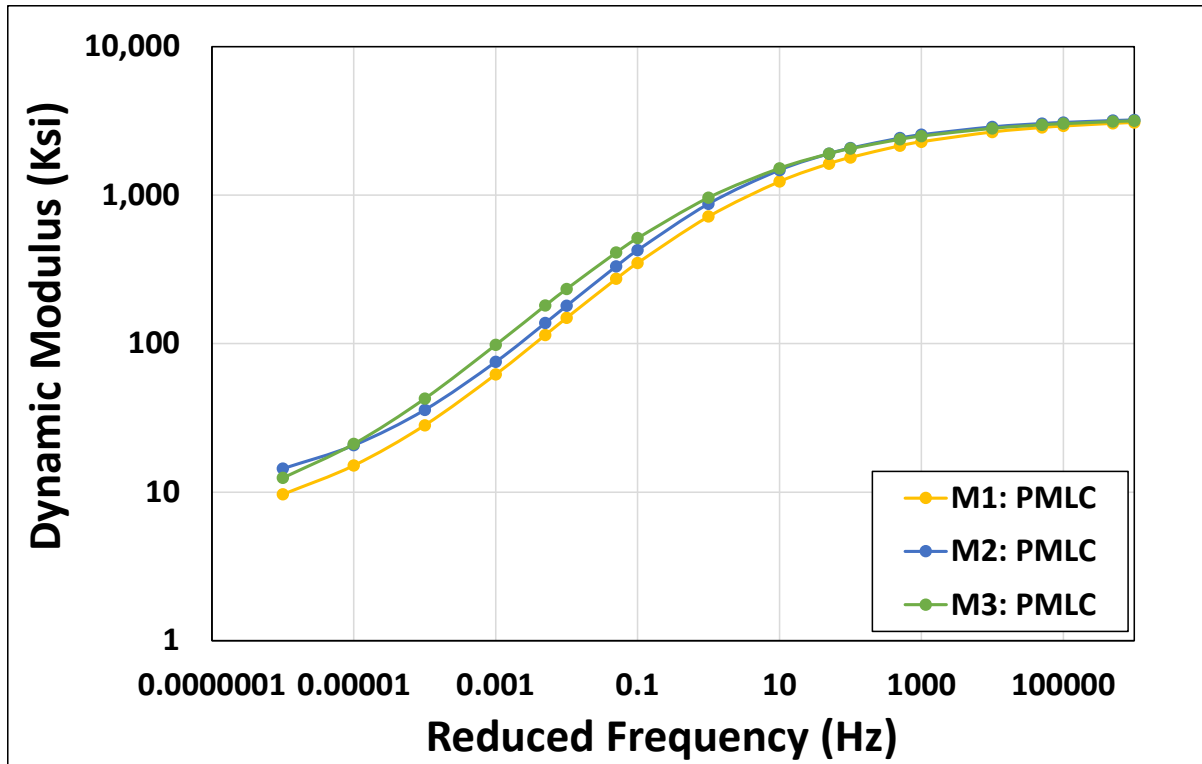


Figure 3.39: Dynamic modulus for PMLC samples

Note: M1: Mix 1-PG70-22ER-Fine gradation
M2: Mix 2-PG70-22ER-Coarse gradation
M3: Mix 3-PG70-22-Coarse gradation

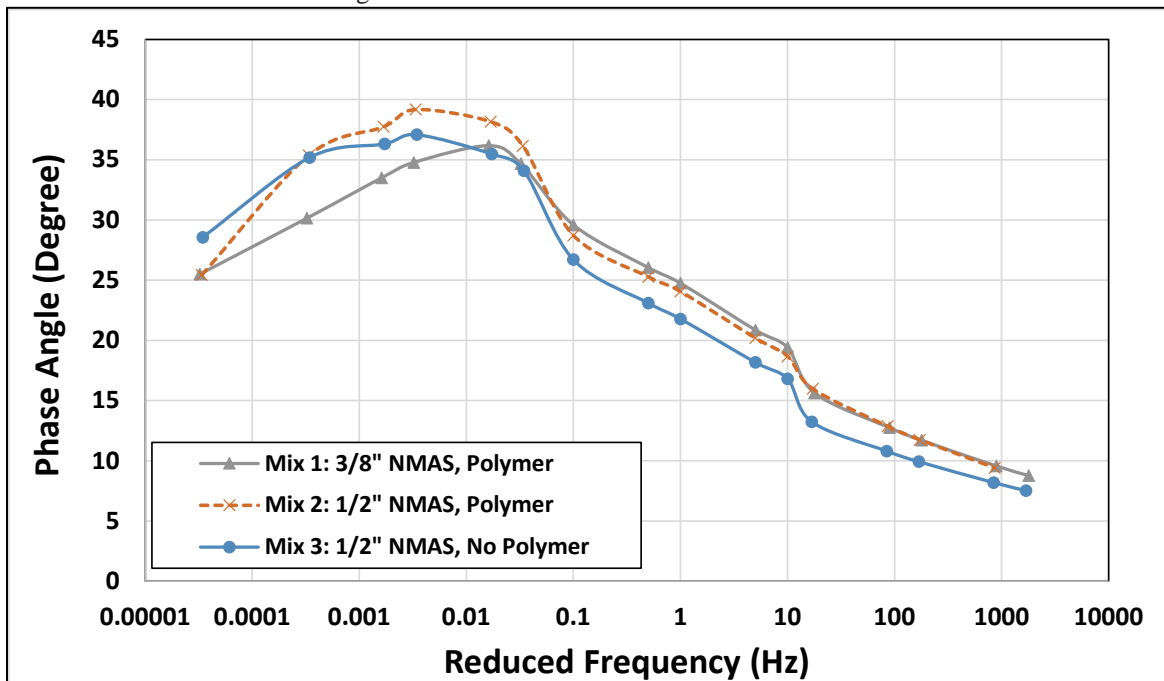


Figure 3.40: Phase angle for PMLC samples

Note: M1: Mix 1-PG70-22ER-Fine gradation
M2: Mix 2-PG70-22ER-Coarse gradation
M3: Mix 3-PG70-22-Coarse gradation

3.6.2.6 Flow Number (FN) Test

The flow number (FN) test is a simple performance test for evaluating rutting performance of asphalt concrete mixtures (Bonaquist et al. 2003). High FN values indicate that asphalt mixtures have high rutting resistance. Since the DM test is a non-destructive test (low strain level), the same samples prepared for DM tests were used for FN tests to compare the rutting resistance of HMA mixtures. Therefore, a total of six tests were conducted (two replicate tests for each mix type). Figure 3.41 illustrates the flow number results for all three mixes. From the figure, it can be observed that Mix 3 had the highest flow number followed by Mix 2 and Mix 1. This trend follows the trend for the dynamic modulus from the DM tests for the three mixes. Therefore, it can be concluded that Mix 3 has the highest rutting resistance while Mix 1 has the lowest. It should be noted that only Mix 3 meets the AASHTO TP 79-13 criteria for FN for the highest traffic level (for Traffic ≥ 30 million ESALs, $FN > 740$) (Rodezno et al. 2015).

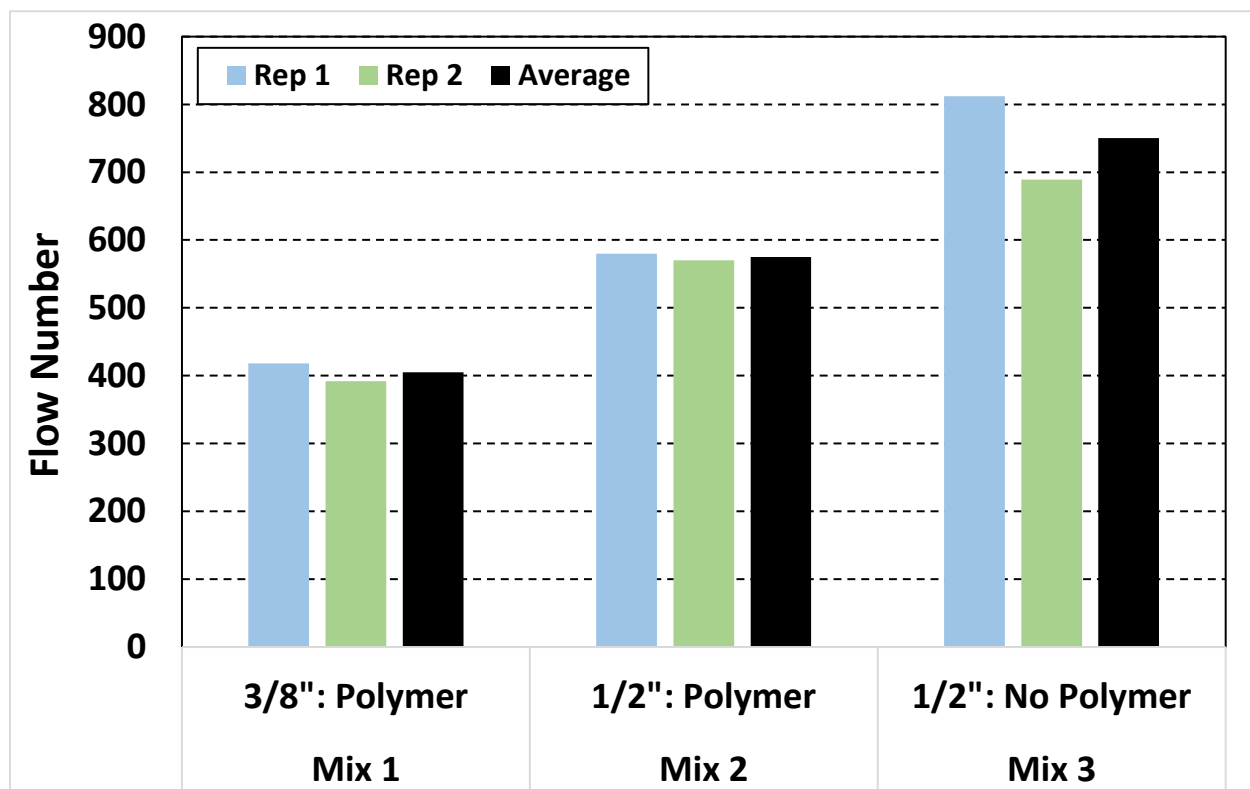


Figure 3.41: Flow number for PMLC samples

Note: Mix 1-PG70-22ER-Fine gradation
Mix 2-PG70-22ER-Coarse gradation
Mix 3-PG70-22-Coarse gradation

3.6.3 Laboratory Mixed-Laboratory Compacted (PMLC) Specimens

In this part of the study, the impact of compaction (field compaction and SGC) and mixing (laboratory and plant mixing) on cracking test results (SCB) were determined. This plan was divided into two parts. The first part (as outlined in Table 3.5) was to compact specimens in the laboratory using the mix obtained from the plant and obtain cores for Mix 2 from the actual pavement sections constructed from the same mix. The aim was to evaluate the difference between laboratory (PMLC) and field compaction (PMFC) on cracking results. In addition, using the aggregates, RAP and binder used for mixture production at the plant, laboratory mixed-laboratory compacted (LMLC) specimens were prepared. By comparing LMLC test results to PMLC test results, the impact of mixing (laboratory versus plant mixing) on measured cracking resistance was determined. The process followed to prepare LMLC specimens is given in Chapter 4.0. The second part was to produce samples in the laboratory using SGC and a laboratory roller compactor. The objective here was to ascertain the impact of compaction type on cracking performance. For this portion, specimens prepared as a part of another ODOT research project conducted by Oregon State University were used (Coleri et al. 2017). The mix used for the second part had a PG58-34 binder, 40% RAP and 6% binder content. Air-void content was the same as PMLC samples (7%). Four SCB test samples were extracted from samples compacted with SGC and roller compactor (a total of 8 SCB specimens).

SCB tests were conducted as described in Section 3.5.1. The only exception here was that the thickness of field cores tested were 38 mm (design thickness for the constructed roadway section) instead of 57 mm. Lower thicknesses for field cores are not expected to affect flexibility index since fracture energy used to calculate flexibility index is calculated by dividing the area under the displacement versus load curve by the ligament area (See Equation 3.3). The force required to break a thinner sample will be less but since ligament area will also be smaller, calculated flexibility index theoretically should not be affected by the specimen thickness.

SCB test results for LMLC, PMLC, and PMFC are presented in Figure 3.42. It can be observed that cracking resistance of laboratory compacted specimens are significantly lower than the cracking resistance of field compacted specimens. On the other hand, cracking resistance of LMLC and PMLC specimens were determined to be close. These results suggested that the mixing method (laboratory or plant) does not have any significant effect on measured cracking performance. However, the compaction method significantly affects the measured response. These results are in agreement with the results from a study conducted by Harvey et al. (2014). Harvey et al. (2014) concluded that SGC compaction creates an unrealistic aggregate skeleton due to excessive compactive effort, which creates an asphalt specimen with higher stiffness and lower ductility. For this reason, SCB test results for SGC compacted specimens cannot be directly compared to the results from field roller compacted specimens. Although compaction type was determined to affect the measured cracking resistance, it is not expected to affect the ranking of performance for different asphalt mixtures.

In order to further confirm this result, specimens prepared as a part of another ODOT research project conducted by Oregon State University (Coleri et al. 2017) were used (PG58-34 binder, 40% RAP and 6% binder content). Samples for the same mixture were compacted using SGC and roller compactor. SCB flexibility indices obtained for these samples are presented in Figure 3.43. Again, it was observed that SGC compacted samples yielded lower flexibility indices as

compared to roller compacted samples. Therefore, it can be concluded that mode of compaction plays an important role in cracking results.

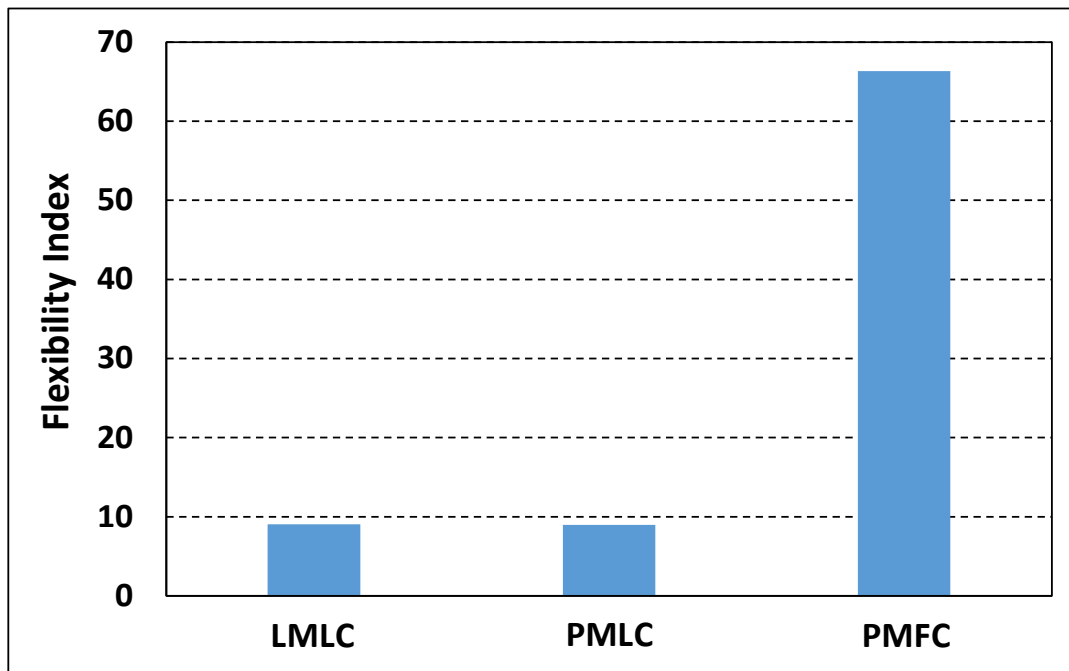


Figure 3.42: The Impact of Mixing Method and Compaction Type on SCB Flexibility Index

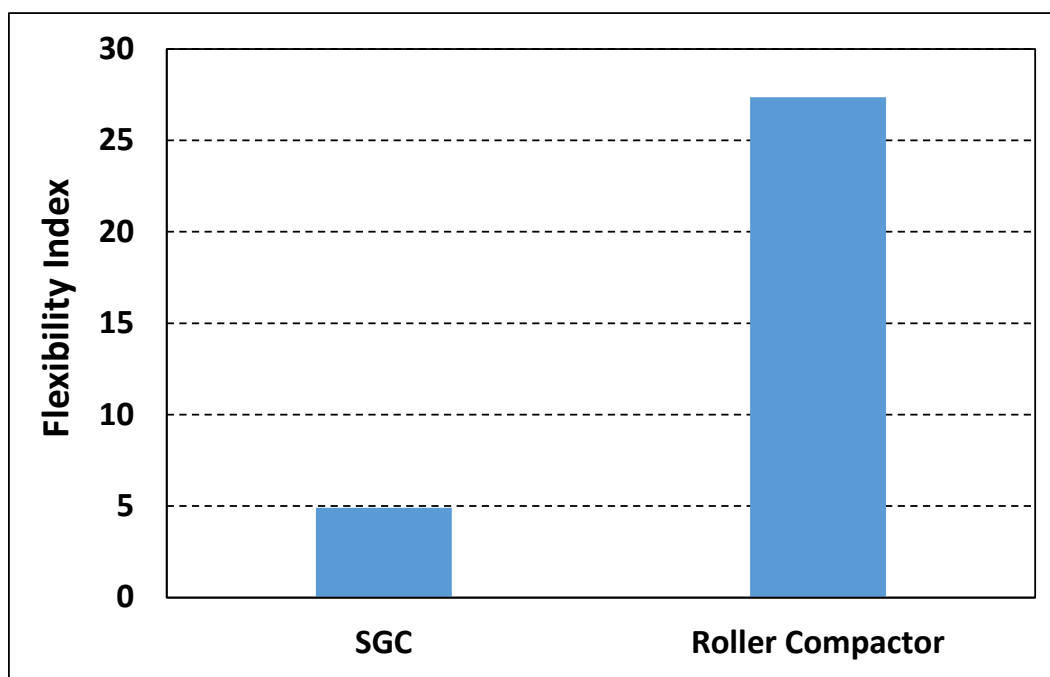


Figure 3.43: SCB Results Evaluating Gyratory and Roller Compaction

3.7 SUMMARY AND CONCLUSIONS

Fatigue cracking is one of the predominant modes of distress in the state of Oregon. Hence, it is necessary to understand the fatigue performance of asphalt mixtures that are being used in asphalt pavement construction. In order to quantify this performance, a laboratory testing procedure is necessary to predict the cracking performance of asphalt mixtures used for pavement construction in Oregon. In this study, four candidate tests (SCB, IDT, BBF and DTCF tests) were used to evaluate the fatigue performance of pavements and asphalt mixes used in Oregon.

In this part of the study, the effectiveness of each laboratory experiment was first evaluated by comparing test results from PMFC-Old (field sections) specimens to the measured in-situ cracking performance of roadway sections. Second, the agreement between the results of different experiments was determined. The major purpose was to determine the effectiveness of different testing methods in identifying the cracking performance of pavements with different mixture properties. Another purpose of this part of the study was to determine the cracking and rutting resistance of Mix 1 (PG70-22ER-Fine gradation), Mix 2 (PG70-22ER-Coarse gradation) and Mix 3 (PG70-22-Coarse gradation) asphalt mixtures that are now commonly used in Oregon for pavement construction. Finally, the impact of compaction (field compaction and SGC) and mixing (laboratory and plant mixing) on cracking test results (SCB) were determined.

The conclusions derived from this study are as follows:

- SCB and IDT tests are the most practical and reliable tests that can be used to evaluate the cracking resistance of asphalt mixtures.
- The SCB test holds a slight advantage against IDT in terms of practicality since just one gyratory sample is required for each mixture type whereas a minimum of two SGC samples are required for IDT testing for each mixture type.
- The flexibility index parameter is an effective parameter in differentiating cracking resistance of asphalt concrete mixtures.
- Test result variability for BBF and DTCF tests were determined to be very high. These two tests were also determined to be ineffective in predicting the in-situ performance of asphalt pavements. Specimen preparation and testing were also determined to be complicated, time consuming and labor intensive.
- For Mix 3 (PG70-22-Coarse gradation), binder content of the production mix is higher than the design binder content.
- Only Mix 3 meets the AASHTO TP 79-13 criteria for FN for the highest traffic level (for Traffic ≥ 30 million ESALs, FN > 740) (Rodezno et al. 2015).

- The mixing method (laboratory or plant) does not have any significant effect on measured cracking performance.
- Compaction method significantly affects the measured cracking resistance. SGC compaction creates an unrealistic aggregate skeleton due to excessive compactive effort which creates an asphalt specimen with higher stiffness and lower ductility. For this reason, SCB test results for SGC compacted specimens cannot be directly compared to the results from field roller compacted specimens. Although compaction type was determined to affect the measured cracking resistance, it is not expected to affect the ranking of performance for different asphalt mixtures.

As a part of this study, the four tests in consideration were ranked based on simplicity, preparation and testing time, test equipment cost, and test results' variability. The simplicity was ranked on a scale from 1 to 5, 1 being the lowest and 5 being the highest. The ratings were based on the consensus of opinion among the operators at Oregon State University. The time factor was divided into preparation time and testing time. Preparation time included the time required for sample preparation and cutting and did not include batching and mixing. For instance, all the tests require almost about the same amount of time until mixing and compaction, but the time required for cutting BBF test samples is much greater than the others. For DTCF testing, the test sample needed to be glued to the loading platens, for which it takes about a day for the epoxy to set. The values presented are the approximate time required for preparing three replicate specimens. Testing time is the time required by one sample from the point of loading to the test termination point. Testing cost is the approximate cost required for the test equipment. For example, the SCB test can be conducted with an independent loading frame whereas the DTCF test requires hydraulic test equipment, which increases the cost. The coefficient of variation was calculated for all the PMLC tests. The rankings are as shown in Table 3.8. It can be observed that SCB and IDT tests are the most practical experiments with lower test equipment costs and lower test results' variability. Although IDT test results have a lower level of variability when compared to SCB test results, the SCB flexibility index parameter was observed to more effectively identify the impact of different mixture properties on cracking resistance.

Table 3.8: Ranking of the Tests

Test	Simplicity	Time		Test equipment cost	Coefficient of variation
		Preparation time	Testing time		
SCB	5	5-6 hours	15-30 min	\$6,000	0.161
IDT	5	10 hours	15-30 min	\$6,000	0.088
BBF	2	1 day	1-5 days	\$30,000	0.977
DTCF	2	1.5 days	1-3 hours	\$65,000	0.550

4.0 CONTRIBUTIONS OF MIXTURE PROPERTIES TO DURABILITY

4.1 INTRODUCTION

Fatigue performance of asphalt mixtures is highly influenced by the binder and air-void contents, binder grade, binder modification, gradation, volumetrics, RAP/RAS content and aging. Air-void and binder contents are considered to be two major factors affecting the fatigue cracking performance of asphalt mixtures. Higher binder content and lower air voids generally improve cracking performance of asphalt pavements. For equal levels of compactive effort, a higher binder content tends to reduce the air-void content of the mix resulting in an increase in mix density. Although increasing mix binder content can be accepted to be a viable strategy for increasing asphalt mix fatigue life, increased binder content also tends to create a softer mix with lower rutting resistance. Over the last two decades, there has been an increase in the use of modified asphalt binders in order to improve cracking resistance of pavements. Although binder modification increases the initial cost of the constructed sections, the increase in service life can significantly reduce long-term life cycle costs for agencies. Therefore, this portion of the study focused on quantifying the impact of air-void content, binder content and polymer modification on cracking resistance of asphalt mixes commonly used in Oregon.

The study was divided into two parts. The purpose of the first part was to reproduce the three mixes from Section 3.4.2 in the laboratory (laboratory mixed-laboratory compacted samples). Two binder contents (5.3% and 6%) and two air-void contents (5% and 7%) were used for each mix type. Mix 1 and Mix 2 had polymer-modified binders while Mix 3 was a non-polymer mixture. Mix 1 had a finer gradation while Mix 2 and Mix 3 had coarse gradations. The results from this Chapter were also compared with the results from Section 3.6.2. The objective was to identify the impact of the difference in mixing processes (laboratory and plant mixing) and short-term aging (plant and laboratory short-term aging) on cracking and rutting resistance of asphalt mixtures

4.2 OBJECTIVES

The major objectives of this part of the study were to:

- Determine the effects of gradation, binder content, air void content (density) and binder type (PG70-22 versus PG70-22ER binder) on the cracking resistance of asphalt mixtures.
- Develop laboratory data (master curves) to conduct Level 1 MEPDG analysis (See Chapter 7.0).

4.3 MATERIALS AND METHODS

4.3.1 Experimental Plan to Determine the Impact of Mixture Properties on Durability

This part of the study intends to reproduce the three plant produced mixes that were used in Chapter 3.0 to determine the most effective cracking experiments. In order to determine the impact of other variables on cracking resistance, mixtures with different binder contents and densities were also prepared in the laboratory. The benefits of increased binder content and density in improving the cracking resistance of asphalt mixtures were quantified. As was shown in Section 3.6.2.1, plant mixes can have properties different from the original mix designs due to production variability and errors. By preparing and testing laboratory mixed-laboratory compacted (LMLC) specimens, the impact of production variability on test results was also eliminated. In this way, the impacts of binder content, density, polymer modification and gradation on performance were more accurately quantified. This section summarizes the experimental plan followed for asphalt mixtures with different gradations, binder contents, air-void contents and binder types (ER and non-ER). The goal was to determine the impact of these variables on mixture durability. The experimental plan followed for durability evaluation is given in Table 4.1.

Table 4.1: Experimental Plan for Durability Evaluation

Test type	Mix Type	Comp. ²	Temp.	Air void content	Binder content	Repl.	Total Tests
SCB	M1 ¹ M2 M3	LMLC ³	25°C	5% 7%	5.3% 6.0%	4	48
Dynamic modulus	M1 M2 M3	LMLC	1 run ⁴	5% 7%	5.3% 6.0%	2	24
Flow number	M1 M2 M3	LMLC	54.7°C	5% 7%	5.3% 6.0%	2	24

Note: ¹ M1: Mix 1-PG70-22ER-Fine gradation
M2: Mix 2-PG70-22ER-Coarse gradation
M3: Mix 3-PG70-22-Coarse gradation

² Comp.=Compaction;

³ LMLC: Laboratory mixed-laboratory compacted;

⁴ Samples were tested at temperatures of 4 °C, 20 °C, and 40 °C and the loading frequencies of 0.1, 0.5, 1, 5, and 10 Hz. A loading frequency of 0.01 Hz was also used for 40 °C tests.

4.3.2 Materials

This section provides information about virgin aggregates, RAP materials and virgin binders used in this study. All the materials were obtained from local producers.

4.3.2.1 Aggregates

This part of the study intends to reproduce the three mixes that were used in Chapter 3.0 to determine the most effective cracking experiments for Oregon. Therefore, the same gradations that were used to prepare asphalt mixtures at the plant were used for laboratory mixture production. Virgin aggregates and RAP materials were obtained from Lakeside Industries in Portland, Oregon while the asphalt binders were taken from the Owens Corning Plant in Portland, Oregon. The aggregate gradations are presented in Section 4.3.3.1.

4.3.2.2 Recycled asphalt pavement (RAP) aggregates

The RAP material was also obtained from Lakeside Industries in Portland, Oregon. RAP content for all mixtures was 20%. All RAP aggregate properties were provided by the Lakeside Industries and are presented in Appendix B. AASHTO T 308-10 was followed for binder extraction and RAP content measurements. The quantity of binder in RAP materials for production Mix 1 was determined to be 5.26% while binder contents of the RAP used for production Mix 2 and Mix 3 were both 5.1%. AASHTO T 30-10 was followed to determine the gradation of extracted RAP aggregates. For five samples of RAP materials for Mix 1, Mix 2, and Mix 3, RAP aggregates were extracted and their gradations were determined, as shown in Table 3.1 and Table 3.2, respectively. Then, to obtain the final RAP aggregate gradation, the percent passing the #200 sieve was reduced by 1 percent. This correction was applied due to the aggregate breakdown in the ignition oven test (AASHTO T 30-10).

4.3.2.3 Binders

Owens Corning in Portland, Oregon provided the virgin binders (PG 70-22 ER and PG 70-22). Temperature curves, mixing temperatures and compaction temperatures were provided by Owens Corning as well. Binder properties and temperature curves are presented in Appendix C. Asphalt mixtures were prepared with two binder contents (5.3%, and 6.0%) in this study. These binder contents are the percentage of the total binder by the weight of the mix, and they include the recycled binder as well. In this study, it was assumed that all the RAP binder was completely blended with virgin binder (100 % blending). RAP content for all tested mixtures was 20%.

4.3.3 Sample preparation

4.3.3.1 Target gradations

Mix 1 followed a Level 4 3/8 in. NMA dense graded mix design and Mixes 2 and 3 followed a Level 4 1/2 in. dense graded mix design. These mix designs are given in Figure

B-1 to Figure B-8. Target gradations from the mix design and the gradations of virgin aggregates and extracted RAP aggregates for Mix 1 are presented in Table 4.2 and Figure 4.1 while the gradations for Mix 2 and Mix 3 are shown in Table 4.3 and Figure 4.2.

Table 4.2. Target, extracted RAP, and stockpiled aggregate gradations for Mix 1

Sieve Size	Percentage Passing		
Stockpile	Virgin Aggregate	RAP	Target Gradation
3/4"	100.0	100.0	100
1/2"	100.0	100.0	100
3/8"	100.0	96.8	99.4
1/4"	85.8	78.4	84.3
#4	64.7	66.4	65.1
#8	39.9	45.1	40.4
#16	28.1	31.5	28.1
#30	21.4	23.8	21.4
#50	14.5	17.4	14.8
#100	10.1	12.9	10.2
#200	8.0	8.4	7.7
Pan	0	0	0

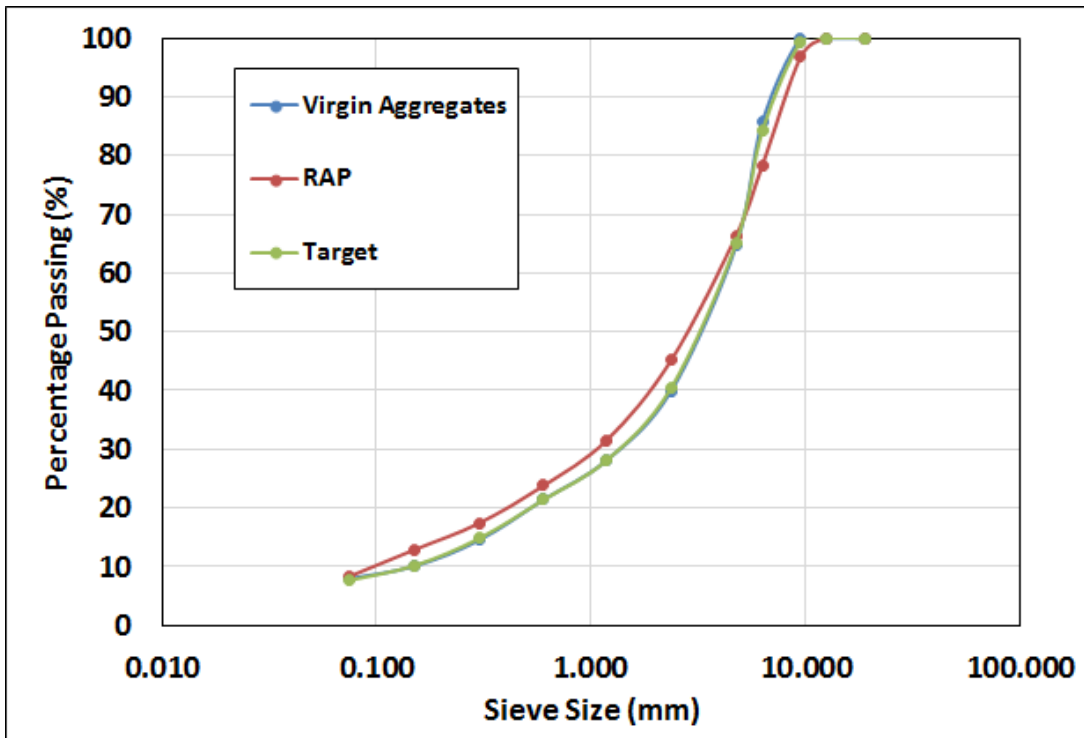


Figure 4.1: Target, extracted RAP, and stockpiled aggregate gradations for Mix 1

Table 4.3. Target, Extracted RAP, and Stockpiled Aggregate Gradations for Mix 2 and Mix 3

Sieve Size	Percentage Passing		
Stockpile	Virgin Aggregate	RAP	Target Gradation
3/4"	100.0	100.0	100
1/2"	94.0	97.6	96
3/8"	81.1	88.3	85
1/4"	61.7	69.8	63
#4	50.4	59.6	50
#8	32.1	42.0	32
#16	22.3	31.0	22
#30	16.5	24.0	17
#50	11.5	17.6	11
#100	8.5	12.6	9
#200	6.4	8.6	6.6
Pan	0	0	0

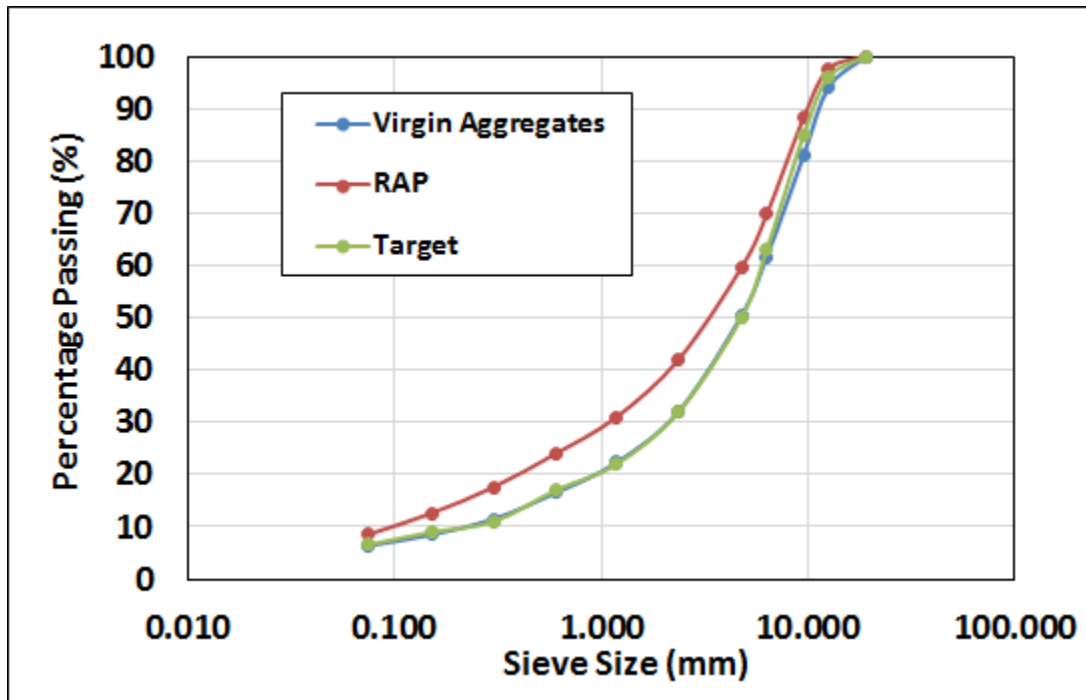


Figure 4.2: Target, extracted RAP, and stockpiled aggregate gradations for Mix 2 and 3

4.3.3.2 Batching

After measuring the gradations of virgin and RAP aggregates, three replicates of each combination of RAP content, binder content and binder grade were mixed according to AASHTO T 312-12 and their G_{mm} values were measured following the procedure described in AASHTO T 209-12. All the measured theoretical maximum specific gravities are presented in Appendix E. Then, aggregates were batched to meet the final gradation to reach 5% and 7% air contents. Knowing G_{mm} , the bulk specific gravity (G_{mb}) required to reach 5% and 7% air-void content of each sample were calculated using Equation 4.1. G_{mb} is the density of asphalt mixture divided by the density of water at 23°C (Pavement Interactive 2017) (Equation 4.2). The total volume of the samples was calculated by using the known dimensions of the laboratory compacted sample. Then, the total mass of the samples was calculated using Equation 4.3. Mass of aggregates and binders were determined afterwards, and samples were batched for mixing and compaction. An example of a batching calculation is given in Appendix F.

$$\text{air voids (\%)} = \frac{G_{mm} - G_{mb}}{G_{mm}} * 100 \quad 4.1$$

$$G_{mb} = \frac{\text{mass per unit volume of asphalt mixture}}{\text{density of water}} \quad 4.2$$

$$\text{total mass of sample} = \text{density of water} * G_{mb} * \text{volume of sample} \quad 4.3$$

4.3.3.3 Mixing and compaction

Batched samples were mixed and compacted by following the AASHTO T 312-12 procedure. Before mixing, aggregates were kept in the oven at 10 °C higher than the mixing temperature, RAP materials were kept at 110 °C (Mcdaniel and Anderson 2001) and binder was kept at the mixing temperature for 2 hours. After mixing, prepared loose mixtures were kept in the oven for 4 hours at 135 °C (AASHTO R 30-10) to simulate short-term aging. The goal of short-term aging is to simulate the aging and binder absorption that occurs during mixing phase of the production process. Then the aged loose asphalt mixtures were kept in the oven for 2 more hours at the compaction temperature prior to compaction.

4.3.3.4 Air void content

All the samples were prepared for the target 5% and 7% air-void content. Air-void contents were measured for all the samples after compaction. To find the air void

contents, the G_{mb} of the samples were measured after compaction by following AASHTO T 166-12. Air-void content for each sample was then determined by using Equation 4.1. Air-void contents for all specimens were required to be within $7\% \pm 1\%$ (Newcomb et al. 2015). In this study, all the samples met the requirement for air content while almost all specimens (except 5 samples) had air-void contents within $7\% \pm 0.5\%$. The measured air-voids for all the samples are presented in Appendix E.

4.3.4 Testing methods

Three tests were carried out in this study (SCB, DM and FN) to evaluate cracking and rutting performance of asphalt mixtures. SCB, DM and FN test methods followed in this study are discussed in Section 3.5.

4.4 RESULTS AND DISCUSSION

This section presents the results of SCB, DM and FN tests for the experimental plan given in Table 4.1. The purpose of this experimental plan was to determine the effects of binder content, air-void content, binder modification and gradation on measured cracking and rutting performance. The three mixes from Chapter 3.0 (Mix 1, Mix 2 and Mix 3), described in Section 3.4.2, were reproduced in the laboratory with two binder contents (5.3% and 6%) and two air-void contents (5% and 7%). A more detailed investigation into the effect of gradation was also performed and is presented in Chapter 5.0. A full factorial experimental plan with SCB, DM and FN tests was followed for all air-void, binder content and mix type combinations (Table 4.1) and results are presented in the subsequent sections.

4.4.1.1 Semi-circular bend (SCB) test

Samples were mixed and compacted to prepare specimens with 150 mm diameter and 130 mm height for each mix type and for each combination of binder content and air void content used in this study. Four replicate SCB test samples were obtained from each sample and a total of 48 samples were tested. The notch depth used was 15 mm (Ozer et al. 2016; Nsengiyumva 2015) and flexibility index was the parameter considered to evaluate the fatigue response of each sample.

Figure 4.3 compares the SCB results for plant mixed (PMLC) and laboratory mixed (LMLC) samples. It was observed that mixing type (plant or laboratory) does not significantly affect the measured flexibility index. Mix 3 was an exception for the reason described in Section 3.6.2.1 (higher production binder content for Mix 3).

Results for the entire test factorial are presented in Figure 4.4. Binder content and air void content significantly affected the measured flexibility index. Polymer modification (ER mixes) created mixtures that are significantly more resistant to cracking. Coleri et al. (2017) suggested a flexibility index of 10 as a threshold for cracking resistance acceptance. It can be observed from Figure 4.4 that none of the cases with PG70-22 binder (Mix 3-Non-ER mix) has a flexibility index close to 10 (the highest one is less than 6). This result suggested that polymer modification creates a significant improvement in cracking resistance of asphalt mixtures. In addition, a 0.7% increase in

binder content increases the flexibility index by 2 to 3 times. This observed significant effect of increased binder content on cracking performance suggested that increasing the binder content of asphalt mixtures currently used in Oregon can create significant savings by improving pavement longevity. By comparing results for M2-BC6%-AV5% and M2-BC6%-AV7%, it can be concluded that increasing asphalt density by 2% (an air-void content reduction from 7% to 5%) can increase flexibility index from 8 to 20. For this reason, producing asphalt mixtures that are easy to compact and utilizing intelligent compaction technologies that are currently being implemented in Oregon can potentially create a significant improvement in the cracking resistance of asphalt mixtures.

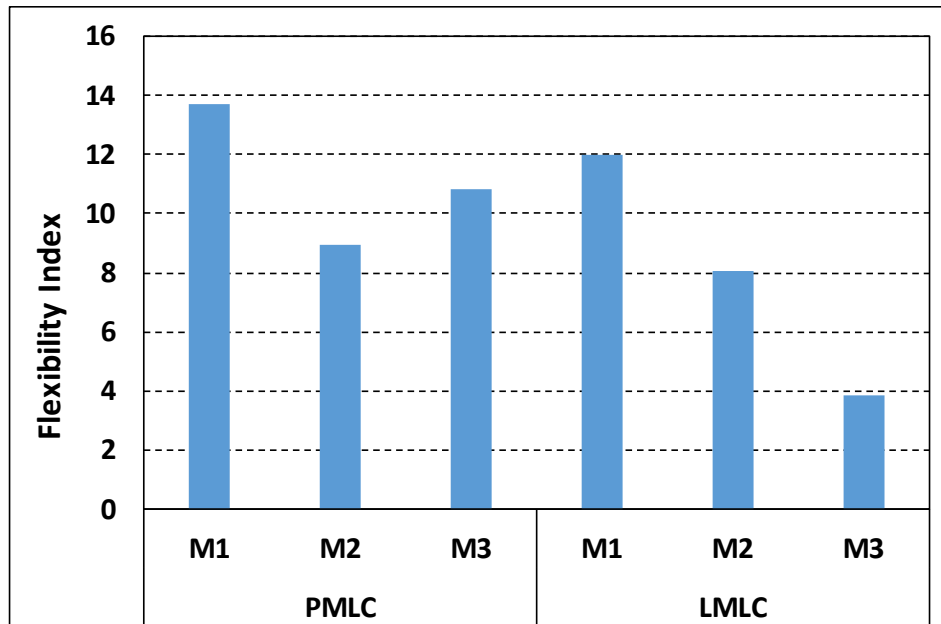


Figure 4.3. SCB results comparing plant and laboratory compaction.

Note: M1: Mix 1-PG70-22ER-Fine gradation
M2: Mix 2-PG70-22ER-Coarse gradation
M3: Mix 3-PG70-22-Coarse gradation

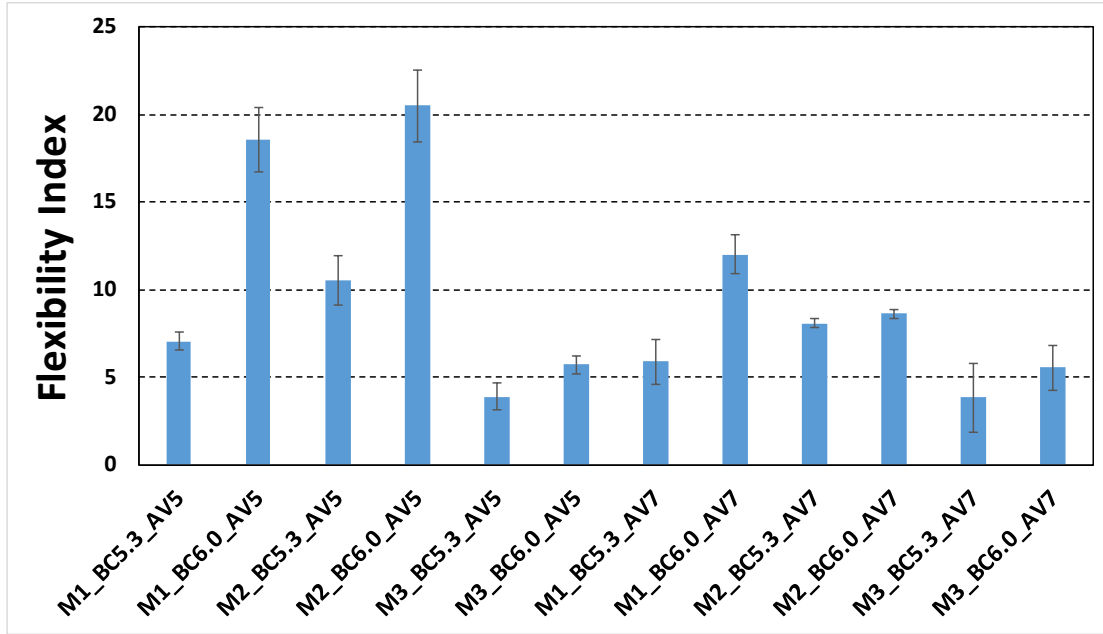


Figure 4.4. SCB results for the mixtures with different binder contents (5.3% and 6%), and air void contents (5%, and 7%).

Note: M1: Mix 1-PG70-22ER-Fine gradation
M2: Mix 2-PG70-22ER-Coarse gradation
M3: Mix 3-PG70-22-Coarse gradation
BC: Binder Content
AV: Air Void Content

ANOVA table

Analysis of Variance (ANOVA) was performed to estimate the effects of mix type, gradation, binder content and air void content on the dependent flexibility index (FI) variable. The F value in ANOVA analyses shows the statistical significance of each independent variable (Seber 1977). Flexibility indices were transformed logarithmically and linearly correlated with the dependent variables. As shown in Table 4.4, all independent variables are important except gradation. Mix type (ER or non-ER) had the most significant effect on FI since it exhibited the highest F value. Binder content and air-void content are the second and third most significant variables, respectively.

Table 4.4. ANOVA Table for the Regression Model Correlating FI Test Results with Mix Type, Gradation, Binder Content and Air Void Content

	Df	Sum of Squares	Mean Sum of Squares	F Value	Pr (F)
MIX	1	2.10	2.10	45.81	0.0003
GRAD	1	0.03	0.03	0.64	0.4504
BC	1	1.02	1.02	22.25	0.0022
AV	1	0.37	0.37	8.17	0.0244
Residuals	7	0.32	0.046		

4.4.1.2 Dynamic modulus (DM) test

In this part of the study, DM tests were conducted on three mixes with different binder contents (5.3% and 6%) and air void contents (5% and 7%). Two replicate experiments were conducted for each combination of the variables and 24 tests in total were conducted at frequencies and temperatures indicated in 3.5.6. The testing procedure described in AASHTO TP 79-13 for unconfined mixtures was followed. Dynamic modulus master curves are presented in Figure 4.5, Figure 4.6 and Figure 4.7. These master curves were used in Chapter 7.0 to perform mechanistic-empirical pavement design simulations.

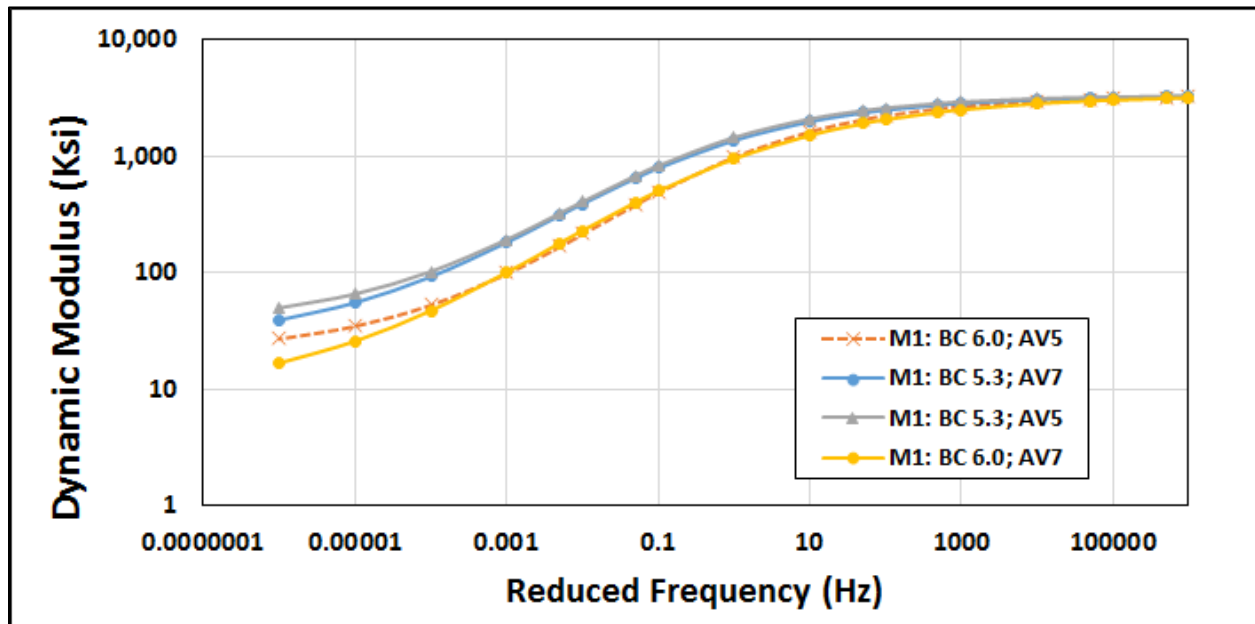


Figure 4.5. Master curves of dynamic modulus for M1 with different binder contents (5.3% and 6%), air void contents (5%, and 7%).

Note: M1: Mix 1-PG70-22ER-Fine gradation
 BC: Binder Content
 AV: Air Void content

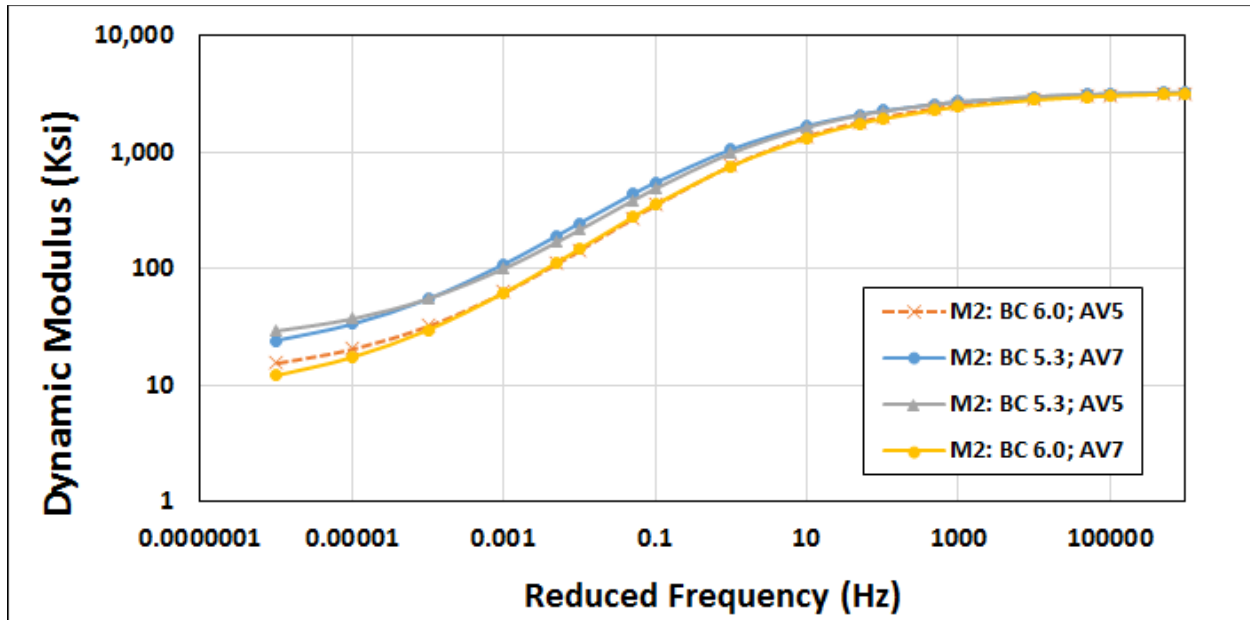


Figure 4.6. Master curves of dynamic modulus for M2 with different binder contents (5.3% and 6%), air void contents (5%, and 7%).

Note: M2: Mix 2-PG70-22ER-Coarse gradation
 BC: Binder Content
 AV: Air Void content

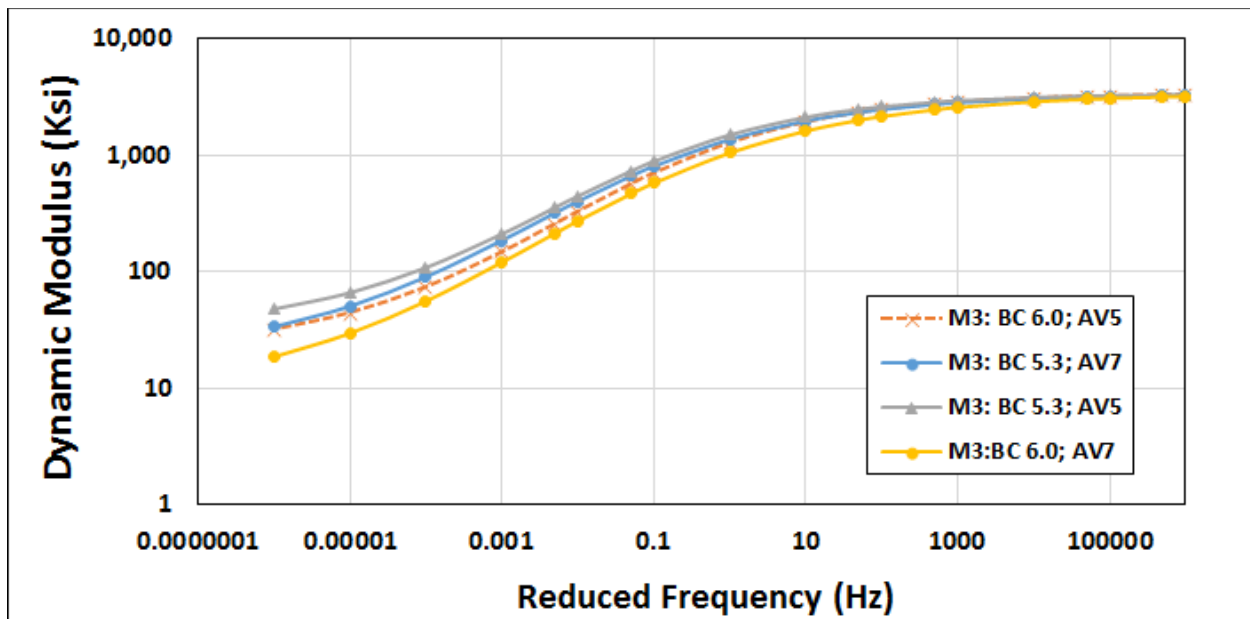


Figure 4.7. Master curves of dynamic modulus for M3 with different binder contents (5.3% and 6%), air void contents (5%, and 7%).

Note: M3: Mix 3-PG70-22-Coarse gradation
 BC: Binder Content
 AV: Air Void content

From Figure 4.5, Figure 4.6 and Figure 4.7, it can be observed that Mix 1 with a binder content of 5.3% and air-void content of 5% was the stiffest and Mix 2 with binder content 6% and air void content 7% was the softest mixture of all combinations. Although decreasing air-void content was determined to improve cracking resistance (See Figure 4.4), air-void content was not observed to have any significant effect on dynamic modulus of mixtures. However, increasing binder content from 5.3% to 6% was observed to significantly reduce the dynamic modulus of asphalt mixtures. It was also observed that although the master curves for Mix 1 and Mix 3 are close, Mix 1 had a significantly higher cracking resistance than Mix 3. This result suggested that although polymer modification does not create a significant change in mixture stiffness, it improved cracking performance due to increased ductility.

In order to evaluate the difference between field mixing and laboratory mixing, master curves of Mix 1 (6% binder content and 7% air voids), Mix 2 (5.3% binder content and 7% air voids) and Mix 3 (5.3% binder content and 7% air voids) prepared by laboratory mixing (LMLC) were compared with the master curves for the same three mixes with the same properties obtained from the plant (PMLC). Figure 4.8 illustrates the master curves for the above-mentioned samples. Although the ranking of the three mixes in terms of stiffness was similar for LMLC and PMLC samples, it was observed that the stiffnesses of the laboratory mixed samples were in general higher than plant mixed samples. One of the important reasons for this difference might be the short-term aging simulation in the laboratory. Four hours of aging at 135°C to simulate short-term aging for LMLC samples may be creating stiffer mixes. However, further investigations are necessary to derive this conclusion.

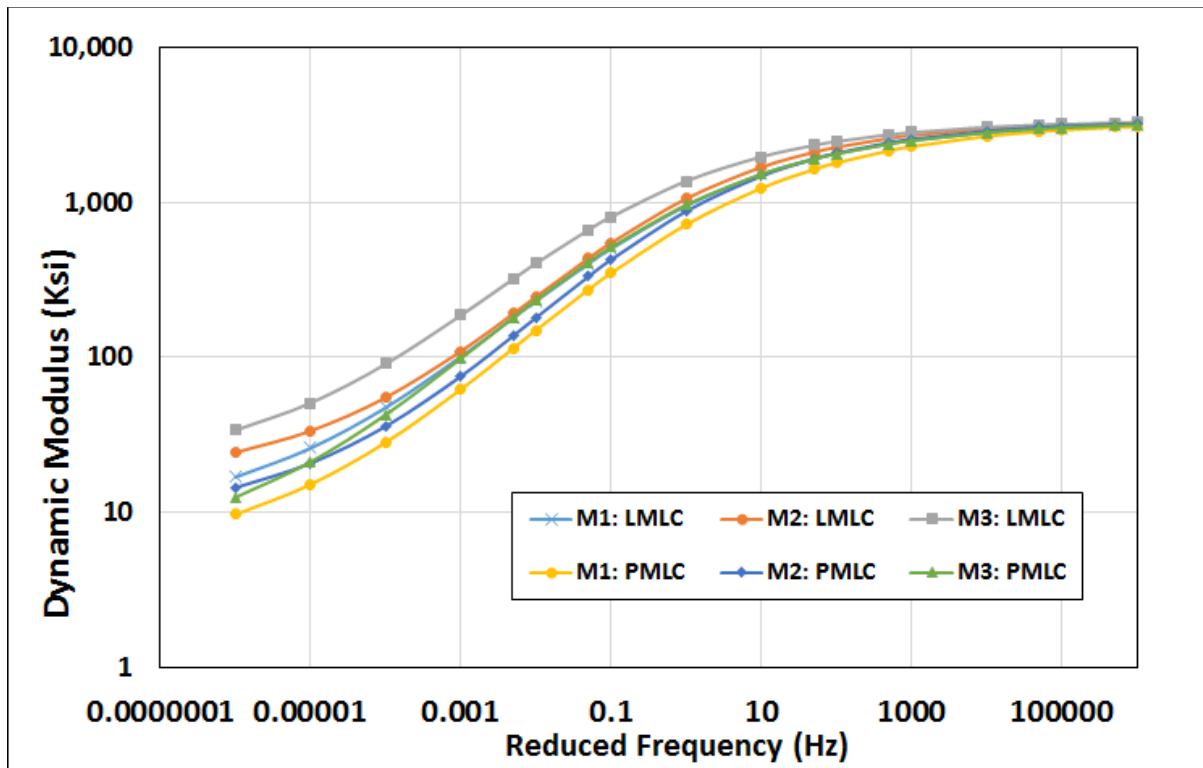


Figure 4.8. Master curves of dynamic modulus comparing field mixed and laboratory mixed samples.

Note: M1: Mix 1-PG70-22ER-Fine gradation
M2: Mix 2-PG70-22ER-Coarse gradation
M3: Mix 3-PG70-22-Coarse gradation
LMLC: Lab Mixed-Lab Compacted
PMLC: Plant Mixed-Lab Compacted

Phase angle master curves for all test results are plotted in Figure 4.9, Figure 4.10 and Figure 4.11. The same shift factor values, which were calculated and used for developing the master curves for DM tests, are used to develop the master curves for phase angles. The reference temperature for all master curves is 20°C.

In general, from Figure 4.9, Figure 4.10 and Figure 4.11, it is evident that decreasing binder content reduces measured phase angles. This result suggests that mixtures with higher binder contents will have higher cracking resistance. On the other hand, air-void content does not significantly affect the phase angle of the asphalt mixtures.

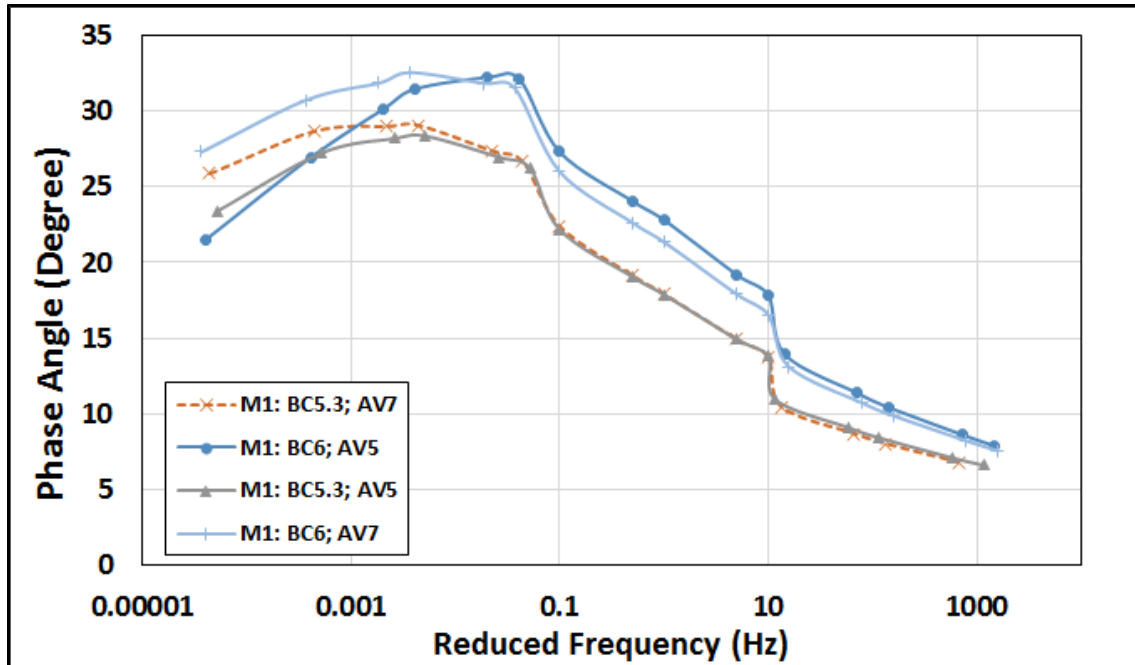


Figure 4.9. Phase angle master curves for M1 with different binder contents (5.3% and 6%), air void contents (5%, and 7%).

Note: M1: Mix 1-PG70-22ER-Fine gradation
 BC: Binder Content
 AV: Air Void content

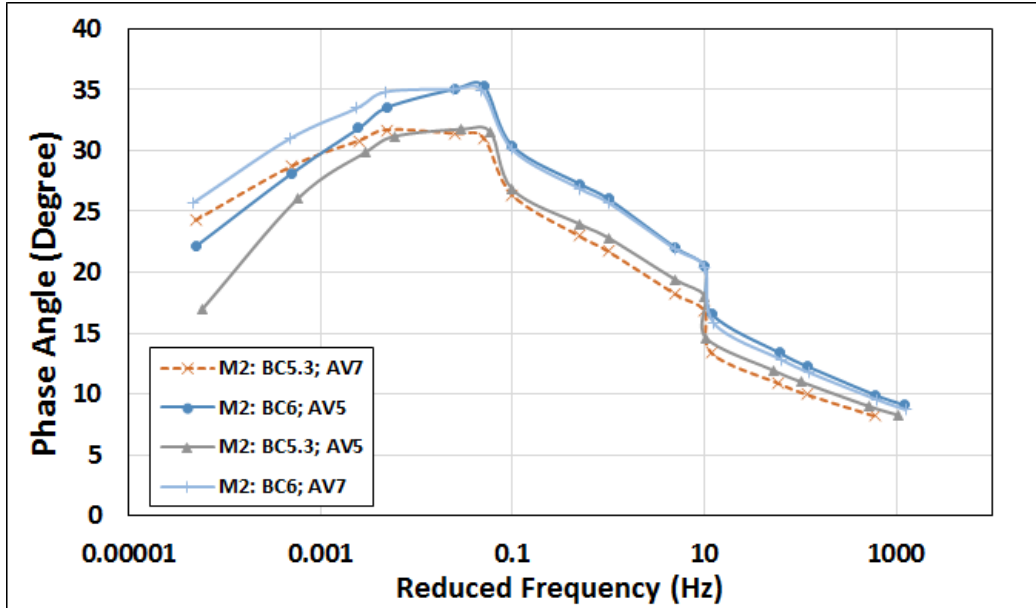


Figure 4.10. Phase angle master curves for M2 with different binder contents (5.3% and 6%), air void contents (5%, and 7%).

Note: M2: Mix 2-PG70-22ER-Coarse gradation
 BC: Binder Content
 AV: Air Void content

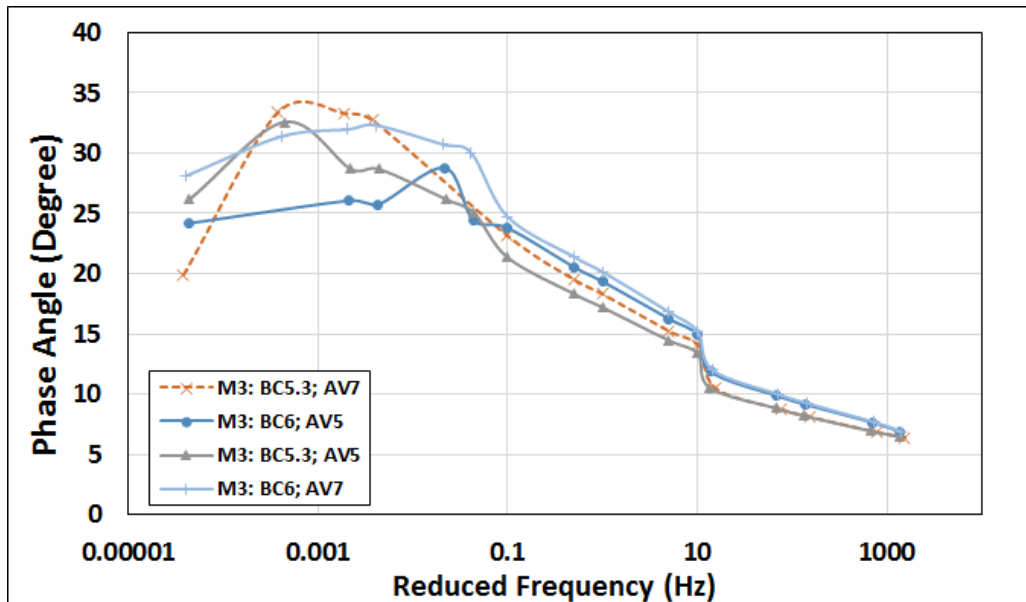


Figure 4.11. Phase angle master curves for M3 with different binder contents (5.3% and 6%), air void contents (5%, and 7%).

Note: M3: Mix 3-PG70-22-Coarse gradation
 BC: Binder Content
 AV: Air Void content

4.4.1.3 Flow number (FN) test

The flow number (FN) test is a simple performance test for evaluating rutting performance of asphalt concrete mixtures (Bonaquist et al. 2003). High FN values indicate that asphalt mixtures have high rutting resistance. Figure 4.12 presents the FN values for all the three mixes with different binder contents and air void contents.

Suggested FN for the traffic level of 10 million to 30 million ESALs is specified as 190 while the FN limit for roadways with ESALs more than 30 million were specified as 740 (AASHTO TP 79-13). In Figure 4.12, dashed and solid red lines show the recommended FN for the traffic levels of 10 to <30 million and ≥ 30 million ESALs, respectively. FN values for all the asphalt mixtures were greater than 740, which is the recommended FN for the traffic level of more than 30 million ESALs. These results suggest that all tested mixtures are stiff enough to resist any rutting failures in the field. This result further suggests that increasing binder content is not going to result in rutting failures in the field while increased binder content will significantly improve cracking resistance of asphalt mixtures. In other words, increasing binder content is an effective strategy to improve pavement longevity.

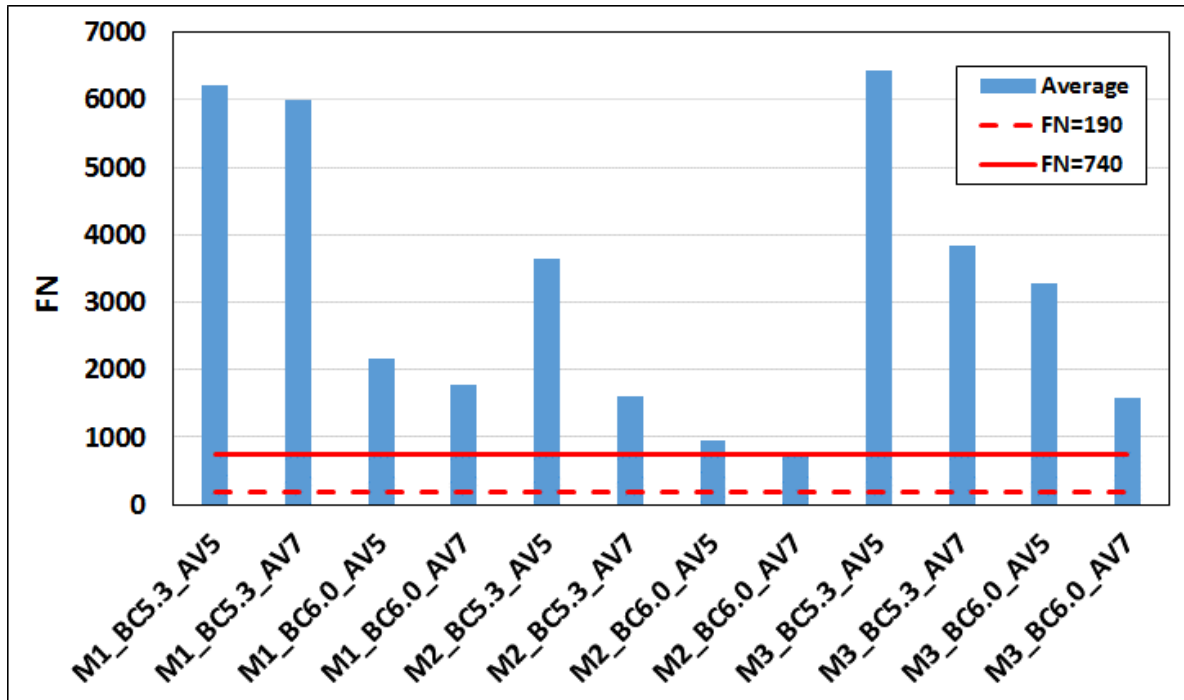


Figure 4.12. Flow number for mixes with different binder contents (5.3% and 6%), air void contents (5% and 7%).

Note: M1: Mix 1-PG70-22ER-Fine gradation
M2: Mix 2-PG70-22ER-Coarse gradation
M3: Mix 3-PG70-22-Coarse gradation
BC: Binder Content
AV: Air Void Content

ANOVA Table

Analysis of Variance (ANOVA) was performed to estimate the effects of mix type, gradation, binder content, and air void content on the dependent flow number (FN) variable. The F value in ANOVA analyses shows the statistical significance of each independent variable (Seber 1977). FN values were transformed logarithmically and linearly correlated with the dependent variables. As shown in Table 4.5, all independent variables are important except gradation. Binder content had the most significant effect on FN since it had the highest F value. Mix type (ER or non-ER) and air-void content are the second and third most significant variables, respectively.

Table 4.5. ANOVA Table for the Regression Model Correlating FN Test Results with Mix Type, Binder Content and Air Void Content

	Df	Sum of Squares	Mean Sum of Squares	F Value	Pr (F)
MIX	2	2.04	1.02	23.03	0.0008
BC	1	2.98	2.98	67.23	0.0001
AV	1	0.56	0.56	12.68	0.0092
Residuals	7	0.31	0.044		

4.5 SUMMARY AND CONCLUSIONS

This portion of the study focused on quantifying the impact of air-void content, binder content, gradation and polymer modification on cracking and rutting resistance of asphalt mixes commonly used in Oregon. The study was divided into two parts. The first part was to reproduce the three mixes from Section 3.4.2 in the laboratory (laboratory mixed-laboratory compacted samples). Two binder contents (5.3% and 6%) and two air-void contents (5% and 7%) were used for each mix type. Mix 1 and Mix 2 had polymer-modified binders while Mix 3 was a non-polymer mixture. Mix 1 had a finer gradation while Mix 2 and Mix 3 had coarse gradations. The results from this Chapter were also compared with the results from Section 3.6.2. The objective was to identify the impact of the difference in mixing (laboratory and plant mixing) and short-term aging (plant and laboratory short-term aging) on cracking and rutting resistance of asphalt mixtures.

The following conclusions were derived from this portion of the study:

- Polymer modification plays an important role in imparting ductility to the mix and thereby significantly increases the cracking resistance of the asphalt mix.
- Binder content significantly affected the measured flexibility index. A 0.7% increase in binder content increases the flexibility index by 2 to 3 times. This observed significant effect of increased binder content on cracking performance suggested that increasing binder content of asphalt mixtures currently used in Oregon can create significant savings by improving pavement longevity.
- Air-void content (density) significantly affected the measured flexibility index. A 2% reduction in air-void content increases the flexibility index by 1.5 to 2 times. For this

reason, producing asphalt mixtures that are easy to compact and utilizing intelligent compaction technologies that are currently being implemented in Oregon can potentially create a significant improvement in the cracking resistance of asphalt mixtures.

- Mixing type (plant or laboratory) does not significantly affect the measured flexibility index.
- According to DM test results, although decreasing air-void content was determined to improve cracking resistance, air-void content was not observed to have any significant effect on dynamic modulus of mixtures. However, increasing binder content from 5.3% to 6% was observed to significantly reduce the dynamic modulus of asphalt mixtures.
- Although polymer modification does not create a significant change in mixture stiffness, it improved cracking performance due to increased ductility.
- The stiffnesses of the laboratory mixed samples were, in general, higher than that of the plant mixed samples. One of the important reasons for this difference might be the short-term aging simulation in the laboratory. Four hours of aging at 135°C to simulate short-term aging for LMLC samples may be creating stiffer mixes.
- FN values for all the asphalt mixtures were greater than 740, which is the recommended FN for the traffic level of more than 30 million ESALs. These results suggest that all tested mixtures are stiff enough to resist any rutting failures in the field. This result further suggests that increasing binder content is not going to result in rutting failures in the field while the increased binder content will also significantly improve the cracking resistance of asphalt mixtures. In other words, increasing binder content is an effective strategy to improve pavement longevity.

5.0 IMPACT OF INCREASED DUST CONTENT ON CRACKING PERFORMANCE

5.1 INTRODUCTION

Aggregate gradation plays a prominent role in cracking performance of asphalt mixtures. Increasing dust content and using finer gradations can reduce the required binder content for the asphalt mix and reduce the initial production costs. This reduction in required binder content is generally a result of the dust particles replacing the binder required to fill the voids in the aggregate microstructure. However, increasing dust content and using finer gradations make the asphalt mixes drier (reduces binder content) and reduce the asphalt film thickness around the aggregates. Thus, reduced binder content and film thickness can reduce the cracking resistance of the asphalt mixture. Reduced asphalt mixture performance can increase the maintenance costs during the service life of the pavement structure.

In this part of the study, a new gradation was created by increasing the dust content. A new mix design was developed for the created high dust content mix. The objective was to evaluate the effect of increased dust content on fatigue performance of asphalt mixtures. SCB tests were conducted to analyze the cracking performance of these mixtures. These results were compared with the results from the control mixes prepared by following the ODOT mix design and target gradations to determine the impact of high dust content on cracking performance.

5.2 OBJECTIVE

The major objective of this part of the study was to determine the cracking performance of asphalt mixtures with higher dust contents. The impact of dust content on cracking performance was determined by comparing two mixtures with similar volumetrics (similar mix designs) but with different binder and dust contents.

5.3 MATERIALS AND METHODS

Materials and Experimental Design

It is possible to achieve similar mixture volumetrics by using different gradations and binder contents. In order to reduce the amount of binder required to reach a specific density level with equal compaction effort (same number of gyrations in a SGC), dust content of the mixture can be increased. The additional dust introduced into the mixture can fill the voids between aggregates with larger sizes and make it possible to reach the required density with less binder. On the other hand, the same density with equal compactive effort can be achieved by increasing the binder content of the asphalt mixture rather than increasing the dust content. Since excessive dust particles in the asphalt mixture reduce the adhesion between aggregates and the binder, higher dust-to-binder ratios in an asphalt mixture are expected to reduce durability. Although increasing dust content to achieve required density is expected to reduce initial costs (material production

costs), a possible reduction in cracking resistance for high dust mixtures can potentially increase life-cycle costs.

In this study, in order to determine the effect of high dust content on performance, first two gradations (a fine and a coarse gradation) were selected. Figure 5.1 shows the gradation curves selected for mixture production. The original gradation is the gradation used by Lakeside industries to produce Mix 3 in this study while the finer gradation is the gradation selected to investigate the high dust content effect on durability. The mix design binder content for the “original gradation” mix was already specified as 5.3% by ODOT and used for production by the plant (See Appendix B). The binder content for the “finer gradation” mix was determined by following the mix design procedure given in AASHTO M 323-12. The procedure followed to design the mix is given in the next section (Section 5.3.2). After the binder content for the “finer gradation” mix was determined, actual test specimens with 7% target air-void content were prepared. In this study, a total of eight SCB tests (Section 3.5.1), four DM tests (Section 3.5.6) and four FN tests (Section 3.5.7) were conducted to determine the effect of increased dust content on durability. The experimental plan followed is given in Table 5.1.

Table 5.1: Experimental Plan for Dust Content Effect Evaluation

Test type	Mix Type	Comp.	Temp.	Binder Grade	Agg. grad.- binder content	Air void	Repl.	Total Tests
SCB	M3 ¹	LMLC ²	25°C	PG 70-22	CA ⁴ -5.3% FA-5.1%	7%	4	8
Dynamic modulus	M3	LMLC	1 run ³	PG 70-22	CA-5.3% FA-5.1%	7%	2	4
Flow number	M3	LMLC	54.7°C	PG 70-22	CA-5.3% FA-5.1%	7%	2	4

Notes:

¹ M3: Mix 3-PG70-22-Fine gradation

² LMLC: Laboratory mixed and Laboratory compacted

³ Samples were tested at temperatures of 4 °C, 20 °C, and 40 °C and the loading frequencies of 0.1, 0.5, 1, 5, and 10 Hz. A loading frequency of 0.01 Hz was also used for 40 °C tests.

⁴ CA: Coarse gradation; FA: Fine gradation

The virgin aggregates and RAP aggregates described in Section 4.3.2 were used in this study. The binder used in this study (PG70-22) was provided by Owens Corning in Portland, Oregon.

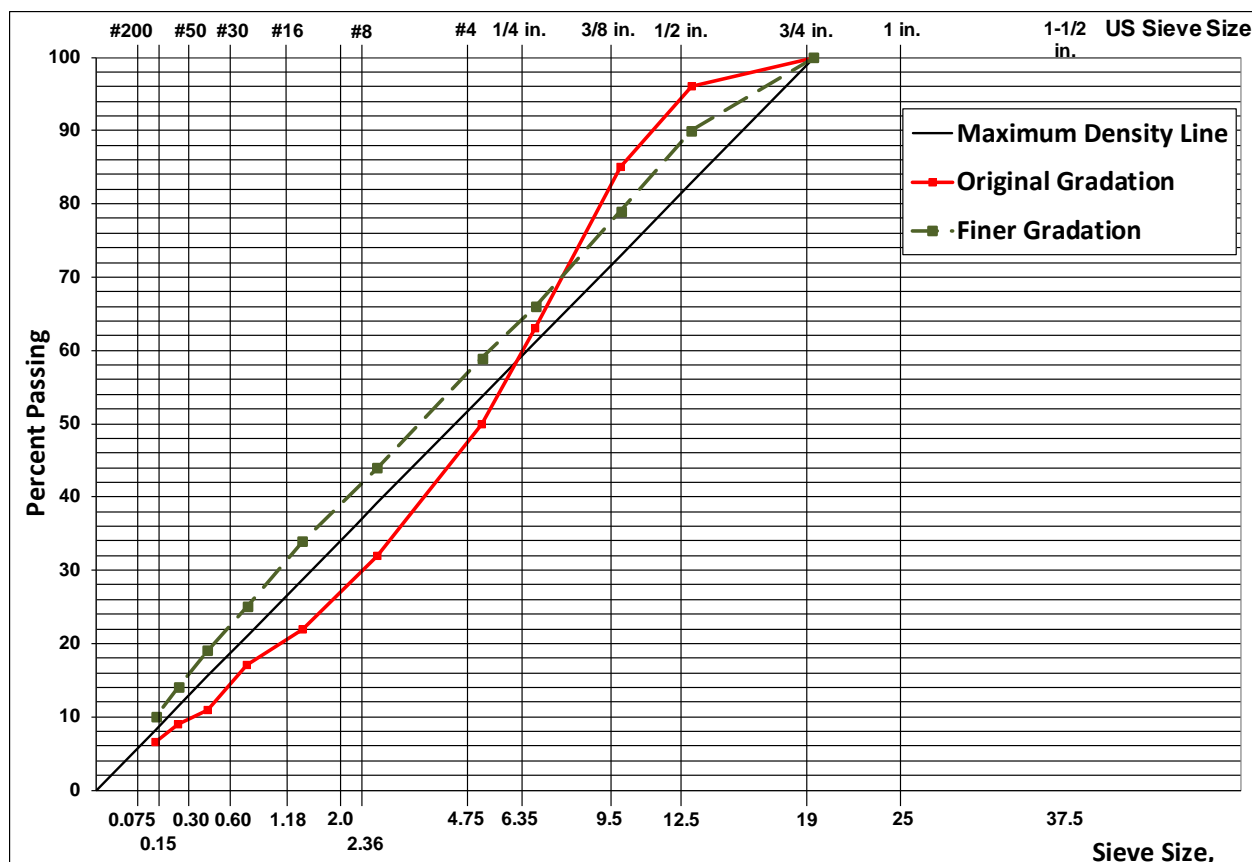


Figure 5.1: Gradations selected to evaluate the effect of increased dust content on durability.

5.3.1 Mix Design Process

After fixing the target gradation, four trial binder contents were chosen (5.0%, 5.5%, 6.0% and 6.5%) for mix design. Three replicate G_{mm} samples for each binder content level (12 G_{mm} samples in total) were mixed according to AASHTO T 312-12 and their G_{mm} values were measured following the procedure described in AASHTO T 209-12. By following the batching procedure described in Section 4.3.3.2, three replicate mix design batches for each binder content level were prepared (12 samples in total). Mixed samples were short-term aged for 4 hours at 135°C and were compacted into cylindrical specimens of 150 mm diameter by fixing the number of gyrations in the gyratory compactor to 100. The volumetrics [air void content (AC), voids in mineral aggregates (VMA) and voids filled with asphalt (VFA)] were determined for each sample. The binder content that met the criteria for AC, VMA and VFA was chosen as the optimum binder content for the high dust mix. Figure 5.2 illustrates the relationship between air-void content and asphalt content. It can be observed that an asphalt content of 5.1% yielded the target 4% air voids. Hence, the optimum binder content was chosen as 5.1% and used for actual test sample preparation (with a target air-void content of 7%) as described in the previous Section (Section 5.3.1). The dust-to-binder ratio for the “original gradation” and the “finer gradation” mixes were determined to be 1.42 and 2.2, respectively.

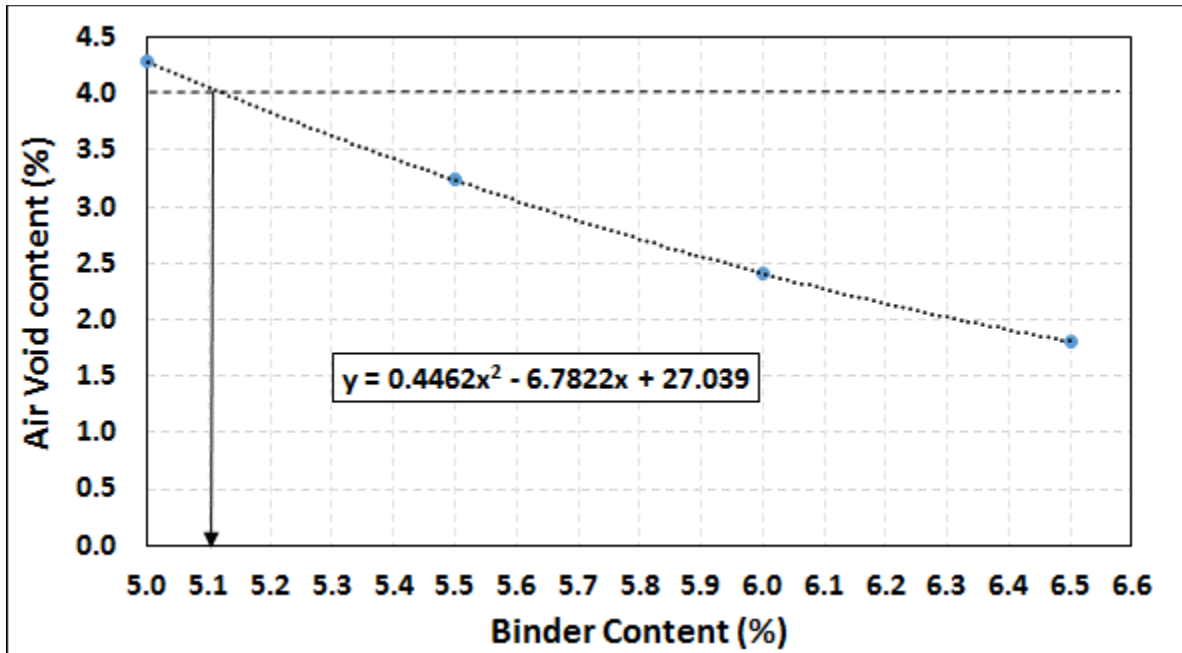


Figure 5.2: Mix design curve – Binder content versus air-void content.

5.4 RESULTS AND DISCUSSION

5.4.1 Semi-Circular Bend (SCB) Test

SCB test results for the “original gradation” and “finer gradation” mixes are presented in Figure 5.3. Both mixtures had similar volumetrics while for the “finer gradation” mix, some of the required binder to fill the voids was replaced with dust particles. For this reason, design binder content for the “finer gradation” mix is about 0.2% lower than the binder content for the “original gradation” mix. It can be observed from Figure 5.3 that average flexibility index (FI) for the “finer gradation” mix is about 25% lower than the “original gradation” mix. This result suggested that increasing the dust content to achieve density targets with less binder content could reduce in-situ cracking performance and reduce pavement longevity. For this reason, lower dust-to-binder ratios should be targeted to improve cracking resistance of asphalt mixtures. As stated in Section 5.3.2, the dust-to-binder ratio for the “original gradation” mix is 1.42. Without changing the gradation, increasing the design binder content for this mix from 5.3% to 6% is expected to reduce the dust-to-binder ratio to about 1.29. It can be observed from Figure 4.4 that the flexibility index for the same mixture with 6% binder content (dust-to-binder ratio of 1.29) is about 31% higher than the mix with a dust-to-binder ratio of 1.42 (FI increases from 3.85 to 5.55).

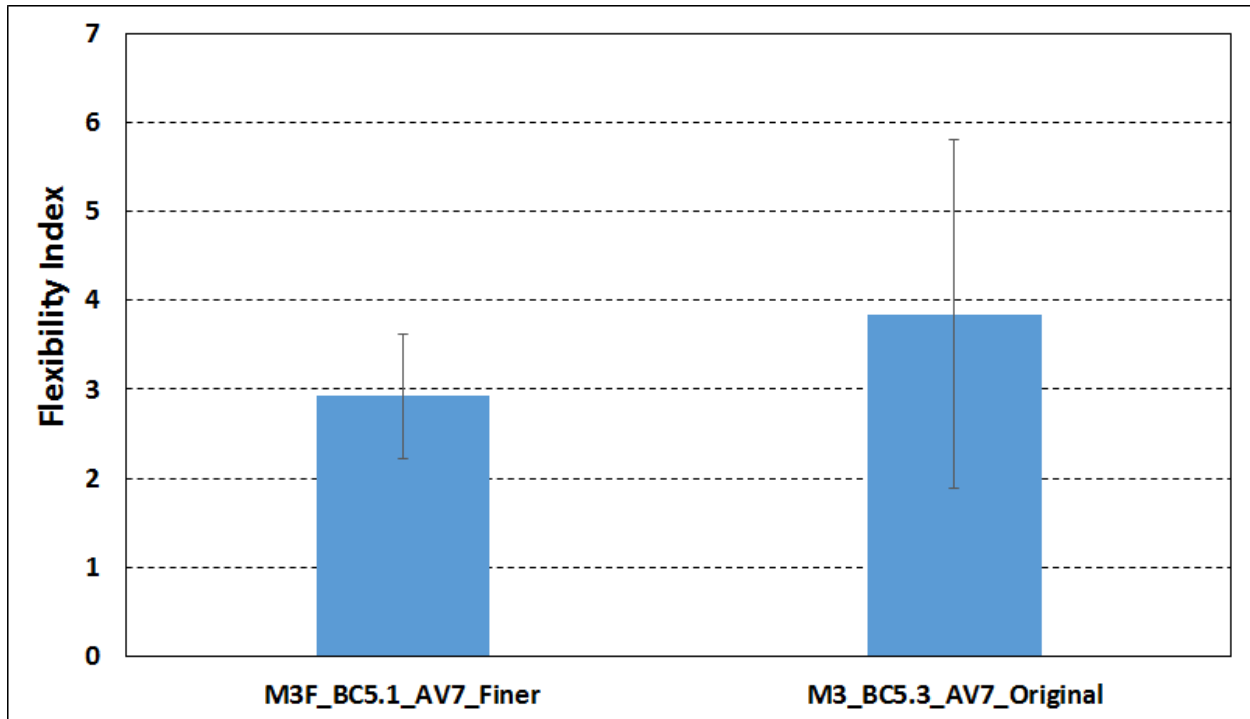


Figure 5.3. SCB results for dust content effect.

Note: M3F: Mix 3-PG70-22-Finer gradation
M3: Mix 3-PG70-22-Original coarse gradation
BC: Binder Content
AV: Air Void Content

5.4.2 Dynamic Modulus (DM) Test

DM tests were conducted with “original gradation” and “finer gradation” mixes. Two replicate experiments were conducted for each combination of the variables and 4 tests were conducted at frequencies and temperatures indicated in Section 3.5.6. The testing procedure described in AASHTO TP 79-13 for unconfined mixtures was followed. Reference temperature for all the master curves is 20°C. Dynamic modulus master curves are presented in Figure 5.4. The master curve for the “finer gradation” mix was compared with the master curve for “original gradation” mix. It was observed that the stiffness of the “finer gradation” mix was higher than the “original gradation” mix. Higher dust content and lower binder content created a stiffer mix with lower cracking resistance.

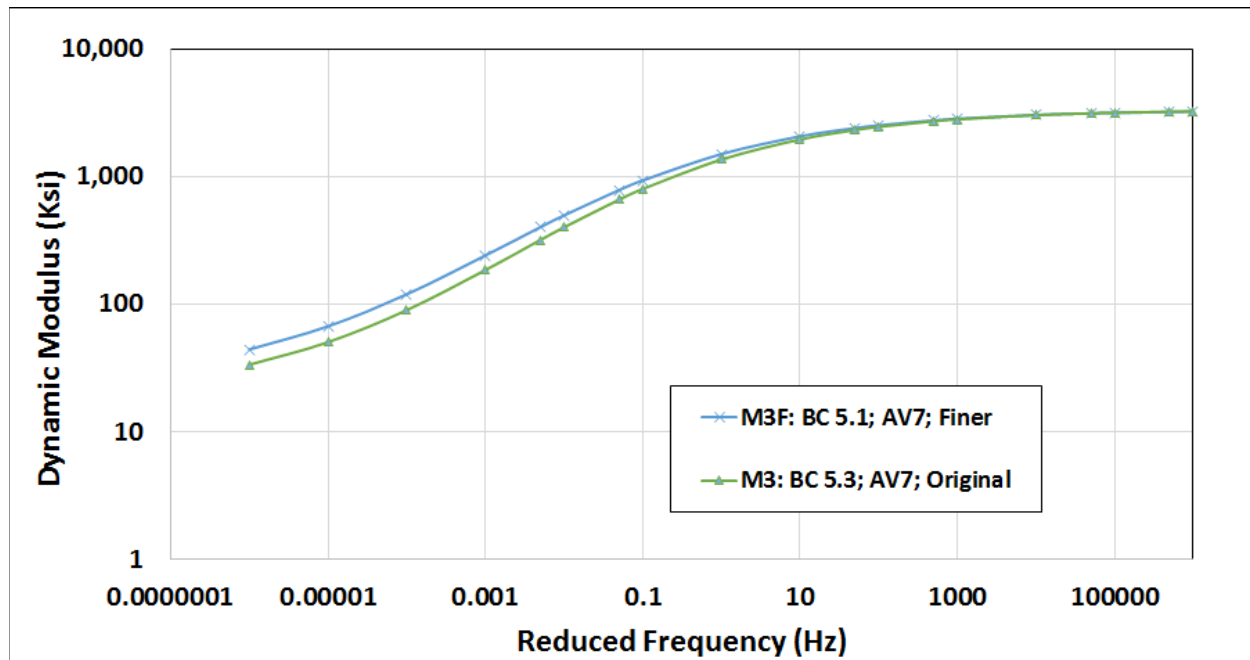


Figure 5.4. DM master curves comparing finer and coarse gradations.

Note: M3F: Mix 3-PG70-22-Finer gradation
M3: Mix 3-PG70-22-Original coarse gradation
BC: Binder Content
AV: Air Void Content

Phase angle master curves for all test results are plotted in Figure 5.5. The same shift factor values, which were calculated and used for developing the master curves for DM tests, were used to develop the master curves for phase angles. Results were in agreement with the dynamic modulus values. The results show that having a higher dust content (more aggregate surface area) and about 0.2% lower binder content resulted in lower phase angle values for the “finer gradation” mix. The lower phase angle for the “finer gradation” mix indicated that this mix is less viscous, less susceptible to rutting and less resistant to cracking.

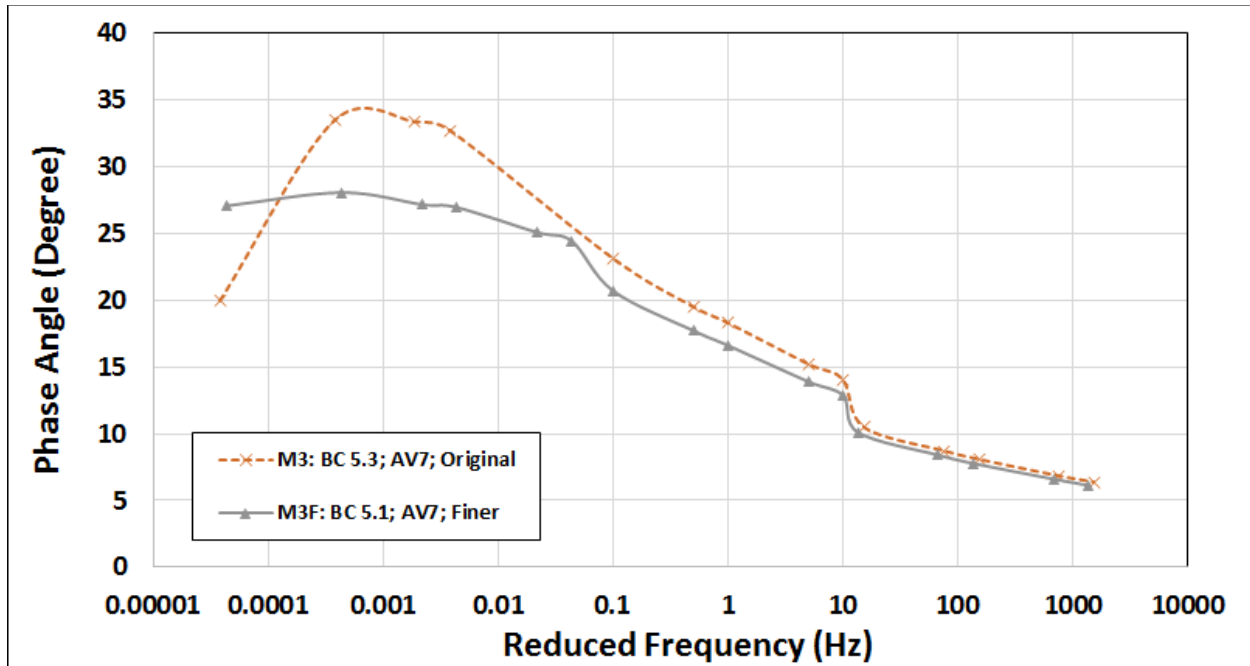


Figure 5.5. DM master curves comparing finer and coarse gradations.

Note: M3F: Mix 3-PG70-22-Finer gradation
M3: Mix 3-PG70-22-Original coarse gradation
BC: Binder Content
AV: Air Void Content

5.4.3 Flow Number (FN) Test

Flow number tests were conducted with each mix to determine the rutting resistance of “original gradation” and “finer gradation” mixtures. Two replicate experiments were conducted for each mix type. FN test results are presented in Figure 5.6. It can be observed that the FN for both mixtures are higher than 740, which is the recommended FN for the traffic level of more than 30 million ESALs. These results suggest that these two mixes are not susceptible to rutting failures in the field. The “Finer gradation” mix was observed to have a higher rutting resistance than the “original gradation” mix.

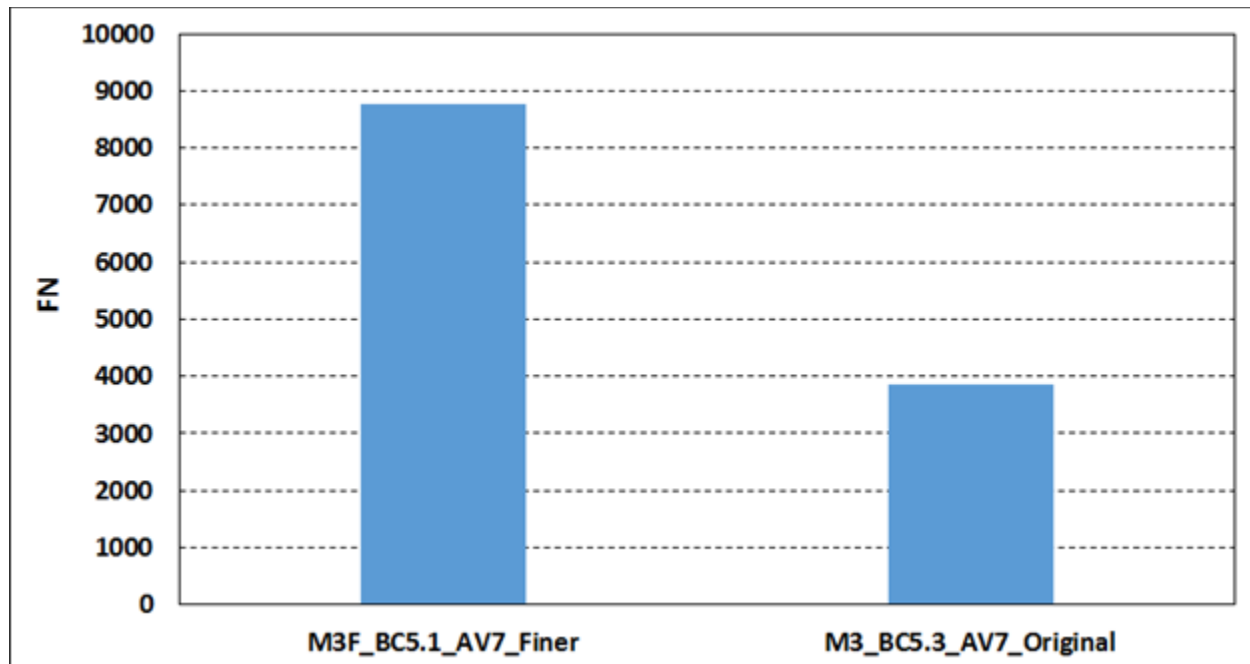


Figure 5.6. FN test results for dust content effect.

Note: M3F: Mix 3-PG70-22-Finer gradation
M3: Mix 3-PG70-22-Original coarse gradation
BC: Binder Content
AV: Air Void Content

5.5 SUMMARY AND CONCLUSIONS

In this part of the study, a new gradation was created by increasing the dust content. A new mix design was developed for the created high dust content mix, which provided about a 0.2% reduction in required binder content when compared to the control mixture. This reduction in required binder content is expected to be a result of the dust particles replacing the binder required to fill the voids in the aggregate microstructure. The objective of this part of the study was to evaluate the effect of increased dust content on fatigue performance of asphalt mixtures. SCB tests were conducted to analyze the cracking performance of these mixtures. These results were compared with the results from the control mixes prepared by following the ODOT mix design and target gradations. Results showed that increased dust content makes the mix drier and reduces the asphalt film thickness around the aggregates. Thus, reduced binder content and film thickness reduces the flexibility index of the asphalt mix. Therefore, the mixture with a high dust-to-binder ratio is expected to be more susceptible to fatigue cracking. For this reason, decreasing the dust-to-binder ratio by limiting the dust content and/or increasing the binder content will provide asphalt mixtures with higher cracking resistance.

6.0 THE EFFECT OF LABORATORY LONG-TERM AGING ON CRACKING PERFORMANCE OF ASPHALT MIXTURES

6.1 INTRODUCTION

The phenomenon of fatigue cracking in asphalt pavements is observed several years after construction. The aromatic compounds, which are a constituent of the asphalt binder, have a tendency to oxidize over time. The oxidation results in the creation of polar carbonyl compounds that increase the elastic modulus and viscosity of the binder. In other words, stiffening of the binder occurs (Glover et al. 2005). This process is known as aging. Aging of asphalt mixtures is a continuous phenomenon, which starts during production and construction and is observed throughout the service life of the pavement. This causes the asphalt mixtures to become brittle, thereby making them more susceptible to cracking. In the past, aging was assumed to be relatively consistent and reasonable correlations have been established between laboratory and field aging (Bell et al. 1994). However, over the last decade, due to the increased use of recycled materials and polymer modification, there is a need to understand the impact of aging on the behavior of asphalt mixtures.

In Chapters 3.0 to 5.0, all LMLC samples were short-term aged to simulate the aging and binder absorption that occurs during mixing phase of the production process. However, none of these mixes were long-term aged to simulate aging within the first 5 to 15 years. In this Chapter, the plant produced loose mixtures described in Section 3.4.2 were further aged in the oven at 85°C for five days after short-term aging at 135 °C for 4 hours (these are called “long-term aged” samples). After long-term and short-term aging, samples were prepared using the SGC and were tested to determine their cracking performance. For this purpose, SCB tests were conducted to measure the flexibility index of the aged samples. Flexibility indices for short and long-term aged samples were compared to the flexibility indices for only short-term aged samples (Figure 3.31) to determine the impact of aging on cracking resistance. DM and FN tests were also conducted to determine the impact of aging on mixture stiffness and rutting resistance.

6.2 OBJECTIVES

The major objectives of this part of the study were to:

- Determine whether the long-term aging process has any impact on the cracking performance ranking of asphalt mixtures, and
- Identify the effect of long-term aging on measured flexibility index values.

6.3 MATERIALS AND METHODS

The three plant produced mixes described in Chapter 3.0 were used in this study to evaluate the effect of aging. After splitting the mix obtained from the plant, the required amount of material for SCB and DM samples were weighed out and short-term aged in the oven at 135°C for 4 hours. They were then placed in the oven at 85°C for five days. It was ensured that the mix was stirred from time-to-time to obtain uniform aging. At the end of the fifth day, the mixtures were heated to compaction temperature and were compacted using SGC (AASHTO T312-12). A total of 12 SCB tests (Section 3.5.1), 6 DM tests (Section 3.5.6) and 6 FN tests (Section 3.5.7) were conducted. The experimental plan is shown in Table 6.1.

Table 6.1: Experimental Plan for Aging Evaluation

Test type	Mix Type	Comp.	Temp.	Repl.	Total Tests
SCB	M1 ¹ M2 M3	PMLC ²	25°C	4	12
Dynamic modulus	M1 M2 M3	PMLC	1 run ³	2	6
Flow number	M1 M2 M3	PMLC	54.7°C	2	6

Note: ¹ M1: Mix 1-PG70-22ER-Fine gradation
M2: Mix 2-PG70-22ER-Coarse gradation
M3: Mix 3-PG70-22-Coarse gradation

² PMLC=Plant Mixed Laboratory Compacted;

³ Samples were tested at temperatures of 4 °C, 20 °C, and 40 °C and the loading frequencies of 0.1, 0.5, 1, 5, and 10 Hz. A loading frequency of 0.01 Hz was also used for 40 °C tests.

6.4 RESULTS AND DISCUSSION

6.4.1 Semi-Circular Bend (SCB) Test

SCB tests were conducted at 25°C to evaluate the fatigue response of laboratory long-term aged asphalt samples. Four replicate experiments for each mix were produced and a total of 12 tests were conducted. SCB test results are presented in Figure 6.1. The flexibility index values obtained were compared with the results from unaged samples (Section 3.6.2.1). It was observed that the flexibility index values for the aged samples, which are expected to be brittle, were lower than that of the unaged samples for the same mix types. The reduction in FI was found to be about 40%. However, it was evident that the performance rankings of the mix types do not change irrespective of aging simulations in the laboratory. For the long-term aged samples, the flexibility index for Mix 1 was higher and was followed by Mix 3 and Mix 2, respectively. The same trend was observed for samples that were only short-term aged (Section 3.6.2.1). Figure 6.2 illustrates the correlation between the FI values of short and long-term aged samples and only short-term aged samples. It can be observed that there is a strong linear correlation between the average measured flexibility index values of short and long-term aged and only short-term aged

samples ($R^2 = 0.953$). However, further research with a larger experimental plan is required to validate this conclusion.

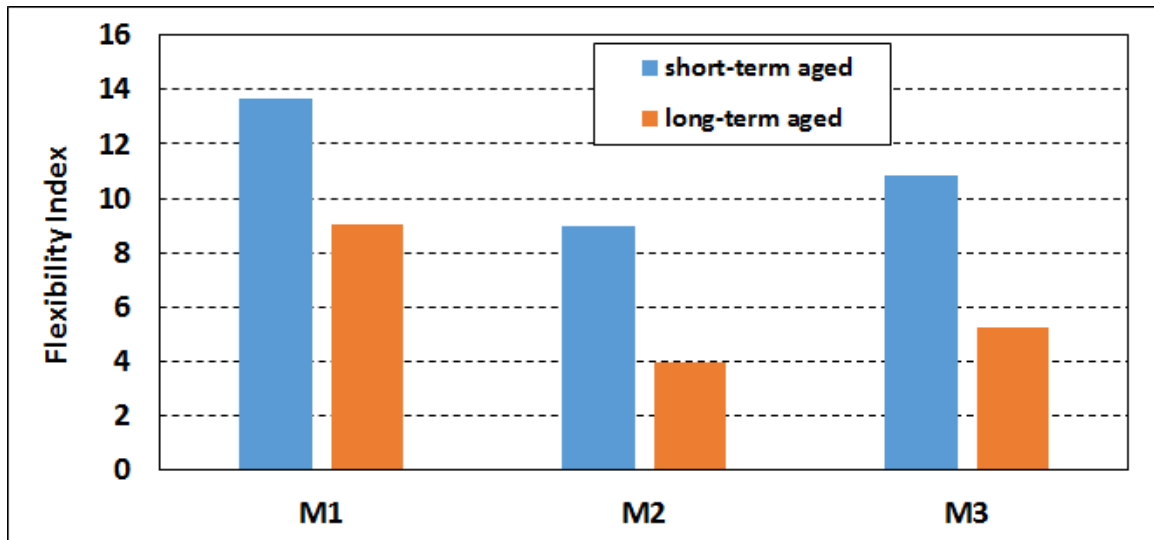


Figure 6.1. SCB results comparing long-term aged and only short-term aged samples.

Note: M1: Mix 1-PG70-22ER-Fine gradation
M2: Mix 2-PG70-22ER-Coarse gradation
M3: Mix 3-PG70-22-Coarse gradation

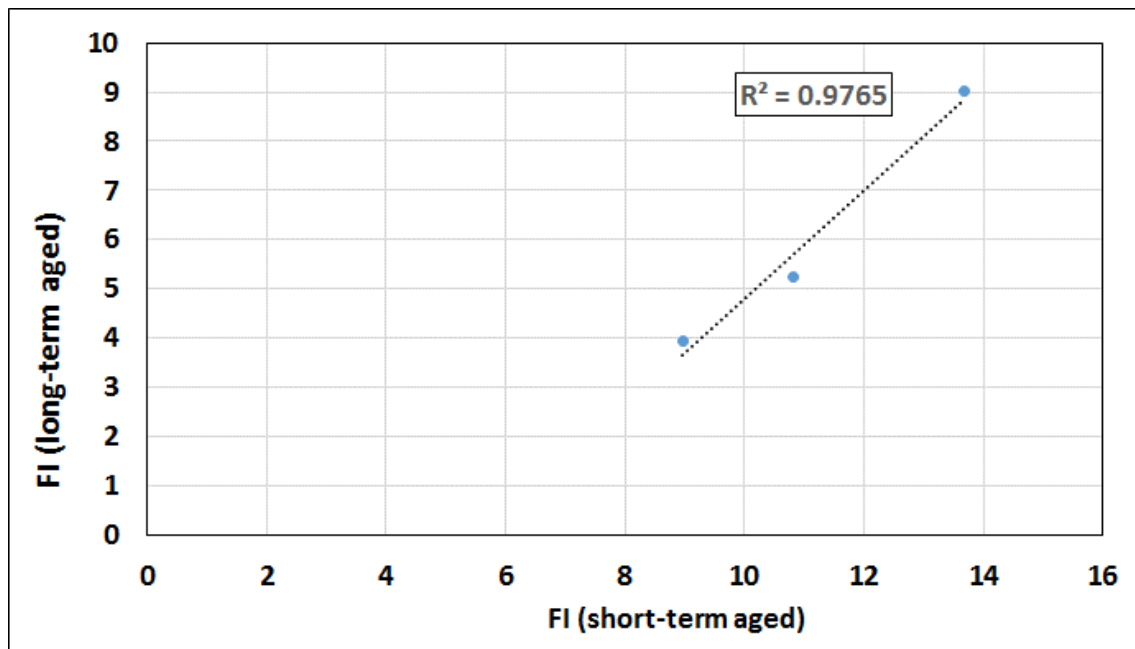


Figure 6.2. Correlation between FI for long-term aged and only short-term aged samples.

6.4.2 Dynamic Modulus (DM) Test

DM tests were also conducted on long-term aged samples in the laboratory. Two replicate experiments were conducted for each mix type. Therefore, six samples were tested at the testing frequencies and temperatures given in Section 3.5.6. The testing procedure without any confining pressure described in AASHTO TP 79-13 was followed. Dynamic modulus and phase angle master curves are presented and discussed in the following sections.

6.4.2.1 Master curves for dynamic modulus

This section presents the dynamic modulus master curves for short and long-term aged asphalt samples and for only short-term aged samples. The average of test results for two replicate mixtures were used to develop each master curve as recommended by AASHTO TP 79-13.

Master curves of dynamic modulus for the short and long-term aged and only short-term aged samples of the three mixtures in consideration are presented in Figure 6.3. Reference temperature for all the master curves is 20°C. As was expected, the aged samples resulted in higher dynamic modulus values than the unaged samples. The dynamic modulus rankings obtained from DM testing were also in agreement with the rankings obtained from the SCB test results described in the previous section. In other words, long-term aging did not affect the dynamic modulus ranking.

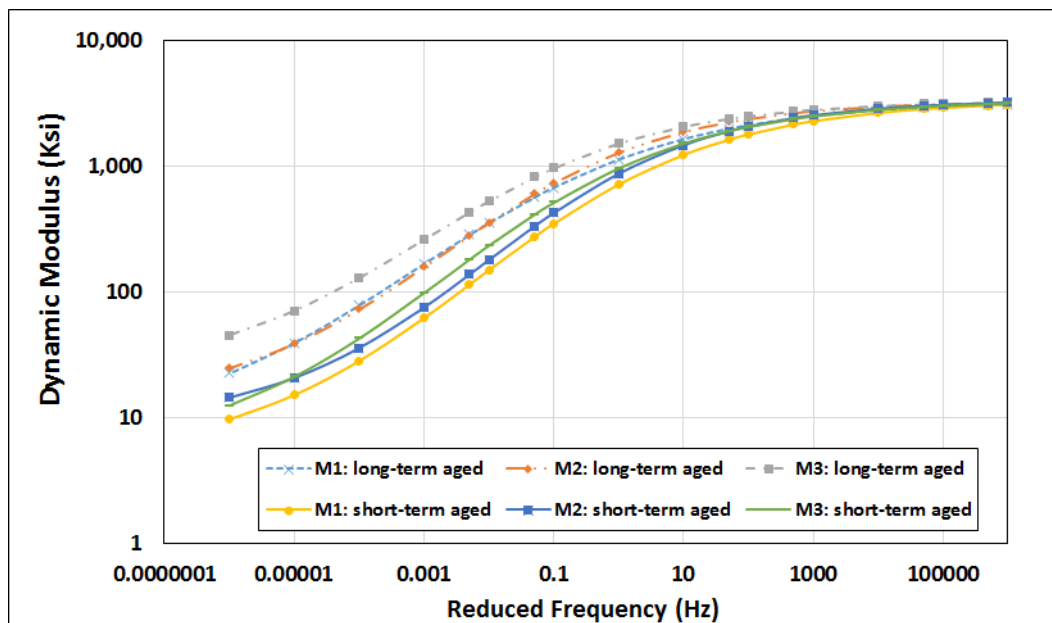


Figure 6.3. DM master curves comparing aged and unaged samples.

Note: M1: Mix 1-PG70-22ER-Fine gradation
M2: Mix 2-PG70-22ER-Coarse gradation
M3: Mix 3-PG70-22-Coarse gradation

6.4.2.2 Master curves for phase angle

Phase angle master curves for all test results are plotted in Figure 6.4. The same shift factor values, which were calculated and used for developing the master curves for DM tests, are used to develop the master curves for phase angles. Reference temperature for all master curves is 20°C. Figure 6.4 depicts that the long-term aged samples, which are expected to be brittle, have lower phase angles indicating that their cracking resistance when compared to the only short-term aged samples will be lower.

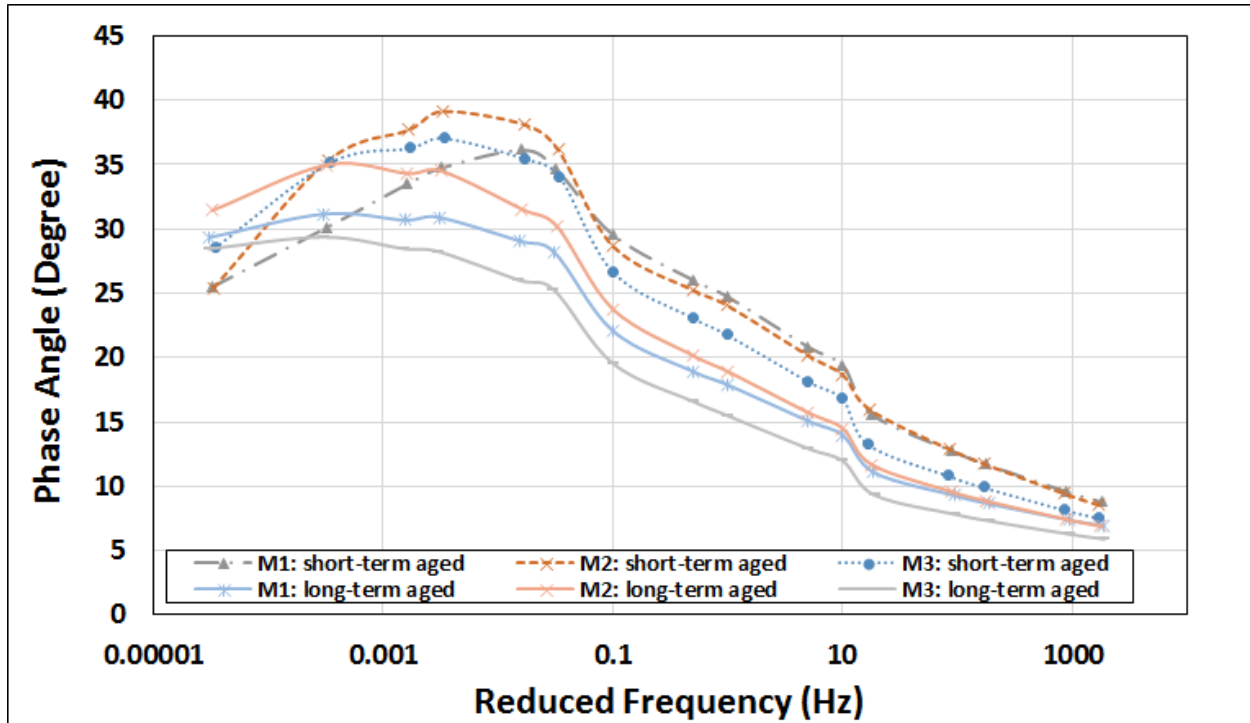


Figure 6.4. Phase angle master curves comparing aged and unaged samples.

Note: M1: Mix 1-PG70-22ER-Fine gradation
M2: Mix 2-PG70-22ER-Coarse gradation
M3: Mix 3-PG70-22-Coarse gradation

6.4.3 Flow Number (FN) Test

Flow number tests were conducted with each mix type to determine the rutting resistance of long-term aged and only short-term aged mixtures. Two replicate experiments were conducted for each mix type. FN test results are presented in Figure 6.5. It can be observed that FN for long-term aged mixtures are significantly higher than the FNs for only short-term aged samples. However, long-term aging does not change the rankings of the mixtures for rutting performance.

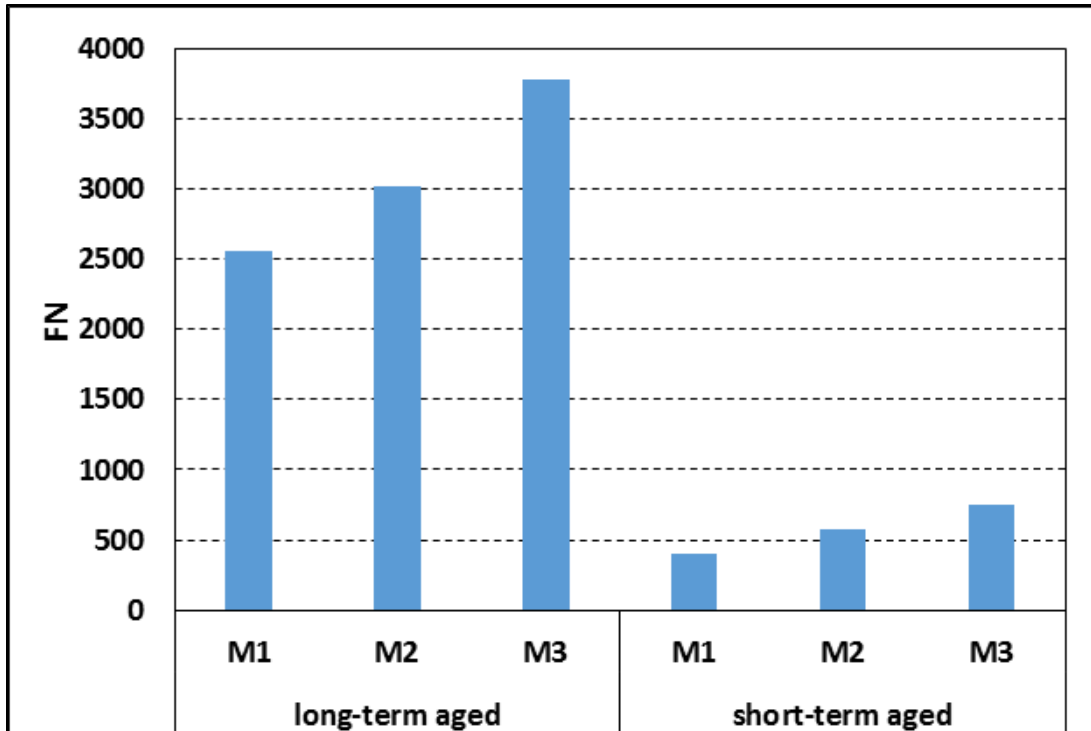


Figure 6.5. FN test results comparing aged and unaged samples.

Note: M1: Mix 1-PG70-22ER-Fine gradation
M2: Mix 2-PG70-22ER-Coarse gradation
M3: Mix 3-PG70-22-Coarse gradation

6.5 SUMMARY AND CONCLUSIONS

In this part of the study, the plant-produced loose mixtures described in Section 3.4.2 were further aged in the oven at 85°C for five days after short-term aging at 135 °C for 4 hours (called as “long-term aged” samples). After long-term and short-term aging, samples were prepared using the SGC and were tested to determine their cracking performance. For this purpose, SCB tests were conducted to measure the flexibility index of the long-term aged samples. Flexibility indices for long-term aged samples were compared to the flexibility indices for only short-term aged samples to determine the impact of aging on cracking and rutting resistance. The following conclusions were derived from this study:

- Laboratory long-term aging does not change the FI, FN and dynamic modulus rankings of the three mixtures used in this study.
- However, long-term aging significantly reduces the flexibility index values of the mixtures thereby making them brittle and more susceptible to cracking.

7.0 MECHANISTIC-EMPIRICAL PAVEMENT DESIGN GUIDE (MEPDG) SIMULATIONS AND LIFE CYCLE COST ANALYSIS

7.1 INTRODUCTION

This portion of the study focused on development of MEPDG models to quantify the impact of polymer modification, binder content, gradation and traffic level on in-situ rutting and alligator cracking (bottom-up cracking) performance. For this purpose, Level 1 MEPDG simulations (the level with highest level of accuracy) were conducted by using the dynamic modulus and binder dynamic shear rheometer test results for lab-mixed lab-compacted mixes given in Chapter 4.0. Measured asphalt mixture properties (effective binder content) for all tested asphalt mixtures were also used to improve model predictions. In this study, MEPDG longitudinal (top-down cracking) cracking models were not used for simulations since the accuracy of these models were determined to be low (Williams and Shaidur 2013). Findings of the NCHRP 9-30 (Von Quintus et al. 2009) also suggested not including current longitudinal cracking models in the local calibration guide.

In this study, a material cost-calculation tool developed by Coleri et al. (2017) was used to calculate the asphalt mixture costs for different mixture types (with and without polymer modification). Using the predicted performance curves and calculated material and agency costs, life-cycle cost analyses (LCCA) were performed to determine the most cost-effective strategies.

7.2 MEPDG RUTTING AND FATIGUE CRACKING MODELS

7.2.1 Fatigue Cracking Models

Miner's law is one of the most basic recursive-incremental damage accumulation methods used in fatigue cracking prediction (Miner 1945). It is based on the cumulative damage theory and defined as the ratio of number of cycles applied at each stress level to the number of cycles to failure, as shown in Equation 7.1. For fatigue cracking, the number of cycles to failure in Miner's law is defined as the number of repetitions to fatigue cracking or allowable number of repetitions. In mechanistic-empirical (ME) pavement design, the number of repetitions to fatigue cracking are calculated for all trucks on a highway section with different loads, speeds and temperatures via transfer functions developed by using laboratory fatigue cracking test results. Then, damage created by a specific axle for a specific time interval (using load, speed and temperature for the corresponding time interval) is calculated by dividing 1 by the calculated number of repetitions to fatigue cracking. By summing up calculated damage created by all truck axles for a specific design period whilst considering variable traffic, climate and changing material properties, the total accumulated damage for the design period can be calculated. Fatigue cracking is assumed to occur when the accumulated damage value reaches a value of '1'.

$$DI = \sum (\Delta DI)_{j,m,l,p,T} = \sum \left(\frac{n}{N_{f-HMA}} \right)_{j,m,l,p,T} \quad 7.1$$

Where:

- n = Actual number of axle load applications within a specific time period
- N_{f-HMA} = Allowable number of axle load applications for a flexible pavement and HMA overlays to fatigue cracking
- j = Axle-load interval
- m = Axle-load type (single, tandem, tridem, quad or special axle configuration)
- l = Truck type using the truck classification groups included in the MEPDG
- p = Month
- T = Median temperature for the five temperature intervals used to subdivide each month

The most common type of model used to predict the number of load repetitions required for initiation of fatigue cracking is a function of the tensile strain and stiffness of the mix. The general form of the number of load repetitions equation (transfer function) used in MEPDG is shown in Equation 7.2 (Witczak et al. 2004).

$$N_f = C k_1 \left(\frac{1}{\epsilon_t} \right)^{k_2} \left(\frac{1}{E} \right)^{k_3} \quad 7.2$$

Where:

- N_f = Number of repetitions to fatigue cracking.
- ϵ_t = Tensile strain at the critical location.
- E = Stiffness of the material.
- k_1, k_2, k_3 = Laboratory regression coefficients.
- C = Laboratory to field adjustment factor.

The damage transfer function for alligator (bottom-up cracking) calculation is given in Equation 7.3.

$$FC_{Bottom} = \left(\frac{6000}{1 + e^{(C_1 * C_1^\delta + C_2 * C_2^\delta * \text{Log}(DI_{Bottom}))}} \right) * \left(\frac{1}{60} \right) \quad 7.3$$

Where:

FC_{Bottom} = Alligator cracking, percent of total area

C_1 = Calibration coefficient

C_2 = Calibration coefficient

C_1^δ = $-2 * C_2^\delta$

C_2^δ = $-2.40874 - 39.748(1 + H_{HMA})^{-2.856}$

H_{HMA} = Total HMAC thickness, inches

DI_{Bottom} = Bottom incremental damage, percent

7.2.2 Rutting Models

Rutting in the asphalt and unbound layers are separately predicted in MEPDG. Total surface rutting is calculated by summing the predicted rutting in all layers. Asphalt layer rutting is calculated by using the field-calibrated equations given below:

$$\Delta_{p(HMA)} = \varepsilon_{p(HMA)} h_{HMA} = \beta_{r1} k_z \varepsilon_{r(HMA)} 10^{k_1} n^{k_2 \beta r2} T^{k_2 \beta r2} \quad 7.4$$

Where:

$\Delta_{p(HMA)}$ = Accumulated permanent or plastic vertical deformation in the HMA layer/sublayer, inches

$\varepsilon_{p(HMA)}$ = Accumulated permanent or plastic axial strain in the HMA layer/sublayer, inches/inches

h_{HMA} = Thickness of the HMA layer/sublayer, inches

n = Number of axle load repetitions

T = Mix or pavement temperature, °F

k_z = Depth confinement factor, inches

$k_{1,2,3}$ = Global field calibration parameters (from the NCHRP 1-40D recalibration;
 $k_1=-3.35412$, $k_2=1.5606$, $k_3=0.4791$)

$\beta_{r_{1,2,3}}$ = Local or mixture field calibration constants; for the global calibration, these constants were all set to 1.0

$$k_z = (C_1 + C_2 D) * 0.328196^D \quad 7.5$$

$$C_1 = -0.1039 * (H_{HMA})^2 + 2.4868 * H_{HMA} - 17.324 \quad 7.6$$

$$C_2 = 0.0172 * (H_{HMA})^2 - 1.7331 * H_{HMA} + 27.428 \quad 7.7$$

Where:

D = Depth below the surface, inches

H_{HMA} = Total HMA thickness, inches

The field-calibrated equation used to calculate unbound layers' vertical deformation is given in Equation 7.8 below:

$$\delta_a(N) = \beta_{s1} k_1 \varepsilon_v h_{soil} \left(\frac{\varepsilon_0}{\varepsilon_r} \right) e^{-\left(\frac{\rho}{n} \right)^\beta} \quad 7.8$$

Where:

$\delta_a(N)$ = Permanent or plastic deformation for the layer/sublayer, inches

n = Number of axle load repetitions

ε_0 = Intercept determined from laboratory repeated load permanent deformation tests, inches/inches

ε_r = resilient strain imposed in laboratory test to obtain material properties ε_0 , β and ρ , inches/inches

ε_v = Average vertical resilient or elastic strain in the layer/sublayer and calculated by the structural response model, inches/inches

h_{soil} = Thickness of the unbound layer/sublayer, inches

k_1 = Global calibration coefficients; $k_1 = 2.03$ for granular materials and 1.35 for fine-grained materials

β_{s1} = Local calibration constant for the rutting in the unbound layers (base or subgrade); the local calibration constant was set to 1.0 for the global calibration effort. Note that β_{s1} represents base layer.

$$\log \beta = -0.61119 - 0.017638(W_e) \quad 7.9$$

$$\rho = 10^9 \left(\frac{C_0}{(1 - (10^9)\beta)} \right)^{\frac{1}{\beta}} \quad 7.10$$

$$C_0 = \ln \left(\frac{a_1 M_r^{b_1}}{a_9 M_r^{b_9}} \right) = 0.0075 \quad 7.11$$

Where:

W_e = Water content, percent

M_r = Resilient modulus of the unbound layer or sublayer, psi

$a_{1,9}$ = Regression constants; $a_1 = 0.15$ and $a_9 = 20.0$

$b_{1,9}$ = Regression constants; $b_1 = 0.0$ and $b_9 = 0.0$

Since rutting in aggregate base and subgrade layers are not expected to be significant in Oregon Williams and Shaidur (2013), calibration factors for aggregate base and subgrade layers are set to 0 in this study.

7.3 LEVEL 1 MEPDG SIMULATIONS USING EXPERIMENTAL RESULTS

Three hierarchical levels of inputs are available in MEPDG. Level 1 input represents the highest level of accuracy and requires laboratory or field test results to characterize material properties. Level 2 analysis requires binder, aggregate and general mixture properties and uses these input variables to estimate HMA stiffnesses by using correlation functions embedded in MEPDG. Level 3 analysis will provide the lowest level of accuracy. Average values for material properties for the U.S. are selected by the user as input parameters. Experiments are not conducted to measure any material properties to use as input variables for modeling.

In this study, MEPDG models were developed to quantify the impact of polymer modification, binder content, gradation, and traffic level on in-situ rutting and alligator cracking (bottom-up cracking) performance. For this purpose, Level 1 MEPDG simulations (the level with highest level of accuracy) were conducted by using the dynamic modulus (presented in Chapter 4.0) and binder dynamic shear rheometer test results. Measured asphalt mixture properties (effective

binder content) for all tested asphalt mixtures were also used to improve model predictions (Appendix B). Table 7.1 shows all the cases modeled with MEPDG to determine the impact of polymer modification, binder content, gradation and traffic level on in-situ rutting and alligator cracking (bottom-up cracking) performance.

Table 7.1: Cases Modeled with MEPDG.

Binder content	RAP content	Binder and mix	Climate	Traffic (AADTT ²)	Number of models
5.3% 6.0%	20%	M1 ¹ M2 M3	Portland	3,000	6
5.3% 6.0%	20%	M1 M2 M3	Portland	6,000	6

Note: ¹ M1: Mix 1-PG70-22ER-Fine gradation

M2: Mix 2-PG70-22ER-Coarse gradation

M3: Mix 3-PG70-22-Coarse gradation

² AADTT: Average annual daily truck traffic.

Mastersolver V2.2, a spreadsheet developed by Dr. Ramon Bonaquist of Advanced Asphalt Technologies, was used to develop master curves and develop the parameters required to perform Level 1 MEPDG analysis.

Williams and Shaidur (2013) performed a local calibration by using the pavement management system data of Oregon Department of Transportation (ODOT). In this study, alligator cracking (bottom-up) and rutting model calibration factors from Williams and Shaidur (2013) (Table 7.2) were used to performed MEPDG simulations. Calibration coefficients from local calibration and Level 1 inputs are expected to provide realistic performance predictions for the cases analyzed in this study. However, it should be noted that MEPDG longitudinal (top-down cracking) cracking models were not used for simulations since the accuracy of these models were determined to be low (Williams and Shaidur 2013). Findings of the NCHRP 9-30 (Von Quintus et al. 2009) also suggested not including current longitudinal cracking models in the local calibration guide.

Table 7.2: Summary of Calibration Factors for Oregon (Williams and Shaidur 2013).

Calibration factor	MEPDG default value	Calibrated value
<i>Alligator cracking</i>		
C1	1	0.560
C2	1	0.225
C3	6,000	6,000
<i>AC rutting</i>		
β_{r1}	1	1.48
β_{r2}	1	1.00
β_{r3}	1	0.90
<i>Base rutting</i>		
β_{s1}	1	0
<i>Subgrade rutting</i>		
β_{s1}	1	0

MEPDG models were developed for identical structures for all cases while the dynamic modulus test results for different mixture types given in Chapter 4.0 were used for material characterization. The typical structure used for model development for the initial rehabilitation is shown in Figure 7.1a. A full friction interface is assumed for all layers. MEPDG rehabilitation analyses were conducted. The top 1 inch of the 3 inch existing layer was milled for the analysis (2 inch thick layer was left for modeling). After milling, 3 inch thick asphalt overlay was constructed as the new layer. Level 1 parameters were entered for the top 3 inch overlay while the existing asphalt layer was assumed to be in “Fair” condition with a PG64-22 binder. After running the initial rehabilitation model and finding the service life, the top layer from the model was milled and a 2nd 3-inch overlay was constructed (Figure 7.1b). These simulations were continued until the total service life of modeled structures exceeded 50 years which is the analysis period for Life Cycle Cost Analysis (LCCA). If a structure was not failing within a 50 year period, a 50 year design life was assumed and used for LCCA. In this study, alligator cracking was considered to be the only distress mechanism for LCCA since almost none of the sections were failing from rutting.

Analyses were conducted with an initial traffic level of 3,000 and 6,000 average annual daily truck traffic (AADTT) with an annual traffic growth rate of 3%. For the 2nd and 3rd rehabilitation models, the last year’s traffic from the previous rehabilitation was used as the starting traffic level for the following rehabilitation to maintain the continuous traffic growth for the section. A climate station from Portland was used for simulations. The typical air temperature distribution for Portland is given in Figure 7.2.

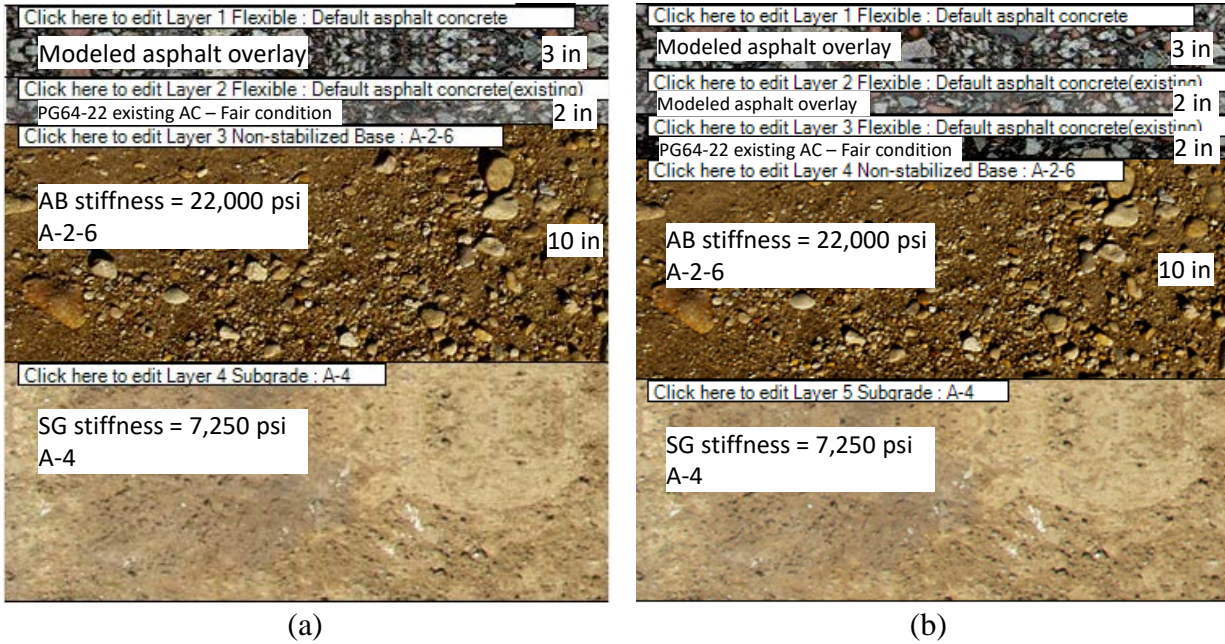


Figure 7.1: Cross sections of structures used for MEPDG modeling (a) initial rehabilitation (overlay) b) Structure after the 2nd rehabilitation.

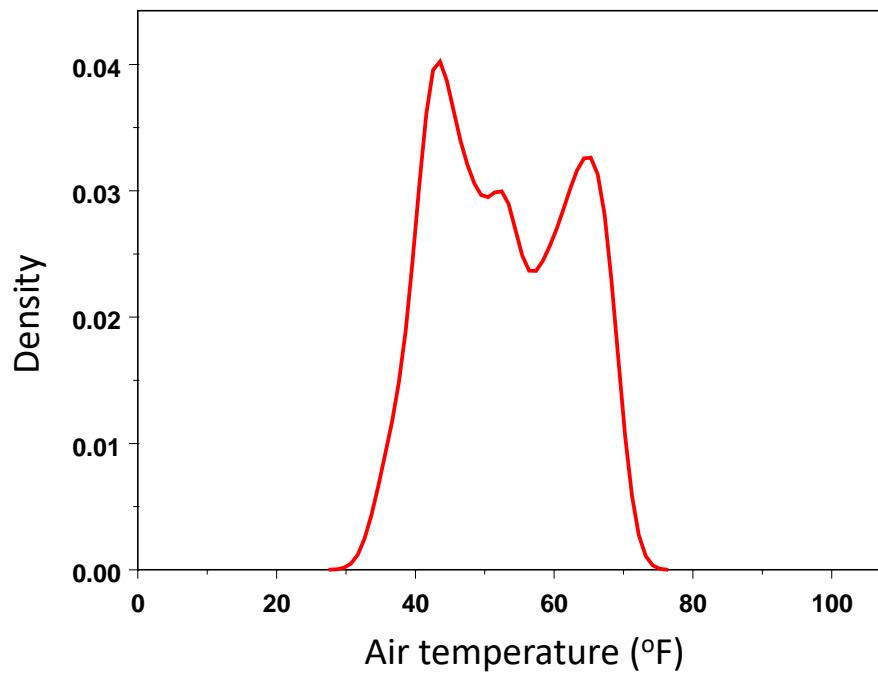


Figure 7.2: Air temperature distribution for Portland.

7.4 COST CALCULATION TOOL

In this study, a material cost-calculation tool developed by Coleri et al (2017) was used to calculate the asphalt mixture costs for different mixture types (with and without polymer modification) and binder contents. A screenshot of the developed tool's input and output tabs are given in Figure 7.3 and Figure 7.4, respectively. In order to use the tool, the user must input data about their HMA mix design, such as target density, binder content and recycled materials content. Input data about the geometry of the pavement section, such as length, lane width, number of lanes and compacted layer thickness, should also be entered. The tool will automatically calculate the volume and weight of HMA material that is anticipated for their target density and pavement section geometry. The user must also input cost data for the materials. The user can input their unit costs for binder, aggregate and recycled materials. Input fields are shown in orange with blue text and calculated fields are shown in gray with orange text. The total mix design cost for the pavement section is shown at the bottom of each mix design spreadsheet in dark gray text.

	A	B	C	D	E
1	RAP & RAS Cost Calculator				
2	Mix Design 1				
3	Inputs:				
4	Product	Cost	Unit	Source	Type
5	Binder Type 1	\$ 375.00	ton		PG 64-22
6	RAP	\$ 20.00	ton		
7	RAS	\$ 40.00	ton		
8	Aggregate	\$ 13.00	ton		
9					
10	Segment Property	Measure	Unit	Source	
11	Geometry	Straight	-	Assumption	
12	Length	1.0	mi	Assumption	
13	Lane Width	12.0	ft	Assumption	
14	Number of Lanes	1.0	each	Assumption	
15	Compacted Layer Thickness	2.0	in	Assumption	
16					
17	Mix Property	Measure	Unit	Source	
18	Compacted Density	150.0	lb/ft^3	NAPA website	
19	Target Binder Content	6.0%	by weight	Estimate	
20	RAP Content	20.0%	by weight	Estimate	
21	RAS Content	3.0%	by weight	Estimate	
22	Aggregate Content	71%	by weight	Calculation	
23	Binder Content (RAP material)	5.0%	by weight	Estimate	
24	Binder Content (RAS material)	15.0%	by weight	Estimate	
25	Virgin Binder Added	4.6%	by weight	Calculation	
26					
27	Outputs:	Measure	Unit		
28	Section Volume	10560	ft^3 (all lanes)		
29	Section Tonnage	792	tons (all lanes)		
30	Mix Cost	\$ 24,942.06	segment		
31					
32					
	Instructions	Mix1	Mix2	Mix3	Mix4
				Summary	+

Figure 7.3: Cost calculation tool input tab (Coleri et al. 2017).

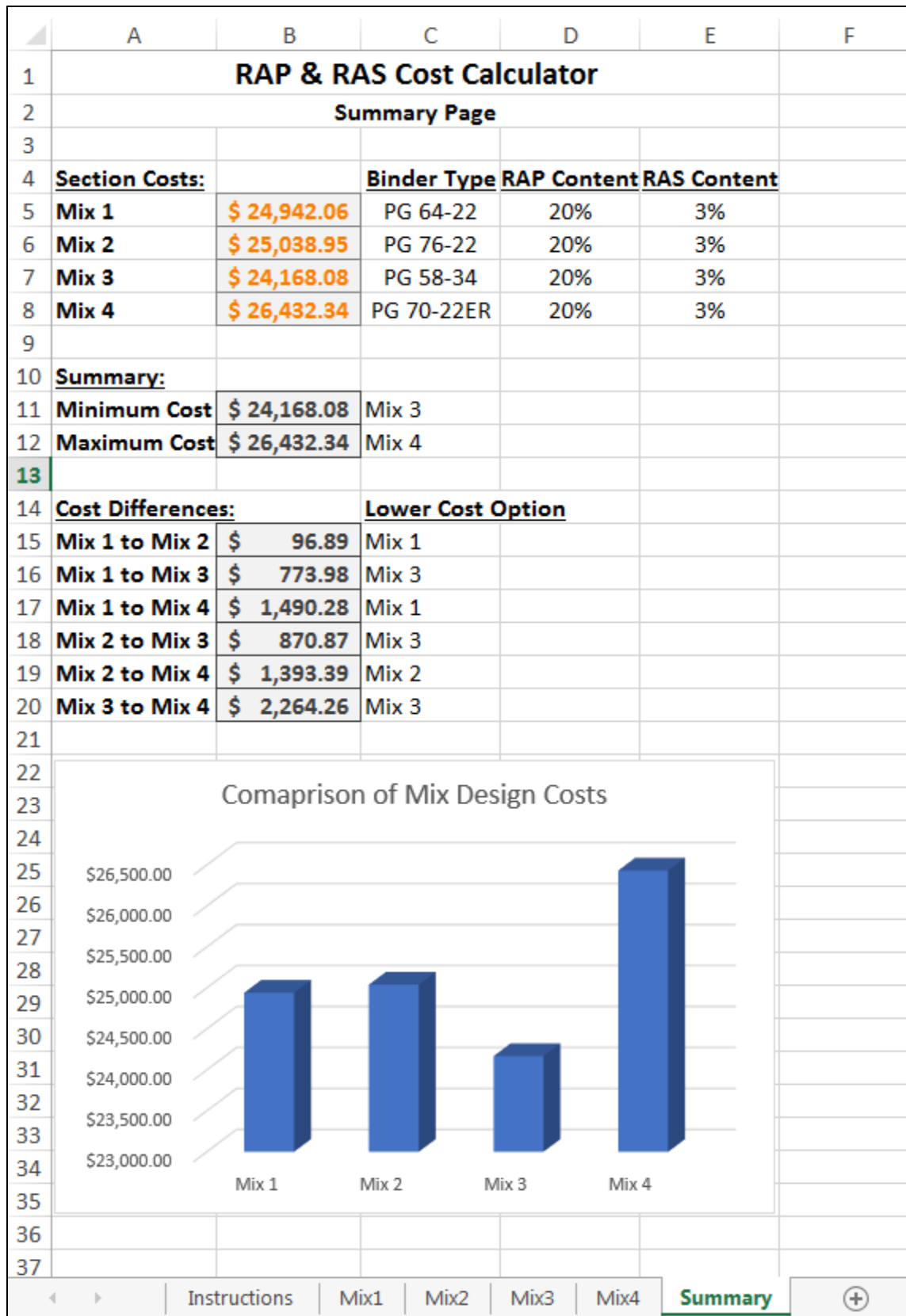


Figure 7.4: Cost calculation tool output tab (Coleri et al. 2017).

In this study, the following costs were used to calculate the total material cost of asphalt mixtures:

- RAP: \$20/ton
- RAS: \$40/ton
- Aggregate: \$13/ton
- PG70-22 binder: \$390/ton
- PG70-22ER binder: \$490/ton

7.5 LIFE-CYCLE COST ANALYSIS

In this study, life-cycle cost analyses (LCCA) were performed by using the service lives for pavement structures obtained from MEPDG simulations described in Section 7.3. Material costs for each strategy (for the cases outlined in Table 7.1) were calculated by using the cost calculation tool described in Section 7.4. Material production costs, plant operation costs and profit were not considered in the analysis. Analyses were performed by only considering material costs to be able to compare the impact of polymer modification, binder content, gradation and traffic level on life cycle costs.

In this study, each section was assumed to be a single-lane having a width of 12 ft (3.7 m) and a length of 1 mile, and material costs were calculated for all the sections based on the asphalt layer thickness of the section. The cost calculation tool described in Section 7.4 was used to calculate material costs.

After finding the service lives for each strategy using MEPDG, material costs were calculated for each year at which the treatment was applied. Net present values (NPV) of material costs were determined afterwards using a 4 percent interest rate for a 50 year analysis period, using Equation 7.12. Analyses were also performed with a 5 percent interest rate to determine the impact of interest rates on the cost effectiveness of each strategy. At the end of the analysis period, NPV of the salvage value of the pavements were computed as the agency benefits and added up to obtain a total NPV benefit.

$$NPV = \sum_{t=0}^T \frac{C_t}{(1+r)^t} \quad 7.12$$

Where:

C_t = estimated agency costs at year t ,

r = interest rate, and

T = number of time periods.

Example Calculation

For the case with PG70-22ER binder, fine gradation, 5.3% binder content and the Portland climate, MEPDG simulations were performed by using the laboratory test results as the input parameter. Service lives were determined to be 6.00 and 30.83 years for first and second rehabilitations, respectively. Using the cost calculation tool, material cost was calculated to be \$41,017 for a 3 inch overlay construction for the 1-mile 1-lane section. After the pavement failed, 1-inch of asphalt was milled and another 3 inch overlay was constructed. For this reason, material costs for the overlays following the initial construction are equal to the cost for the initial construction. Milling costs were not used for the analysis. Figure 7.5 shows example diagrams used for LCCA. Using Equation 7.13, NPV for both cases were calculated as follows:

$$\begin{aligned} NPV_{6\%BC} &= \frac{\$41,017}{(1 + 0.04)^0} + \frac{\$41,017}{(1 + 0.04)^{6.00}} + \frac{\$41,017}{(1 + 0.04)^{36.83}} - \frac{36.83}{50} \cdot \frac{\$41,017}{(1 + 0.04)^{50}} \\ &= \$78,857 \end{aligned}$$

7.13

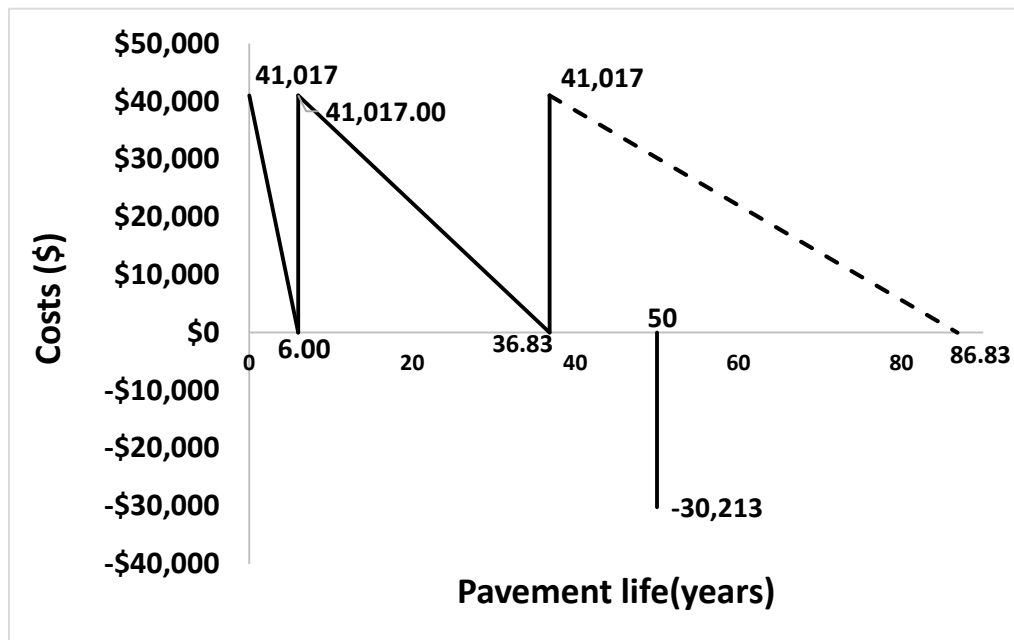


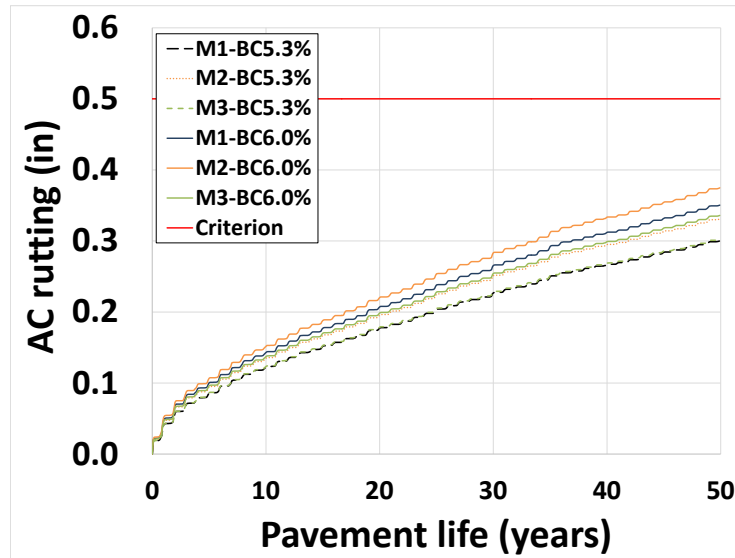
Figure 7.5: Diagram used for LCCA - PG70-22ER binder, fine gradation, 5.3% binder content, and Portland climate.

7.6 RESULTS AND DISCUSSION

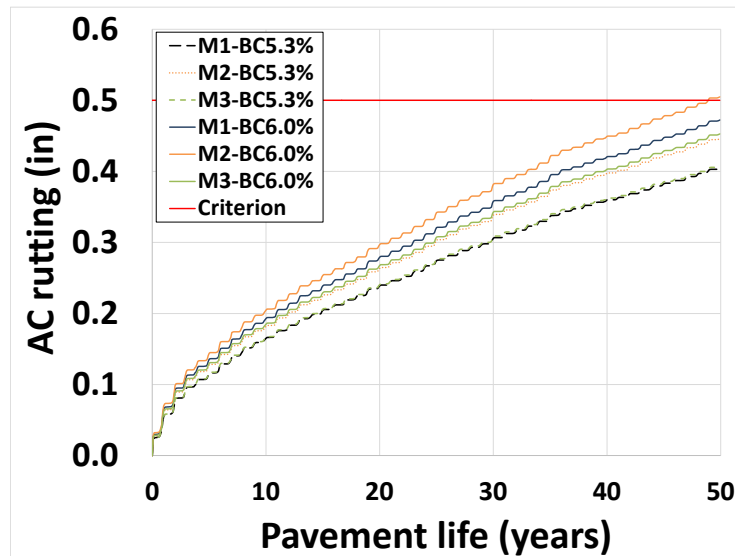
7.6.1 MEPDG Performance Predictions

Level 1 MEPDG simulations were performed using the input parameters given in Section 7.3. Predicted asphalt concrete rutting for all sections for the Portland climate are shown in Figure 7.6. It can be observed that rutting accumulation rates for the sections with 6% binder content were higher than the sections with 5.3% binder content. The mixture with PG70-22ER binder, coarse gradation and 6% binder content was determined to have the lowest rutting resistance. The mixture without any polymer modification and coarse gradation had the highest rutting resistance. It should be noted that PG70-22ER-FA mix had a 6% binder content in the mix design while the design binder content for PG70-22ER-CA and PG70-22-CA mixes were 5.3%.

Results also show that none of the sections fail from rutting within the first 45 years for a failure criteria of 0.5 inch rut depth while majority of the sections do not fail within the 50 year analysis period. Since asphalt aging is going to significantly increase asphalt stiffnesses during this long time period, it is highly likely that none of the sections will fail from rutting. For this reason, alligator cracking was used as the only failure criteria for LCCA.



(a)



(b)

Figure 7.6: Predicted asphalt concrete (AC) rutting for all mixes (a) AADTT=3,000 (b) AADTT=6,000.

Note: M1: Mix 1-PG70-22ER-Fine gradation
M2: Mix 2-PG70-22ER-Coarse gradation
M3: Mix 3-PG70-22-Coarse gradation

Predicted bottom-up cracking for all sections (Table 7.1) for the Portland climate are shown in Figure 7.7. It can be observed that cracking accumulation rates for the sections with 5.3% binder content were higher than the sections with 6.0% binder content. The mixture with PG70-22ER binder, coarse gradation and 6% binder content was determined to have the highest cracking resistance. The mixture without any polymer modification and coarse gradation (M3) had the lowest cracking resistance. It should be noted that PG70-22ER-FA mix had a 6% binder content

in the mix design while the design binder content for PG70-22ER-CA and PG70-22-CA mixes were 5.3%. When actual design binder contents are considered, mixtures with polymer modification (PG70-22ER) have significantly higher cracking resistance.



(a)



(b)

Figure 7.7: Predicted bottom-up cracking (alligator) for all mixes (a) AADTT=3,000 (b) AADTT=6,000.

Note: M1: Mix 1-PG70-22ER-Fine gradation
M2: Mix 2-PG70-22ER-Coarse gradation
M3: Mix 3-PG70-22-Coarse gradation

All rutting and cracking curves presented in this section are for the structure shown in Figure 7.1a (a 3 inch asphalt overlay on a 2 inch milled existing asphalt layer). To be able to determine service lives after initial failure, simulations were also performed after first failure (structure in Figure 7.1b) by milling 1 inch from the existing overlay surface and placing a new 3 inch asphalt overlay. Traffic levels were also adjusted for all simulations to have continuous 3% increasing in AADTT throughout the analysis period. This process was repeated until the total life of all constructed pavements reach or exceed the 50 year analysis period.

Figure 7.8 shows the bottom-up cracking performance curves for the section with PG70-22ER binder, fine gradation, 5.3% binder content and the Portland climate. In this study, the asphalt overlay was constructed when the bottom-up cracking reached 5% of the lane area (rehabilitation trigger value or failure criteria). Since total service life did not reach 50 years (analysis period) after two rehabilitations, the structure in Figure 7.1b was milled 1 inch and a 3 inch thick asphalt overlay was constructed for the third time. Since the thickness of the section was increasing by 2 inches with every asphalt overlay construction, service life is increasing. Using the service lives for each construction (6.00, 30.83, and 50.00 years for the case in Figure 7.8) and calculated costs, LCCAs were performed in the next section.

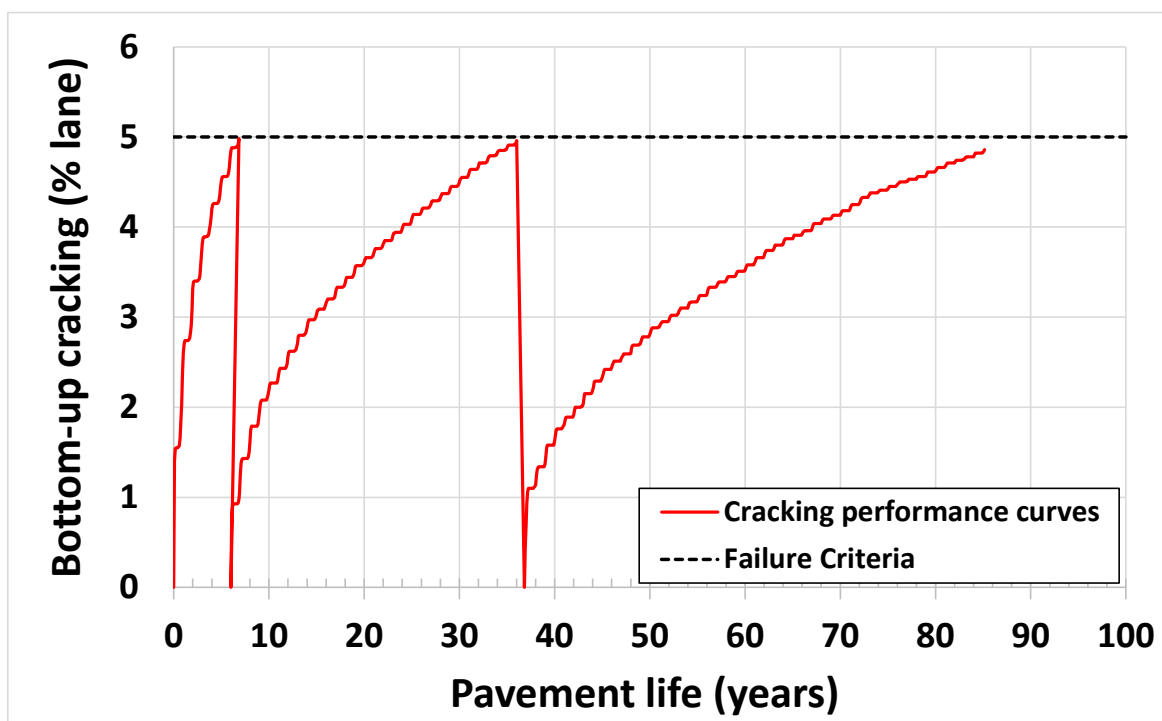


Figure 7.8: Cracking performance curves for the section with for the section with PG70-22ER binder, fine gradation, 5.3% binder content, and Portland climate.

7.6.2 Life-Cycle Cost Analysis

LCCA was performed by following the process described in Section 7.5. Material cost of each strategy (for the cases outlined in Table 7.1) were calculated by using the cost calculation tool described in Section 7.4. Material production costs, plant operation costs and profit were not considered in the analysis. Analyses were performed by only considering material costs to be able to compare the impact of polymer modification, binder content, gradation and traffic level on life cycle costs. Table 7.3 shows the service lives and material costs for all cases. Calculated salvage values and NPVs for all cases are also given in Table 7.3. Figure 7.9 compares the NPVs for all cases. An interest rate of 4% was used for NPV calculations.

It can be observed from Figure 7.9 and Table 7.3 that although increasing binder content increases the mixture costs, for some of the cases, increased performance results with higher cracking resistance and lower life-cycle costs. This result suggests that increasing the binder content of an asphalt mixture can be an effective strategy to improve the condition of highway network and reduce long-term costs. Since the cost of PG70-22 binder (\$390/ton) is lower than PG70-22ER (\$490/ton) binder, life-cycle costs for the sections constructed with PG70-22 were determined to be lower. For mixtures Mix 1 and Mix 3, increasing traffic makes the mixes with high binder contents (6% rather than 5.3%) more cost effective. Results also suggested that for sections with lower traffic levels, using non-ER mixtures can be more cost effective.

Table 7.3: Results of Life Cycle Costs Analysis.

Mix	AADTT ₂	Cost T#1 (\$)	Service life#1	Cost T#2 (\$)	Service life#2	Cost T#3 (\$)	Service life#3	Salvage value (\$)	NPV (\$)
M1 ¹ -BC5.3	3,000	41,017	10.83	41,017	49.00	-	-	8,229	66,681
M1-BC6.0	3,000	44,984	13.17	44,984	50.00	-	-	11,849	70,153
M2-BC5.3	3,000	41,203	12.00	41,203	50.00	-	-	9,889	69,169
M2-BC6.0	3,000	45,170	14.83	45,170	50.00	-	-	13,397	68,534
M3-BC5.3	3,000	36,119	10.83	36,119	50.00	-	-	7,823	58,637
M3-BC6.0	3,000	39,254	12.67	39,254	50.00	-	-	9,947	61,736
M1-BC5.3	6,000	41,017	6.00	41,017	30.83	41,017	50.00	30,213	78,857
M1-BC6.0	6,000	44,984	7.92	44,984	48.92	-	-	6,290	77,071
M2-BC5.3	6,000	41,203	7.00	41,203	39.92	41,203	50.00	38,665	73,616
M2-BC6.0	6,000	45,170	8.83	45,170	50.00	-	-	7,977	75,996
M3-BC5.3	6,000	36,119	6.00	36,119	30.92	36,119	50.00	26,670	69,400
M3-BC6.0	6,000	39,254	7.67	39,254	43.17	-	-	764	68,203

Note: ¹ M1: Mix 1-PG70-22ER-Fine gradation

M2: Mix 2-PG70-22ER-Coarse gradation

M3: Mix 3-PG70-22-Coarse gradation

² AADTT: Average annual daily truck traffic

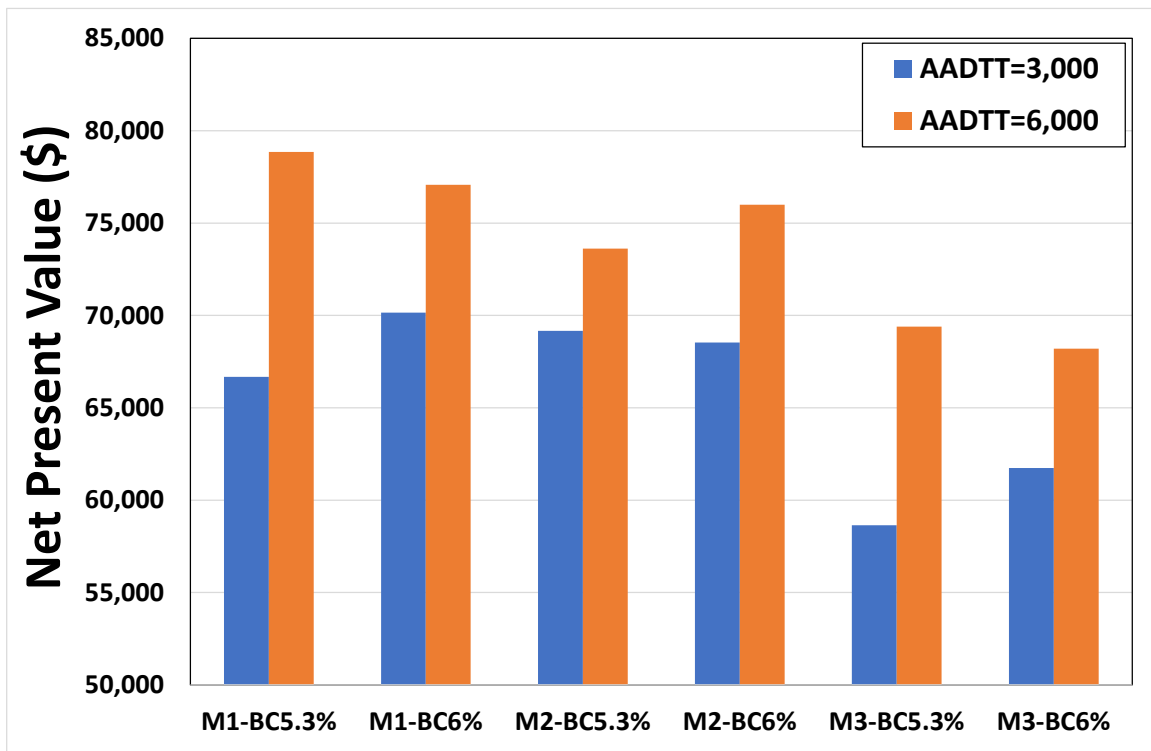


Figure 7.9: Calculated material cost NPVs for all cases for 4% interest rate.

In order to determine the impact of interest rate on NPV ranking of the analyzed cases, NPVs for all cases were also calculated using a 5% interest rate (rather than the 4% initially used). Figure 7.10 shows the calculated NPVs for a 5% interest rate. Figure 7.11 shows the correlation between NPVs calculated by using 4% and 5% interest rates. Although using a 5% interest rate reduces the calculated NPVs (as expected), a strong linear correlation between NPVs for 4% and 5% interest rates suggests that increasing interest rate does not change the rankings and conclusions except for the M2 low traffic case. For M2-AADTT:3,000, using a 6% binder content becomes more cost effective when a 4% interest rate is used.

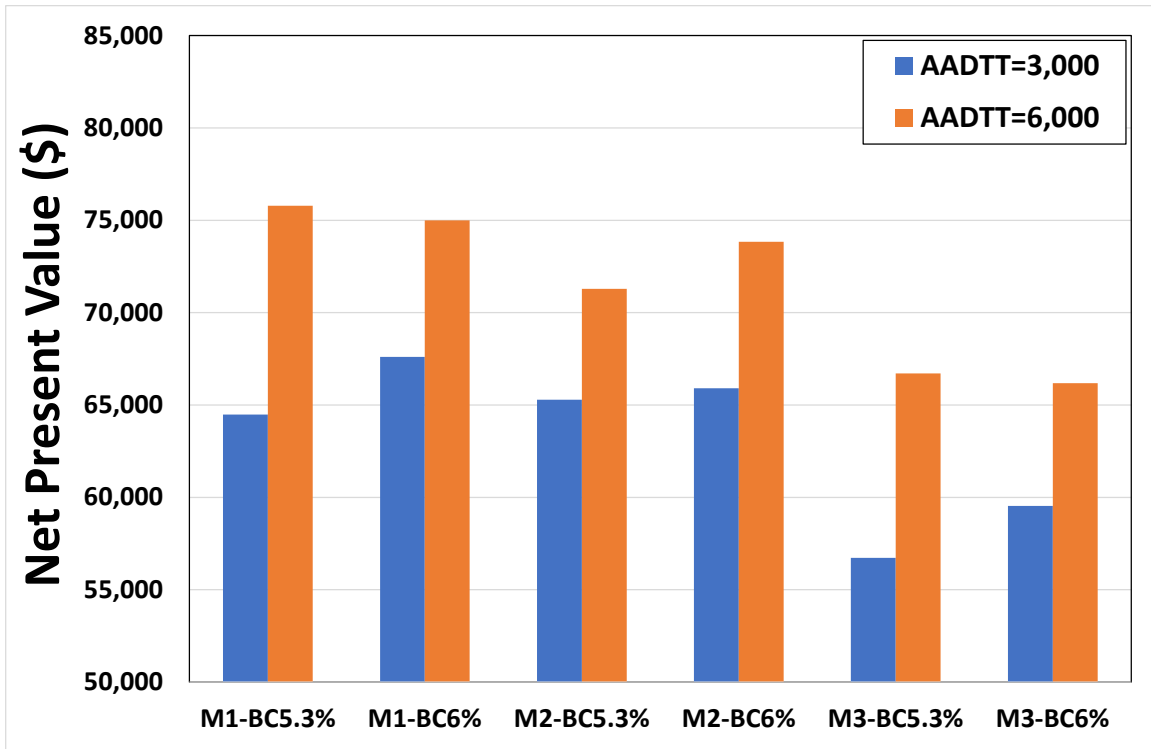


Figure 7.10: Calculated material cost NPVs for all cases for 5% interest rate.

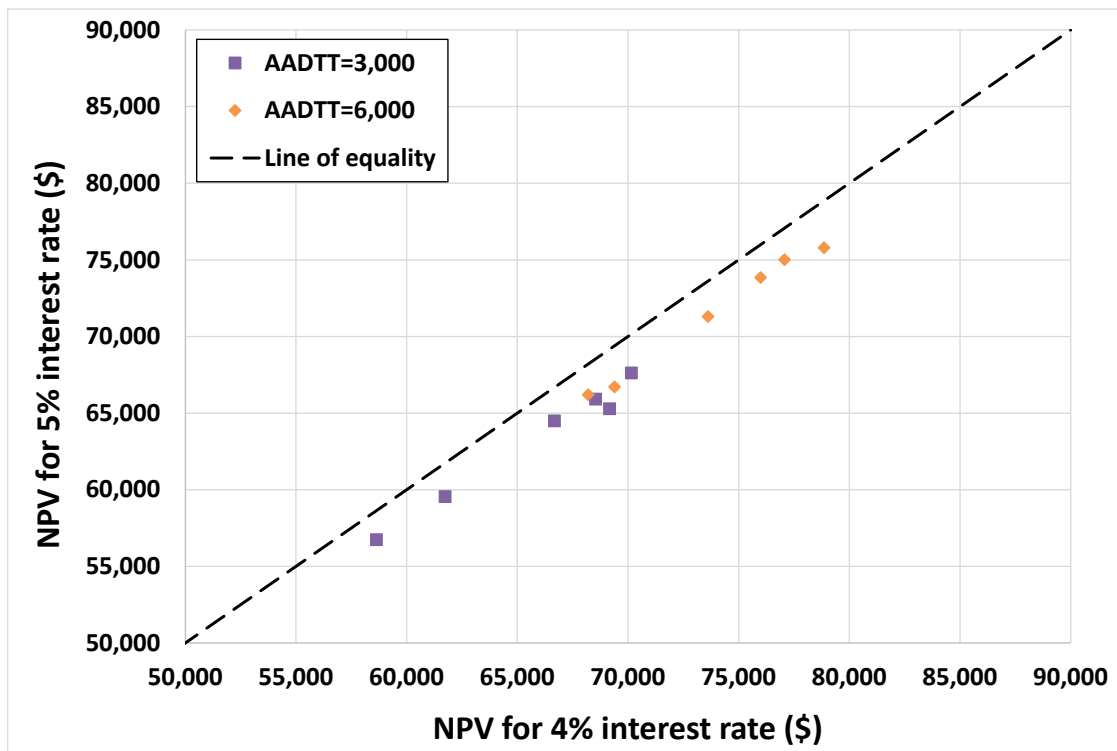


Figure 7.11: Correlation between NPVs calculated by using 4% and 5% interest rates.

7.7 SUMMARY AND CONCLUSIONS

This portion of the study focused on development of MEPDG models to quantify the impact of polymer modification, binder content, gradation and traffic level on in-situ rutting and alligator cracking (bottom-up cracking) performance. The material cost-calculation tool developed by Coleri et al. (2017) was also used to calculate the asphalt mixture costs for different binder contents and binder types. Using the predicted performance curves and calculated material costs, life-cycle costs analyses (LCCA) were performed to determine the most cost effective strategies.

The analysis presented in this chapter have yielded the following conclusions:

- Rutting accumulation rates for the sections with 6% binder content were higher than the sections with 5.3% binder content.
- The mixture with PG70-22ER binder, coarse gradation and 6% binder content was determined to have the lowest rutting resistance. The mixture without any polymer modification and coarse gradation had the highest rutting resistance.
- Results also show that none of the sections fail from rutting within the first 45 years for a failure criteria of 0.5 inch rut depth while the majority of the sections do not fail within the 50 year analysis period.
- Cracking accumulation rates for the sections with 5.3% binder content were higher than the sections with 6.0% binder content.
- Mixture with PG70-22ER binder, coarse gradation and 6% binder content was determined to have the highest cracking resistance. The mixture without any polymer modification and coarse gradation (M3) had the lowest cracking resistance.
- When actual design binder contents are considered, mixtures with polymer modification (PG70-22ER) have significantly higher cracking resistance.
- Although increasing binder content increases the mixture costs, for some of the cases, increased performance results in higher cracking resistance and lower life-cycle costs. This result suggests that increasing the binder content of the asphalt mixture can be an effective strategy to improve the condition of highway network and reduce long-term costs.
- For mixtures Mix 1 and Mix 3, increasing traffic makes the mixes with high binder contents (6% rather than 5.3%) more cost effective.
- For sections with lower traffic levels, using non-ER mixtures can be more cost effective.
- Although using a 5% interest rate reduces the calculated NPVs (as expected), a strong linear correlation between NPVs for 4% and 5% interest rates suggests that increasing interest rate does not change the rankings and conclusions except for the Mix 2 low

traffic case. For M2-AADTT:3,000, using 6% binder content becomes more cost effective when a 4% interest rate is used.

8.0 SUMMARY AND CONCLUSIONS

This study focuses on characterizing the cracking performance of asphalt pavements in Oregon by considering four tests commonly used to evaluate fatigue cracking resistance and proposing implementation of the most cost-effective and efficient test procedure for agencies and contractors. Also, the impacts of asphalt mixture properties, such as binder content, air-void content, aggregate gradation, and polymer modification, and aging on cracking performance of asphalt mixtures were investigated. Mechanistic-empirical (ME) design modeling and life-cycle cost analyses (LCCA) were also conducted to determine cost and performance effectiveness of asphalt mixtures with varying properties. Finally, recommended strategies were proposed for Oregon to address the issue of early pavement fatigue failure based on the test results, statistical analysis, ME models and LCCA.

The goal of this study is to provide a better decision-making structure during the pavement design stage to address fatigue cracking susceptibility, with the intent of avoiding premature pavement failure and expensive early maintenance and rehabilitation. Additionally, the study aims to reliably facilitate an increase in recycled materials content in asphalt pavement through advanced testing procedures and design recommendations proposed in this study. These recommendations will reduce the life cycle cost of pavements in Oregon, reduce network-level pavement roughness and increase the sustainability of the paving industry.

Conclusions based on the experimental and analytical findings, recommendations and additional research are discussed in the following sections.

8.1 CONCLUSIONS

The major conclusions drawn from the results of this study are as follows:

Implementation of performance tester to evaluate fatigue cracking of asphalt concrete

1. SCB and IDT tests are the most practical and reliable tests that can be used to evaluate the cracking resistance of asphalt mixtures. The SCB test holds a slight advantage against IDT in terms of practicality since just one gyratory sample is required for each mixture type whereas a minimum of two SGC samples are required for IDT testing for each mixture type.
2. The flexibility index parameter is an effective parameter in differentiating cracking resistance of asphalt concrete mixtures.
3. Variability in test results for BBF and DTCF tests were determined to be very high. These two tests were also determined to be ineffective in predicting the in-situ performance of asphalt pavements. Specimen preparation and testing were also determined to be time consuming and labor intensive.
4. For Mix 3 (PG70-22-Coarse gradation), the binder content of the production mix is higher than the design binder content.
5. Mixing method (laboratory or plant) does not have any significant effect on measured cracking performance.
6. Compaction method significantly affects the measured cracking resistance. For this reason, SCB test results for SGC compacted specimens cannot be directly compared to the results from

field roller compacted specimens. Although compaction type was determined to affect the measured cracking resistance, it is not expected to affect the ranking of performance for different asphalt mixtures.

Contributions of mixture properties to durability

7. Polymer modification plays an important role in imparting ductility to the mix and thereby significantly increases the cracking resistance of the asphalt mix.
8. Binder content significantly affected the measured flexibility index. A 0.7% increase in binder content increased the flexibility index by 2 to 3 times. This observed significant effect of increased binder content on cracking performance suggests that increasing binder content of asphalt mixtures currently used in Oregon can create significant savings and improve pavement longevity.
9. Air-void content (density) significantly affected the measured flexibility index. A 2% reduction in air-void content increases the flexibility index by 1.5 to 2 times. For this reason, producing asphalt mixtures that are easy to compact and utilizing intelligent compaction technologies that are currently being implemented in Oregon can potentially create a significant improvement in the cracking resistance of asphalt mixtures.
10. According to DM test results, although decreasing air-void content was determined to improve cracking resistance, air-void content was not observed to have any significant effect on the dynamic modulus of mixtures. However, increasing binder content from 5.3% to 6% was observed to significantly reduce the dynamic modulus of asphalt mixtures.
11. Although polymer modification does not create a significant change in mixture stiffness, it improved cracking performance due to increased ductility.
12. The stiffness of the laboratory-mixed samples were, in general, higher than that of the plant mixed samples. One of the important reasons for this difference might be the short-term aging simulation in the laboratory. Four hours of aging at 135°C to simulate short-term aging for LMLC samples may be creating stiffer mixes.
13. FN values for all the asphalt mixtures were greater than 740, which is the recommended FN for the traffic level of more than 30 million ESALs. These results suggest that all tested mixtures are stiff enough to resist any rutting failures in the field. This result further suggests that increasing binder content is not going to result in rutting failures in the field, while increased binder content will significantly improve cracking resistance of asphalt mixtures. In other words, increasing binder content is an effective strategy to improve the longevity of Oregon pavements.

Impact of increased dust content on cracking performance

14. Increased dust content makes the mix drier and reduces the asphalt film thickness around the aggregates. Thus, reduced binder content and film thickness reduces the flexibility index of the asphalt mix. Therefore, mixtures with high dust-to-binder ratios are expected to be more susceptible to fatigue cracking. For this reason, decreasing the dust-to-binder ratio by limiting the dust content and/or increasing the binder content will provide asphalt mixtures with higher cracking resistance.

The effect of laboratory long-term aging on cracking performance of asphalt mixtures

15. Laboratory long-term aging does not change the FI, FN and dynamic modulus rankings of the three mixtures used in this study.
16. Long-term aging significantly reduces the flexibility index values of the mixtures, thereby making them brittle and more susceptible to cracking.

Mechanistic-empirical pavement design guide (MEPDG) simulations and life cycle cost analysis

17. The mixture with PG70-22ER binder, coarse gradation and 6% binder content was determined to have the lowest rutting resistance. The mixture without any polymer modification and coarse gradation had the highest rutting resistance.
18. The mixture with PG70-22ER binder, coarse gradation and 6% binder content was determined to have the highest cracking resistance. The mixture without any polymer modification and coarse gradation (M3) had the lowest cracking resistance.
19. None of the sections fails from rutting within the first 45 years for a failure criteria of 0.5 inch rut depth while majority of the sections do not fail within the 50 year analysis period.
20. When actual design binder contents are considered, mixtures with polymer modification (PG70-22ER) have significantly higher cracking resistance.
21. Although increasing binder content increases the mixture costs, for some of the cases, increased performance resulted in higher cracking resistance and lower life-cycle costs. This result suggests that increasing the binder content of asphalt mixture can be an effective strategy to improve the condition of the highway network and reduce long-term costs.
22. For mixtures Mix 1 and Mix 3, increasing traffic makes the mixes with high binder contents (6% rather than 5.3%) more cost effective.
23. For sections with lower traffic levels, using non-ER mixtures can be more cost effective.

8.2 RECOMMENDATIONS AND FUTURE WORK

8.2.1 Implementation of Performance Tester to Evaluate Fatigue Cracking of Asphalt Concrete

This study constructs the beginnings of a performance-based balanced mix design method. It was determined that typical FI values for production mixtures (plant-produced) range from 9 to 14. However, more experiments need to be conducted to determine exact threshold for FI that will provide acceptable long-term pavement cracking performance. In a future study, flow number and SCB experiments should be conducted with several production mixtures from different sources to develop a distribution of FI and FN for Oregon mixtures. Cracking and rutting performance of the sections constructed with these mixtures should be monitored to determine the acceptable thresholds for FN and FI.

The results showed that SCB testing and flexibility index parameter can effectively be used to characterize the cracking resistance of asphalt mixtures. The effectiveness of SCB testing to identify moisture sensitivity and low-temperature cracking resistance of Oregon asphalt mixtures should also be determined.

8.2.2 Contributions of Mixture Properties to Durability

The results showed that binder content significantly affected the measured flexibility index. A 0.7% increase in binder content increased the flexibility index by 2 to 3 times while the increased binder content did not result in FNs lower than the required threshold ($FN > 740$). This observed significant effect of increased binder content on cracking performance suggested that increasing binder content of asphalt mixtures currently used in Oregon can create significant savings and improve pavement longevity. However, field verification of this finding needs to be sought. Pilot sections should be constructed with mixes with binder contents higher than the design binder contents. Suggestions with higher FIs (> 15) should be selected for pilot section construction to minimize the risk of cracking. Since rutting is going to be the expected failure distress for these highly flexible mixtures, rutting performance of the sections should be monitored for 2 to 4 years.

The results of this study also showed that air-void content (density) significantly affected the measured flexibility index. A 2% reduction in air-void content increases the flexibility index by 1.5 to 2 times. For this reason, producing asphalt mixtures that are easy to compact can create significant benefits. For this reason, in a future study, compactability of asphalt mixes designed with current mix design process (mostly controlled by gyration levels) should be determined by preparing lab samples with the SGC and hydraulic roller compactor (HRC) (directly simulating field compaction). The compactive effort required for different mix designs should be quantified using the HRC. The impacts of filler content, gradation, aggregate size, binder type, binder content, additives (rejuvenators and warm mix technologies), thickness of the layer being compacted, maximum aggregate size to lift thickness ratio, and temperature (to evaluate the impact of time between roller and paver) on compactive effort should be quantified by using both SGC and HRC. Required gyration levels and parameters for mix design to achieve 95-96% density during construction should be determined. Pilot sections should be constructed to determine the effectiveness of using the suggested mix design process and guidelines to achieve higher density.

8.2.3 Impact of Increased Dust Content on Cracking Performance

The results showed that increased dust content makes the mix drier and reduces the asphalt film thickness around the aggregates. Thus, reduced binder content and film thickness reduces the flexibility index of the asphalt mix. Therefore, the mixture with a high dust-to-binder ratio is expected to be more susceptible to fatigue cracking. Similar analysis should be conducted to determine the improvement in cracking resistance that can be created by reducing the dust content of asphalt mixtures. The dust-to-binder ratio for the “original gradation” and the “finer gradation” mixes were determined to be 1.42 and 2.2, respectively. The impact of reducing dust-to-binder ratio to 1 to 1.2 range (by limiting the dust content and/or increasing the binder content) on cracking and rutting performance of asphalt mixtures should be determined.

8.2.4 The Effect of Laboratory Long-Term Aging on Cracking Performance of Asphalt Mixtures

The results of this study showed that laboratory long-term aging does not change the FI, FN and dynamic modulus rankings of the three mixtures used in this study. Although this result suggested that it is not necessary to perform long-term aging to accurately rank the cracking performance of different asphalt mixtures, additional mixtures with different RAP contents need to be tested by following the same procedure to validate this conclusion. The possibility of developing an aging versus flexibility index reduction curve to use for long-term aging effect prediction should also be investigated.

8.2.5 Mechanistic-Empirical Pavement Design Guide (MEPDG) Simulations and Life Cycle Cost Analysis

In this study, MEPDG simulations were conducted to determine the rutting and bottom-up cracking performance of different asphalt mixtures. MEPDG longitudinal (top-down cracking) cracking models were not used for simulations since the accuracy of these models were determined to be low (Williams and Shaidur 2013; Von Quintus et al. 2009). Since top-down cracking is the major distress mode in Oregon, using top-down cracking models for performance prediction and LCCA will provide more realistic results. More effective models that can explain the mechanism behind top-down cracking are currently being developed in research project NCHRP 01-52. The analysis performed in this research study should also be performed with top-down fatigue cracking as the main failure mode to evaluate the cost and performance effectiveness of different high RAP strategies in Oregon.

9.0 REFERENCES

- AASHTO. *Standard Specification for Superpave Volumetric Mix Design*. Publication M 323-12. American Association of State and Highway Transportation Officials, Washington, D.C., 2012.
- AASHTO. *Standard Practice for Mixture Conditioning of Hot Mix Asphalt (HMA)*. Publication R 30-10. American Association of State and Highway Transportation Officials, Washington, D.C., 2010.
- AASHTO. *Standard Practice for Reducing Samples of Hot Mix Asphalt (HMA) to Testing Size*. Publication R 47-14. American Association of State and Highway Transportation Officials, Washington, D.C., 2014.
- AASHTO. *Bulk Specific Gravity (Gmb) of Compacted Hot Mix Asphalt (HMA) using Saturated Surface-Dry Specimens*. Publication T 166-12. American Association of State and Highway Transportation Officials, Washington, D.C., 2012.
- AASHTO. *Theoretical Maximum Specific Gravity (Gmm) and Density of Hot Mix Asphalt*. Publication T 209-12. American Association of State and Highway Transportation Officials, Washington, D.C., 2012.
- AASHTO. *Preparing and Determining the Density of Hot Mix Asphalt (HMA) Specimens by Means of the Superpave Gyratory Compactor*. Publication T 312-12. American Association of State and Highway Transportation Officials, Washington, D.C., 2012.
- AASHTO. *Standard Method of Test for Determining the Fatigue Life of Compacted Hot-Mix Asphalt (HMA) Subjected to Repeated Flexural Bending*. Publication T 321-07. American Association of State and Highway Transportation Officials, Washington, D.C., 2007.
- AASHTO. *Standard Method for Determining the Dynamic Modulus and Flow Number for Hot Mix Asphalt (HMA) Using the Asphalt Mixture Performance Tester (AMPT)*. Publication TP 79-13. American Association of State and Highway Transportation Officials, Washington, D.C., 2013.
- AASHTO. *Standard Method of Test for Determining the Fracture Energy of Asphalt Mixtures Using the Semicircular Bend Geometry (SCB)*. Publication TP 105-13. American Association of State and Highway Transportation Officials, Washington, D.C., 2013.
- AASHTO. *Determining the Damage Characteristic Curve of Asphalt Concrete from Direct Tension Cyclic Fatigue Tests*. Provisional Standard TP 107. American Association of State and Highway Transportation Officials, Washington, D.C., 2014.

Arega, Z.A., A. Bhasin, and R. De. Kesel. Influence of Extended Aging on the Properties of Asphalt Composites Produced Using Hot and Warm Mix Methods. In *Construction and Building Materials*, Vol. 44, 2013, pp. 168–174.

Asphalt Institute. *Research and Development of the Asphalt Institute's Thickness Design Manual (MS-1)*. 9th Edition. Research Report, 1982.

ASTM.. *Standard Test Method for Quantitative Extraction of Asphalt Binder from Asphalt Mixtures*. Publication D2172. ASTM International, West Conshohocken, PA, 2017.

ASTM. *Standard Test Method for Indirect Tensile (IDT) Strength of Asphalt Mixtures*. Publication D6931-12. ASTM International, West Conshohocken, PA, 2012.

ASTM. *Standard Test Method for Determining the Resilient Modulus of Bituminous Mixtures by Indirect Tension Test*. Publication D7369-11. ASTM International, West Conshohocken, PA, 2011.

Baek, C., S.B. Underwood, and Y.R. Kim. Effects of Oxidative Aging on Asphalt Mixture Properties. In *Transportation Research Record: Journal of the Transportation Research Board*, No. 2296, TRB, National Research Council, Washington, D.C., 2012, pp. 77–85.

Bahia, H.U., D.I. Hanson, M. Zeng, H. Zhai, M.A. Khatri, and R.M. Anderson. In *Characterization of Modified Asphalt Binders in Superpave Mix Design*. NO. Project 9-10 FY'96, 2001.

Bell, C.A, and D. Sosnovske. Aging : Binder Validation. In *Strategic Highway Research Program, National Research Council*, SHRP-A-384, Washington, D.C.,1994.

Bell, C.A, Y. Abwahab, M E. Cristi, and D. Sosnovske. Selection of Laboratory Aging Procedures for Asphalt-Aggregate Mixtures. In *Strategic Highway Research Program. National Research Council*, SHRP-A-383, Washington, D.C., 1994.

Biligiri, K., K. Kaloush, M. Mamlouk, and M. Witczak. Rational Modeling of Tertiary Flow for Asphalt Mixtures. In *Transportation Research Record: Journal of the Transportation Research Board*, TRB, National Research Council, Washington, D.C., 2007, pp.63-72.

Birgisson, B., B. Sangpetngam, and R. Roque. Prediction of the Viscoelastic Response and Crack Growth in Asphalt Mixtures using the Boundary Element Method. In *Transportation Research Record: Journal of the Transportation Research Board*, No. 1789, TRB, National Research Council, Washington, D.C., 2002, pp. 129-135.

Bolzan, P.E., and G. Huber. Direct Tension Test Experiments. In *Strategic Highway Research Program, National Research Council*, SHRP-A-641, Washington, D.C., 1993.

Bonaquist, R.F., D.W. Christensen, and W. Stump. Simple Performance Tester for Superpave Mix Design: First-Article Development and Evaluation. In *Transportation Research Board*, Vol. 513. TRB, National Research Council, Washington, D.C., 2003, pp. 9-29.

- Bonnetti, K., K. Nam and H. Bahia. Measuring and Defining Fatigue Behavior of Asphalt Binders. In *Transportation Research Record: Journal of the Transportation Research Board*, No. 1810, TRB, National Research Council, Washington, D.C., 2002, pp. 33–43.
- Bonnaure, F., A. Gravois, and J. Udrón. A New Method of Predicting the Fatigue Life of Bituminous Mixes. In *Journal of the Association of Asphalt Paving Technologists*, Vol. 49, 1980, pp. 499-529.
- Brock, J.D. Segregation of Asphaltic Mixtures. In *Proceedings of Association of Asphalt Paving Technologists*, Vol. 55, 1986, pp. 269-277.
- Chang, C., G.Y. Baladi, and T.F. Wolff. Using Pavement Distress Data to Assess Impact of Construction on Pavement Performance. In *Transportation Research Record: Journal of the Transportation Research Board*, No. 1761, TRB, National Research Council, Washington, D.C., 2001, pp. 15–25.
- Coleri, E., R. Wu, J.M. Signore, and J.T. Harvey. Rutting of Rubberized Gap-Graded and Polymer-Modified Dense-Graded Asphalt Overlays in Composite Pavements. In *Transportation Research Record: Journal of the Transportation Research Board*, No. 2304, TRB, National Research Council, Washington, D.C., 2012, pp. 195–204.
- Coleri, E., S., Haddadi, S. Sreedhar, S. Lewis, Y. Zhang, and B. Wruck. *Binder-Grade Bumping and High Binder Content to Improve Performance of RAP-RAS Mixtures*. Final Report. SPR 797, Draft report for Oregon Department of Transportation, Salem, OR, (under review by TAC), 2017.
- Daniel, J.S., and A. Lachance. Mechanistic and Volumetric Properties of Asphalt Mixtures With Recycled Asphalt Pavement. In *Bituminous Paving Mixtures*, No. 1929, 2005, pp. 28–36.
- Darnell Jr, J. and C.A. Bell. *Performance Based Selection of RAP/RAS in Asphalt Mixtures*. Federal Highway Administration. Publication FHWA-OR-RD-16-08. FHWA, U.S. Department of Transportation, 2015.
- De Freitas, E., P. Pereira, L. Picado-Santos, and A. Papagiannakis. Effect of Construction Quality, Temperature, and Rutting on Initiation of Top-Down Cracking. In *Transportation Research Record: Journal of the Transportation Research Board*, No. 1929, TRB, National Research Council, Washington, D.C., 2005, pp. 174–182.
- Dongré, R., J. D'Angelo, and A. Copeland. Refinement of Flow Number as Determined by Asphalt Mixture Performance Tester: Use in Routine Quality Control—Quality Assurance Practice. In *Transportation Research Record: Journal of the Transportation Research Board*, No. 2127, TRB, National Research Council, Washington, D.C., 2009, pp.127-136.
- Francken, L. *Pavement Deformation Law of Bituminous Road Mixes in Repeated Load Triaxial Compression*. Presented at Fourth International Conference on the Structural Design of Asphalt Pavements, University of Michigan, Ann Arbor, MI, 1977.

Gauff, N. *Tire Management - Rubberized Asphalt Concrete*. December 2010.
<http://www.calrecycle.ca.gov/Tires/RAC/Default.htm>.

Ghuzlan, K., and S. Carpenter. Energy-Derived, Damage-Based Failure Criterion for Fatigue Testing. In *Transportation Research Record: Journal of the Transportation Research Board*, No. 1723, TRB, National Research Council, Washington, D.C., 2000, pp. 141–149.

Glover, C.J., R.R. Davison, C.H. Domke, Y. Ruan, P. Juristyarini, D.B. Knorr, and S.H. Jung. *Development of a New Method for Assessing Asphalt Binder Durability with Field Validation*. Publication No. FHWA/TX-05/1872-2. FHWA, U.S. Department of Transportation, 2005.

Harmelink, D., S. Shuler, and T. Aschenbrener. Top-Down Cracking in Asphalt Pavements : Causes, Effects, and Cures. In *Journal of Transportation Engineering, ASCE*, Vol. 134(1), 2008, pp. 1–6.

Hartman, A.M., and M.D. Gilchrist. Evaluating Four-Point Bend Fatigue of Asphalt Mix Using Image Analysis. In *Journal of Materials in Civil Engineering, ASCE*, Vol. 16(1), 2004, pp. 60–68.

Harvey, J., and B.W. Tsai. Effects of Asphalt Content and Air Void Content on Mix Fatigue and Stiffness. In *Transportation Research Record: Journal of the Transportation Research Board*, No. 1543(1), TRB, National Research Council, Washington, D.C., 1996, pp. 38–45.

Harvey, J., Liu, A., Zhou, J., Signore, J.M., Coleri, E., He, Y. *Superpave Implementation Phase II: Comparison of Performance-Related Test Results*. UCPRC-RR-2015-01, July 2014.

Hu, S., F. Zhou, T. Scullion. Factors That Affect Cracking Performance in Hot Mix Asphalt Mix Design. In *Transportation Research Record: Journal of the Transportation Research Board*, No. 2210, TRB, National Research Council, Washington, D.C., 2011, pp. 37–46.

Hudson, W.R., F.N. Finn, B.F. McCullough, K. Nair, and B.A. Vallergera. *Systems Approach to Pavement Systems Formulation, Performance Definition and Materials Characterization*. Final Report, NCHRP Project 1-10, Materials Research and Development, Inc., 1968.

Isola, M., S. Chun, R. Roque, J. Zou, C. Koh, and G. Lopp. Development and Evaluation of Laboratory Conditioning Procedures to Simulate Mixture Property Changes Effectively in the Field. In *Transportation Research Record: Journal of the Transportation Research Board*, No. 2447, TRB, National Research Council, Washington, D.C., 2014, pp. 74–82.

Jones, D. R. SHRP Materials Reference Library : Asphalt Cements : A Concise Data Compilation. In *Strategic Highway Research Program, National Research Council*, Washington, DC. 1993.

Kaloush, K.E., M.I. Souliman, W.A. Zeiada, J.J. Stempihar. *Sensitivity of Mixture Performance Tests to Identical PG Binders from Different Suppliers*. Proceedings of Transportation Research Board 91st Annual Meeting, 2012.

Kandhal, P.S., S.S. Rao, D.E. Watson, and B. Young. Performance of Recycled Hot Mix Asphalt Mixtures in Georgia. In *Transportation Research Record: Journal of the Transportation Research Board*, No. 1507, TRB, National Research Council, Washington, D.C., 1995, pp. 67-77.

Kennedy, T.W., R.B. McGennis, and R.J. Holmgreen. Asphalt Mixture Segregation: Diagnostics And Remedies. In *Association of Asphalt Paving Technologists, Proc* (Vol. 56), 1987.

Khedaywi, T., and T. White. Effect of Segregation Fatigue on Fatigue Performance of Asphalt Paving Mixtures, In *Transportation Research Record: Journal of the Transportation Research Board*, No. 1543, TRB, National Research Council, Washington, D.C., 1996, pp. 63–70.

Khosla, N.P., and S. Sadasivam. *Determination of Optimum Gradation for Resistance to Permeability, Rutting and Fatigue Cracking*, Publication FHWA/NC/2004-12. FHWA, U.S. Department of Transportation, 2005.

Kim, Y.R. and D.N. Little. One-Dimensional Constitutive Modeling of Asphalt Concrete. In *ASCE Journal of Engineering Mechanics*, Vol. 116 (4), 1990, pp. 751–772.

Kim, Y.R., C. Baek, B.S. Underwood, V. Subramanian, M.N. Guddati, K. Lee. Application of Viscoelastic Continuum Damage Model Based Finite Element Analysis to Predict the Fatigue Performance of Asphalt Pavements. In *KSCE Journal of Civil Engineering*, Vol. 12(2), 2008, pp. 109-120.

Kim, Y.R. *Modeling of Asphalt Concrete*. American Society of Civil Engineers Press, VA, USA, 2009.

Lee, H.J. and Y.R. Kim. A Viscoelastic Continuum Damage Model of asphalt concrete with healing. In *ASCE Journal of Engineering Mechanics*, Vol. 124 (11), 1998, pp. 1224–1232.

Lee, H.J., J.S. Daniel, and Y.R. Kim. Continuum Damage Mechanics-Based Fatigue Model of Asphalt Concrete. In *Journal of Materials in Civil Engineering*, ASCE, Vol. 12(2), 2000, pp. 105-112.

Li, X., M.O. Marasteanu, R.C. Williams, and T.R. Clyne. Effect of Reclaimed Asphalt Pavement (Proportion and Type) and Binder Grade on Asphalt Mixtures. In *Transportation Research Record: Journal of the Transportation Research Board*, No. 2051, TRB, National Research Council, Washington, D.C., 2008, pp. 90–97.

Luo, X., R. Luo, R.L. Lytton. Characterization of Asphalt Mixtures Using Controlled-Strain Repeated Direct Tension Test. In *Journal of Materials in Civil Engineering*, ASCE. Vol. 25(2), 2013, pp. 194-207.

McDaniel, R., and R. M. Anderson. *NCHRP Web Document 30: Recommended Use of Reclaimed Asphalt Pavement in the Superpave Mix Design Method—Project 9-12*. Final Report, 2001.

Miner, M.A. Cumulative Damage in Fatigue. In *Journal of Applied Mechanics*, Vol. 12, 1945, pp. A159–A164.

Mohammad, L.N., M. Kim, M. Elseifi. Characterization of Asphalt Mixture's Fracture Resistance Using the Semi-Circular Bending (SCB) Test. 7th RILEM International Conference on Cracking in Pavements, 2012, pp. 1-10.

Monismith, C.L. Fatigue Characteristics of Asphalt Paving Mixtures and Their Use in Pavement Design. 18th Paving Conf., Univ. of New Mexico, Albuquerque, N.M, 1981.

Monismith, C.L., J.S. Coplantz, J.A. Deacon, F.N. Finn, J.T. Harvey, and A.A. Tayebali. Fatigue Response of Asphalt-Aggregate Mixtures. In *Strategic Highway Research Program, National Research Council*, Washington, DC. SHRP-A-404, 1994.

Newcomb, D., A.E. Martin, F. Yin, E. Arambula, E.S. Park, A. Chowdhury, R. Brown, C. Rodezno, N. Tram, E. Coleri, and D. Jones. *NCHRP Report 815: Short-Term Laboratory Conditioning of Asphalt Mixtures*. Washington DC: National Cooperative Highway Research Program, Transportation Research Board, National Research Council, 2015.

Norouzi, A., D. Kim, and Y.R. Kim. Numerical Evaluation of Pavement Design Parameters for the Fatigue Cracking and Rutting Performance of Asphalt Pavements. In *Materials and Structures*, Vol. 49(9), 2016, pp.3619-3634.

Nsengiyumva, G. *Development of Semi-Circular Bending (SCB) Fracture Test for Bituminous Mixtures*, 2015.

Oregon Department of Transportation, Pavement Services Unit. *2012 Pavement Condition Report*, 2013.

Ozer, H., Al-Qadi, I.L., Lambros, J., El-Khatib, A., Singhvi, P., & Doll, B. Development of the Fracture-Based Flexibility Index for Asphalt Concrete Cracking Potential Using Modified Semi-Circle Bending Test Parameters. In *Construction and Building Materials*, Vol. 115, 2016, 390–401

Paris, P., and F. Erdogan. A Critical Analysis of Crack Propagation Laws. In *Journal of Basic Engineering, Transactions of the American Society of Mechanical Engineers*, December 1963, pp. 528-534.

Pavementinteractive.org. *Flexural Fatigue*. 1 July 2011.
<http://www.pavementinteractive.org/article/flexural-fatigue/> Accessed on 26 November 2015.

Pellinen, K.T. The Effect of Volumetric Properties on Mechanical Behavior of Asphalt Mixtures. In *Transportation Research Record: Journal of the Transportation Research Board No. 2403*, TRB, National Research Council, Washington, D.C., 2003.

Pellinen, T., D. Christensen, G. Rowe, and M. Sharrock. Fatigue-Transfer Functions: How Do They Compare? In *Transportation Research Record: Journal of the Transportation Research Board, No. 1896*, TRB, National Research Council, Washington, D.C., 2004, pp. 77–87.

- Prowell, B.D., E.R. Brown, R.M. Anderson, J.S. Daniel, A.K. Swamy, H.V. Quintus, S. Maghsoodloo. *NCHRP Report 646: Validating the Fatigue Endurance Limit for Hot Mix Asphalt*. Transportation Research Board of the National Academies, Washington, DC, 2010.
- Raad, L., S. Saboundjian, and G. Minassian. Field Aging Effects on Fatigue of Asphalt Concrete and Asphalt-Rubber Concrete. In *Transportation Research Record: Journal of the Transportation Research Board*, No. 1767, TRB, National Research Council, Washington, D.C., 2001, pp.126–134.
- Rice, J. R. A Path Independent Integral and the Approximate Analysis of Strain Concentration by Notches and Crack. In *Journal of Applied Mechanics*, V 35, 1968, pp. 379–386.
- Rodezno, M.C., West, R. and Taylor, A. Flow Number Test and Assessment of AASHTO TP 79-13 Rutting Criteria: Comparison of Rutting Performance of Hot-Mix and Warm-Mix Asphalt Mixtures. In *Transportation Research Record: Journal of the Transportation Research Board*, No. 2507, TRB, National Research Council, Washington, D.C., 2015, pp.100-107.
- Roque, R., Z. Zhang, and B. Sankar. Determination of Crack Growth Rate Parameters of Asphalt Mixtures Using the Superpave IDT. In *Journal of the Association of Asphalt Paving Technologists*, Vol. 68, 1999, 404-433.
- Roque, R., B. Birgisson, Z. Zhang, B. Sangpetngam, and T. Grant. *Implementation of SHRP Indirect Tension Tester to Mitigate Cracking in Asphalt Pavements and Overlays*. Final Report, Florida Department of Transportation, Florida, 2002.
- Roque, R., J. Zou, Y.R. Kim, C.M. Baek, S. Tirunavukkarasu, B.S. Underwood, and M.N. Guddati. *NCHRP Web-Only Document 162: Top-Down Cracking of Hot Mix Asphalt Layers: Models for initiation and Propagation. Final Report. NCHRP 1-42A*. Transportation Research Board of the National Academies, Washington, D.C., 2010.
- Roque, R., S. Chun, J. Zou, G. Lopp, and C. Villiers. *Construction of Superpave Projects Monitoring*. Final Report, Florida Department of Transportation, Tallahassee, Florida, 2011.
- Schapery, R.A. Deformation and Fracture Characterization of Inelastic Composite Materials Using Potentials. In *Polymer Engineering and Science*, Vol. 27 (1), 1987, pp. 63–76.
- Schapery, R.A. A Theory of Mechanical Behavior of Elastic Media with Growing Damage and other Changes in Structure. In *J. Mech. Phys. Solids*, Vol. 38, 1990, pp. 215–253.
- Schorsch, M., C.M. Chang, G.Y. Baladi, C. Petit, I.L. Al-Qadi, and A. Millien. Effects of Segregation on the Initiation and Propagation of Top-Down Cracks. In *Fifth International RILEM Conference on Reflective Cracking in Pavements*, No. 7361, 2003, pp. 3–10.
- Seber, G.A.F. *Linear Regression Analysis*. John Wiley & Sons, 1977.
- SHRP-A-404. *Fatigue Response of Asphalt-Aggregate Mixes*. Strategic Highway Research Program, National Research Council, Washington DC, 1994.

Sousa, J., J. Pais, M. Prates, R. Barros, P. Langlois, and A. M. Leclerc. Effect of Aggregate Gradation on Fatigue Life of Asphalt Concrete Mixes. In *Transportation Research Record: Journal of the Transportation Research Board*, No. 1630, TRB, National Research Council, Washington, D.C., 1998, pp. 62–68.

Tangella, S.C.S., J. Craus, J.A. Deacon, and C.L. Monismith. *Summary Report on Fatigue Response of Asphalt Mixtures*. No. SHRP-A-312, Strategic Highway Research Program, National Research Council, 1990.

Tayebali, A.A., G.M. Rowe, J.B. Sousa. Fatigue Response of Asphalt-Aggregate Mixtures. In *Journal of the Association of Asphalt Paving Technologists*, Vol. 61, 1992, pp. 333-360.

Texas Department of Transportation (TxDOT). *Standard Specifications for Construction and Maintenance of Highways, Streets, and Bridges*. Austin, TX, 2004.

Tsai, B.W., J. Harvey, and C. Monismith. WesTrack Fatigue Performance Prediction Using Miner's Law. In *Transportation Research Record: Journal of the Transportation Research Board*, No. 1809, TRB, National Research Council, Washington, D.C., 2002, pp. 137–147.

Uhlmeier, J., K. Willoughby, L. Pierce, and J. Mahoney. Top-Down Cracking in Washington State Asphalt Concrete Wearing Courses. In *Transportation Research Record: Journal of the Transportation Research Board*, No. 1730, TRB, National Research Council, Washington, D.C., 2000, pp. 110–116.

Underwood, B.S., Y.R. Kim, and M.N. Guddati. Improved Calculation Method of Damage Parameter in Viscoelastic Continuum Damage Model. In *International Journal of Pavement Engineering*, Vol. 11(6), 2010, pp. 459-476.

Underwood, B. S., C. Baek, and Y. R. Kim. Simplified Viscoelastic Continuum Damage Model as Platform for Asphalt Concrete Fatigue Analysis. In *Transportation Research Record: Journal of the Transportation Research Board*, No. 2296, TRB, National Research Council, Washington, D.C., 2012, pp. 36-45.

Von Quintus, H., J. Mallela, R. Bonaquist, C. Schwartz, and R.L. Carvalho. *Calibration of Rutting Models for HMA Structural and Mixture Design–Project 9-30*. Final Report, 2009.

Walker, D. (2014). <http://asphaltmagazine.com/the-benefits-of-modified-asphalts/>

Wambura, J.H.G., J. Maina, and H.R. Smith. Kenya Bituminous Materials Study. In *Transportation Research Record: Journal of the Transportation Research Board*, TRB, National Research Council, Washington, D.C., 1999, pp. 129–137.

West, R.C., G.R. Rada, J.R. Willis, and M.O. Marasteanu. Improved Mix Design, Evaluation, and Materials Management Practices for Hot Mix Asphalt with High Reclaimed Asphalt Pavement Content. In *Transportation Research Record: Journal of the Transportation Research Board*, No. 752 TRB, National Research Council, Washington, D.C., 2013, pp. 1-100

Williams, R.S., and R. Shaidur. *Mechanistic Design Guide Calibration for Pavement Rehabilitation*. SPR, Final Report for Oregon Department of Transportation, Salem, Oregon, 2013.

Williams, R.S., R. Shaidur. *SPR 734: Premature Asphalt Concrete Pavement Cracking*. Final Report for Oregon Department of Transportation, Salem, Oregon, 2015.

Witczak, M.W., and M.W. Mirza. *AC Fatigue Analysis for 2002 Design Guide*. Research Report for NCHRP 1-37A. Project. Arizona State University, Tempe, AZ, 2000.

Witczak, M.W., D. Andrei, and W.N. Houston. *Guide for Mechanistic–Empirical Design of New and Rehabilitated Pavement Structures*. Transportation Research Board of the National Research Council, 2004, pp. 1-19.

Wu, Z., N.L. Mohammad, L.B. Wang, M.A. Mull. Fracture Resistance Characterization of Superpave Mixtures Using Semi-Circular Bending Test. In *Journal of ASTM International*, Vol. 2(3), 2005.

Zhang Z., R. Roque, and B. Birgisson. Evaluation of Laboratory-Measured Crack Growth Rate for Asphalt Mixtures. In *Transportation Research Record: Journal of the Transportation Research Board*, No. 1797, TRB, National Research Council, Washington, D.C., 2001, pp. 67-75.

APPENDIX A

A.0 PAVEMENT MANAGEMENT SYSTEM DATA SHEETS (PMS) FOR FIELD SECTIONS

Field specimens were collected from the following sections: Sections US20-U and OR99-U with no cracking and sections OR99W-C and OR99EB with cracking. The pavement condition data were obtained from ODOT's PMS database. Figure A.1 through Figure A.4 illustrate the PMS data for the four sections.

Oregon State Highway Report

SECTION: OR 22: SUBLIMITY INTCHG SECT (RW2-WB)
 DIRECTION: W
 TYPE: DGAC THK
 SURFACE: C-MIX
 AGE: 6

HWY NO: 162
 BEGIN MP: 12.11
 END MP: 13.80
 LENGTH: 1.69
 REGION: 2 DIST: 03

CONSTRUCTION HISTORY

DATE	THKN	MTRL	THKN	MTRL	THKN	MTRL	CPPR	THKN	BASE	THKN	SUB	V-FILE	CON #
2010	2	C	3	C	5	C		11	AG	0.1	GE	41V-15	C13439
COMMENTS: 1" thicker near structures													

TRAFFIC

ADT: 0	20 YEAR ESALS: 0	SPEED: 55
--------	------------------	-----------

CURRENT DISTRESS

% FATIGUE: 0%	% PATCHING: 0%	% RAVELING: 0%
# T-CRACKS / 0.1 MILE: 0	# POTHOLES / MILE: 0	% BLEEDING: 0%

CONDITION HISTORY

	1994	1995	1996	1997	1998	1999	2001	2003	2004	2006	2008	2010	2012	2014	2016
RATING:							100	100	100	100			98	98	98
RUT:															0.10
IRI:															
SKID:															

CONDITION GRAPH

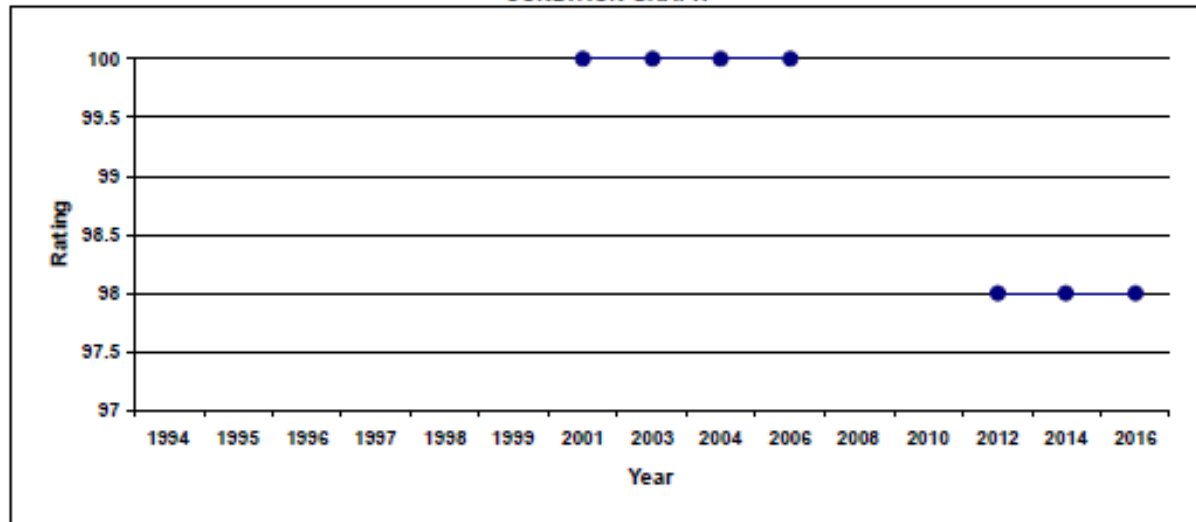


Figure A.1: PMS for OR-22 Sublimity Section

Oregon State Highway Report

SECTION: OR 99W: JCT HWY 058 - FLAT CREEK
 DIRECTION: S
 TYPE: DGAC THK
 SURFACE: B-MIX
 AGE: 23

HWY NO: 091
 BEGIN MP: 108.76
 END MP: 108.92
 LENGTH: 0.16
 REGION: 2 DIST: 04

CONSTRUCTION HISTORY

DATE	THKN	MTRL	THKN	MTRL	THKN	MTRL	CPPR	THKN	BASE	THKN	SUB	V-FILE	CON #
1993	2	B	3	B	5	B		12	PA	0.01	GE	24V-125	C11252
COMMENTS: 108.52-108.60 4" ovly of PCC													

TRAFFIC

ADT: 12,000	20 YEAR ESALS: 6,000,000	SPEED: 30
-------------	--------------------------	-----------

CURRENT DISTRESS

% FATIGUE: 0%	% PATCHING: 0%	% RAVELING: 7%
# T-CRACKS / 0.1 MILE: 0	# POTHoles / MILE: 0	% BLEEDING: 0%

CONDITION HISTORY

	1994	1995	1996	1997	1998	1999	2001	2003	2004	2006	2008	2010	2012	2014	2016
RATING:	98	98	98	98	95	90	90	90	90	85	85	92	79	74	57
RUT:		0.13		0.21		0.18	0.19	0.35		0.44		0.34	0.30	0.35	0.24
IRI:		172		181		191	194	231		194		185	146	165	
SKID:	49				52				47		40	53	54		

CONDITION GRAPH

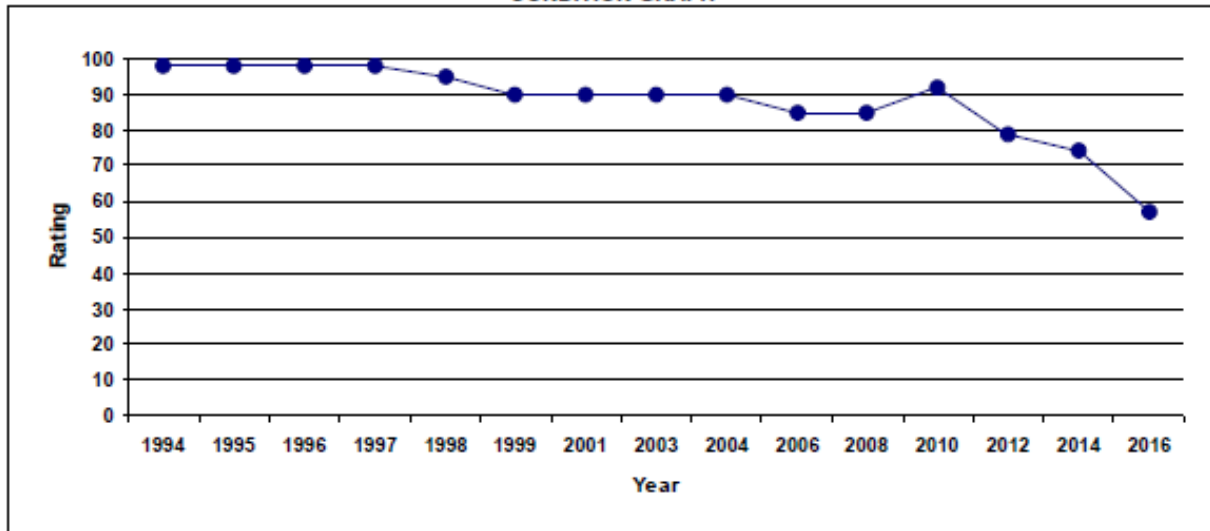


Figure A.2: PMS for OR-99W JUNCTION CITY

Oregon State Highway Report

SECTION: OR 99W: BRUTSCHER ST - JCT HWY 151
 DIRECTION: S
 TYPE: DGAC THK
 SURFACE: C-MIX
 AGE: 14

HWY NO: 091
 BEGIN MP: 21.80
 END MP: 23.76
 LENGTH: 1.93
 REGION: 2 DIST: 03

CONSTRUCTION HISTORY

DATE	THKN	MTRL	THKN	MTRL	THKN	MTRL	CPPR	THKN	BASE	THKN	SUB	V-FILE	CON#
2002	2	C2	2	C2	6.5	L	2					34V-25	C12504
COMMENTS: 23.17-23.76 - rebuilt													
1963	1.5	B	2	B				2	AG	17	AG	7V-275	C06195
COMMENTS: widen to 5 lanes, 1.5"B ovly JCP under A-lanes & median, 22.89-23.2 (1956) 5V-137													
1937	1	AU	3	AU				6	AG			2V-241	
COMMENTS: 22' wide, ovly extg 5" bit road, PCC 21.03-22.44													

TRAFFIC

ADT: 35,000	20 YEAR ESALS: 6,000,000	SPEED: 35
-------------	--------------------------	-----------

CURRENT DISTRESS

% FATIGUE: 44%	% PATCHING: 0%	% RAVELING: 0%
# T-CRACKS / 0.1 MILE: 1	# POTHOLES / MILE: 0	% BLEEDING: 0%

CONDITION HISTORY

	1994	1995	1996	1997	1998	1999	2001	2003	2004	2006	2008	2010	2012	2014	2016
RATING:	22	32	24	18	17	22		100	100	91	86	60	62	54	46
RUT:		0.46		0.71		0.47	0.59	0.10	0.18	0.31	0.25	0.32	0.33	0.29	0.38
IRI:		145		167		178	205	87	90	96	116	110	103	104	110
SKID:	47		56		52				50	47	51		52	48	46

CONDITION GRAPH

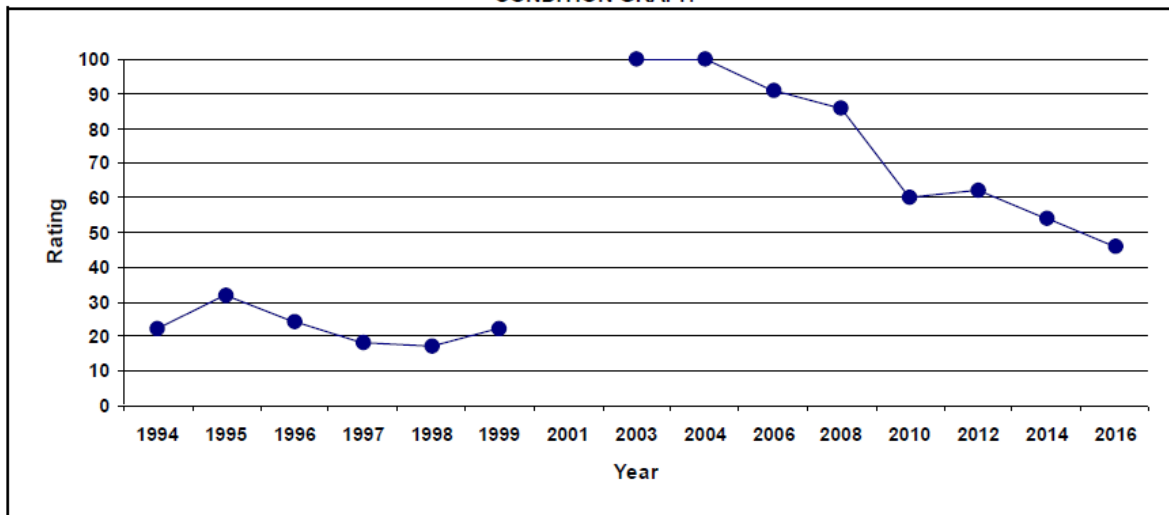


Figure A.3: PMS for OR-99W BRUTSCHER ST

Oregon State Highway Report

SECTION: OR 99EB: JCT HWY 001 - LIBERTY ST
 DIRECTION: S
 TYPE: DGAC THK ON CTB
 SURFACE: C-MIX
 AGE: 12

HWY NO: 072
 BEGIN MP: 0.43
 END MP: 3.34
 LENGTH: 2.91
 REGION: 2 DIST: 03

CONSTRUCTION HISTORY

DATE	THKN	MTRL	THKN	MTRL	THKN	MTRL	CPPR	THKN	BASE	THKN	SUB	V-FILE	CON #
2004	2	C	2	B								37V-50	C12986
COMMENTS: 2.58-3.34 - 2"ovly/2.5"inly													
1984	2	B	2	B				11	CT	6	CE	16V-133	C09491
COMMENTS: 3.34-3.63 widen & ovly													

TRAFFIC

ADT: 25,000	20 YEAR ESALS: 10,000,000	SPEED: 55
-------------	---------------------------	-----------

CURRENT DISTRESS

% FATIGUE: 65%	% PATCHING: 0%	% RAVELING: 0%
# T-CRACKS / 0.1 MILE: 8	# POTHOLES / MILE: 1	% BLEEDING: 0%

CONDITION HISTORY

	1994	1995	1996	1997	1998	1999	2001	2003	2004	2006	2008	2010	2012	2014	2016
RATING:	75	55	55	50	50	40	40	40		98	92	65	52	43	35
RUT:		0.21		0.20		0.19	0.26	0.30	0.05	0.22	0.13	0.16	0.19	0.20	0.22
IRI:		108		113		118	116	117	63	63	105	75	81	80	91
SKID:	53		52		47				52		53	54	56	48	56

CONDITION GRAPH

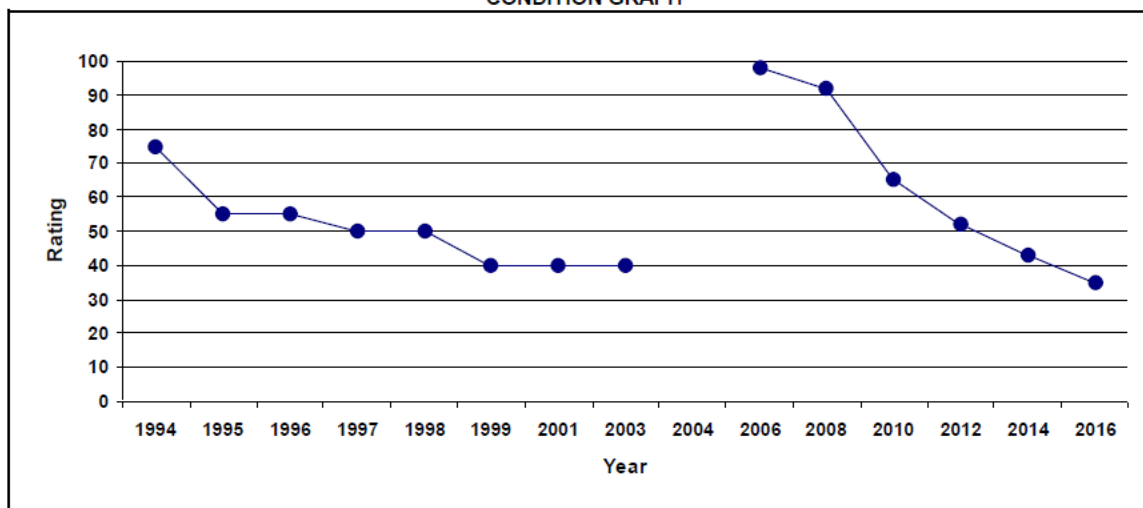


Figure A.4: PMS for OR-99EB JCT HWY

APPENDIX B

B.0 MIX DESIGN SHEETS FOR PLANT MIXTURES

This section presents the bituminous mix design summary and consensus aggregate properties of Mix 1, Mix 2, and Mix 3 provided by Lakeside Industries Portland, Oregon.

Figure B.1 through Figure B.4 show the mix design properties of Mix 1. Figure B.5 through Figure B.8 show the mix design properties of Mix 2 and Mix 3.

OREGON DEPARTMENT OF TRANSPORTATION
MATERIALS LABORATORY
800 AIRPORT ROAD SE
SALEM, OR 97301-4758

503.585.3000
Fax: 503.585.3096

Contract No.: C14905	EA: CON03839	F.A. No. NHPP-S092(057)	Lab No. 16-MD0095
Project Name: US30: NW McNamee Rd - NW Bridge Ave		Amendment 1 Date:	
Highway: Lower Columbia River Highway	County: Multnomah	Amendment 2 Date:	
Begin MP: 6.40	End MP: 13.03	Amendment 3 Date:	
Contractor: Kerr Contractors Oregon, Inc.			
Project Manager: Marge West		Use: Level 4 3B* Dense Mix	

BITUMINOUS MIX DESIGN REVIEW

Lab Name: Lakeside Industries	Certified Mix Design Technician: Laura Nelson
Mix Producer: Lakeside Industries	Contractor Mix Design No.: LAN0418
Asphalt Supplier: Owens Corning	Transferred from Lab No.:
Asphalt Grade: PG 70-22ER	Antistrip Information: %
Gb (60°/180° F): 1.037	

Stockpile Information	1/2" - #4	#4 - #8	#4 - 0	RAP			
Stockpile Size	05-004-1	05-004-1	05-004-1	Front Av			
Stockpile Source	0.0	23.0	67.0	20.0	0.0	0.0	0.0
Stockpile Percentage	2.893	2.895	2.840	2.848	0.100	0.100	0.100
Bulk Specific Gravity (Gsb)							

Job Mix Formula	Slave	% Pass	Paving Course	% Asphalt by WL of Mixture (Pb)	Maximum Specific Gravity (Gmm):
3/4" (19mm)	-----	100	Wearing	8.0	2.480
1/2" (12.5mm)	-----	100	Base		
3/8" (9.5mm)	-----	99	Levelling		
1/4" (6.25mm)	-----	84	Temporary		
No. 4 (4.75mm):	-----	65			
No. 3 (2.36mm):	-----	40			
No. 16 (1.18mm):	-----	26	VMA: 15.4	VFA: 74	
No. 30 (0.60mm):	-----	21	Percent A/C in Rap: 5.3	Combined Aggregate Gravity (Gsb): 2.847	
No. 50 (0.30mm):	-----	15	Number of Gyration: 100	Gmb Sample Weight: 4690	
No. 100 (0.15mm):	-----	10	Void Target (Va): 4.0	Mixing Temp Range: 315-322 F	
No. 200 (0.075mm):	-----	7.7	Tensile Strength Ratio: 87	Placement Temp Range: 300-307 F	

Compliance Statement:	Based on the information submitted for review, this mix design does comply with specifications.	Total Lab Charges: \$0.00
-----------------------	---	----------------------------------

 Reviewed by Signature	25 August 2016 Date
--	-------------------------------

C: Flex; Project Manager; Chris Daman, Pavements; Bituminous; Region 1 QA Coord; Kerr Contractors Oregon, Inc.
Larry Ig, Pavements

Figure B.1: ODOT mix design summary-Mix 1

PROJECT	US30: McNamee Rd. NW Bridge Ave.
CONTRACT NO.	14905
MIX PRODUCER	Lakeside Industries
CMDT (print)	Laura Nelson

MIX CLASS	Dense Graded 3/8"
LEVEL (2,3,4)	4
PROJECT MANAGER	Marge West
CMDT JMF MIX ID NO.	LAN0416
BID ITEM #	570


AGGREGATE & OTHER CONSTITUENTS (RAP, BL. SAND, LIME, ETC.)

STOCKPILE SIZES	#4-88	#4-0	RAP
SOURCE NUMBER	05-004-1	05-004-1	Front Ave
STOCKPILE PERCENTAGE (P _{st})	23	57	20
Bulk Specific Gravity (G _{sb})	2.685	2.840	2.648
Apparent Specific Gravity (G _{sa})	2.779	2.777	2.795

Design developed with "dryback" Gmm (Y/N)?

N

MIXTURE AT DESIGN ASPHALT CONTENT

Maximum Specific Gravity (G _{max})	2.480
Gyratory Bulk Gravity (G _{mb})	2.382
Combined Aggregate (G _{sa})	2.847
Effective Specific Gravity (G _{se})	2.724
Combined Apparent Gravity (G _{sa})	2.781
Absorbed Asphalt, % (P _{ba})	1.09
Effective Asphalt Content, % (P _{ba})	4.39
P ₂₀₀ / P ₁₀ Ratio	1.5
Air Voids, % (V _a)	4.0
VMA, %	15.4
VFA, %	74
Tensile Strength Ratio (TSR)	85.7
TSR Compaction Blows	NA
VIR	12.83
APA Rut depth - mm	pending
Gmb Sample Weight @ JMF	4690
Number of Gyration	100
Dust Pul, %	NA
Draindown % (open graded)	
Date	8/2/2016
CMDT Signature	
CMDT Card #	44014

COMMENTS: BLEND CHOSEN? Medium
REASON? Flare request

JOB MIX FORMULA

Aggregate Gradation	Blend	CA & FA Ratios
Sieve		
3/4" (19 mm)	100	
1/2" (12.5 mm)	100	CA
3/8" (9.5 mm)	99	0.708
1/4" (6.3 mm)	84	
No. 4 (4.75 mm)	65	FA
No. 8 (2.36 mm)	40	0.406
No. 16 (1.18 mm)	28	0.431
No. 30 (0.60 mm)	21	0.53
No. 50 (0.30 mm)	15	0.528
No. 100 (0.150 mm)	10	0.477
No. 200 (0.075 mm)	7.7	0.519
	FA Average	0.482
	FA Std Dev	0.053
Asphalt content, % (P _b)	6.0	
RAP AC, % (P _{ba})	5.26	
Virgin Binder Repl., %	17.5	
Antistrip, %	NA	
Agg. Treatment, %	NA	
Asphalt Brand	Owens Corning	
Asphalt Grade	70-22ER	
Mixing temp. range	315 - 322 F	
Placement temp. range	300 - 307 F	
Asphalt SpGr (G _b) 77 °F	1.033	
Asphalt SpGr (G _b) 80 °F	1.037	

Figure B.2: ODOT mix design summary-Mix 1 (continued)

AASHTO T-86: Specific Gravity and Absorption of Coarse Aggregate									
Size	Source	A4-43 (146)		Average		#4-10 (146)		Average	
		US-054-1				US-054-1			
A) Mass of Dry Sample		2402.6	2317.2			2183.3	2047.1		
B) Mass of SSD Sample		3438.9	2343.9			2220.8	2041.0		
C) Mass of Sample Immersed		1630.1	1483.6			1508.5	1310.3		
Bulk Specific Gravity (G_m)		2.667	2.654			2.666	2.656		2.658
Bulk Specific Gravity (G_{SD})		2.707	2.708			2.701	2.700		2.700
Apparent Specific Gravity (G_a)		2.779	2.776			2.778	2.778		2.760
Absorption (%)		1.51	1.57			1.69	1.60		1.65
Average									
Average									
Average									
Average									
Average									
Average									
Average									
Average									
Average									
Average									
Average									
Average									
Average									
Average									
Average									
Average									
Average									
Average									
Average									
Average									
Average									
Average									
Average									
Average									
Average									
Average									
Average									
Average									
Average									
Average									
Average									
Average									
Average									
Average									
Average									
Average									
Average									
Average									
Average									
Average									
Average									
Average									
Average									
Average									
Average									
Average									
Average									
Average									
Average									
Average									
Average									
Average									
Average									
Average									
Average									
Average									
Average									
Average									
Average									
Average									
Average									
Average									
Average									
Average									
Average									
Average									
Average									
Average									
Average									
Average									
Average									
Average									
Average									
Average									
Average									
Average									
Average									
Average									
Average									
Average									
Average									
Average									
Average									
Average									
Average									
Average									
Average									
Average									
Average									
Average									
Average									
Average									
Average									
Average									
Average									
Average									
Average									
Average									
Average									
Average									
Average									
Average									
Average									
Average									
Average									
Average									
Average									
Average									
Average									
Average									
Average									
Average									
Average									
Average									
Average									
Average									
Average									
Average									
Average									
Average									
Average									
Average									
Average									
Average									
Average									
Average									
Average									
Average									
Average									
Average									
Average									
Average									
Average									
Average									
Average									
Average									
Average									
Average									
Average									
Average									
Average									
Average									
Average									
Average									
Average									
Average									
Average									
Average									
Average									
Average									
Average									
Average									
Average									
Average									
Average									
Average									
Average									
Average									
Average									
Average									
Average									
Average									
Average									
Average									
Average									
Average									
Average									
Average									
Average									
Average									
Average									
Average									
Average									
Average									
Average									
Average									
Average									
Average									
Average									
Average									
Average									
Average									
Average									
Average									
Average									
Average									
Average									
Average									
Average									
Average									
Average									
Average									
Average									
Average									
Average									
Average									
Average									
Average									
Average									
Average									
Average									
Average									
Average									
Average									
Average									
Average									
Average									
Average									
Average									
Average									
Average									
Average									
Average									
Average									
Average									
Average									
Average									
Average									
Average									
Average									
Average									
Average									
Average									
Average									
Average									
Average									
Average									
Average									
Average									
Average									
Average									
Average									
Average									
Average									
Average									
Average									
Average									
Average									
Average									
Average									
Average									
Average									
Average									
Average									
Average									
Average									
Average									
Average									
Average									
Average									
Average									
Average									
Average									
Average									
Average									
Average									
Average									
Average									
Average									
Average									
Average									
Average									
Average									
Average									
Average									
Average									
Average									
Average									
Average									
Average									
Average									
Average									
Average									
Average									
Average									
Average									
Average									
Average									
Average									
Average									
Average									
Average									
Average									
Average									
Average									
Average									
Average									
Average									
Average									
Average									

PROJECT	US30: McNamée Rd. NW Bridge Ave Sec.	MIX CLASS	3/8"
CONTRACT	14905	LEVEL (2,3,4)	4
MIX PROJ	Lakeside Industries	PROJECT MANAGER	Marge West
CMDT (pr)	Laura Nelson	CMDT JMF MIX ID NO	LAN0416

JMF - BATCH VERIFICATION									
SIEVE SIZE	Virgin %			RAP %		COMBINED		TOLERANCE	SIEVE SIZE
	MASS 1	MASS 2	TOTAL MASS	% RET	% PASS	% PASS	% PASS		
3/4"	0.0		0.0	0.0	100.0	100.0	100.0	100.0	3/4"
1/2"	0.0		0.0	0.0	100.0	100.0	100.0	100.0	1/2"
3/8"	0.0		0.0	0.0	100.0	96.8	99.4	99.4	3/8"
1/4"	212.4		212.4	14.2	85.8	78.4	84.4	84.3	1/4"
#4	317.8		317.8	21.2	64.7	66.4	65.0	65.1	#4
#8	372.0		372.0	24.8	39.9	45.1	40.9	40.4	#8
#16	176.5		176.5	11.8	28.1	31.5	28.8	28.1	#16
#30	100.5		100.5	6.7	21.4	23.8	21.9	21.4	#30
#50	102.6		102.6	6.8	14.5	17.4	15.1	14.8	#50
#100	67.3		67.3	4.5	10.1	12.9	10.6	10.2	#100
#200	30.5		30.5	2.0	8.0	8.4	8.1	7.7	#200
PAN	8.4		8.4	0.6					
TOTAL MASS (g)			1388						

NIT. DRY MASS (g)	1500	DRY WASHED MASS (g)	1387.3	SIEVE LOSS %	0.05%
Certified Technician and Card Number:			Laura Nelson #441014		

Figure B.4: Field worksheet for HMAC (plant report)-Mix 1

This section represents the bituminous mix design summary, and consensus aggregate properties of Mix 2 and 3 provided by Lakeside Industries Portland, Oregon.

OREGON DEPARTMENT OF TRANSPORTATION
MATERIALS LABORATORY
800 AIRPORT ROAD SE
SALEM, OR 97301-4798

503.986.3000
Fax: 503.986.3096

Contract No.: **C14607** EA: **CON03539** F.A. No JTA-S047(109) Lab No. **16-MD0019**
Project Name: **US26 @ Brookwood/Helvetia (Shute Rd)** Amendment 1 Date:
Highway: **Sunset Highway** County: **Washington** Amendment 2 Date:
Begin MP: **0.00** End MP: **0.00** Amendment 3 Date:
Contractor: **Wildish Standard Paving Co.**
Project Manager: **Ron Larson** Use: **Level 4** 1/2" Dense Mix

BITUMINOUS MIX DESIGN REVIEW

Lab Name: **Lakeside Industries** Certified Mix Design Technician: **Laura Nelson**
Mix Producer: **Lakeside Industries** Contractor Mix Design No.: **LAN0509**
Asphalt Supplier: **Owens Corning** Transferred from Lab No.: **09-MD0022**
Asphalt Grade: **PG 70-22ER** Antistrip Information: %
G_b (60°/60° F): **1.037**
This JMF updated for 2016.

Stockpile Information							
Stockpile Size	1/2" - #4	#4 - #8	#4 - 0	RAP			
Stockpile Source	05-004-1	05-004-1	05-004-1	Front Av			
Stockpile Percentage	28.0	8.0	44.0	20.0	0.0	0.0	0.0
Bulk Specific Gravity (G _{sb})	2.693	2.667	2.650	2.689	0.100	0.100	0.100

Job Mix Formula		Paving Course	% Asphalt by Wt. of Mixture (P _b)	Maximum Specific Gravity (G _{mm}):
Sieve	% Pass			
3/4" (19mm)	100	Wearing <input checked="" type="checkbox"/>		
1/2" (12.5mm)	96	Base <input type="checkbox"/>	5.3	2.502
3/8" (9.5mm)	85	Leveling <input type="checkbox"/>		
1/4" (6.25mm)	63	Temporary <input type="checkbox"/>		
No. 4 (4.75mm):	50			
No. 8 (2.36mm):	32	VMA: 14.8	VFA: 73	
No. 16 (1.18mm):	22	Percent A/C in Rap: 5.1	Combined Aggregate Gravity (G _{sb}): 2.671	
No. 30 (0.60mm):	17	Number of Gyration: 100	G _m Sample Weight: 4740	
No. 50 (0.30mm):	11	Void Target (V _a): 4.0	Mixing Temp Range: 315-322 F	
No. 100 (0.15mm):	9	Tensile Strength Ratio: 92	Placement Temp Range: 300-307 F	
No. 200 (0.075mm):	6.6			

Compliance Statement: Based on the information submitted for review, this mix design does comply with specifications.

Total Lab Charges: \$0.00

Reviewed by Signature

31 March 2016
Date

C: Files; Project Manager; Chris Duman, Pavements; Bituminous; Region 1 QA Coord;
Larry Ilg, Pavements

Wildish Standard Paving Co.

Figure B.5: ODOT mix design summary – Mix 2 and Mix 3

ODOT CONTRACTOR MIX DESIGN SUMMARY

PROJECT	US26 @ Brookwood/ Helevita (Shute Rd)
CONTRACT NO.	C14607
MIX PRODUCER	Lakeside Industries
CMDT (print)	Laura Nelson

MIX CLASS	Dense Graded 1/2"
LEVEL (2,3,4)	4
PROJECT MANAGER	Ron Larson
CMDT JMF MIX ID NO.	LAN0509/ 13-MD0023
BID ITEM #	1430


AGGREGATE & OTHER CONSTITUENTS (RAP, BL. SAND, LIME, ETC.)

STOCKPILE SIZES	1/2"-#4	#4-#8	#8-#16	RAP			
SOURCE NUMBER	05-004-1	05-004-1	05-004-1	Front Ave			
STOCKPILE PERCENTAGE (P _{sp})	28	8	44	20			
Bulk Specific Gravity (G _{sb})	2.693	2.667	2.650	2.689			
Apparent Specific Gravity (G _{sa})	2.785	2.781	2.777	2.795			

Design developed with "dryback" Gmm (Y/N)?

N

MIXTURE AT DESIGN ASPHALT CONTENT

Maximum Specific Gravity (G _{mm})	2.502
Gyratory Bulk Gravity (G _{mb})	2.403
Combined Aggregate (G _{ab})	2.671
Effective Specific Gravity (G _{se})	2.719
Combined Apparent Gravity (G _{sa})	2.783
Absorbed Asphalt, % (P _{ba})	0.68
Effective Asphalt Content, % (P _{be})	4.65
P ₂₀₀ / P _{be} Ratio	1.42
Air Voids, % (V _a)	4.0
VMA, %	14.8
VFA, %	73
Tensile Strength Ratio (TSR)	92
TSR Compaction Blows	
VIR	12.8
APA Rut depth - mm	2.6
Gmb Sample Weight @ JMF	4740
Number of Gyrations	100
Dust Pull, %	NA
Draindown % (open graded)	
Date	3/29/14
CMDT Signature	
CMDT Card #	44014

COMMENTS: BLEND CHOSEN? Medium

REASON?: History of mix

JOB MIX FORMULA

Aggregate Gradation	Blend	CA & FA Ratios
Sieve		
3/4" (19 mm)	100	
1/2" (12.5 mm)	96	CA
3/8" (9.5 mm)	85	0.851
1/4" (6.3 mm)	63	
No. 4 (4.75 mm)	50	FA
No. 8 (2.36 mm)	32	0.374
No. 16 (1.18 mm)	22	0.442
No. 30 (0.60 mm)	17	0.525
No. 50 (0.30 mm)	11	0.514
No. 100 (0.150 mm)	9	0.52
No. 200 (0.075 mm)	6.6	0.577
	FA Average	0.492
	FA Std Dev.	0.072
Asphalt content, % (P _b)	5.3	
RAP AC, % (P _{br})	5.1	
Virgin Binder Repl., %	19.2	
Antistrip, %	NA	
Agg. Treatment, %	NA	
Asphalt Brand	Owens Corning	
Asphalt Grade	70-22ER	
Mixing temp. range	315F-322F	
Placement temp. range	300F-307F	
Asphalt SpGr (G _b) 77 °F	1.033	
Asphalt SpGr (G _b) 60 °F	1.037	

Figure B.6: ODOT mix design summary– Mix 2 and Mix 3 (continued)

AASHTO T-85: Specific Gravity and Absorption of Coarse Aggregate

Size	1/2" #4	Average	#4-#8 (+#8)	Average	#4-0 (+#8)	Average
Source	05-004-1		05-004-1		05-004-1	
A) Mass of Dry Sample	2834.4		2301.1		2385.6	
B) Mass of SSD Sample	2868.4		2336.7		2424.0	
C) Mass of Sample Immersed	1816.4		1473.5		1527.2	
Bulk Specific Gravity (G_{sb})	2.894	2.693	2.666	2.669	2.662	2.661
Bulk Specific Gravity (SSD)	2.727	2.726	2.707	2.709	2.703	2.704
Apparent Specific Gravity (G_{sa})	2.784	2.785	2.780	2.782	2.779	2.779
Absorption (%)	1.23	1.23	1.55	1.52	1.61	1.60

AASHTO T-84: Specific Gravity and Absorption of Fine Aggregate

Size	#4-0 (-#8)	Average	Average	Average
Source	05-004-1			
S) Mass of SSD Sample	500.0			
B) Mass of Pyc. + Water	648.7			
C) Mass of Pyc. + H ₂ O + Sample	962.8			
Mass of Dry Sample + Pan	874.6			
Mass of Pan	383.7			
A) Mass of Dry Sample	490.9			
Bulk Specific Gravity (G_{sb})	2.641	2.639	#DIV/0!	#DIV/0!
Bulk Specific Gravity (SSD)	2.690	2.688	#DIV/0!	#DIV/0!
Apparent Specific Gravity (G_{sa})	2.777	2.776	#DIV/0!	#DIV/0!
Absorption (%)	1.85	1.90	#DIV/0!	#DIV/0!

Combined Specific Gravity

Size	1/2" #4	#4-#8	#4-0
Split Sieve	#4	#8	#8
Percent Passing Split Sieve			
Bulk Specific Gravity (G_{sb})	2.693	2.667	2.680
Bulk Specific Gravity (SSD)	2.726	2.708	2.696
Apparent Specific Gravity (G_{sa})	2.766	2.781	2.777
Absorption (%)	1.23	1.54	1.74

Comments:

Certified Technician and Card Number:

Figure B.7: Specific gravity and absorption of coarse and fine aggregates– Mix 2 and Mix 3

FIELD WORKSHEET FOR HMAC (PLANT REPORT)

PROJECT NAME SECTION		US26 @ Brookwood/Helvetia		MIX DESIGN NO. 15MD0716		TEST NO. 1		CONTRACT NUMBER C14607	
Contractor or Supplier Lakeside Industries		PROJECT MANAGER Ron Larson		DATE 10/18/2015		AMOUNT REPRESENTED 100		SHEET NUMBER	
SOURCE (HMAC)		Santosh		TIME 8:30am		DRC OR HMAC		DATA NORMAL SIZE 1/2"	
PLANT/NOVEL		Gencor		TYPE Drum		SIZE 550		TO BE USED IN HMAC	
SIEVE		Sieve Analysis		CORRECTED		JOB MIX FORMULA		SIEVE	
MASS 1	MASS 2	TOTAL MASS	% RET	% PASS	TARGET	ACTION LIMITS	PAN TARE	AGG. MOISTURE	
0	0	0	0.0	100.0	100	100	327-338	311	
3/4	96.1	96.1	6.0	94.0	94	95	WET MASS (A)	1588.1	
1/2	204.6	204.6	12.8	87.1	81	82	WET MASS (B)	2548.3	
3/8	309.0	309.0	19.4	80.6	62	61	WET MASS (C)	1495.7	
1/4	180.8	180.8	11.3	88.7	50	50	WET MASS (D)	1495.4	
4	290.5	290.5	18.2	81.8	32	32	WET MASS (E)	1655.0	
8	157.1	157.1	9.9	90.1	22	23	WET MASS (F)	1653.5	
16	92.6	92.6	5.8	94.2	16	16	WET MASS (G)	0.12	
30	78.4	78.4	4.9	95.1	12	12	WET MASS (H)	MIX MOISTURE	
50	49.3	49.3	3.1	96.9	9	9	WET MASS (I)	255	
100	33.2	33.2	2.1	97.9	6.4	6.4	WET MASS (J)	430.5	
200	3.8	3.8	0.2	99.8	5.30	5.30	WET MASS (K)	1655.0	
PAN							WET MASS (L)	1653.5	
INITIAL DRY MASS		1693.7		% ASPHALT, P/B		4.9-5.9		RAP MOISTURE	
METER READINGS									
ASPHALT	WET AGG	WET RAP			BASKET TARE		T 3014.6		PAN TARE (T)
BEGINNING					MIX MASS & BASKET		A 4705.5		WET MASS (A)
ENDING					A EG MASS & BASKET		B 4606.0		WET MASS (B)
SUB TOTAL					COOL AGG & BASKET		4607.7		WET MASS (C)
MOISTURE	4.13	% 5.02	% (B)	% (C)	% (D)	% (E)	0.12		WET MASS (D)
TOTAL					MIX MOISTURE		5.77		WET MASS (E)
ASPHALT METER CORRECTION					(M) = (A-T)/(T-%M/100)		0.44		WET MASS (F)
%					300.0		1688.8		WET MASS (G)
PLANT MOISTURE AND DRY READINGS					305.0		1591.4		WET MASS (H)
%					plant waste total		10.00		WET MASS (I)
%					coated waste (half of total)		5.00		WET MASS (J)
%					uncoated waste (half of total)		5.00		WET MASS (K)
%					rejected mix		0.00		WET MASS (L)
SIGNATURE		DATE		10/18/15		QUALITY CONTROL VERIFICATION		INDEPENDENT ASSURANCE	
Bryan Aschim #44173		Lakeside Industries							

Figure B.8: Field worksheet for HMAC (plant report) – Mix 2 and Mix 3

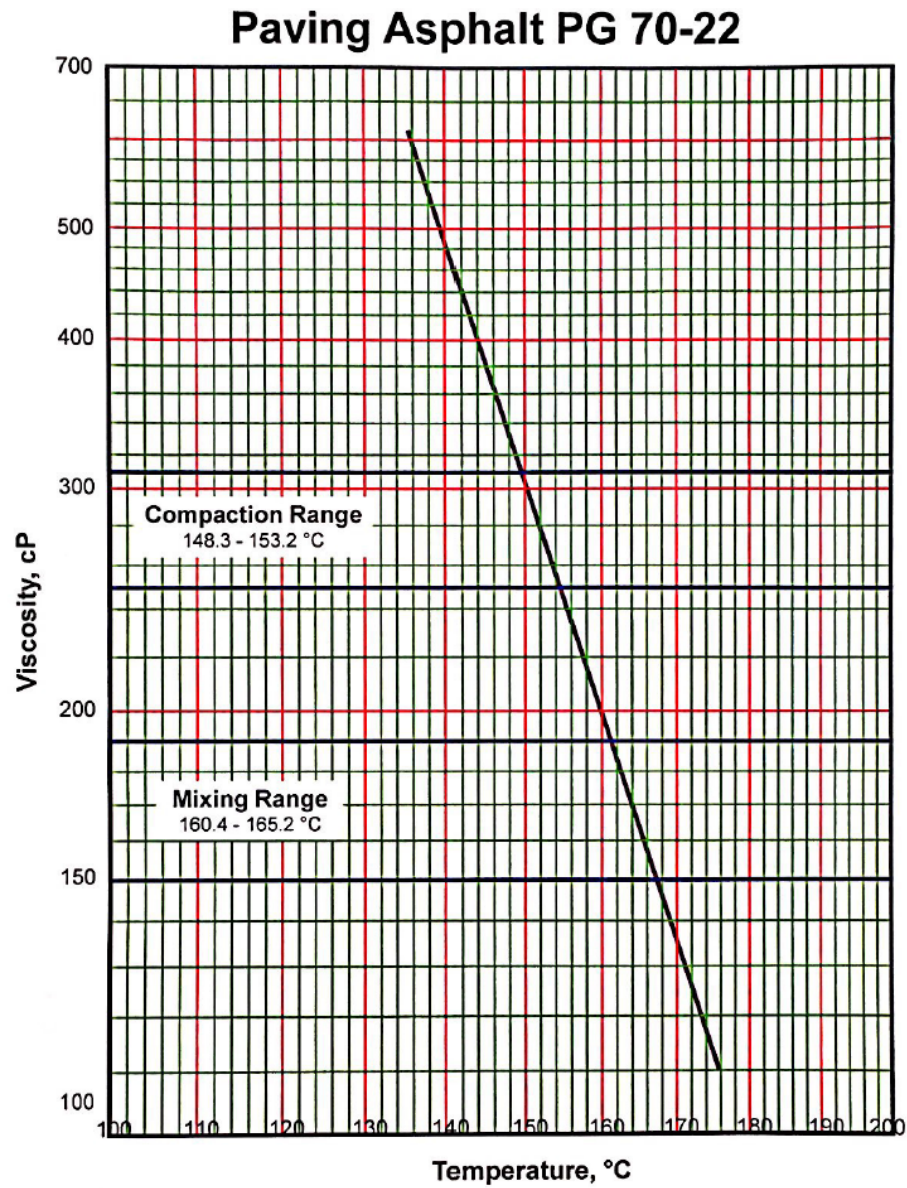
APPENDIX C

C.0 BINDER PROPERTIES PROVIDED BY THE PLANT

Figure C.1 through Figure C.4 illustrate the binder consensus properties and mixing and compaction curves for PG70-22 and PG70-22ER binder types.

CERTIFICATE OF ANALYSIS		Sample ID: T08091316-01	
For Owens Corning Trumbull Asphalt 11910 NW ST. HELENS ROAD Portland OR 97231		Testing Performed by BLM Owens Corning Roofing & Asphalt 11910 NW St Helens Road Portland Oregon 97231 AASHTO MP 320 table 1 Specification	
DATE 9/14/16	Sample Date 9/13/16	Tank 8	
Product: PG 70-22			
Test	Result	Test Method	Specification
Appearance	Homogenous, free of water, no foam		
Penetration, 100g /5 seconds	47	ASTM D5	0.1dmm
Specific Gravity @ 15.6 °C	1.037	AASHTO T228	Report
Rotational Viscosities @ 135.0 °C Pa.s	0.606	AASHTO T316	< 3.00 Pa.s
Softening Point, Ring & Ball, °F	128	ASTM D36	Report
Flash Point, COC °C	327	AASHTO T48	230 °C minimum
DSR @ 70.0 °C (ORIG) G* kPa	1327.00		Report
Phase Angle @ 70.0 °C	83.9	AASHTO T315	Report
DSR @ 70.0 °C G*/sin delta, kPa	1.33		1.00 minimum
Rolling Thin Film Oven Mass change, 163.0 °C, %	-0.071	AASHTO T240	-1.00 maximum
DSR @ 70.0 °C (RTFO) G* kPa	3592.00		Report
Phase Angle @ 70.0 °C	80.5	AASHTO T315	Report
DSR @ 70.0 °C G*/sin delta, kPa	3.64		2.20 minimum
PAV, 2.1 Mpa @ 20 hours	Perform	AASHTO R28	100 °C
DSR @ 28.0 °C (PAV) G* kPa	4.25E+00		Report
Phase Angle @ 28.0 °C	42.9	AASHTO T315	Report
DSR @ 28.0 °C G*(sin delta) kPa	2891		5000 maximum
BBR @ -12.0 °C MPa. Est. Stiffness	187		300 maximum
BBR PAV @ -12.0 °C (m-value)	0.309	AASHTO T313	0.300 minimum
<p>This report is for the exclusive use of stated client. No copy or other reproduction in any form should be made without the client's written permission. The test results, opinions, or interpretations contained herein are based upon work performed in a laboratory setting. Owens Corning and its Trumbull Asphalt Division assume no responsibility and make no warranty or other representation whatsoever regarding the actual performance of the material, products or processes reported on herein.</p> <p>This material was found to meet AASHTO M320 Table 1 specifications. Analysis by Brendan McGillicuddy (NBTC #A1162)</p> <p>Reported by Frank Burg</p>			

Figure C.1: PG 70-22 binder consensus properties



Specific Gravity at 15°C: 1.039

Source: Portland, OR

Mixing and Compaction temperatures calculated are based on the latest edition of Asphalt Institutes' *SuperPave Mix Design* (SP-2) publication. They are calculated using recommended viscosity ranges of 170±20cP for mixing temperatures and 280±30cP for compaction temperatures. These ranges are only a recommended starting point for laboratory analysis, and must be verified by detailed mix designs for field use.

Every care has been taken in the preparation of this information. To the extent permitted by applicable law, all warranties and/or representations, express or implied, as to the accuracy of the information are disclaimed, and no liability is accepted for the accuracy or completeness of the same.

Figure C.2: PG 70-22 binder mixing and compaction curve

<p align="center">CERTIFICATE OF ANALYSIS</p> <p align="center">For Owens Corning Trumbull Asphalt 11910 NW ST. HELENS ROAD Portland OR 97231</p>		<p>Sample ID: T06090116-01</p> <p>Testing Performed by BLM Owens Corning Roofing & Asphalt 11910 NW St Helens Road Portland Oregon 97231 AASHTO MP 320 table 1 Specification</p>	
DATE 9/2/16	Sample Date 9/1/16		
Tank 6	Product: PG 70-22ER		
Test	Result	Test Method	Specification
Appearance	Homogenous, free of water, no foam		
Penetration, 100g /5 seconds	64	ASTM D5	0.1dmm
Specific Gravity @ 15.6 °C	1.034	AASHTO T228	Report
Rotational Viscosities @ 135.0 °C Pa.s	0.712	AASHTO T316	< 3.00 Pa.s
Softening Point, Ring & Ball, °F	126	ASTM D36	Report
Flash Point, COC °C	310	AASHTO T48	230 °C minimum
DSR @ 70.0 °C (ORIG) G* kPa	1112.00		Report
Phase Angle @ 70.0 °C	76.5	AASHTO T315	Report
DSR @ 70.0 °C G*/sin delta, kPa	1.14		1.00 minimum
Rolling Thin Film Oven			
Mass change, 163.0 °C, %	-0.128	AASHTO T240	-1.00 maximum
DSR @ 70.0 °C (RTFO) G* kPa	2572.00		Report
Phase Angle @ 70.0 °C	74.61	AASHTO T315	Report
DSR @ 70.0 °C G*/sin delta, kPa	2.67		2.20 minimum
Elastic Recovery			
Per cent Recovery at 77°F	69	AASHTO T301	50% per ODOT
PAV, 2.1 Mpa @ 20 hours	Performed	AASHTO R28	100 °C
DSR @ 28.0 °C (PAV) G* kPa	2.33E+00		Report
Phase Angle @ 28.0 °C	48.7	AASHTO T315	Report
DSR @ 28.0 °C G*(sin delta) kPa	1747		5000 maximum
BBR @ -12.0 °C MPa. Est. Stiffness	147		300 maximum
BBR PAV @ -12.0 °C (m-value)	0.332	AASHTO T313	0.300 minimum
<p>This report is for the exclusive use of stated client. No copy or other reproduction in any form should be made without the client's written permission. The test results, opinions, or interpretations contained herein are based upon work performed in a laboratory setting. Owens Corning and its Trumbull Asphalt Division assume no responsibility and make no warranty or other representation whatsoever regarding the actual performance of the material, products or processes reported on herein.</p> <p>This material was found to meet AASHTO M320 Table I specifications, Analysis by Brendan McGillicuddy (NBTC#162)</p> <p>Reported by Frank Burg</p>			

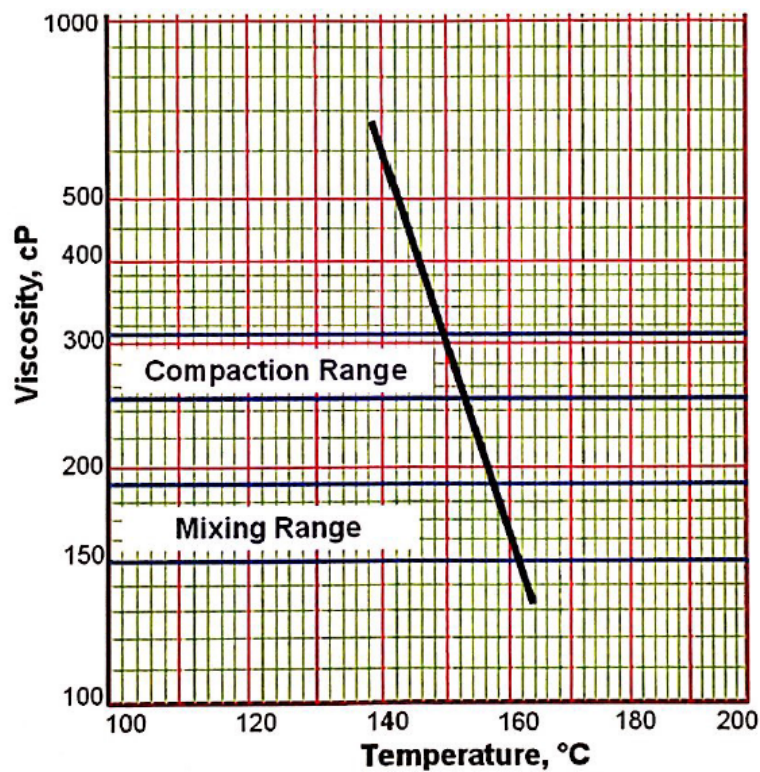
Figure C.3: PG 70-22ER binder consensus properties



INNOVATIONS FOR LIVING®

Asphalt Binder PG 70-22ER

Mixing and Compaction Curve



Specific Gravity: 1.036

This report is for the exclusive use of stated client. No copy or other reproduction in any form should be made without the client's written permission. The test results, opinions, or interpretations contained herein are based upon work performed in a laboratory setting. Owens Corning and its Trumbull Asphalt Division assume no responsibility and make no warranty or other representation whatsoever regarding the actual performance of the material, products or processes reported on herein.

Figure C.4: PG 70-22ER binder mixing and compaction curve

APPENDIX D

D.0 EFFECTS OF RECYCLED ASPHALT PAVEMENT AND BINDER CONTENT ON THE FLEXURAL STIFFNESS OF ASPHALT CONCRETE USING BBF

Twelve beam samples were tested using the four-point bending beam fatigue device. Four different mixture variations were used, with three replicates for each variation. The variations being tested consisted of a 6% binder content with 30% RAP content mixture, a 6.4% binder content with 30% RAP content mixture, a 6.4% binder content with 40% RAP content mixture and a 6.8% binder content with 40% RAP content mixture.

The stiffness and cycle number were first plotted from each of the test results to examine how the stiffness decreased with the applications of the cyclic loads. The results were plotted per binder content in the mixture and can be seen below in Figure D.1 through Figure D.3:

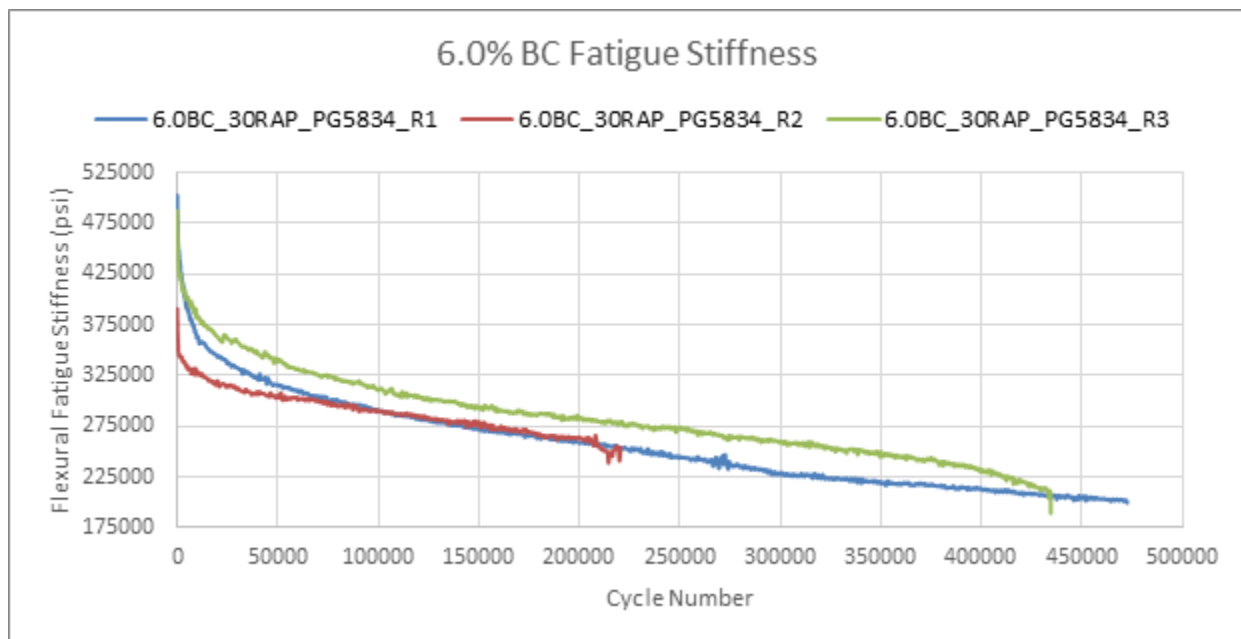


Figure D.1: Flexural fatigue stiffness versus cycle number for 6.0% BC

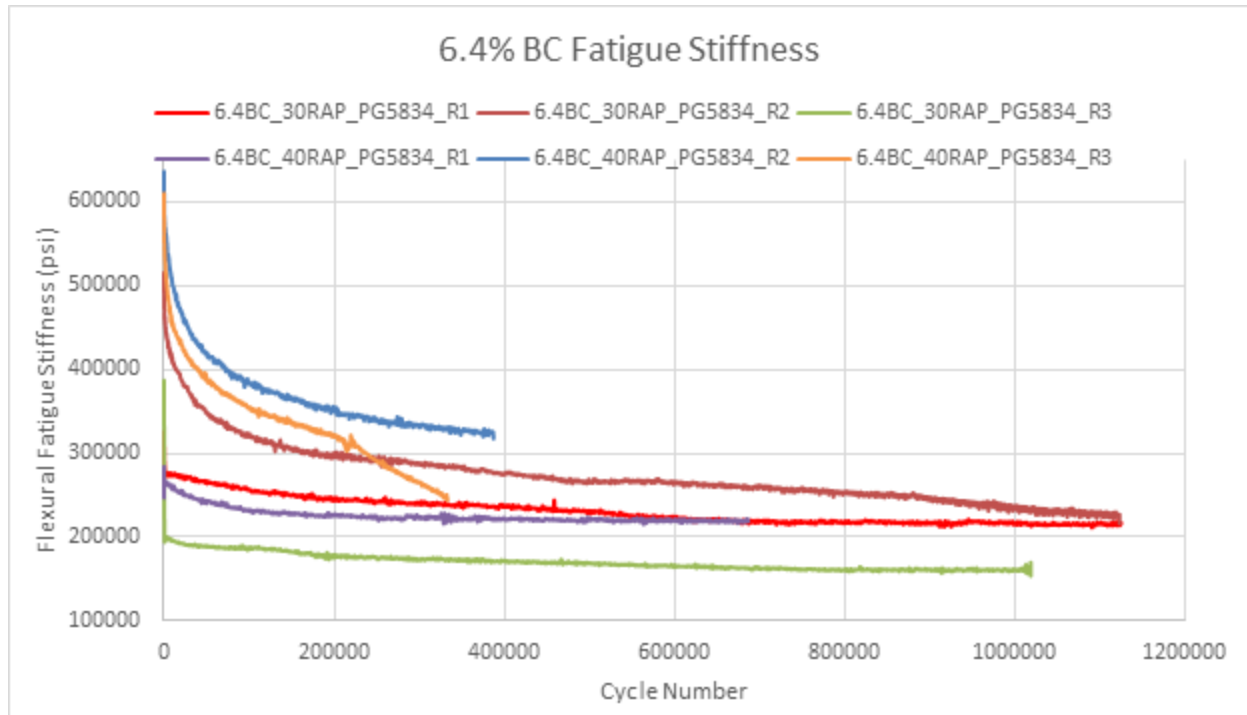


Figure D.2: Flexural fatigue stiffness versus cycle number for 6.4% BC

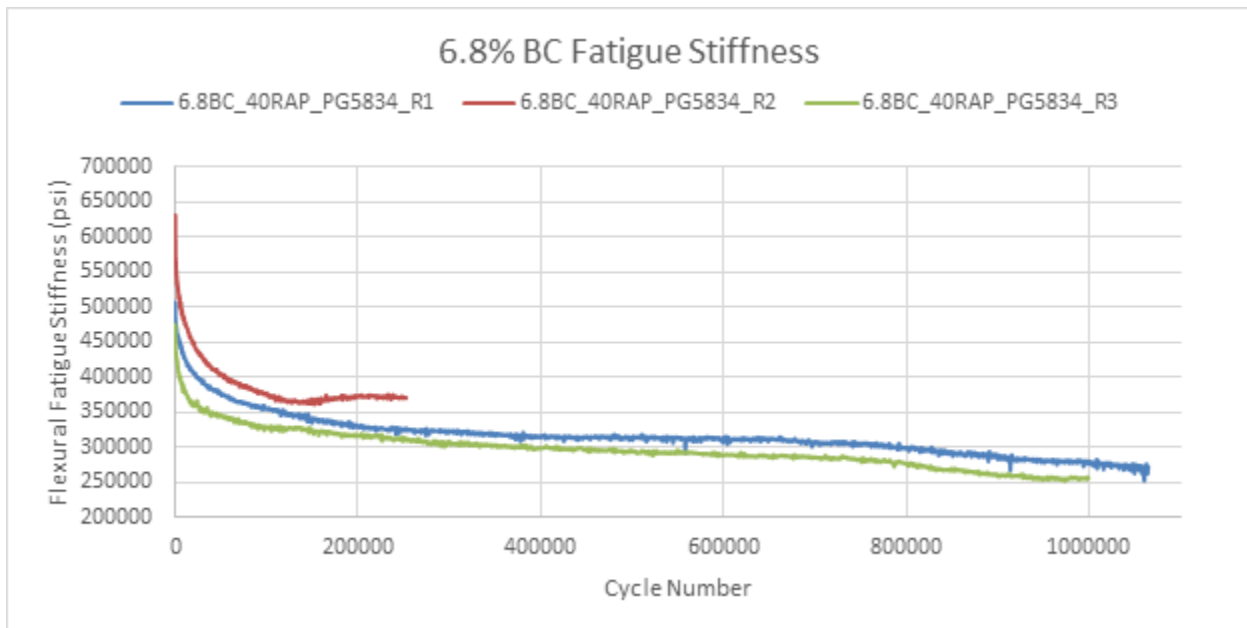


Figure D.3: Flexural fatigue stiffness versus cycle number for 6.8% BC

Immediately, it can be seen that a high level of variability exists between replicates of the same binder and RAP contents. Each of the three replicates for each mix variation were cut from the same asphalt block, thus the discrepancy between replicates is not a sample preparation issue. From the above plots, it can be seen that the flexural fatigue stiffness of each beam decreases at a

negative exponential rate. In general, the stiffness decreases rapidly over the first 50,000 to 100,000 loading cycles before transitioning to a constant rate of stiffness reduction.

Plotting the percentage of stiffness reduction against the number of cycles using a logarithmic scale provides a clearer interpretation of the flexural performance of each mixture variation. The beam sample is considered as failed once it reaches a 50 percent reduction in initial stiffness. To effectively compare each mix variation, the number of cycles required to achieve a 50 percent reduction in initial stiffness was determined.

For various reasons, four of the beam samples did not reach the 50 percent stiffness reduction failure criteria at the conclusion of the testing. In these situations, the existing data was modeled using a Weibull distribution. A trendline was then fit to a portion of the data and the cycle number at which the sample reached 50 percent of its initial stiffness was estimated using the equation of the trendline.

Conclusions

The number of cycles required to reach a 50 percent reduction in stiffness are shown in Table D.1 below, along with the average value for each mixture variation. There were several outliers in the data which were not considered when determining the average number of cycles to failure. The samples not considered were Replicate 2 (R2) from the 6.0BC_30RAP mixture, and Replicates 1 and 3 (R1 and R3) from the 6.4BC_30RAP mixture.

Table D.1. Number of Cycles Required to Reach a 50% Reduction in Stiffness

6.0BC_30RAP				6.4BC_30RAP			
Number of Cycles of Failure				Number of Cycles of Failure			
R1	R2	R3	AVG	R1	R2	R3	AVG
232,003	1,085,838	357,006	294,505	-	658,520	499	658,520

6.4BC_40RAP				6.8BC_40RAP			
Number of Cycles of Failure				Number of Cycles of Failure			
R1	R2	R3	AVG	R1	R2	R3	AVG
21,000	387,007	213,002	207,003	1,060,525	559,646	1,153,434	924,535

By comparing the number of cycles to failure for each mixture, as can be seen below in Figure D.4, conclusions can be drawn regarding the effects of binder and RAP content in an asphalt pavement mixture. In both the 30% and 40%RAP cases, holding the RAP content constant and increasing only the binder content will increase the fatigue life of the mixture. This is as expected, since additional binder will increase the pavement's flexibility. By comparing the 6.4BC_30RAP and 6.4BC_40RAP mixtures, one can see that increased RAP contents will have a negative impact on the fatigue life of the pavement, which is also to be expected since aged RAP is less flexible than virgin material. Comparing the 6.0BC_RAP30 mixture to the 6.4BC_RAP40 mixture shows that these two mixtures have similar fatigue lives despite having significantly different mixture characteristics. One could draw the conclusion that by increasing the binder content in a mixture, the RAP content could also be increased without a loss in

performance of the asphalt pavement. This strategy could be implemented to decrease the material costs while also improving the sustainability of a roadway.

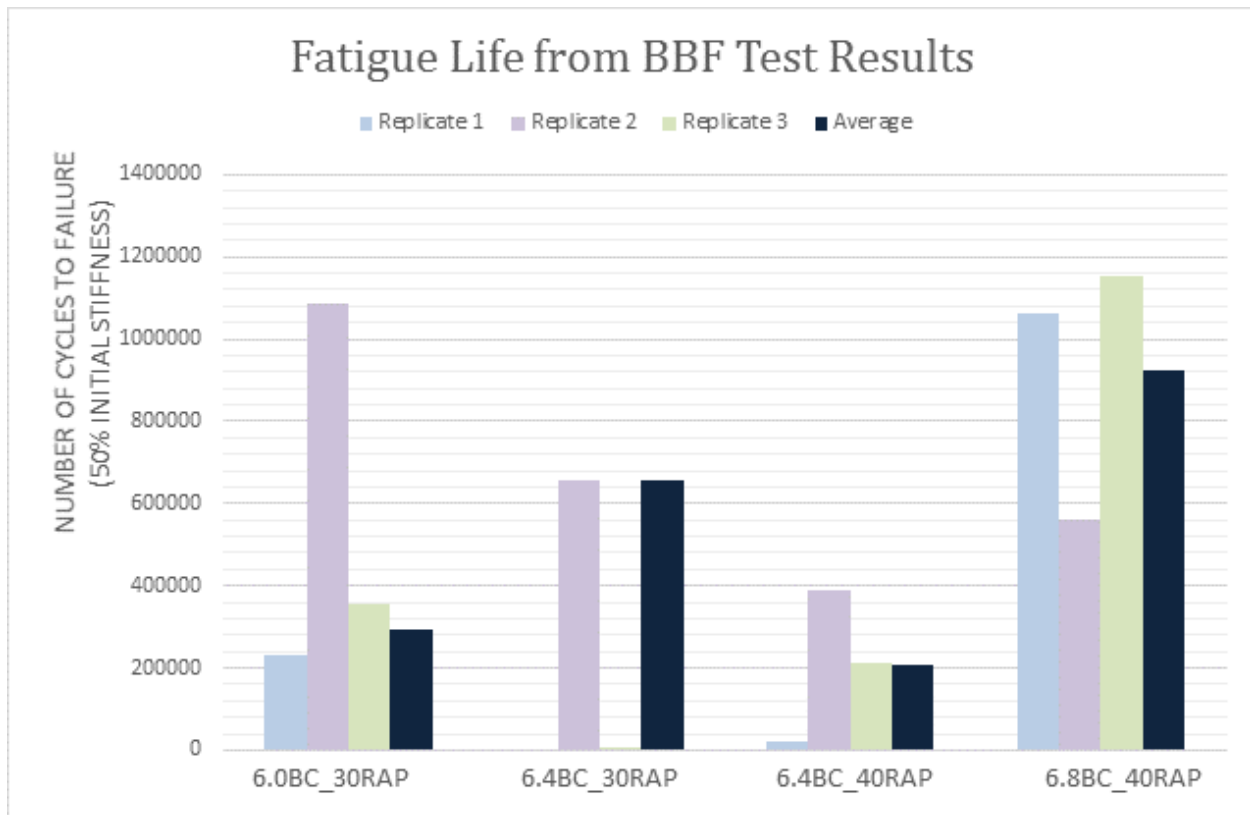


Figure D.4: Number of BBF cycles required to reach failure of samples with varying RAP and binder contents.

APPENDIX E

E.0 GMM AND AIR VOIDS

Table E-1 shows G_{mm} and air voids for Mix 1:

Table E.1: G_{mm} and air voids for Mix 1

ID	A	B	C	D	E	F
	mass of sample in air, A (g)	mass of SSD sample in air, B (g)	mass of sample in water, C (g)	Gmb (A/(B-C))	Gmm (g/cm³)	Air voids (%)
SCB_5.3AC_5.0AV_S1	5430.5	5440.5	3192.0	2.415	2.562	5.73
SCB_5.3AC_7.0AV_S1	5319.0	5352.0	3102.0	2.364	2.562	7.73
SCB_6.0AC_5.0AV_S1	5331.0	5341.0	3098.0	2.377	2.518	5.61
SCB_6.0AC_7.0AV_S1	5238.0	5256.0	3011.0	2.333	2.518	7.34
DM_5.3AC_5.0AV_S1	7143.0	7155.0	4205.0	2.421	2.562	5.49
DM_5.3AC_5.0AV_S2	7127.0	7139.0	4194.0	2.420	2.562	5.54
DM_5.3AC_7.0AV_S1	7009.0	7026.0	4084.5	2.383	2.562	6.99
DM_5.3AC_7.0AV_S2	6992.0	7007.0	4067.5	2.379	2.562	7.16
DM_6.0AC_5.0AV_S1	7025.5	7035.0	4087.0	2.383	2.518	5.36
DM_6.0AC_5.0AV_S2	7017.5	7026.0	4084.0	2.385	2.518	5.27
DM_6.0AC_7.0AV_S1	6874.5	6889.0	3956.5	2.344	2.518	6.90
DM_6.0AC_7.0AV_S2	6868.5	6885.0	3949.0	2.339	2.518	7.09

Table E-2 shows G_{mm} and air voids for Mix 2:

Table E.2: G_{mm} and air voids for Mix 2

ID	A	B	C	D	E	F
	mass of sample in air, A (g)	mass of SSD sample in air, B (g)	mass of sample in water, C (g)	Gmb (A/(B-C))	Gmm (g/cm³)	Air voids (%)
SCB_5.3AC_5.0AV_S1	5441.5	5451.0	3212.0	2.430	2.561	5.10
SCB_5.3AC_7.0AV_S1	5343.6	5365.6	3129.8	2.390	2.561	6.68
SCB_6.0AC_5.0AV_S1	5365.5	5373.5	3142.5	2.405	2.526	4.79
SCB_6.0AC_7.0AV_S1	5248.5	5259.0	3032.5	2.357	2.526	6.68
DM_5.3AC_5.0AV_S1	7131.0	7140.5	4217.0	2.439	2.561	4.76
DM_5.3AC_5.0AV_S2	7127.0	7137.0	4206.5	2.432	2.561	5.04
DM_5.3AC_7.0AV_S1	6987.0	7004.5	4058.5	2.372	2.561	7.39
DM_5.3AC_7.0AV_S2	6978.0	6998.0	4074.0	2.386	2.561	6.82
DM_6.0AC_5.0AV_S1	7020.0	7029.0	4100.5	2.397	2.526	5.10
DM_6.0AC_5.0AV_S2	7015.0	7025.5	4103.5	2.401	2.526	4.96
DM_6.0AC_7.0AV_S1	6869.0	6884.5	3969.5	2.356	2.526	6.71
DM_6.0AC_7.0AV_S2	6875.0	6895.0	3978.0	2.357	2.526	6.70

Table E-3 shows G_{mm} and air voids for Mix 3:

Table E.3: G_{mm} and air voids for Mix 3

ID	A	B	C	D	E	F
	mass of sample in air, A (g)	mass of SSD sample in air, B (g)	mass of sample in water, C (g)	G_{mb} (A/(B-C))	G_{mm} (g/cm ³)	Air voids (%)
SCB_5.3AC_5.0AV_S1	5434.0	5445.0	3206.4	2.427	2.550	4.81
SCB_5.3AC_7.0AV_S1	5305.0	5330.4	3097.2	2.376	2.550	6.84
SCB_6.0AC_5.0AV_S1	5393.6	5402.6	3166.6	2.412	2.538	4.96
SCB_6.0AC_7.0AV_S1	5281.8	5301.2	3064.4	2.361	2.538	6.96
DM_5.3AC_5.0AV_S1	7088.5	7103.5	4175.0	2.421	2.550	5.08
DM_5.3AC_5.0AV_S2	7095.5	7108.5	4184.0	2.426	2.550	4.85
DM_5.3AC_7.0AV_S1	6943.5	6970.0	4044.5	2.373	2.550	6.92
DM_5.3AC_7.0AV_S2	6936.5	6961.5	4043.5	2.377	2.550	6.78
DM_6.0AC_5.0AV_S1	7075.5	7089.5	4173.0	2.426	2.538	4.41
DM_6.0AC_5.0AV_S2	7055.5	7052.0	4140.0	2.423	2.538	4.53
DM_6.0AC_7.0AV_S1	6898.0	6910.5	3986.5	2.359	2.538	7.05
DM_6.0AC_7.0AV_S2	6906.5	6919.0	3995.0	2.362	2.538	6.93

APPENDIX F

F.0 AN EXAMPLE OF BATCHING SHEET

The following example (Table F-1 and Table F-2) shows the procedure of calculating the quantity of materials for the Mix 1 with 20% RAP, 5.3% binder content and binder grade of PG 70-22ER.

Table F.1: Quantity of virgin aggregates and RAP materials for the mixture with 20% RAP, 5.3% binder content, and binder grade of PG 70-22ER

stockpile	Virgin	RAP	Comparison: Combined vs. Target					
stockpile percentage, Ps	80	20						
total percentage	100		combined aggregate					
sieve size	percentage passing	%retained	cum. Retained	%passing	target %pass	Diff	Diff^2	
3/4"	100.0	100.0	0.0	0.0	100.0	100	0.0	0.0
1/2"	100.0	100.0	0.0	0.0	100.0	100	0.0	0.0
3/8"	100.0	96.8	0.6	0.6	99.4	99.4	0.0	0.0
1/4"	85.8	78.4	15.0	15.7	84.3	84.3	0.0	0.0
#4	64.7	66.4	19.3	35.0	65.0	65.1	0.1	0.0
#8	39.9	45.1	24.1	59.1	40.9	40.4	-0.5	0.3
#16	28.1	31.5	12.2	71.2	28.8	28.1	-0.7	0.5
#30	21.4	23.8	6.9	78.1	21.9	21.4	-0.5	0.2
#50	14.5	17.4	6.8	84.9	15.1	14.8	-0.3	0.1
#100	10.1	12.9	4.4	89.3	10.7	10.2	-0.5	0.2
#200	8.0	8.4	2.6	91.9	8.1	7.7	-0.4	0.1
pan	0	0	8.1	100.0	0.0	0	0.0	0.0
binder content	---	5.26	root mean square error					

stockpile	Virgin	RAP	Virgin	RAP (agg)	RAP (total)	Virgin Agg	RAP Agg
stockpile percentage, Ps	80	20	80	20	20		
total percentage	100		batch mass, grams				
sieve size	percentage retained						
3/4"	0.0	0	0.0	0.0	0.0	0.0	0.0
1/2"	0.0	0.0	0.0	0.0	0.0	0.0	0.0
3/8"	0.0	3.2	0.0	35.5	37.4	0.0	58.3
1/4"	14.2	18.4	629.8	204.0	215.3	629.8	238.3
#4	21.1	12	935.8	133.0	140.4	935.8	151.8
#8	24.8	21.3	1099.9	236.2	249.3	1099.9	282.3
#16	11.8	13.6	523.3	150.8	159.2	523.3	189.9
#30	6.7	7.7	297.1	85.4	90.1	297.1	113.5
#50	6.9	6.4	306.0	71.0	74.9	306.0	68.1
#100	4.4	4.5	195.1	49.9	52.7	195.1	17.4
#200	2.1	4.5	93.1	49.9	52.7	93.1	42.8
pan	8	8.4	354.8	93.1	98.3	354.8	7.9
			total weight				
			4434.93	1108.73	1170.288917	4434.9	1170.29

Table F.2: Quantity of binder, RAP materials, and total aggregates for Mix 1 with 20% RAP, 5.3% binder content, and binder grade of PG 70-22ER

target binder content %	5.3
aggregate mass, g	5543.658599
mixture mass, g	5853.916155
RAP binder (gr)	61.56
virgin binder (gr)	248.70
Gmm	2.562
Gmb	2.434
airvoid content (%)	5
gyratory height	0.13
mass of sample in GC (g)	5575.158243